

## CHAPTER 51

# Ultraviolet Radiation and Polymers

Anthony L. Andradý

*Camille Dreyfus Laboratory, Research Triangle Institute, Research Triangle Park, NC 27709*

---

<b>51.1</b>	Mechanisms of Photodegradation.....	859
<b>51.2</b>	Effects of Solar UV Induced Degradation.....	861
	References.....	865

---

The energies associated with near-ultraviolet radiation quanta are about 3.0–4.3 eV which correspond to 72–97 kcal/mol. Common covalent bonds encountered in polymers have bond dissociation energies which for the most part are either lower or within this energy range. Provided the ultraviolet radiation is absorbed by the polymer and suitable pathways are available for the photoexcited singlet ( $S$ ) and triplet ( $T$ ) species to transfer the absorbed energy to cause photochemical reactions, light-induced damage to the polymer can take place. In most systems a variety of competing photophysical processes, such as phosphorescence (from  $(T_1 \rightarrow S_0)$  transition) or fluorescence (from  $(S_1 \rightarrow S_0)$  transition), may preclude chemical reaction. When photochemical reactions of polymers do take place, they tend to involve the triplet excited states of molecules rather than the ground or singlet stage species because of the relatively longer lifetime of the former. The lowest excited triplet state,  $T_1$ , is formed by radiationless intersystem crossing from the lowest excited singlet state,  $S_1$ . Higher triplet states can form only from a triplet-triplet absorption where a molecule in the  $T_1$  state absorbs a photon.

When photochemical pathways are available, they often involve sequences of chemical reactions with specific energy requirements. The number of photochemical degradative pathways available to polymers is quite extensive.

As the photon energy is a function of the wavelength of radiation, it is reasonable to expect the high energy, short wavelength ultraviolet radiation to be more effective than visible light in promoting a wider range of these reactions. This is found to be the case; for instance, solar UV-B range (extending from about 290 nm to 315 nm) is well known to be the most deleterious wavelengths to polymers exposed to sunlight.

Absorption of electromagnetic radiation is a necessary prerequisite for photodegradation; Table 51.1 summarizes the ultraviolet cut-off wavelength and relative stability of commodity polymers and biopolymers. Polymers such as polyolefins, which theoretically should be transparent to ultraviolet (UV) light, nevertheless do absorb UV radiation due to the presence of impurities from several sources. In most practical applications, the compounding ingredients in the formulation and the processing operation itself yield sufficient chromophores to allow these polymers to absorb UV radiation and therefore to undergo photodegradation.

Also included in Table 51.1 is data on spectral sensitivity of common polymers. Wavelength sensitivity of a given photodegradation process can be measured experimentally using either monochromatic radiation or a specific source such as a white light source. In the former technique, the change in a specific property (such as yellowness or absorbance at a selected wavelength) per unit available photon is obtained. When a specific light source is used, samples of the polymer are exposed behind a series of cut-on filters. Each cut-on filter allows only the fraction of light having a wavelength longer than the cut-on value to reach the sample. Samples exposed to the same source behind different cut-on filters therefore photodegrade at different rates and sometimes even via different mechanisms. A comparison of the changes in a selected property of the samples exposed behind different filters allows the identification of the approximate spectral region which causes the most damage. This range is both source-dependent and damage-dependent. The data in Table 51.1 pertain to white light spectrum from borosilicate-filtered xenon source radiation, which is similar to direct solar radiation at unit air mass. However, the spectral sensitivity depends on the property or mode of damage used in its determination and also on compounding

**TABLE 51.1.** Absorption of UV-visible radiation by common synthetic and natural polymers.

Polymer	Cut-off [nm] <sup>a</sup>	Abs.max. [nm]	Stability <sup>b</sup>	Ref. <sup>c</sup>	Spectral sensitivity	
					Range [nm]	Property
Polyethylene	<180		4		260–360	Optical density
Polypropylene	<180		5		315–330	Extensibility
Polyoxymethylene	<210		4		—	
Poly(vinyl chloride)	<240		4		310–325	Yellowing
Polyamides	~240		3			
Polystyrene	~270		4		280	Chain scission
Polycarbonate	~280		4		310–340	Yellowing
Poly(phenyleneoxide)	~280		3			
Polyurethanes	~280		3			
Poly(ethylene terephthalate)	~310		2			
Poly(vinyl acetate)		240		[3]		
Poly(methylmethacrylate)	~240		1		300 <sup>e</sup>	Chain scission
Poly(methyl vinyl ketone)		~290		[3]		
Poly(phenyl vinyl ketone)		240		[3]		
Cellulose		270 <sup>d</sup>	4	[4]		
Lignin-softwood		280–285 <sup>d</sup>	5	[5]	334–354	Yellowing
-hardwood		274–276 <sup>d</sup>		[5]		
Wool		205, 280	3	[6]	340–420	Yellowing
Chitosan (acetylglucosamine)		193, 197	4	[7]		

<sup>a</sup>Cut-off wavelength indicated is that at which absorbance of a 10-micron film reaches 1.0.

<sup>b</sup>Stability is a relative, qualitative measure of the resistance of the polymer to terrestrial solar radiation.

<sup>c</sup>Data from [1] where not otherwise indicated. Data on spectral sensitivity are from [2]. Absorption maxima indicated in column 3, are for solution spectra.

<sup>d</sup>Biopolymers shown absorb very strongly at wavelengths shorter than the absorption maximum indicated.

<sup>e</sup>Based on quantum yield measurements.

ingredients in the polymer sample used. Therefore, the spectral sensitivity data in Table 51.1 are specific to the formulation and source used in their determination.

Irradiation of a polymer *in vacuo* or in an inert gas can lead to photolysis of the covalent bonds and sometimes subsequent rearrangement of the macroradical. However, in practical applications, UV-visible irradiation is carried out in air, and oxygen plays a key role in the photodegradation process. It is convenient to discuss the photodegradation process in terms of three stages: initiation, propagation, and termination. Initiation reactions lead to generation of free-radicals on absorption of radiation by polymers which contain a suitable chromophore (either as a part of macro-molecular structure or as an additive or impurity). The mechanism of initiation of even the common polymers, especially the relative significance of hydroperoxides, ketones, charge transfer processes, and singlet oxygen is a controversial topic. Typically, the propagation reactions take place between the polymer radical species and either oxygen or a polymer chain. The macromolecular oxy radicals formed may undergo  $\beta$  scission or other reactions. At a given instant during photodegradation, the polymer substrate would contain a variety of macroradicals which may terminate by bimolecular interaction or unimolecular processes.

The extent of primary photodegradation caused by the absorption of a single photon is a measure of the efficiency

of the photoprocess. With most photodegradation processes, the photoproducts formed during controlled exposure of the polymer to UV radiation can be accurately determined. The chain scission and/or crosslinking in the irradiated samples can also be estimated from physical techniques (such as gel permeation chromatography, or solution viscosity). Reliable quantum yields for different products can therefore be calculated. Some typical quantum yields for photodegradative processes of common polymers are given in Table 51.2.

The photochemical initiation process is of particular interest from a mechanistic as well as a practical point of view. A better understanding of initiation allows the selection of polymers which are inherently photostable under a given exposure scenario, and also helps in the design of new light stabilizers. However, even for commodity thermoplastics, the initiation process is not fully understood. The complexity of the photoinitiation process is due to the many competing reactions involved. In polypropylene for instance, photolysis of hydroperoxides and peroxides yield radical species with a quantum yield of about 2. While this is likely to be a key initiation route, oxidation products such as carbonyles and unsaturated groups, as well as charge transfer complexes and catalyst residues, are believed to be involved in the photoinitiation process. With most common polymers, the key species contributing to the initiation

**TABLE 51.2.** Quantum yields for product formation in common polymers.

Polymer	Process	Quantum yield (mol/Einstein)		$\lambda$ [nm]	Reference
		In air or O <sub>2</sub>	In N <sub>2</sub> or Vacuo		
Poly(vinyl chloride)	HCl evolution	0.015	0.011	254–400	[1]
	Chain scission	0.003	0.003		
	Crosslinking	0.0006	0.0014		
	Carbonyl formation	0.005	—	514.5 (laser)	[8]
	HCl evolution	0.009	0.005		
Poly(vinyl acetate)	Acetic Acid formation	0.01	—	254	[9]
	CO <sub>2</sub> formation	0.0065			
	CO formation	0.0069			
	Methane formation	0.0038			
	Chain scission	0.05	0.066		[10]
	Crosslinking	0.0025	0.047		
Polystyrene	Oxygen absorption (600 torr)	0.027		254	[11]
	Hydroperoxide formation	0.0009			
	Acetophenone formation	0.0006			
	Ketone formation	0.0011			
	Water formation	0.0095			
	Chain scission	0.0056	0.0039	254	[12]
	Crosslinking	0.0004	0.0009		
Poly (ethyleneterephthalate)	CO <sub>2</sub> formation	0.0002		254 or 313	[13]
	CO formation	0.0006			
	Crosslinking	0.0006			

process have been reported. While some controversy exists on the relative importance of these, data are summarized in Table 51.3 for common polymers.

### 51.1 MECHANISMS OF PHOTODEGRADATION

Polymers irradiated in air with solar UV radiation invariably breakdown due to a combination of photodegradative

as well as photo-initiated thermo-oxidative mechanisms. Both mechanisms can operate simultaneously or one can be dominant at a given stage of degradation depending on the chemical structure of the substrate polymer. With polymers such as the rigid poly(vinyl chloride) formulations used in building materials the visible damage is primarily a result of photodegradation. The photo-dehydrochlorination of the polymer results in the formation of conjugated double bonds along the chain, and leads to the characteristic

**TABLE 51.3.** Techniques commonly used to measure changes in common polymers due to UV irradiation.<sup>a</sup>

Changes	Property	Technique	Polymer	Reference
Surface degradation	Yellowing	Colorimetry	i) Poly(vinyl chloride)	[14]
			ii) Polycarbonate	[15]
			iii) Polystyrene foam	[16]
	Morphology	Electron microscopy	i) Poly(methyl methacrylate)	[17]
			ii) Polypropylene fiber	[18]
	Wettability	Contact angle	i) Polystyrene and Poly(methylvinylketone)	[19]
ii) Poly(vinyl chloride) film			[20]	
Bulk physical change	Appearance	Visual evaluation	i) Chalking of Poly(vinyl chloride)	[21]
	Mass	Gravimetry	i) Polyoxymethylene	[22]
			ii) Polyethylenes	[23]
	Density	Pycnometry	i) Polyethylene	[24]
	Transport	Gas permeability	i) Polyethylenes (CO <sub>2</sub> and H <sub>2</sub> O)	[25]
			ii) Poly(ethyleneterephthalate)	[26]

TABLE 51.3. Continued.

Changes	Property	Technique	Polymer	Reference	
	Crystallinity	Water vapor permeability	i) Polyethylene films	[27]	
		x ray analysis	i) (Ethylene - carbon monoxide) <sup>b</sup> copolymer	[25] [28]	
		ESCA (x ray photoelectron spectroscopy)		[29]	
Thermal properties	Transitions	Calorimetry	ii) Polyethylene	[30]	
			iii) Polystyrene		
			i) Polycarbonate, Poly(vinyl chloride), and Polystyrene	[31]	
Mechanical properties		Tensile properties	i) Common polymers	[32]	
			ii) Polyethylene	[33] [34]	
			iii) Polypropylene	[35] [36]	
			iv) Polystyrene	[37]	
			v) Poly(vinyl chloride)	[38] [39]	
			vi) Polyamides	[40] [41]	
		Flexural properties	i) Polyamides	[42]	
		Hardness	i) Polyethylene	[24]	
		Tear properties	i) Wool fabric	[43]	
Functional groups	Absorption of light energy	UV/Visible spectroscopy	i) Polypropylene	[44]	
			ii) Poly(vinyl chloride)	[45] [46]	
			iii) Polyamide	[44]	
			FTIR spectroscopy	i) Polyethylene	[47] [48] [49]
				ii) Poly(vinyl chloride)	[50]
				iii) Poly(ethyleneterephthalate)	[51]
			Photoacoustic FTIR	i) Polyethylene	[52]
				ii) Ethylene - propylene copolymer	[53]
				iii) Poly(vinyl chloride)	[54]
			NMR spectroscopy	i) Polyethylene	[55]
			ii) Poly(vinyl chloride)	[56]	
			iii) Polystyrene	[57]	
			iv) Polyisoprene	[58]	
		ESR spectroscopy	i) Polyethylene	[59]	
			ii) Polypropylene	[60]	
			iii) Polystyrene	[61]	
			iv) Poly(vinyl chloride)	[62]	
Other properties	Emission of light energy	Chemiluminescence	i) Polypropylene	[63]	
		Dielectric properties	i) Polyethylene	[64]	
			ii) Polystyrene	[65]	
Macromolecular changes	Molecular weight	Gel permeation	i) Polyethylene	[49]	
	Cross linking	Chromatography Sol/gel analysis	ii) Polystyrene	[66]	
			i) Polyethylene	[67]	
			ii) Polystyrene	[61]	

<sup>a</sup>Ultraviolet radiation exposure includes both solar ultraviolet exposure encountered in natural and/or accelerated weathering, as well as exposure to UV sources in the laboratory.

<sup>b</sup>ECO - (Ethylene - carbon monoxide ~1%) copolymer.

yellow discoloration of the material. In polyolefins, however, the only contribution of the solar UV radiation is in promoting initiation of the free radical reaction sequence. This occurs via the photolysis of the hydroperoxides and lead to an auto-oxidative reaction sequence. As hydroperoxide dissociation is catalyzed by metal compounds, the photodegradation of polyolefins is enhanced by the presence of transition metal salts.

In yet other polymers, such as with bisphenol polycarbonates both photodegradation and photo-initiated oxidative reactions take place simultaneously. The direct photoreaction is a Frie's rearrangement reaction, while the oxidative reactions result in chain scission and discoloration of the polymer. The chemical pathways involved in the latter process are not well understood.

While outdoor lifetimes of decorative and even some other building materials are limited by the rapidity with which they discolor, the more serious outcome of solar irradiation of polymers is the scission and/or crosslinking of chains that occur during exposure. Some crosslinking leading to the formation of an insoluble gel fraction as well as chain-scission leading to a low molecular weight sol fraction are generally obtained on exposure of common polymers to solar UV wavelengths. Chain scission measured by gel permeation methods or from the reduction in solution viscosity results in drastic irreversible changes in the mechanical properties of the material.

Based on the different pathways for breakdown available the photodegradation behavior can be generally classified as belonging to one of four categories:

1. Photodegradation with no significant chain scission

*Dehydrochlorination of poly(vinyl chloride) and photFrie's reaction in polycarbonates.*

2. Photodegradation with significant chain scission.

*Photodegradation of ethylene-carbon monoxide copolymers by Norrish reactions.*

3. Photoinitiated oxidation with significant chain scission

*Autoxidation of polyisoprene, and thermoplastic polyolefins.*

4. Photoinitiated oxidation with no significant chain scission

*Hydroperoxidation of unsaturated side chains with singlet oxygen in EPDM*

The above discussion pertains mostly to the pure polymer; most, polymers used in practical applications, especially those used outdoors tend to be compounded with a variety of additives. Some of these such as opacifiers, UV absorbers, and light stabilizers are intentionally added to the compound to control photodegradation and related oxidation reactions, to extend the outdoor lifetime of the material. Others such as fillers, reinforcing agents, lubricants, and

flame retardants are added to improve unrelated properties of the material. These, however, can very significantly impact the photostability of the polymer. Any change in copolymer composition or the presence of a second polymer can similarly alter the photodegradability of the mix.

Blending methyl methacrylate-butadiene-styrene copolymer with poly(vinyl chloride) for instance was shown to decelerate the dehydrochlorination (leading to discoloration). The gel content, surface energy, and the spectroscopic characteristics of the blend was altered by the presence of the second polymer [158]. In ethylene-propylene-diene rubber EPDM where the third monomer is ethylene-2-norbornene (NB), the photo-oxidation rate as measured by the accumulation of typical products such as hydroperoxides, varied linearly with the NB content [159]. The same held true for peroxide-crosslinked compounds of the same EPDM except that the linear relationship was found between the relative carbonyl absorbance on photooxidation and the amount of peroxide used to crosslink the material [160]. Additives can also have a similar effect; decabromodiphenyl ether flame retardant in polypropylene was shown to enhance oxidation. Furthermore, where hindered-amine light stabilizers HALS were present in the compound, the degradation product HBr reacted with it to form the ammonium salt that has no photostabilizer effectiveness [161].

The direct and indirect effects of fillers on the photostability of polymer compositions are well known. With the recent interest in nanopowdered fillers reports of their effectiveness as photostabilizers is beginning to be reported in the literature. For instance ZnO and TiO<sub>2</sub> nanoparticles (primary particle size 25–70 nm) were studied in acrylic coatings. A layer that carried at least 5 weight percent of the nanoparticles was needed to shield the underlying layers from UV exposure and hence degradation [162]. Nanoscale titania was also evaluated as a stabilizer in epoxy coatings [163].

## 51.2 EFFECTS OF SOLAR UV INDUCED DEGRADATION

Photochemical changes in the polymer invariably affect the physical, chemical, and mechanical properties of the material. These changes are often used to quantify the photodegradation process. As the changes in different properties are brought about by different light-induced processes, the rates at which they change on exposure to radiation may differ. Understandably, most studies have concentrated on those polymer characteristics of either fundamental importance (such as changes in average molecular weights) or those of practical relevance (such as surface discoloration). The consequences of photodegradation, which are of relevance to applications of polymers, include discoloration of the surface, surface damage such as cracking or chalking, loss of integrity as evidenced by reduced

**TABLE 51.4.** *Initiating species in photodegradation of common polymers.*

Polymer	Potential initiating species	Reference
Polyethylene <sup>a</sup>	-O-O- -OOH -C=O groups C=C groups from processing or from oxidation. Pigments (titania), and metal catalyst residues. Charge transfer complexes with O <sub>2</sub> .	[75–84]
Polypropylene <sup>b</sup>	Tertiary -OOH -O-O- groups from processing or from oxidation. In-chain and terminal -C=O groups. Catalyst residues. Charge-transfer complex with O <sub>2</sub> .	[76,80,82, 85–87]
Poly(vinyl chloride) <sup>c</sup>	Unsaturated centers, specially ~ CH <sub>2</sub> -CH=CH-CH <sub>2</sub> Cl and ~ CHCl-CH=CH-CH <sub>2</sub> ~. ~CHCl-CO=CHCl~ or side group carbonyl functionalities. $\alpha,\beta$ -unsaturated ketones ~CH=CH-CO~. Photolysis of -OOH and -O-O- groups from processing or from oxidation.	[88–94]
Polystyrene	Structural defects, pigments, and plasticizers. Direct photoexcitation/photoxidation of phenyl rings. Charge-transfer complex with oxygen. -C=O and -OOH groups from processing or from oxidation.	[32,95–101]
Polymethacrylates	Interactions with singlet oxygen. -C=O groups via Norrish I reactions. Direct photolysis of ester or methyl side groups. Photolysis of -O-O- groups from processing or from oxidation.	[102–107]
Polycarbonates	-O-C=O group in the main chain. Photo-Fries rearrangement.	[108, 109]
Aromatic Polyester (thermoplastic)	Light absorption by ester functionality, followed by main chain or side group scission. Norrish I and II reactions.	[110–113]
Polyamides	$\alpha,\beta$ -unsaturated carbonyl group impurities. Photolysis of OOH groups. H-bonding - mediated photoreactions of CONH group. Photolysis of C-N bond in main chain.	[90,114–117]

<sup>a</sup>Polyethylene and (ethylene-carbon monoxide) copolymer: Carbonyl photolysis in the early stages of photooxidation is via Norrish II process which occurs with a quantum efficiency  $\phi = 0.067$  in the presence or absence of oxygen [68,69]. Norrish I process can occur at a lower efficiency ( $\phi = 0.01$ ) but does not yield radicals [69]. Carbonyl moieties may also yield radicals by a primary process; intermolecular hydrogen - abstraction from polymer chains [70,71]. Photolysis of hydroperoxides is a key initiation pathway in early photodegradation of polyethylenes; in spite of their low absorbance, the quantum yield of radicals is high ( $\phi = 1$ ) [70]. Hydroperoxides produced in thermal processing is believed to be the most important initiating species, followed by carbonyl groups, and then the charge transfer complexes with oxygen [68].

<sup>b</sup>Polypropylene: Initiation process in polypropylene (and in polyolefins in general) is still controversial. While many possible initiating species have been identified, the relative importance of these is as yet unresolved. In the case of polypropylene Carlsson [70] ranked the candidate species in the following decreasing order of importance; peroxides, titanium catalyst residues, polynuclear aromatic pollutants, carbonyl compounds, and charge-transfer complexes with oxygen. Singlet oxygen and polynuclear aromatic compounds (PNA) [72], have also been proposed as possible initiators of photodegradation and photooxidative degradation in polyolefins. Water, oxygen, and compounding ingredients commonly present in polyolefins can readily react with singlet oxygen, making it unavailable for slower-reacting unsaturated centers in the polymer. PNAs are not present in the polymer but sorbed from air where the compounds may exist as pollutants.

<sup>c</sup>Poly(vinyl chloride): Unsaturated centers (generally 1–3 per 1000 repeat units) are believed to be the most important initiating species [73]. Conjugated polyene sequences in the polymer have very high extinction coefficients in the UV. Depending on the initial concentration in the polymer, carbonyl groups are the next important initiator. Not only can these undergo Norrish reactions, but excited carbonyl groups can also transfer energy to unsaturated centers [74]. Hydroperoxides and peroxides formed during autooxidation of the polymer also contributes to initiation process. Photolysis of hydroperoxide yields alkoxy radicals with a quantum yield of about unity [18].

**TABLE 51.5.** *Consequences of exposure of polymers to ultraviolet radiation.*

Polymer	Degradation	Mechanism	Published data	Reference
Polyethylene	a) Product yield	Basic autoxidation scheme and secondary oxidations of products.	Percentages of major products formed.  Same for (ethylene-ketone) copolymers.	[118–121]
	b) Carbonyl group formation	Photo-reactions of hydroperoxide.	Empirical equations for [C=O] build-up in natural and artificial exposures.  Change in [C=O] on irradiation for LDPE including those of different crystallinity.	[48,49,122]  [61,123]
	c) Change in tensile properties	Chain scission and crosslinking.	Correlation between the extensibility and [C=O] of films.	[34,79,118]
	d) Change in hardness	Chain scission and crosslinking reactions.	Correlation between Vicker's Hardness and [C=O].	[24]
	e) Decrease in average molecular weight	Chain scission reactions.	GPC data correlated with extensibility of weathered LDPE films.	[49]
	f) Gel formation	Crosslinking reactions.	Gel formation in LDPE. Change in density and dynamic modulus.	[118,124] [125]
	g) Other properties			
Polypropylene	a) Product yield	Same as for polyethylene.	Product yield as a function of the atactic content. FTIR study of products.	[126–128]
	b) Carbonyl group formation	Same as for polyethylene.	Data for samples of different tacticity.	[48,129]
	c) Change in hardness	Chain scission and crosslinking reactions.	Changes in brittleness, tensile properties, and FTIR, on irradiation. Surface changes.	[126,130]
Poly(vinyl chloride), (PVC)	a) HCl yield	Photodehydrochlorination yielding conjugated polyenes.	a) Kinetics of HCl evolution $E_a = 14$ KJ/mol.	[131–133]
			b) For exposure of film to $\lambda > 254$ nm.	
			c) Rate is unaffected by light intensity. At 20–90°C, in N <sub>2</sub> , $E_a = 8.3$ KJ/mol.	
			d) Effect of radiation wavelength.	
	b) Carbonyl and hydroperoxide yield	Photooxidation reactions.	The $E_a$ for carbonyl build-up for photo-oxidation in O <sub>2</sub> , $E_a = 21$ KJ/mol. Spectroscopic study of [C=O] and [ROOH] for PVC film. Effect of tacticity.	[118,134,135]
c) Gel formation	Crosslinking.	For crosslinking of PVC film, $E_a = 1.4 \times 10^{-3}$ (air) and $3.1 \times 10^{-3}$ KJ/mole(N <sub>2</sub> ).	[136]	
d) Discoloration	Yellowing due to formation of conjugated polyene sequences.	Yellowing of extruded PVC compounds.  Photobleaching of PVC yellowness at $\lambda > 514$ nm.	[14,129,138]	
e) Decrease in average molecular weight	Oxidative chain-scission.	Change in molecular weight distribution during weathering. For chain scission, $E_a = 1.7 \times 10^{-4}$ KJ/mole. Correlation between chain scission and [C=O].	[132,139,140]	

TABLE 51.5. *Continued.*

Polymer	Degradation	Mechanism	Published data	Reference
Polystyrene	f) Change in tensile properties	Chain scission and crosslinking.	Linear dependence of tensile strength on reciprocal molecular weight.	[141]
	a) Discoloration	Yellowing due to formation of unidentified chromophores.	Yellowing on exposure to solar UV radiation and to a filtered - xenon source radiation.	[142–144]
	b) Carbonyl and/or hydroperoxide yield	Photo-oxidation reactions.	[C=O] as a function of irradiation time at different temperatures.	[61,145]
	c) Decrease in molecular weight	Oxidative chain scission.	Random scission on photolysis in solution. Changes in molecular weight at different depths.	[12,146–147]
Polymethacrylate	d) Gel formation	Crosslinking.	Gel formation on irradiation in air at different temperatures.	[12,61,143]
	a) Decrease in average molecular weight	Oxidative chain scission.	Reduction in average molecular weight (depending on residual monomer concentration), on exposure to a filtered xenon source.	[148]
Polycarbonate	a) Discoloration	Yellowing due to photo-fries and oxidative processes.	Yellowing on exposure to solar UV radiation.	[15,149–152]
	b) Decrease in average molecular weight	Oxidative chain scission.	Change in molecular weight due to photo-degradation.	[149,153]
	c) Change in tensile properties	Chain scission and crosslinking.	Change in extensibility with exposure time in natural weathering.	[149]
Polyester (Polyethylene terephthalate)	a) Product yield	Photooxidative reactions and direct cleavage via Norrish reactions:	Quantum yields, $\phi$ ., for CO, CO <sub>2</sub> , -OH and -COOH products formed on photolysis of PE.	[110,154] [166]
	Polyamide	a) Change in mechanical properties	Chain scission and crosslinking.	Changes in tenacity, yield strength and flexural strength of nylons on exposure to solar UV and to xenon source.
b) Changes in average molecular weight		Oxidative chain scission.	Change in molecular weight on exposure to a filtered-xenon source, at different pH values.	[156]

strength or extensibility, changes in impact strength of the polymer, and changes in physical properties such as solubility. A large fraction of the reported literature is devoted to effects of solar UV radiation on polymers. With the practical lifetimes of polymers used outdoors being routinely determined by photodegradation rates, this interest in solar UV-B is not surprising. With recent observations of global stratospheric ozone depletion and the concomitant increase in UV-B fractions in the terrestrial solar spectrum, there is renewed interest in weatherability and stabilization of polymers used in outdoor applications.

A wide range of analytical approaches is available to study the effects of UV exposure on polymers. Table 51.4

summarizes the more common of these techniques and illustrates their use with selected examples. Table 51.5 attempts to summarize some of the published data on various effects of UV exposure on common polymers. Typical data are cited to illustrate the main types of physical and chemical changes obtained with different polymers. Data include those pertaining to exposure to solar radiation (solar UV-B effects), exposure to laboratory-filtered xenon sources or other UV-visible sources, and exposure to monochromatic UV wavelengths. Table 51.5 is not intended to be a comprehensive review but a set of selected examples to indicate the diversity of changes brought about by exposure to UV radiation.



EPDM rubber	Carbonyl absorption	Oxidative chain scission	Effect of crosslinking	[158]
Epoxy resin	(a) Indentation for hardness (b) Spectroscopy (ATR-FTIR) (c) Differential scanning calorimetry	Chain scission	Presence of nanofiller TiO <sub>2</sub> in the compound improved photostability	[163]
Polyurethane acrylate	(a) FTIR spectroscopy	Urethane linkage was found to be most susceptible	Weathering resistance of the coating was established	[164]
Softwood and hardwood pulps	(a) Brightness measurements	Yellowing and brightness changes	Effectiveness of stabilizers against brightness reversion established	[165]

## REFERENCES

- D. J. Carlsson and D. M. Wiles, in *Encyclopedia of Polymer Science and Engineering*, Vol. 4, edited by H. F. Mark, N. M. Bikales, C. G. Overberger, and G. Menges (John Wiley & Sons, New York, 1986a), p. 665.
- A. L. Andrady, M. B. Amin, S. H. Hamid *et al.*, in *Environmental Effects Panel Report. 1991 Update* (United Nations Environmental Program, Nov. 1991b), p. 45.
- W. Schnabel, in *Polymer Degradation. Principles and Practical Applications* (Hanser Publishers, 1981), p. 98.
- N. S. Hon, *J. Polymer Sci.*, A1 **13**, 1347 (1975).
- A. Sakakibara, in *Wood and Cellulosic Chemistry*, edited by D. N.-S. Hon, and N. Shiraiishi (Marcel Dekker, New York, 1991), p. 114.
- F. G. Lennox, M. G. King, I. H. Leaver *et al.*, *Appl. Polym. Symp.*, No. **18**, 353 (1971).
- R. A. A. Muzzarelli and R. Rocchetti, *Chitin in Nature and Technology*, edited by R. Muzzarelli, C. Jeuniaux, and G. W. Gooday (Plenum Press, New York, 1986), p. 385.
- C. Decker and M. Balandier, *J. Photochem.* **15**, 213 (1981b).
- G. Geuskens, M. Borsu, and C. David, *Europ. Polym. J.* **8**, 883 (1972); *ibid.* 1347 (1972).
- D. David, M. Borsu, and G. Gueskins, *Eur. Polym. J.* **6**, 959 (1970).
- G. Gueskins, G. Delaunois, D. Baeyens-Volant *et al.*, *Eur. Polym. J.* **14**, 291 (1978).
- C. David, D. Baeyens-Volant, G. Delaunois *et al.*, *Europ. Polym. J.* **14**, 501 (1978).
- F. B. Marcotte, D. Campbell, J. A. Cleaveland *et al.*, *J. Polymer Sci.*, A1 **5**, 481 (1967).
- A. L. Andrady and N. D. Searle, *J. Appl. Polym. Sci.* **37**, 2789 (1989).
- A. L. Andrady, N. D. Searle, L. F. E. Crewdson, *Polym. Deg. Stab.* **35**, 235-247 (1992).
- A. L. Andrady, K. Fueki, and A. Torikai, *J. Polym. Sci.* **42**, 2105 (1991).
- A. Blaga and R. S. Yamasaki, *Durability Building Mater.* **4**, 21 (1986).
- D. J. Carlsson and D. M. Wiles, in *Ultraviolet Light Induced Reactions in Polymers*, ACS Symposium Ser. 25 (American Chemical Society, Washington DC, 1976), p. 321.
- K. Esumi, K. Meguro, A. M. Schwartz *et al.*, *Bull. Chem. Soc. Jpn.* **55**, 1649 (1982).
- R. B. Fox and T. R. Price, *J. Polym. Sci. A1* **3**, 2303 (1965).
- W. V. Titow, in *PVC Technology* (Elsevier Applied Science Publishers, New York, 1984), p. 473.
- A. Davis, *Polym. Deg. Stab.* **3**, 187 (1981).
- J. H. Cornell, A. M. Kaplan, and M. R. Rogers, *J. Appl. Polym. Sci.* **29**, 2581 (1984).
- Y. Watanabe and T. Shiota, *Kenkyu Hokoku Kogyo Gijutsuin* **2**, 141 (1981).
- A. L. Andrady, J. E. Pegram, and S. Nakatsuka, *J. Environ. Polym. Degradn.* **0**, 00 (1994).
- P. Mercea, T. Virag, D. Silipas *et al.*, *Polym. Comm.* **28**, 31 (1987).
- S. G. Croll, *Prog. Org. Coat.* **15**, 223 (1987).
- R. Gooden, D. D. Davis, M. Y. Hellman *et al.*, *Macromolecules* **21**, 1212 (1988).
- A. Dilks, *J. Polym. Sci.*, A1 **19**, 1319 (1981).
- D. T. Clark and H. S. Munro, *Polym. Deg. Stab.* **8**, 195 (1984); **8**, 213 (1984).
- M. M. Quayyum and J. R. White, *Arabian Journal for Science and Engineering* **13**, 547 (1988).
- G. Geuskens, G. Delaunois, Q. Lu-Vinh *et al.*, *Eur. Polym. J.* **18**, 387 (1982).
- A. Torikai, H. Shirakawa, S. Nagaya *et al.*, *J. Appl. Polym. Sci.* **40**, 1637 (1990).
- A. L. Andrady, J. E. Pegram, and S. Nakatsuka, *J. Environ. Polym. Degradn.* **1**, 31 (1993).
- C. S. Schollenberg and H. D. F. Meijer, *Polymer* **32**, 438 (1991).
- M. Raab, L. Kotulak, J. Kolarik *et al.*, *J. Appl. Polym. Sci.* **27**, 2457 (1982).
- G. Geuskens, P. Bastin, Q. Lu-Vinh *et al.*, *Polym. Deg. Stab.* **3**, 295 (1980).
- G. Scott and M. Tahan, *Europ. Polym. J.* **13**, 997 (1977).
- A. Kaminska and H. Kaczmarek, *Angew. Makromol. Chem.* **139**, 63 (1986); **144**, 139 (1986).
- G. A. George and M. S. O'Shea, *Polym. Deg. Stab.* **28**, 289 (1990).
- Y. W. Mai and B. Cotterell, *J. Appl. Polym. Sci.* **27**, 4885 (1982).
- A. Davis and D. Sims, in *Weathering of Polymers* (Applied Science Publishers, London, 1983), p. 139.
- C. M. Carr and I. H. Leaver, *J. Appl. Polym. Sci.* **33**, 2087 (1987).
- N. S. Allen, *Polym. Deg. Stab.* **6**, 193 (1984); N. S. Allen, *Polym. Deg. Stab.* **8**, 55 (1984).
- C. Decker, *J. Appl. Polym. Sci.* **28**, 97 (1983).
- R. Sastre, G. Martinez, F. Castillo *et al.*, *Makromol. Chem. Rapid Commun.* **5**, 541 (1984).
- J. Lacoste, R. Arnaud, and J. Lemaire, *J. Appl. Polym. Sci. A-1* **22**, 3855 (1984).
- F. Gugumus, *Die Angew. Makromol. Chem.* **182**, 85 (1990a).
- A. L. Andrady, J. E. Pegram, and Y. Tropsha, *J. Env. Polym. Deg.*, 117-126 (1993a).
- J. L. Gardette and J. Lemaire, *Polym. Deg. Stab.* **16**, 147 (1986); *ibid.* **25**, 293 (1989).
- P. Blais, M. Day, and D. M. Wiles, *J. Appl. Polym. Sci.* **17**, 1895 (1973).
- R. A. Costa, L. Coltro, and F. Galembek, *Angew. Makromol. Chem.* **180**, 85 (1990).
- R. O. Carter, P. M. Paputa, and D. J. Bauer, *Polym. Deg. Stab.* **23**, 121 (1989).
- H. C. Pendey and A. K. Kulshreshtha, *Eur. Polym. J.* **24**, 599 (1988).
- L. W. Jelinski, J. J. Dumais, J. P. Luongo *et al.*, *Macromolecules* **17**, 1650 (1984).
- F. Mori, M. Koyama, and Y. Oki, *Angew. Makromol. Chem.* **68**, 137 (1979); *ibid.* **64**, 89 (1977).
- H. C. Beachell and L. H. Smiley, *J. Polym. Sci.*, A1 **5**, 1635 (1967).
- M. A. Golub, M. L. Rosenberg, and R. V. Gemmer, *Rubber Chem. Technol.* **50**, 704 (1977).
- H. Kubota and M. Kimura, *Polym. Deg. Stab.* **38**, 1 (1992).
- H. Kubota, K. Takahashi, and Y. Ogiwara, *Polym. Deg. Stab.* **33**, 115 (1990).
- A. Torikai, A. Takeuchi, and K. Fueki, *Polym. Deg. Stab.* **14**, 367 (1986).
- J. F. Rabek, T. A. Skowronsky, and B. Ranby, *Polymer* **21**, 226 (1980).
- G. A. George and M. Gahemy, *Polym. Deg. Stab.* **33**, 411 (1991).
- F. P. La Mantia and R. Schifani, *Polym. Deg. Stab.* **10**, 67 (1985).
- N. A. Weir, *Dev. Polym. Deg.* **1**, 67 (1977).
- I. Mita, T. Takagi, K. Horrie *et al.*, *Macromolecules* **17**, 2256 (1984).
- R. M. Ikeda, F. F. Rogers, S. Tocker *et al.*, in *Ultraviolet Light Induced Reactions in Polymers*, edited by S. S. Labana, ACS Symposium Series **25**, 76 (1976).
- G. Scott, in *Ultraviolet Light Induced Reactions with Polymers*, edited by S. S. Labana, ACS Symp. Ser. No. 25 (ACS, Washington, DC, 1976), p. 340.

69. G. H. Hartley and J. E. Guillet, *Macromolecules* **1**, 165 (1968).
70. D. J. Carlsson, A. Garton, and D. M. Wiles, *Macromolecules* **9**, 695 (1976).
71. N. S. Allen and J. F. McKellar, *Chem. Soc. Revs.* **4**, 533 (1965).
72. G. Scott, in *Singlet Oxygen*, edited by B. Ranby and J. F. Rabek (Wiley Interscience, London, 1978).
73. C. Decker, in *Degradation and Stabilization of PVC*, edited by E. D. Owen (Elsevier Applied Science Publishers, London, 1984), p. 95.
74. E. D. Owen, in *Developments in Polymer Photochemistry*, edited by N. S. Allen (Applied Science Publishers Ltd., London, 1982), p. 165.
75. S. Al-Malaika and G. Scott, *Europ. Polym. J.* **16**, 709 (1980).
76. D. J. Carlsson, K. H. Chan, A. Garton *et al.*, *Pure Appl. Chem.* **52**, 289 (1980).
77. A. Garton, D. J. Carlsson, and D. M. Wiles, *Makromol. Chem.* **181**, 1841 (1980).
78. C. H. Chew, L. M. Gan, and G. Scott, *Europ. Polym. J.* **13**, 361 (1977).
79. F. Gugumus, *Die Angew. Makromol. Chem.* **176/177**, 27 (1990).
80. N. S. Allen, K. O. Fatinikun, J. Luc-Gardette *et al.*, *Polym. Deg. Stab.* **4**, 95 (1982).
81. F. M. Rugg, J. J. Smith, and L. H. Waterman, *J. Polym. Sci.* **11**, 1 (1953).
82. D. J. Carlsson and D. M. Wiles, *J. Macromol. Sci. Rev. Macromol. Chem. C* **14**, 65 (1976).
83. J. Buil and J. Verdu, *Europ. Polym. J.* **15**, 389 (1979).
84. F. Gugumus, *Makromol. Chem., Macromol. Symp.* **27**, 25 (1989).
85. D. J. Carlsson and D. M. Wiles, *Macromolecules* **2**, 597 (1969).
86. D. C. Mellor, A. B. Moir, and G. Scott, *Europ. Polym. J.* **9**, 219 (1973).
87. N. S. Allen, K. O. Fatinikun, J. Luc-Gardette, and J. Lemaire, *Polym. Deg. Stab.* **4**, 95 (1982).
88. N. S. Allen, J. F. McKellar, and G. O. Phillips, *J. Polym. Sci., A1* **12**, 1233 (1974).
89. L. Ackerman and W. J. McGill, *South Afr. Chem. Inst.* **26**, 82 (1973).
90. N. S. Allen, J. F. McKellar, and D. Wilson, *J. Photochem.* **6**, 337 (1976).
91. N. S. Allen, in *Degradation and Stabilization of Polyolefins* (Applied Science Publishers, Ltd., London, 1993).
92. N. S. Allen, A. Chirinois-Padron, and J. H. Appleyard, *Polym. Deg. Stab.* **6**, 149 (1984).
93. L. Ratti, F. Visani, and M. Ragazzani, *Eur. Polym. J.* **9**, 429 (1973).
94. A. Caraculacu, E. C. Buruiana, and G. Robila, *J. Polymer Sci., Polym. Chem. Ed.* **16**, 2741 (1978).
95. G. Geuskens, D. Baeyens-Volant, G. Delaunois *et al.*, *Europ. Polym. J.* **14**, 299 (1978).
96. J. F. Rabek and B. Ranby, *J. Polymer Sci., A1* **12**, 295 (1974).
97. M. Nowakowska, J. Najbar, and B. Waligor, *Europ. Polym. J.* **12**, 387 (1975).
98. J. R. MacCallum and D. A. Ramsey, *Eur. Polym. J.* **13**, 945 (1977).
99. N. Yamamoto, S. Akaishi, and H. Subomura, *Chem. Phys. Lett.* **15**, 458 (1972).
100. N. A. Weir, *Dev. Polym. Deg.* **4**, 143 (1982).
101. B. Rándy and J. Lucki, *Pure Appl. Chem.* **52**, 295 (1980).
102. B. Dickens, J. W. Martin, and D. Waksman, *Polymer* **25**, 706 (1984).
103. S. G. Bond and J. R. Ebdon, *Polym. Commun.* **32**, 290 (1991).
104. D. Panke and W. J. Wunderlich, *J. Appl. Polym. Sci., Appl. Polym. Symp.* **35**, 321 (1979).
105. A. Torikai and K. Fueki, *J. Polym. Photochem. Photobiol.* **2**, 297 (1982).
106. F. R. Mayo and A. A. Miller, *J. Am. Chem. Soc.* **80**, 2493 (1958).
107. N. S. Hon, *J. Polymer Sci., A1* **14**, 2497 (1976).
108. J. S. Humphrey, A. R. Schultz, and D. B. G. Jaquiss, *Macromolecules* **6**, 305 (1973).
109. A. Rivaton, D. Sallet, and J. Lemaire, *Polym. Photochem.* **3**, 463 (1983).
110. M. Day and D. M. Wiles, *J. Appl. Polym. Sci.* **16**, 203 (1972a).
111. P. S. R. Cheung, C. W. Roberts, and K. B. Wagner, *J. Appl. Polym. Sci.* **24**, 1809 (1979).
112. M. Day and D. M. Wiles, *J. Appl. Polym. Sci.* **16**, 175 (1972b).
113. C. V. Stephenson, J. C. Lacey, and W. S. Wilcox, *J. Polym. Sci.* **55**, 177 (1961).
114. N. S. Allen, J. F. McKellar, and D. Wilson, *J. Polym. Sci., A1* **15**, 2973 (1977).
115. C. H. Do, E. M. Pearce, B. J. Bulkin *et al.*, *J. Polym. Sci., A1* **25**, 2301 (1987).
116. A. Roger, D. Sallet, and J. Lemaire, *Macromolecules* **19**, 579 (1986).
117. J. F. McKellar and N. S. Allen, in *Photochemistry of Man-Made Materials* (Applied Science Publishers Ltd., London, 1979), p. 128.
118. G. Scott and M. Tahan, *Europ. Polym. J.* **11**, 535 (1975).
119. J. H. Adams, *J. Polymer Sci., A1*, **8**, 1279 (1970).
120. S. K. L. Li and J. E. Guillet, *J. Polym. Sci., A1* **18**, 2221 (1980).
121. M. U. Amin, G. Scott, L. M. K. Tillerkeratne, *Europ. Polym. J.* **11**, 85 (1975).
122. K. Tsuji and H. Nagata, *Rep. Prog. Polym. Phys. Jpn.* **18**, 517 (1975).
123. P. Vink, in *Degradation and Stabilization of Polyolefins*, edited by N. S. Allen (Applied Science Publishers, London, England, 1983), p. 228.
124. R. Geetha, A. Torikai, S. Nagaya *et al.*, *Polym. Deg. Stab.* **19**, 279 (1987).
125. G. Scott, *J. Polym. Sci., Polym. Symp.* **57**, 357 (1976a).
126. J. H. Adams and J. E. Goodrich, *J. Polymer Sci., A1* **8**, 1279 (1970).
127. Y. Kato, D. J. Carlsson, and D. M. Wiles, *J. Appl. Polym. Sci.* **13**, 1447 (1969).
128. G. Geuskens and M. S. Kabamba, *Polym. Deg. Stab.* **5**, 399 (1983).
129. C. Decker and M. Balandier, *Polym. Photochem.* **1**, 221 (1981).
130. D. J. Carlsson and D. M. Wiles, *Macromolecules* **4**, 174, 179 (1971).
131. W. H. Gibb and J. R. MacCallum, *Europ. Polym. J.* **8**, 1233 (1972).
132. C. Decker and M. Balandier, *J. Photochem.* **15**, 221 (1981a).
133. D. Braun and S. Kull, *Angew. Makromol. Chem.* **85**, 79 (1980).
134. D. Braun and S. Kull, *Angew. Makromol. Chem.* **86**, 171 (1980).
135. G. Martinez, C. Mijangos, and J. Millan, *J. Appl. Polym. Sci.* **29**, 1735 (1984).
136. C. Decker and M. Balandier, *Europ. Polym. J.* **18**, 1085 (1982).
137. A. L. Andrady, A. Torikai, and K. Fueki, *J. Appl. Polym. Sci.* **37**, 935 (1989).
138. J. F. Rabek, B. Ranby, B. Ostenson *et al.*, *J. Appl. Polym. Sci.* **24**, 2407 (1979).
139. S. Matsumoto, H. Ohshima, Y. Hosuda, *J. Polym. Sci., Polym. Chem. Ed.* **22**, 869 (1984).
140. F. Mori, M. Koyama, and Y. Oki, *Angew. Makromol. Chem.* **64**, 89 (1977).
141. G. Geuskens and C. David, *Pure Appl. Chem.* **51**, 2385 (1979).
142. A. L. Andrady and J. E. Pegram, *J. Appl. Polym. Sci.* **42**, 1589 (1991).
143. N. A. Weir, *Dev. Polym. Deg.* **4**, 143 (1982).
144. F. Gugumus, *Dev. Polym. Stab.* **1**, 8 (1978).
145. A. Ghaffar, A. Scott, and G. Scott, *Eur. Polym. J.* **12**, 615 (1976).
146. T. R. Price and R. B. Fox, *J. Polym. Sci.* **4**, 771 (1966).
147. Z. Osawa, F. Konomo, S. Wu *et al.*, *Polym. Photochem.* **7**, 337 (1986).
148. M. Day and D. M. Wiles, *Can. Text. J.* **6**, 69 (1972).
149. A. Ram, O. Zilber, and S. Kenig, *Polym. Eng. Sci.* **25**, 535 (1985).
150. Andrady, 1991a.
151. A. Davis and J. H. Golden, *J. Macromol. Sci., Rev. Macromol. Chem. C* **3**, 49 (1969).
152. A. Factor and M. L. Chu, *Polym. Deg. Stab.* **2**, 203 (1980).
153. J. D. Webb and A. W. Czanderna, *Sol. Energy Mater.* **15**, (1987).
154. M. H. Tabankia and J.-L. Gardette, *Polym. Deg. Stab.* **14**, 351 (1986).
155. A. Anton, *J. Appl. Polym. Sci.* **9**, 1631 (1965).
156. K. E. Kyllö and C. M. Ladisch, *ACS Symposium Series* **318**, 343 (1986).
157. K. E. Kyllö and C. M. Ladisch, *ACS Symposium Ser.* **318**, 343 (1986).
158. C. Xudong, W. Jiasheng, and J. Shen, *Polym. Degrad. Stab.* **87**(3), 527 (2005).
159. E.A. Snijders, A. Boersma, B. van Baarle, and P. Gijsman, *Polym. Degrad. Stab.* **89**(3), 484 (2005).
160. E.A. Snijders, A. Boersma, B. van Baarle, and P. Gijsman, *Polym. Degrad. Stab.* **89**(2), 200 (2005).
161. K. Antos, and J. Sedlar, *Polym. Degrad. Stab.* **90**(1), 180 (2005).
162. P. Katangur, S. B. Warner, P. K. Patra, Y. K. Kim, S. K. Mhetre, and A. Dhanote, Continuous Nanophase and Nanostructured Materials). In *Materials Research Society Symposium Proceedings*. Materials Research Society. 589–594 (2003).
163. S. Scierka, P. L. Drzal, A. L. Forster, and S. Svetlik, *Mater. Res. Soc. Symp. Proc.* 217–222 (2005).
164. C. Decker, F. Masson, and R. Schwalm, *Polym. Degrad. Stab.* **83**(2), 309 (2004).
165. C. Li, D. Kim, and A. J. Ragauskas, *J. Wood Chem. Technol.* **24**(1), 39 (2004).
166. G. J. M. Fechine, M. S. Rabello, R. M. S. Maior, and L. H. Catalani, *Polym. Degrad. Stab.* **45**(7), 2303 (2004).

## CHAPTER 52

# The Effects of Electron Beam and $\gamma$ -Irradiation on Polymeric Materials

K. Dawes\*, L. C. Glover<sup>†</sup>, and D. A. Vroom<sup>†</sup>

*\*Department of Materials Science and Engineering, North Carolina State University  
Campus Box 7907 Raleigh, NC, 27695-7907;*

*<sup>†</sup>Tyco Electronics 305 Constitution Dr Menlo Park, CA 94025*

---

<b>52.1</b>	Introduction . . . . .	867
<b>52.2</b>	General Effects of Electron Beam and $\gamma$ -Irradiation on Polymeric Materials . . . . .	868
<b>52.3</b>	Specific Effects on Polymeric Groups . . . . .	873
<b>52.4</b>	Additives . . . . .	884
<b>52.5</b>	Summary . . . . .	884
	References . . . . .	884

---

### 52.1 INTRODUCTION

The effect of high-energy irradiation on polymeric materials has been intensely studied over the past 60 years. These studies parallel the growth in the types and usage of polymeric materials and the availability of electrically generated radiation sources. The electron beam has been a commercially acceptable processing technique for the last 50 years and is the preferred radiation source for polymer modification. Several books are available that cover the high-energy irradiation of polymeric materials [1–6].

The effect of radiation on materials has importance in the areas of wire and cable insulation, heat-shrinkable articles, curing of elastomers, plastics, paints and inks, electron beam lithography, medical sterilization, polymer property control, and outer space applications.

In general, the effects of exposure of polymers to high-energy radiation will lead to some change in the properties of the polymer. Its interaction with a high-energy electron is a complex and random process. The energies involved are much greater than the electron binding energy of any electron to an atomic nucleus. In this respect it differs from ultraviolet (UV) irradiation in which the energy carried per particle (photon) is lower than the ionization energy of an atom or molecule. Ultraviolet irradiation is therefore very selective, whereas high-energy irradiation is nonselective. The changes are primarily a consequence of:

1. Electron linear energy transfer (LET) to a molecule, followed by bond cleavage to give radicals.
2. Radical combination leading to the formation of crosslinks and end-links or disproportionation to give scission.
3. Gas evolution is mainly a consequence of (2) and direct formation of gaseous molecules.

#### 52.1.1 Radiation Sources

The sources of high-energy ionizing radiation are [7]:

1. Cobalt-60 sources of  $\gamma$ -rays (1.17–1.33 MeV) [8,9];
2. Cesium-137 sources of  $\gamma$ -rays (0.66 MeV) [10];
3. Electron accelerators (0.1–12 MeV) [11];
4. Bremstrahlung X-rays from accelerators (3–10 MeV) [12].

The International System unit of absorbed dose is the Gray (Gy), which is equal to the energy imparted by ionizing radiation to a mass of matter corresponding to 1 joule per kilogram. The other unit of radiation dose is a special unit, the rad, which is equal to the energy absorption of 0.01 joule per kilogram, that is, 0.01 Gray. Until recently the most common unit of dose used to be the

Megarad (Mrad). The Gray is now the most commonly used unit in the literature:

$$1\text{Mrad} = 10^4\text{Gy} = 10\text{kGy}$$

$$1\text{Gy} = 6.25 \times 10^8 \text{ eVKg}^{-1}.$$

$\gamma$ -Ray sources give a deeper penetration into a material, (sometimes an order of magnitude deeper) but at a much slower dose rate for example, kGy per hour when compared to electron accelerators which have a much lower penetration but have a much higher dose rate, for example, kGy per second. This difference becomes important for irradiation in air or oxygen.

The amount of radiation absorbed can be measured either directly or indirectly using a variety of dosimeters. Several reviews of dosimeters are available [13–15].

## 52.2 GENERAL EFFECTS OF ELECTRON BEAM AND $\gamma$ -IRRADIATION ON POLYMERIC MATERIALS

### 52.2.1 G-Factors

The common way to investigate the effects of irradiation by either electron beam or  $\gamma$ -rays is to determine the yield of an event. An event change may involve the measurement of the changes in, for example, molecular weight, solution viscosity or gel content, or the measurement of the amounts of specific gaseous materials evolved during exposure.

The standard measurement of the yield for an event resulting from the irradiation process is expressed as the  $G$  factor. This factor is universally accepted [16] and is defined as the event yield per 100 eV of energy deposited in the material. The SI unit for  $G$  is  $\mu\text{mol J}^{-1}$ . For the purposes of this review events per 100 eV will be used throughout. The most commonly quoted  $G$  factors are for crosslinking, chain scission, and gas evolution,  $G(X)$ ,  $G(S)$ , and  $G(\text{Gas})$ , respectively. There may be several different values for the  $G$ -factor in the literature since several different methods of measurement may be used to determine the event yield. If different methods or standards are used to determine molecular weights, they can lead to widely different  $G$ -factors. For example, in the case of a low density polyethylene values for  $G(X)$  of 0.9 or 1.7 are obtained using the hydrogenated polybutadiene or polystyrene calibrations, respectively [17].

### 52.2.2 Changes in Molecular Weight Distribution

As stated above one of the main effects of exposure of polymeric materials to high energy radiation is that the material undergoes scission of the main chain and the creation of free radicals, unsaturation (double bonds),

crosslinks, and end-links. Change in the molecular size distribution will be a consequence of main chain scission, crosslinking, and end linking. Much of the early theoretical expressions relating to the effect of radiation processes on molecular weight distribution were derived by Charlesby [18–20] and Saito [21–24].

### Main Chain Scission

In deriving the basic equation for main chain scission, the following assumptions are made: (1) all polymer molecules are linear; (2) every structural unit is fractured with equal probability; (3) average molecular weight is sufficiently large; and (4) the total number of main chain scissions is sufficiently smaller than the total number of structural units.

The basic equation, derived by Saito [25], which expresses the change in molecular size distribution of linear polymer molecules undergoing main chain scission is

$$\frac{\partial w(p,y)}{\partial y} = -pw(p,y) + 2p \int_p^\infty \frac{w(l,y)}{l} dl,$$

where

$$y = \int_0^t r dt$$

and

$$G(S) = \frac{100N_A y}{D}$$

where  $t$  is the time,  $p$  is the degree of polymerization of the polymer molecule,  $r$  is the probability that a structural unit undergoes scission in unit time, and  $w(p,y)$  is the weight fraction of polymer molecules having  $p$  structural units,  $N_A$  is Avogadro's number,  $D$  is the radiation dose, and  $G(S)$  is the yield of main chain scissions. The first term,  $-pw(p,y)$ , corresponds to the decrease of the molecules having  $p$  structural units due to main chain scission, and the last term corresponds to the increase of the molecules having  $p$  structural units due to the scissions of those molecules having  $l$  units. The number of main chain scissions per structural unit is  $y$ , and since  $r$  is usually independent of  $t$  then  $y$  is equal to  $rt$ . Solution of the above equation leads to

$$w(p,y) = \left[ w(p,0) + py \int_p^\infty \frac{(2+yl-yp)}{l} w(l,0) dl \right] \exp(-py),$$

where  $w(p,0)$  is the initial weight fraction. Calculation of the average molecular weight can be obtained from the following expression.

$$f_j(y) = \int_0^\infty p^{j-1} w(p,y) dp, \quad j = 0, 1, 2, 3, \dots$$

The change in the average molecular weights due to main chain scission can be calculated from the last two equations. The number average degree of polymerization  $P_n$  in the absence of any crosslinking is given by

$$\frac{1}{P_n} = \frac{1}{u_n} + y,$$

where  $u_n$  is the number average degree of polymerization prior to irradiation. This relationship holds for any initial molecular size distribution. If  $M_n^0$  and  $M_n$  are the number average molecular weight before and after irradiation, respectively, then

$$uy = \frac{[M_n^0 - M_n]}{M_n}.$$

Therefore the changes in the number average molecular weight depend only on  $M_n^0$  and the number of chain scission per structural unit and not on the initial molecular weight distribution.

The changes in the weight average molecular weight after irradiation are dependent on the initial molecular weight distribution.

For initial uniform distribution then

$$\frac{M_w}{M_w^0} = \frac{2(u_n - 1 + e^{u_n y})}{(u_n y)^2}.$$

For initial random distribution then

$$\frac{M_w}{M_w^0} = \frac{1}{(1 + u_n y)}.$$

For an initial Schulz-Zimm distribution then

$$\frac{M_w}{M_w^0} = \left[ u_n y - 1 + \left( \frac{1 + u_n y}{\sigma} \right)^{-\sigma} \right] \frac{2\sigma}{(1 + \sigma)(u_n y)^2},$$

where

$$\sigma = \frac{M_n}{M_w - M_n}.$$

When only degradation occurs with a polymer the molecular weight distribution will always approach the random case, that is

$$\frac{M_w}{M_n} = 2.$$

### Simultaneous Crosslinking and Scission

For crosslinking, the basic equation which expresses the change in molecular size distribution of linear polymer molecules is

$$\frac{1}{p} \frac{\partial w(p, x)}{\partial x} = -2w(p, x) \int_0^\infty w(l, x) dl + \int_0^p w(l, x) w(p - 1, x) dl,$$

where  $x$  is the number of crosslinks per structural unit, or the density of crosslinks. The assumptions made for this equation are as follows: (1) Crosslinks are produced at random; (2) every structural unit crosslinks with the same probability regardless of its position in the polymer molecule; (3) the number of crosslinks is sufficiently small in comparison to the total number of structural units; and (4) intramolecular linkings in molecules of finite size are negligible.  $G(X)$  is the yield of crosslinks:

$$G(X) = \frac{100N_A x}{D}.$$

When crosslinks and main chain scissions are produced simultaneously by irradiation it is assumed that they are independent of each other. The change in molecular size distribution can be obtained by first calculating the effect of all the scission on the initial distribution and then calculating the effect of all the crosslinking on the resultant distribution. This assumes that crosslinking occurs after all the main chain scissions have taken place. When crosslinking and scission occur simultaneously, the number average degree of polymerization  $P_n(x, y)$ , for any arbitrary shape of the initial molecular weight distribution, is given

$$\frac{1}{P_n(x, y)} = \frac{1}{u} + y - x$$

and

$$\frac{M_n}{M_n^0} = \frac{1}{1 + u_n(y - x)}.$$

The number average molecular weight resulting from simultaneous chain scission and crosslinking is independent of the initial molecular weight distribution, whereas the weight average molecular weight is not. The weight average degree of polymerization  $P_w(x, y)$  for an initial random distribution is given by

$$\frac{1}{P_w(x, y)} = \frac{1}{2u} + \frac{y}{2} - 2x$$

and

$$\frac{M_w}{M_w^0} = \frac{1}{[1 + u_n(y - 4x)]}.$$

If the initial distribution is uniform then

$$\frac{M_w}{M_w^0} = \frac{2(e^{-u_n y} + u_n y - 1)}{[u_n y^2 - 4u_n x(e^{-u_n y} + u_n y - 1)]}$$

and the initial Schulz-Zimm distribution

$$\frac{M_w}{M_w^0} = \frac{2\{u_n y - 1 + [1 + (\frac{u_n y}{\sigma})]^{-\sigma}\}}{(u_n x)^2 - 4\{u_n y - 1 + [1 + (\frac{u_n y}{\sigma})]^{-\sigma}\}u_n x}.$$

### Gelation

When a polymeric material undergoes radiation crosslinking the weight average molecular weight and intrinsic viscosity increase with radiation dose, until they finally tend to infinitely large values. A part which is insoluble in any solvent grows within the polymeric substance as the radiation level is increased. The phenomenon is called gelation and the insoluble part is the gel. The instance when an incipient gel is formed is the gel point. The density of crosslinks at the gel point,  $x_g$ , is given by

$$x_g = \frac{1}{2P_w^0}.$$

The number of crosslinks at the gel point is equal to half the ratio of the total number of structural units to the weight average degree of polymerization,  $P_w^0$ , prior to undergoing crosslinking.

When crosslinking and main chain scission occurs simultaneously, for an initial random distribution then

$$x_g = \frac{y}{4} + \frac{1}{2P_w^0}.$$

### 52.2.3 Determination of G Factors

#### Charlesby–Pinner Equation

In a paper published in 1959 [26] Charlesby and Pinner developed the Charlesby–Pinner equation which allows the experimentalist to determine the  $G(S)$  and  $G(X)$  ratios. The derivation of the equation is based on an initial random molecular weight distribution and relates to the sol fraction,  $s$ , to the crosslinking index,  $\gamma'$ , when both main chain scission and crosslinking occur.

$$s + \sqrt{s} = \frac{1}{\gamma'}.$$

The basic equation, which is a slight modification of an earlier equation [18,19] is expressed as follows:

$$s + \sqrt{s} = \frac{p_0}{q_0} + \frac{1}{q_0 u_1 D},$$

where  $p_0$  is the probability of main chain scission per monomer unit per unit dose,  $q_0$ , the probability of crosslinking per monomer unit per unit dose,  $u_1$ , the number average degree of polymerization, and,  $D$ , the radiation dose in Mrads.

The expression relates the sol fraction to the crosslinking and scission processes. The expression can also be written in terms of the ratio of  $G(S)$  to  $G(X)$  and the initial number average molecular weight,  $M_n^0$ , as follows:

$$s + \sqrt{s} = \frac{G(S)}{2G(X)} + \frac{9.6 \times 10^5}{2G(X)M_n^0 D}.$$

A plot of  $s + \sqrt{s}$  against  $1/D$  should yield a straight line with the intercept giving the ratio of scission to crosslinking. The plot is only linear for initial random molecular weight distribution and deviations occur when  $M_w/M_n \neq 2$ . For an initial distribution, which is either very broad or very narrow and for a moderate value of the ratio of the scission rate to crosslinking rate, considerable deviations from the Charlesby–Pinner relationship occur [27]. At high radiation doses, the assumptions for the Charlesby–Pinner relationship that there is no intramolecular crosslinking and that endlinking is negligible may not be valid since both these processes would be expected to occur at high doses. With polyethylene, extrapolation of the Charlesby–Pinner relation at higher doses yields a value for  $p_0/q_0$  of zero [28], a decrease in the main chain scission rate with increasing dose suggesting that scission then becomes a minor component. Also, when  $G(S) > 4G(X)$  [29] the polymer will remain completely soluble even though the polymer is still undergoing considerable modification; therefore, the Charlesby–Pinner relationship would not be applicable in this case since no gel would be formed.

Several modifications to the Charlesby–Pinner relationship that deal with deviation from the initial random distribution have been published [30–32]. In some cases a plot of  $s + \sqrt{s}$  against  $D^{-k}$ , where  $k$  can vary from 0.42 to 0.55 leads to a better linear relationship for polyethylenes [28]. Vinyl group endlinking can also be taken into account with the following relationship [33]:

$$\ln \phi = (q_0 u_1 + k)D,$$

where  $\ln \phi$  is the ratio of number of molecules before and after irradiation and,  $k$  The probability of one molecule of the  $i$ th species being removed through vinyl endlinking.

The Charlesby–Pinner equation can also be expressed in dimensionless quantities as

$$s + \sqrt{s} = \frac{G(S)}{2G(X)} + \left(2 - \frac{G(S)}{2G(X)}\right) \left(\frac{D_g}{D}\right),$$

where  $D_g$  is the dose to the gel point. The initial slope of the  $s + \sqrt{s}$  vs  $D_g/D$  curve is more helpful in many cases in determining the ratio of  $G(S)$  to  $G(X)$  [34].

#### Other Methods

The yield of scission can be determined by the change in the number average molecular weight of the polymer using the equation [35]:

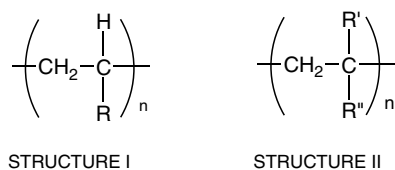
$$\frac{1}{M_n} = \frac{1}{M_n^0} + 1.04 \times 10^7 G(S)D.$$

The yield of crosslinking can be determined using the equation [36]:

$$G(X) = \frac{0.48 \times 10^6}{M_w D_g}$$

### 52.2.4 Polymeric Structure

The chemical structure of the polymer can determine the type of change that a polymer will undergo upon high energy irradiation. In very general terms, polymers of structure I will undergo crosslinking upon irradiation and those of structure II will undergo scission.



An example of this is the case of poly(methyl acrylate), which has structure I ( $\text{R} = \text{COOCH}_3$ ) and readily crosslinks,  $G(\text{crosslinking}) \approx 0.5$  [37]. In contrast, poly(methyl methacrylate), PMMA, which has structure II ( $\text{R}' = \text{CH}_3$ ,  $\text{R}'' = \text{COOCH}_3$ ) readily degrades via chain scission,  $G(\text{scission}) 2.28$  [38]. Table 52.1 gives a list of the types of polymers that are prone to either crosslinking or scission.

The presence of unsaturation in the polymer chain can enhance the effects and increase the yields of crosslinking. Purified natural rubber (*cis*-1,4-polyisoprene) is highly unsaturated and is readily crosslinked upon irradiation in vacuo with either  $\gamma$ -rays or electron beam [39], giving a yield for physical crosslinking,  $G(\text{X})$ , of 3.5. Some polymers that contain high levels of unsaturation also undergo a high yield for loss of unsaturation upon irradiation. For example synthetic polyisoprenes composed of 1,2 and 3,4 isomers give a  $G(\text{loss of unsaturation})$  of  $\approx 130$  [40,41], whereas  $G(\text{X})$  is  $\approx 2$ . Intramolecular cyclization upon irradiation appears to be a dominant process in this case.

If in structure I,  $\text{R} = \text{X}$ , that is a halogen atom, the carbon-halide bond is broken upon irradiation and dehydrohalogenation, loss of hydrogen halide gas can be the dominant process. The relative ease of loss of the halogen will depend

on the carbon-halogen bond strength, following the order  $\text{I} > \text{Br} > \text{Cl} > \text{F}$ . Polyvinylchloride, PVC, although often cited [42] as a crosslinking polymer upon irradiation, readily and rapidly dehydrochlorinates on exposure to either electron beam or  $\gamma$ -irradiation. The yield for production of hydrogen chloride gas,  $G(\text{HCl})$ , is 13 at 30 °C [43].

The structural type of  $\text{R}$ ,  $\text{R}'$ , and  $\text{R}''$  can also influence reaction yields. In general, the larger the amount of aromaticity that is present, the lower the yield of any reaction occurring as a consequence of irradiation. The yields of aromatic-containing polymers can often be an order of magnitude lower than the corresponding hydrocarbon. In fact, some of the highly aromatic polymers are very resistant to the effects of irradiation. The aromatic unit has a protective effect, the resonant structure of the aromatic ring enabling a considerable amount of energy to be absorbed without any rupture of the bonds. An example of the protective effect of aromatic rings on the yield for crosslinking,  $G(\text{X})$ , is the case of polystyrene,  $\text{R} = \text{phenyl}$ , where  $G(\text{X})$  is around 0.05, compared to polyethylene, structure I,  $\text{R}' = \text{H}$ , and  $G(\text{X})$  is  $> 1$  [44].

### 52.2.5 Effect of Atmosphere During Irradiation

A major effect of irradiation of polymeric materials is the atmosphere in which the material is exposed. As mentioned earlier, the irradiation process produces radical species, and depending on the relative stability of these species, several competing reactions can happen:

1. The radical can remain as a stable species within the polymeric matrix. In an inert atmosphere radicals can exist for extensive periods of time (up to many days or weeks).
2. The radical undergoes some reaction either with another radical to form a crosslink or undergoes disproportionation that leads to scission and the development of unsaturated groups in the polymer.

**TABLE 52.1.** Generic types of polymers that either undergo crosslinking or scission.

Prone to crosslinking	Prone to scission
Polyacrylates	Polyisobutylene
Polyvinylchloride	Poly $\alpha$ -methylstyrene
Polysiloxanes	Polymethacrylates
Polyamides	Polymethacrylamides
Polystyrene	Poly(vinylidene chloride)
Polyacrylamides	Polytetrafluoroethylene(PTFE)
Polyethylene copolymers such as EVA, EEA, EMA, EBA	Polytrifluorochloroethylene
Unsaturated elastomers	Polypropylene ether
Ethylene propylene elastomers	Cellulose and derivatives
Polyacrolein	
Polyethylene	

- In the presence of oxygen, either already present in the polymeric material or by diffusion into the polymer, there are processes that compete with (1) and (2). Oxygen will react with radicals to form peroxides or hydroperoxides. Inevitably the presence of oxygen will lead to an increase in the extent or rate of the scission process and degradation of the polymer.

A good example of the effect of oxygen is the case of polypropylene which degrades when irradiated in oxygen, whereas crosslinking occurs when the irradiation takes place in vacuo. Another example is poly(tetrafluoroethylene) (PTFE) which readily degrades in air upon irradiation, whereas irradiation in the absence of air has much less of an effect on properties [45]. However in the case of poly(methyl methacrylate), which is very prone to degradation, the rate of degradation is lower in air than in vacuo [38].

As mentioned earlier, the dose rate can affect the choice of atmosphere used. For example, in the case of  $\gamma$ -irradiation the dose rate is of the order of kGy per hour. At this rate oxygen can readily diffuse into the polymer, react with radicals and lead to degradation. In general, irradiation with  $\gamma$ -rays is usually done in an inert atmosphere, unless you want to intentionally degrade the material. With an electron beam the dose rate is much higher at kGy per second; therefore, the competition with oxygen is reduced as it cannot diffuse into the material at a rate equal to the radiation induced reaction, although not totally eliminated.

### 52.2.6 Trapped Electrons/Radicals

If the polymeric material is in the glassy state, that is, below the glass transition temperature ( $T_g$ ) or has some crystallinity, trapped electrons and trapped radicals can be produced upon irradiation with either electron beam or  $\gamma$ -irradiation. Phenomena such as thermoluminescence, electrical conductivity, color changes in the polymer, and imperfections within crystals have attributed to ionic species. Trapped electrons have been identified in  $\gamma$ -irradiated polyethylene [46].

In general, amorphous materials do not have the tendency to produce trapped electrons. Table 52.2 shows the yield of trapped electrons,  $G(e_t^-)$  for a range of hydrocarbon polymers with different crystalline content that have been  $\gamma$  irradiated at 77 K [47,48]. The initial  $G(e_t^-)$  was deter-

mined from ESR experiments by comparison with ( $e^-$ ) in 2-methyltetrahydrofuran (MTHF) and based on a value of  $G(e^-)$  of 2.6 for MTHF. All the polymers were free of antioxidants and stabilizers.

The materials with trapped electrons undergo photo-bleaching when exposed to near-infrared light ( $\lambda > 1,000nm$ ).

### 52.2.7 Effect of the Temperature During Irradiation

Any effect of irradiation, in general, is increased with increasing temperature. At temperatures below  $T_g$ , a significant number of stable radicals are formed (radicals trapped in the glassy state) and, in general, crosslinking is reduced due to immobility in the glassy state. At temperatures above  $T_g$  the tendency to crosslink is usually increased, although scission processes will also increase.

An example of the change above  $T_g$  is illustrated for the case of the fluorocopolymer, FEP. Irradiation of FEP with high energy radiation above  $T_g$  (80 °C for 14% hexafluoropropylene) leads to crosslinking with maximum efficiency being at temperatures between 300 °C and 320 °C. Above 320 °C thermal degradation becomes a major factor [49,50]. On the other hand, polystyrene shifts from crosslinking below  $T_g$  (approximately 100 °C) to scission above  $T_g$  [44].

### 52.2.8 Effects in Semicrystalline Polymers

Semicrystalline polymers are polymers that contain both crystalline and amorphous states. In general, the major effect of irradiation, either electron beam or  $\gamma$ -rays, on the crystalline region is to cause some imperfections. At high levels of irradiation the original crystalline structure tends to be progressively destroyed and is nearly always accompanied by a drop in the crystalline melting point,  $T_m$ . An example is that of poly(ethylene terephthalate), which shows a decrease in melting point of approximately 25 °C after irradiation (20 MGy) [51].

On the other hand, some polymers show an initial increase in crystallinity, demonstrated by an increase in density. At relatively low doses (< 200 kGy), ultra high molecular weight polyethylene (UHMWPE) appears to show an increase in crystallinity. Since UHMWPE has a

**TABLE 52.2.** Effect of crystallinity on trapped electrons yields in  $\gamma$ -irradiated hydrocarbon polymers.

Polymer	Crystallinity (%)	Initial $G(e_t^-)$ (electrons/100 eV)
HDPE (Marlex 6050)	≈ 82	0.46
LDPE (Alathon 1414)	≈ 45	0.12
Isotactic PP (Phillips Petroleum Co.)	≈ 70	0.17
Atactic PP (Hercules Inc.)	0	<0.02
Isotactic Poly(4-methylpentene-1) (Mitsui)	≈ 40	0.08
Polyisobutylene (Exxon)	0	0



relatively low amount of crystallinity but a very high molecular weight, the effect is best explained by a scission process thereby reducing the molecular weight and reducing entanglements. Both these effects will increase mobility of the polymer chains and allow more crystallization [52]. Similar effects are seen with poly(tetrafluoroethylene) PTFE and poly(vinylidene fluoride) PVDF.

## 52.3 SPECIFIC EFFECTS ON POLYMERIC GROUPS

### 52.3.1 Elastomers

An excellent review on the radiation chemistry of elastomers up to 1980 has been published [53].

Elastomers such as *cis*-1,4-polyisoprene (natural rubber), polybutadiene, polybutadiene-styrene (SBR), and polychloroprene have large amounts of unsaturation in the polymer backbone and all undergo crosslinking upon irradiation with either electron beam or  $\gamma$ -irradiation. Table 52.3 gives some values for  $G(X)$  and the ratio of scission to crosslinking  $G(S)/G(X)$  for several elastomers. The protective effect of the aromatic ring is shown by the decrease in yield as the percentage of styrene is increased for the SBR series.

Polychloroprene also undergoes loss of the chlorine atom, which leads to a high yield of hydrogen chloride gas,  $G(HCl)$  is 3.3 [54], as well as crosslinking. For a crystallizable polychloroprene both crosslinking and scission occur in the amorphous region [55].

The radiation effects on ethylene-propylene rubber (EPR) are modestly dependent on the ethylene content [63]. As the ethylene content is increased a shift to a larger yield for crosslinking occurs and the polymer is less prone to scission, the relationship is not linear since similar results for yields are found at 42 and 69% ethylene.

The irradiation of ethylene-propylene-diene-monomer (EPDM) elastomers, which contain some specific side

chain unsaturation, leads to an increase in both crosslinking and scission. The type of diene monomer can affect the yield of crosslinking (curing) with 1,4-hexadiene being more effective than 5-ethylidene-2-norbornene (EN) [65] and EN more effective than dicyclopentadiene (DCP) [64]. The higher the levels of diene content the faster the crosslinking rate but this is also accompanied by an increase in the scission yield [64,66]. The properties of radiation cured EPDM are superior when compared to the more common sulfur cured material (conventional cure), with greatly improved compression set and oil resistance [65].

The block copolymer elastomeric materials such as styrene-butadiene-styrene (SBS) and styrene-isoprene-styrene (SIS) are readily crosslinked by an electron beam [67]. The increase in the properties such as dynamic and static moduli is consistent with crosslinking.

Polyphosphazene elastomers undergo crosslinking when  $\gamma$ -irradiation is performed in a vacuum. The yield of crosslinking,  $G(X)$ , varies from about 1 to 12 depending on the percentage of allyl groups in the polymer chain [68].

### 52.3.2 Polyethylene and Copolymers

Polyethylene (PE) is the most widely studied and commercially irradiated polymer class, with studies ranging from *n*-alkane waxes [69,70] as model compounds to UHMWPE [52,71–73].

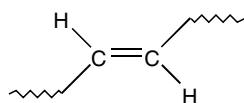
The types of polyethylene can vary depending on the method of manufacture, the amount of comonomer and the type of comonomer, that is, whether hydrocarbon or polar. Polyethylene manufactured by the older high pressure process leads to the production of highly branched and long branched low density polyethylene (LDPE). With modern polymerization technology, which uses much lower pressures, polyethylenes are more linear in nature. They can be made with random short chain branches such as methyl, ethyl, butyl, and hexyl which arise from copolymerization

**TABLE 52.3.**  $G(X)$  and  $G(S)/G(X)$  values for some common elastomers.

Elastomer	$G(X)$	$G(S)/G(X)$
Purified natural rubber (in vacuo)	3.5 [39]	0.14, 0.11 [56], 0.18, 0.03 [57]
Natural rubber (in air)	1.05 [58]	
Polybutadiene ( <i>cis</i> -1,4) [59]	5.3	0.1
Polybutadiene (90% vinyl 1,2) (in vacuo) [60]	$\approx 10$	
SBR (16% styrene) [61]	2.9	–
SBR (28% styrene) [61]	1.5	–
SBR (85% styrene) [61]	0.3	–
Polychloroprene [62]	3.2–4.8	–
EPR( $\approx$ 4% ethylene) [63]		0.44
EPR(42% ethylene) [63]	0.46	0.21
EPR(69% ethylene) [63]	0.50	0.23
EPR(60 mole% ethylene) [64]	0.26	0.61
EPDM(56 mole% ethylene +1.9 mole% DCP) [64]	0.91	0.32
EPDM(57 mole% ethylene +2.0 mole% EN) [64]	2.18	0.26

with the corresponding alkene monomer. Linear low density PE (LLDPE) and high density PE (HDPE) are made using a low pressure technique in either liquid or gas phase.

The backbone structural feature of two hydrogen atoms per carbon leads to several unique responses to irradiation including hydrogen gas evolution, formation of *trans* vinylene unsaturation, the decay of vinyl end groups and extremely high crosslinking efficiency.



*Trans* Vinylene

The formation of the *trans* vinylene unsaturation is not molecular weight dependent, is linear over a substantial dose range and is used as a dosimeter [15]. From numerous investigations [15,74,75], the formation of *trans* vinylene unsaturation appears to be a primary process of irradiation with the detachment of a hydrogen molecule being a one step process. The  $G(\text{H}_2)$  value is relatively high, 3–4 at room temperature and 3–6 at elevated temperatures (130 °C). The  $G$  values for some of the other processes are shown in Table 52.4. The values all show a relatively wide variation, due to the complexity of the polyethylene materials studied. Table 52.5 gives some values for the yield of crosslinking for a wide range of polyethylenes [33]. The materials cover a wide range of initial molecular weight distribution, density and initial vinyl content. However, the average measured  $G(X)$  for LDPE, LLDPE, and HDPE is about 1. Chain scission in polyethylenes appears to be low with  $G(S)$  values  $<0.1$  [28].

Linear polyethylene (low pressure process) has been most widely studied where the effects of molecular weight, polydispersity, temperature, crystallinity, the presence or absence of terminal unsaturation, branching and postirradiation treatment have been shown to effect the previously mentioned main irradiation consequences. The consequences have been thoroughly reviewed [15,79–81].

Since polyethylene mainly crosslinks, the effect of irradiation is to generally enhance the physical properties. For example, for HDPE an increase in both the yield stress and secant modulus at 0.5% strain is observed [52]. The effect on the properties above the melting point have been extensively studied [82] and there is a direct relationship of the elastic modulus measured at 160 °C to the dose. For irradi-

ated polyethylenes, the elastic modulus measured at 160 °C shows a growth rate of 3.8 and 3.9 Pa Gy<sup>-1</sup> for LDPE and HDPE, respectively.

The effect of irradiation on the crystallinity of UHMWPE has already been described. Irradiation of UHMWPE in the melt leads to a high yield of crosslinks with effectively no chain scission occurring, and with increasing crosslink density a change from lamellar to micellar-like crystallization was found [83]. More recent thorough studies of UHMWPE often at sterilizing doses of around 25–50 kGy, show both scission and crosslinking as well as a “transition” zone within and below the polymer mass [84–87].

Polar copolymers of ethylene, such as ethylene-vinyl acetate (EVA) and ethylene-ethyl acrylate (EEA), are readily crosslinked upon exposure to high energy irradiation [88]. In fact, the melt index of EVA can be controlled by the use of low doses ( $<50$  kGy) of irradiation [89]. The presence in polar ethylene copolymers of comonomer units such as vinyl acetate or alkyl acrylates (methyl, ethyl and *n*-butyl) proportionately reduces the level of crystallinity, and since the majority of radiation responses of interest take place in the amorphous phase, the responses are more uniform throughout the polymer mass. When the irradiation is done at room temperature, the physical properties after irradiation follow the same trend as polyethylene [90].

### 52.3.3 Polypropylene

Polypropylenes can be a semicrystalline polymer (atactic/isotactic), (atactic/syndiotactic) or a purely amorphous polymer (atactic). The effect of crystallinity on the yield of trapped electrons (Table 52.2) has already been discussed.

Although polypropylene is classed as a crosslinking type polymer, the initial studies on polypropylene [91,92] showed that the polymer, in the early stages of irradiation, undergoes scission, but at around 500 kGy a gel point was reached indicating the formation of crosslinks;  $G(X)$  was found to be around 0.6. Irradiation at  $>500$  kGy leads to further degradation. In fact polypropylene undergoes both scission and crosslinking at about equal amounts.

The mechanical degradation that arises after irradiation with  $\gamma$ -rays has been shown to be independent of the conditions of irradiation (air or vacuum) [93]. The post-irradiation effects of oxygen dominate, which will lead to a drop in both the tensile strength, modulus of elasticity, and elongation over time. Table 52.6 gives some changes for isotactic

**TABLE 52.4.**  $G$  values for the generation of alkyl[ $G(\text{alkyl})$ ], allyl[ $G(\text{allyl})$ ], and dienyl[ $G(\text{dienyl})$ ] radicals, and *trans* vinylene [ $G(V_i)$ ] for irradiated polyethylenes.

Polymer	$G(\text{alkyl})$	$G(\text{allyl})$	$G(\text{dienyl})$	$G(V_i)$	$G(X)$
HDPE	1.3–3.0 [76]	0.2–0.4	0.015 [77]	2.0+/-0.3 [78]	0.1–1.34 [79]
LLDPE	–	–	–	–	0.7–1.09
LDPE	–	–	–	1.7	0.8–1.25

**TABLE 52.5.** Yields for crosslinking for a range of polyethylenes [33].

Resin	Density	G(X)
LDPE	0.920	1.09
LDPE	0.935	0.8
LDPE	0.930	1.09
HDPE	0.962	1.0
HDPE	0.950	0.70
HDPE	0.945	0.50
HDPE	0.962	1.1
LLDPE	0.937	1.0
LLDPE	0.924	0.96
LLDPE	0.919	0.99

polypropylene after  $\gamma$  irradiation [94]. An increase in temperature will accelerate the process. For isotactic polypropylene the drop in elongation follows first order kinetics with an activation energy of 9 kcal/mole<sup>-1</sup> [95].

The major gases evolved during irradiation under a vacuum are hydrogen and methane. In the presence of oxygen, carbon dioxide and carbon monoxide are also produced. Table 52.7 gives the yields for gas evolution for powdered isotactic polypropylene; similar values are found for polypropylene film [95].

Some values for the yields of crosslinking and scission are given in Table 52.8 for atactic and isotactic polypropylenes.

The G(S)/G(X) ratio also tends to be a function of dose, with the value decreasing with increasing dose [97].

The irradiation will also show an effect on the level of crystallinity and melting point. For example, after a dose of 6 MGy the crystallinity was 73% of the original value and the melting point changed from 160°C to 105°C [98].

### 52.3.4 Fluoropolymers

#### General Trends in Fluoropolymers

A review of the effects of high energy radiation on fluoropolymers has recently been published [99] and provides a wealth of information. There is a relationship between the effect of high energy irradiation on a fluoropolymer and the amount of hydrogen atoms in the fluoropolymer. The trend can be approximately expressed as follows:

For crosslinking

PVF > PVDF > ETFE > FEP > PFA > PTFE

and for degradation

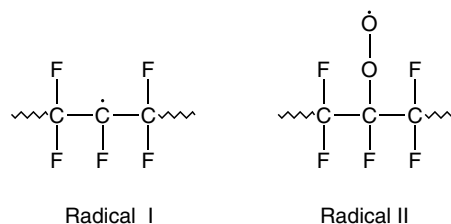
PTFE > PFA  $\approx$  FEP > ETFE > PVDF > PVF

In general, the higher the hydrogen content the higher the tendency of the fluoropolymer to crosslink. The presence of hydrogen does lead to dehydrohalogenation (loss of hydrogen fluoride, HF) upon irradiation. The use of crosslinking promoters are advantageous since relatively high levels of crosslinking can be achieved without compromising the thermal stability of the polymer [99]. Recent work has reinforced the difference in radiation response between perfluoropolymers and those containing hydrogen with a study of the influence of low doses (10–200 kGy) of gamma irradiation on PVF, PVDF, ETFE, FEP, and PFA [100]. Also, gamma irradiated PVF has been shown to have much better UV stability than gamma irradiated PVDF [101].

### 52.3.5 Perfluoropolymers

Poly(tetrafluoroethylene) (PTFE) is very sensitive to irradiation with either an electron beam or  $\gamma$  source. It predominately undergoes degradation when irradiated [102,103] in fact high energy irradiation is used commercially to induce degradation to reduce and control the molecular weight of PTFE. The effect of irradiation on the high temperature (380 °C) viscosity measurements and the number average molecular weight are shown in Table 52.9.

The effect of gamma irradiation on the physical properties of PTFE film are shown in Table 52.10. The falloff in physical properties is dramatic, even after irradiation in vacuo followed by exposure to air. The radicals produced by irradiation have been shown to have a long lifetime even after heating to 300 °C [103]. By looking at the electron spin resonance spectrum, radical I is detected for irradiation in vacuo and peroxy radical II is detected after exposure to air [105].

**TABLE 52.6.** Variation in the tensile strength, modulus of elasticity, elongation, and some electrical properties with irradiation dose in polypropylenes.

Dose (kGy)	0	1,000	280	800	1,200	1,600
Tensile strength (MN m <sup>-2</sup> )	37.5	35.1	30.0	17.1	18.0	16.5
Modulus of elasticity (MN m <sup>-2</sup> )	1.45	1.35	1.30	1.20	1.15	
Elongation (%)	$\approx$ 900	$\approx$ 200	$\approx$ 90	$\approx$ 50	$\approx$ 40	$\approx$ 20
Dielectric rigidity (MV m <sup>-1</sup> )	168	165	150	100	99	98
Electrical permittivity (@ 50 Hz)	2.19	2.16	2.20	2.17	2.20	2.34

**TABLE 52.7.** Yields for gas evolution for  $\gamma$ -irradiation (300 kGy) of powdered isotactic polypropylene in a vacuum or in air [95].

Condition	G(H <sub>2</sub> )	G(CH <sub>4</sub> )	G(CO)	G(CO <sub>2</sub> )
Vacuum	2.9	0.09	–	–
Air	2.5	0.17	1.2	2.1

**TABLE 52.8.** G-factors for crosslinking and scission for polypropylenes.

Polymer	G(X)	G(S)	G(S)/G(X)
Atactic PP [96]	0.27	0.22	0.8
Isotactic PP [96]	0.16	0.24	1.5

**TABLE 52.9.** Molecular weights and high temperature viscosity of vacuum irradiated PTFE [104].

Dose (kGy)	M <sub>n</sub> (× 10 <sup>6</sup> )	Viscosity at 380 °C (poise)
0	>10	3.2 × 10 <sup>11</sup>
150	2.5	2.8 × 10 <sup>9</sup>
750	2.1	1.4 × 10 <sup>8</sup>
750*	0.9	8.0 × 10 <sup>6</sup>

\*Air sintered material, other materials were vacuum sintered.

An interesting, and somewhat surprising effect of high energy irradiation on PTFE is an increase in the level of crystallinity at relatively modest doses (<1 MGy) [106–108]. The changes in crystallinity with increasing dose are shown in Table 52.11 [107]. By studying the change in specific volume for PTFE it has been shown that when the irradiation dose is increased beyond 1 MGy, the trend is reversed and the crystallinity level starts to decrease; that is, the specific volume will start to increase [108].

The explanation for the increase in crystallinity at relatively low irradiation doses is chain scission when irradiated in the presence of oxygen. Scission will relieve stresses or entanglements within the polymer, leading to a lower molecular weight, more mobility, and further crystallization. It is well established that for PTFE the lower the molecular weight, the higher the density and correspondingly, the higher the crystallinity.

Recently, irradiation of PTFE in vacuo has shown evidence of crosslinking when the temperature during irradiation is above 200 °C. There is a significant increase in the tensile strength and elongation, measured at 200 °C, for PTFE that had been irradiated (2 kGy) above the melting point of 327 °C (330–340 °C), in vacuo [109,110]. Radical I may well be the source of crosslinking for in vacuo irradiation at high temperature.

The electron beam irradiation of a series of perfluoro copolymers of PTFE shows that the copolymers with hexafluoropropylene (HFP), octafluorobutylene, and perfluoroheptene-1 undergo crosslinking when irradiated at a temperature of between 200 – 250 °C [111]. On the other hand, irradiation of poly(hexafluoropropylene) and a copolymer of HFP and perfluoroheptene-1 underwent scission. The crosslinking of FEP at above the  $T_g$  has been mentioned earlier [49,50]. All these evaluations involved the determination of a change in the melt viscosity. For a series of FEP polymers with levels of HFP, from 4.7% to 29.8%, the higher the level of HFP the larger the increase in melt viscosity after irradiation at 250 °C in nitrogen [111].

The yields of volatile gases evolved after the irradiation of PTFE and FEP in vacuo and air [112] are given in Table 52.12. The results show relatively low yields in vacuo, but in oxygen the gas yield is high and almost entirely comprises carbonyl fluoride (COF<sub>2</sub>).

Irradiation of the copolymers of PTFE at ambient temperature will generally lead to degradation of the polymer. Both FEP and poly(tetrafluoroethylene-co-perfluoropropylvinylether) PFA undergo predominantly chain scission which is also accompanied with a reduction of the mechanical properties [113]. However, with PFA, when the percentage of the comonomer is at a relatively high level, ca. 30% of perfluoro (methyl vinyl ether), there is some evidence of crosslinking [102]. The crosslinking may be due to the more “rubbery” nature of this copolymer at ambient temperature.

Poly(perfluoroethers) is another class of polymers that undergoes chain scission when subjected to high energy irradiation [114,115]. There appears to be no evidence for any crosslinking. The main products of degradation are the gaseous products COF<sub>2</sub> and CF<sub>4</sub>; the G Factors for these gases are given in Table 52.13 [116,117].

### 52.3.6 ETFE and ECTFE Copolymers

These polymers are fluorocopolymers that have alternating units of ethylene and, respectively, TFE or CTFE. They are sometimes additionally modified with a third perfluoro monomer.

An increase in the high temperature (200 °C) tensile properties of the ethylene-tetrafluoroethylene copolymer, ETFE, after irradiation in nitrogen at room temperature followed by heat treatment at 162 °C in nitrogen for 20 min indicates some crosslinking [118]. On the other hand, irradiation carried out in air showed very little crosslinking [119]. ETFE behaves in some ways similar to polyvinylidene fluoride (PVDF) in that there is competition between crosslinking and scission. Some of the tensile properties, measured at 200 °C, of irradiated ETFE are shown in Table 52.14 [119].

ECTFE, the copolymer of ethylene and chlorotrifluoroethylene, has been shown to undergo some crosslinking

**TABLE 52.10.** Tensile strength and elongation properties for  $\gamma$ -irradiated PTFE film [105].

Condition	Dose (kGy)	Tensile strength (kg cm <sup>-2</sup> )	Elongation at break (%)	Sample thickness (mm)
Untreated	0	175	104	0.1
Irradiated in vacuo*	10	154	98	0.1
Irradiated in air	10	110	15	0.1
Untreated	0	269	129	0.04
Irradiated in vacuo*	104	136	10	0.04
Irradiated in air	104	0	0	0.04

\*Tensile properties were measured in air.

**TABLE 52.11.** Effect of dose on crystallinity levels of PTFE after  $\gamma$ -irradiation [106].

Irradiation dose (KGy)	Density (g/cc)	Crystallinity (%)
0	2.17	59
250	2.23	79
500	2.24	83
750	2.24	83
1,000	2.24	83

**TABLE 52.12.** Yields of volatile gases from the  $\gamma$ -irradiation of PTFE and FEP in vacuo and oxygen [112].

	G(CO)	G(CF <sub>4</sub> )	G(CO <sub>2</sub> )	G(total gas)
PTFE (Vacuo)	0.03	0.006	0.08	0.43
FEP (Vacuo)	0.02	0.03	0.10	0.18
PTFE (Oxygen)	–	n. d.**	–	3.5*
FEP (Oxygen)	–	–	–	6.2*

\*The main component of the total gas was almost entirely COF<sub>2</sub>.

\*\*Not detected within the limits of experimentation.

**TABLE 52.13.** Yields for gas evolution for the electron beam irradiation of a series of poly(perfluoroethers).

Polymer	G(COF <sub>2</sub> )	G(CF <sub>4</sub> )	G(CF <sub>3</sub> CFO)
-(CF <sub>2</sub> -O) <sub>x</sub> -(CF <sub>2</sub> CF <sub>2</sub> -O) <sub>y</sub>	7.7	0.35	–
HO-CH <sub>2</sub> CF <sub>2</sub> -O-(CF <sub>2</sub> -O) <sub>x</sub> -(CF <sub>2</sub> CF <sub>2</sub> -O) <sub>y</sub> -CF <sub>2</sub> CH <sub>2</sub> -OH	6.2	–	–
-(CF <sub>2</sub> -O) <sub>x</sub> -(CF(CF <sub>3</sub> )CF <sub>2</sub> -O) <sub>y</sub>	1.7	1.1	0.3
-(CF <sub>2</sub> CF <sub>2</sub> CF <sub>2</sub> -O) <sub>x</sub>	1.2	0.22	–
-(CF(CF <sub>3</sub> )CF <sub>2</sub> -O) <sub>x</sub>	1.0	0.7	0.1

**TABLE 52.14.** Tensile properties measured at 200 °C, of irradiated ETFE.

Dose (kGy)	Temperature of irradiation (°C)	Tensile yield strength (psi)	Tensile strength (psi)	Ultimate elongation (%)
0	–	347	347	12
7	r. t.*	541	840	545
7	150–198	541	813	421
10	220–245	471	701	340

\*Irradiation followed by heat treatment at about 160 °C for 20 min.

after irradiation with  $\gamma$ -rays [120], although there is competition between crosslinking and scission. Table 52.15 gives some data for high temperature (200 °C) tensile properties. The increase in both tensile strength and elongation is indicative of crosslinking, although at the higher doses the elongation starts to fall. The room temperature properties, Table 52.16, show a maintenance of tensile strength even up to 700 kGy, but they are accompanied by a steady decrease in elongation.

### 52.3.7 Vinylidene Fluoride Polymers

For the major polymer in this series, polyvinylidene fluoride (PVDF), the effects of high energy irradiation have been studied [99,119]. PVDF is a polymer that undergoes both crosslinking and scission with relatively high yields for both processes [121–124].

The radicals formed from electron and proton irradiation (50–5000 kGy) have been characterized by electron paramagnetic resonance (EPR). The radicals decay when exposed to normal light; however, when kept in the dark, no

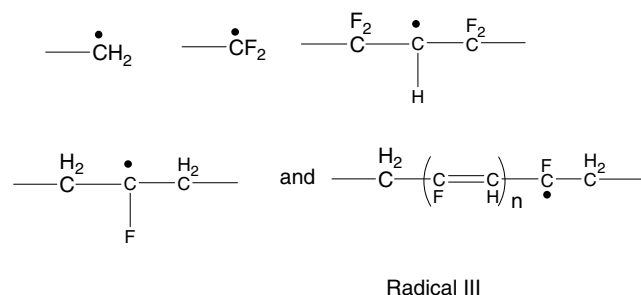
**TABLE 52.15.** Mechanical properties measured at 200 °C of an ECTFE polymer after  $\gamma$ -irradiation.

Dose (kGy)	Tensile strength (kg/cm <sup>2</sup> )	Elongation (%)
0	13	37
40	33	679
70	44	660
100	43	377
700	85	132

**TABLE 52.16.** Mechanical properties measured at room temperature of an ECTFE polymer after  $\gamma$ -irradiation.

Dose (kGy)	Tensile strength (kg/cm <sup>-2</sup> )	Elongation (%)
0	486	309
40	453	298
70	430	268
100	452	224
700	479	72

decay was observed after 180 days [125]. The radical types identified are:



Previous work had identified the five peaks in the spectra [126–128]. Radical III is a singlet and is long lived.

The thermal stability of the polymer after irradiation varies inversely with the radiation dose [129]. The yields for crosslinking and scission for several PVDF grades and its copolymers are given in Table 52.17. No substantial differences have been found for the radiation induced crosslinking of the  $\alpha$ -,  $\beta$ -, and  $\gamma$ -crystalline forms of PVDF [130].

At relatively low doses, < 300 kGy, there is virtually no change in the room temperature tensile properties of PVDF when irradiated with an electron beam. For higher doses, > 300 kGy, there is an increase in the Young's modulus and a decrease in both tensile strength and elongation at break [124]. A recent study of the dependence of irradiation dose on the physical, chemical, and thermal properties of PVDF has been carried out [133].

The crystallinity of PVDF films has been shown to increase after irradiation with an electron beam followed by: (1) aging at ambient temperature for various periods and (2) uniaxial orientation [134]. The other observation from this work shows that in addition to the increase in crystallinity upon orientation there was a change in the crystalline form with a shift from the  $\alpha$  form to the  $\beta$  form. The ratio of  $\alpha$  to  $\beta$  after an irradiation dose of 200 kGy followed by aging and orientation was 32:68, and the degree of crystallinity increased from 0.40 to 0.66. The explanation for increasing crystallinity may be similar to that for PTFE, but may also be due to the effect of orientation.

A study of the irradiation of PVDF in vacuo has demonstrated the increase in crystallinity at low doses. However, the crystalline melting point decreased rapidly at approximately 3 °C/100 kGy between 100 and 300 kGy dose [135].

PVDF is known to exhibit a strong piezoelectric effect [136] with the Phase I ( $\beta$  form) being the most effective crystalline form for piezoelectric activity. Since molecular relaxation modes also contribute to overall piezoelectricity, high energy irradiation will affect the piezoelectric activity. This is due mainly to the effect of crosslinking which will increase the mechanical strength and change the molecular mobility of the polymer chains. A restriction in chain mobility will reduce reorientation of the molecular electric

**TABLE 52.17.** Yields of crosslinking and scission for PVDF and copolymers after irradiation.

Polymer	G(X)	G(S)	G(S)/G(X)	Remarks
PVDF [121]	1.0	0.3	0.30	
PVDF [122]	0.78	0.37	0.47	Solef 1010 Homopolymer
PVDF [131]	0.78	0.8	1.03	KF 1,000 irradiation at 61 °C
PVDF [128]	0.75	0.77	1.03	KF 1100 irradiation at 61 °C
PVDF [128]	0.90	0.85	0.94	Kynar 200 irradiation at 61 °C
PVDF [128]	0.70	0.57	0.81	Kynar 450 irradiation at 61 °C
VDF + HFP [121]	1.7	1.3	0.76	Fluoroelastomer Viton A
VDF + CTFE [121]	0.9	1.4	1.56	Fluoroelastomer Kel-F 3,700
PVDF [113]	0.60	0.29	0.48	Copolymer 3.5% tetrafluoroethylene
PVDF-HFP [122]	1.5	0.58	0.39	Solef 11010 Copolymer 6% (HFP)
PVDF-HFP [121,132]	3.4	1.3	0.4	

moments at the interphase. High energy irradiation of mainly  $\beta$  form PVDF leads to a lowering of the piezoelectric constant [137] and leads to improvement in the thermal stability of the  $\beta$  form and a slower piezoelectric decay [138].

An interesting comparison of the effect of electron beam irradiation on PVDF and ETFE, which differ only in chemical structure and have the same chemical composition, has shown that the irradiation has a more detrimental effect on tensile strength for ETFE than PVDF [139]. In fact, PVDF shows an increase in tensile strength compared to ETFE which shows a decrease. In both cases, the elongation at break dropped with increasing dose, indicating crosslinking.

The copolymers of PVDF with trifluoroethylene and tetrafluoroethylene generally crystallize into the  $\beta$  form [140]. Irradiation with either electron beam or  $\gamma$ -radiation has been shown to induce solid-state ferroelectric to paraelectric transition in these copolymers as well as a decrease in their Curie temperature [141].

### 52.3.8 Other Fluoropolymers

Poly(vinylfluoride) (PVF) undergoes predominantly crosslinking when exposed to high energy irradiation [142] with a  $G(X)$  of 3.4 to 5.7  $G(S)$  of 0.95 to 1.6 and  $G(S)/G(X)$  of 0.28. The tensile strength of PVF almost doubles upon gamma irradiation of 10 kGy indicating the predominance of crosslinking [113].

Poly(trifluoroethylene) undergoes both crosslinking and chain scission with the former dominating. The  $G(X)$  and  $G(S)$  values are 1.1 and 0.4, respectively [121].

Poly(chlorotrifluoroethylene) (PCTFE) only degrades on exposure to high energy radiation. The  $G(S)$  value is 0.67 from number average molecular weight determination [132]. The tensile properties degrade with relatively low doses of irradiation [143,144], Table 52.18, but slightly less rapid than PTFE. Irradiation in air will eventually give a yellow powder, as the critical dose for electrical breakdown is approached [145].

### 52.3.9 Polyvinylchloride

Polyvinylchloride (PVC) is one of the most reactive plastics when irradiated with either an electron beam or  $\gamma$ -rays. The major process is degradation via the loss of hydrogen

**TABLE 52.18.** Mechanical properties of irradiated PCTFE [144].

Dose (kGy)	Tensile strength(psi)	Shear strength (psi)	Elongation (%)
0	2,550	3,410	264
10	2,400	3,650	230
100	1,670	1,850	73
1,000	Failed	Failed	Failed

chloride gas (dehydrochlorination). The dehydrochlorination is accompanied by a severe color change to a dark brown material [146], the color is due to the production of highly conjugated double bonds [147]. The degradation process is more pronounced in the presence of air and occurs after the irradiation has stopped (postirradiation effect) [43]. The dehydrochlorination process is dependent on temperature and increases with increasing temperature, as does the postirradiation effect [148]. At 90°C, that is, above  $T_g$ , gelation is observed at relatively low doses (120 kGy). For irradiation under nitrogen and at 150°C gelation occurs at < 50 kGy [43], although at temperatures above  $T_g$  thermal dehydrochlorination will also be a major factor. Some yields for gas evolution under a variety of conditions are given in Table 52.19.

The physical properties of PVC film show an increase in elongation at low dose (>0.1 MGy) and then a dramatic fall off in elongation at 0.3 MGy. Above doses of 0.3 MGy the material becomes brittle and has no elasticity.

When PVC is irradiated at very high doses (20 MGy), a material is formed that appears to have a structure that is mainly composed of carbon and in some cases is crystalline in nature [150,151].

### 52.3.10 Polyacrylates and Polymethacrylates

These are an interesting group of materials since they are clear examples of how the structure of the polymer can dramatically affect the changes that occur with either  $\gamma$  or electron beam irradiation. The poly(alkyl acrylates) undergo radiation crosslinking, whereas the poly(alkyl methacrylates) degrade so rapidly that they are used as positive-working electron beam resists [152]. Tables 52.20 and 52.21 give the yields for crosslinking and scission

**TABLE 52.19.**  $G$ -Factors for degradation of PVC under vacuum and in the presence of oxygen.

Condition	$G(HCl)$	$G(H_2)$	$G(CH_4)$	$G(CO_2)$	$G(CO)$	Dose (kGy)
Vacuum [149]	2.38	0.19	0.0013	0.007	0.001	300
Oxygen [110]	3.02	0.2	0.0063	0.115	0.1	300
-145 to -90°C [19]	5.6	-	-	-	-	-
30°C [19]	13	-	-	-	-	-
70°C [19]	23	-	-	-	-	-

**TABLE 52.20.** The yields for crosslinking  $G(X)$ , scission  $G(S)$  and the ratio  $G(S)/G(X)$  for a series of poly(alkyl acrylates).

Polymer	$G(X)$	$G(S)$	$G(S)/G(X)$
Poly (methyl acrylate) [37]	0.5	–	0.07
Poly (ethyl acrylate) [153]	0.07	0.07	0.23
Poly ( <i>n</i> -butyl acrylate)	0.21 [153]	–	0.07 [37], 0.14 [153]
Poly (iso-butyl acrylate) [37]	–	–	0.07
Poly (sec-butyl acrylate) [37]	–	–	0.10
Poly (tert-butyl acrylate) [37]	–	–	0.3–0.35

**TABLE 52.21.** The yields for crosslinking  $G(X)$ , scission  $G(S)$  and the ratio  $G(S)/G(X)$  for a series of poly(methacrylates).

Polymer	$G(X)$	$G(S)$	$G(S)/G(X)$
Poly methyl methacrylate	–	1.63 (vacuo)	–
Poly methyl methacrylate	–	0.77 (air) [154]	–
Poly phenyl methacrylate	–	0.44 [155]	–
Poly benzyl methacrylate	–	0.14 [155]	–
Poly (1-naphthyl methacrylate)	–	0.14 [155]	–
Poly (2-naphthyl methacrylate)	–	0.19 [155]	–
Poly (Si methyl methacrylate) [156]	0.11	0.25	2.3
Poly (Si ethyl methacrylate) [156]	0.14	0.21	1.5
Poly (Si propyl methacrylate) [156]	0.54	0.58	1.07
Poly (Si Butyl methacrylate) [156]	0.99	0.77	0.78

for a series of poly(acrylates) and poly(methacrylates), respectively.

Modification of the alkyl methacrylate with a silicone group can cause a shift to a polymer that is more prone to crosslinking poly(Si butyl methacrylate) [156].

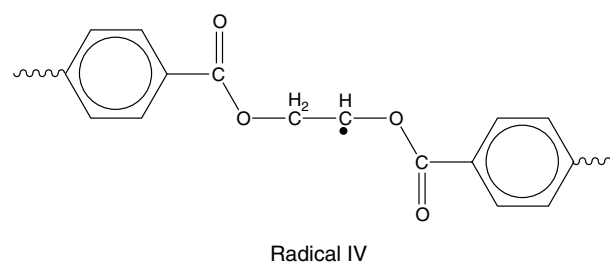
### 52.3.11 Polyesters

The dominant effect of high energy irradiation on a polyester is chain scission, although both crosslinking and scission occur. With the aromatic polyesters such as polyethylene terephthalate (PET) and polybutylene terephthalate (PBT) the aromatic groups will act as protection, and the yields of any process will have a tendency to be low.

Upon irradiation with an electron beam the aliphatic polyester, poly(butylene adipate)diol (PBAD) undergoes predominantly scission at low doses (< 50 kGy) along with an increase in the level of crystallinity, whereas above 100 kGy both crosslinking and scission occur and the level of crystallinity decreases [157].

Although PET is regarded as relatively radiation resistant polymer, irradiation at relatively high dose (>1 MGy) with an electron beam in vacuo yields both crosslinking and scission with crosslinking predominating [158]. The initially semicrystalline material also becomes completely amorphous after high doses. Poly-1,6-hexamethylene terephthalate (PHT) behaves in a similar manner to PET but has higher yield of crosslinking. There is some evidence that

both polymers undergo some crosslinking in the crystalline region as well as the amorphous region [159]. The radical produced from PET is shown as radical IV; there is evidence for the radical in both the amorphous and crystalline states. Two different decay rates are observed, the fast decay being attributed to the amorphous region and the slower decay to the crystalline region [160].



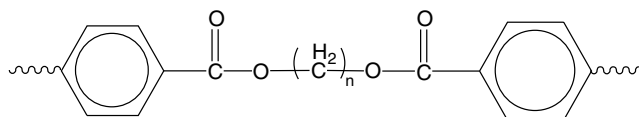
Irradiation of PET, in vacuo, is dose rate dependent [161] with  $\gamma$ -irradiation resulting in more degradation, leading to the production of acid groups,  $-\text{COOH}$  and evolution of the gases  $\text{CO}_2$ ,  $\text{CO}$ ,  $\text{H}_2$  and  $\text{CH}_4$  [162]. The yields of these products are shown in Table 52.22.

There appears to be some relationship between the number of methylene ( $-\text{CH}_2-$ ) groups in poly(alkylene terephthalates), structure III, and irradiation, with even number of methylenes having a different effect in magnitude to the odd number of methylenes [164,165].



**TABLE 52.22.** Yields for the products of electron beam and  $\gamma$ -irradiation of PET in vacuo [163].

	$G(\text{H}_2)$	$G(\text{CO})$	$G(\text{CO}_2)$	$G(\text{X})$	$G(\text{S})$	$G(\text{CH}_4)$
$\gamma$ -rays	0.016	0.11	0.17	—	>0.8	0.003
E. beam	0.016	—	0.08	0.08	0.16	—



Structure III

### 52.3.12 Polyamides

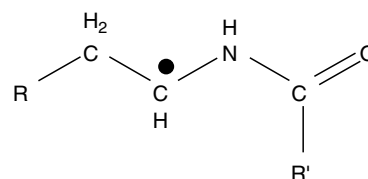
Polyamides are classed in the family of crosslinking polymers when irradiated with either electron beam or  $\gamma$ -rays. Both crosslinking and scission occur, the yields for both processes  $G(\text{X})$  and  $G(\text{S})$  have been shown to be independent of the irradiation dose [166] but have been shown to be dependent on the number of hydrogen atoms or methylene groups in the amine residue [167]. Table 52.23 gives the yields of crosslinking and scission for a series of dry polyamides.

The yield of crosslinking correlates well with the number of methylene groups ( $-\text{CH}_2-$ ) present in the polyamide structure. Absorbed water in the polyamide enhances crosslinking at higher concentration, and inhibits the process at low concentration. The presence of water does not appear to significantly affect the scission process.

Polyamides show a color change upon irradiation with either electron beam or  $\gamma$ -rays; the change is a consequence of radical formation. The radical is generally formed on the  $\alpha$ -carbon, adjacent to the amide nitrogen [168], (radical V). Blocking of the hydrogen atom on the  $\alpha$ -carbon with, for example, phenyl groups (Nylon MPD10) leads to a large reduction in the yields of both crosslinking and scission.

**TABLE 52.23.** Yields of crosslinking and scission for a series of polyamides [131].

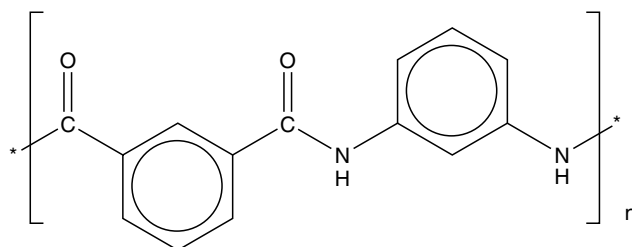
Polyamide	$G(\text{X})$	$G(\text{S})$
Nylon 6	0.67	0.68
Nylon 6,6	0.50	0.70
Nylon 6,10	0.62	0.76
Nylon 11	0.92	0.85
Nylon 12	0.92	0.85
Nylon 10,10	1.12	1.10
Nylon 12,10	1.14	1.10
Nylon MPD10	0.07	0.07



Radical V

As with many other polymers, the effects of irradiation on the physical properties of polyamides are highly dependent on the atmosphere during irradiation. For example, irradiation of a high tenacity Nylon 6,6 with an electron beam in an atmosphere free of oxygen showed only a 4% loss of tensile strength after 200 kGy and 35% loss after 2,000 kGy; the elongation to break showed little change. However, under similar irradiation conditions in air, after 2,000 kGy the tensile strength retention was 19% and the elongation to break was about a third of the original value [169].

Aromatic polyamides are much more resistant to irradiation than aliphatic polyamides, much of the effect is due to the protective effect of the aromatic groups. The highly aromatic polyamide, Nomex<sup>®</sup>, can retain about 80% of its tensile strength after a 6,000 kGy dose in air [170].



NOMEX

### 52.3.13 Polystyrene

Polystyrene is relatively resistant to the effects of high energy irradiation due to the “protective” effect of the aromatic groups. It does undergo crosslinking as the dominant process [171,172] with yields for crosslinking  $G(\text{X})$  being in the range, 0.019 to 0.051, depending on the method of determination. The effect of the irradiation temperature has already been discussed [44] in section 52.2.7.

The main volatile material evolved during the irradiation of polystyrene is hydrogen, the yield for hydrogen  $G(\text{H}_2)$  is in the range, 0.022–0.026 with  $\gamma$ -irradiation [38,173,174]. Small amounts of benzene and methane have also been detected after irradiation with  $G(\text{C}_6\text{H}_6)$  and  $G(\text{CH}_4)$  being 0.008 and  $10^{-5}$ , respectively [38].

The closely related polymer poly( $\alpha$ -methylstyrene) undergoes scission when irradiated with high energy [175] illustrating the importance of polymer structure. Polystyrene has structure I whereas poly( $\alpha$ -methylstyrene) has structure II and readily degrades [173]. Table 52.24 gives some crosslinking and scission yields for a variety of polystyrenes. The *p*-bromostyrene undergoes a high level of crosslinking, whereas the *p*-cyano and *p*-nitro show relatively high stability after irradiation [44].

The physical properties of polystyrene remain relatively stable even after high doses of irradiation. The hardness, tensile strength, and shear strength are all within 75% of the original values up to doses of  $10^2$  MGy [177]. The glass transition temperature is reported to increase by about  $10^\circ\text{C}$  and the crystalline melting point increases to  $150^\circ\text{C}$  after the irradiation of crystalline isotactic polystyrene to 40 MGy [178].

#### 52.3.14 Polysiloxanes

Polysiloxanes readily undergo crosslinking when irradiated with high energy irradiation. Table 52.25 gives some *G* values for crosslinking for a series of polysiloxanes, poly(dimethyl siloxane) (PDMS), poly(phenylmethylsiloxane) (PPMS), and poly(diphenylsiloxane) (PDPS) and copolymers of dimethylsiloxane with phenylmethylsiloxane and diphenylsiloxane. As the percentage of aromaticity increases, the protective effect of the aromatic group leads to more radiation resistant polysiloxanes.

The gases evolved upon irradiation of PDMS comprise hydrogen, methane, and ethane. The total yield of gases is relatively high; *G*(Total gas) is 3.0 for PDMS [179].

There is a positive temperature effect, in that increasing temperature leads to increasing yield for crosslinking. For example, irradiation of a 1,000 centistokes dimethylsiloxane fluid gave *G*(X) values of 2.6, 2.8, 3.1, and 4.7 at  $-78^\circ\text{C}$ ,  $0^\circ\text{C}$ ,  $20^\circ\text{C}$ , and  $150^\circ\text{C}$ , respectively [182].

The curing of silicone elastomers by irradiation leads to the typical properties of a cured elastomer, that is, an increase in hardness and tensile strength. Interestingly, the curing of PDMS using a peroxide cure system is very inefficient [183].

#### 52.3.15 Highly Aromatic Polymers

All of the highly aromatic polymers are resistant, relative to the nonaromatic polymers, to irradiation with either electron beam or  $\gamma$ -rays. When irradiated in a vacuum many of these polymers are very stable and can show no change in physical properties even after high beam doses. For example, Kapton<sup>TM</sup> and Vespel<sup>TM</sup> aromatic polyimides have been shown to have resistance to both  $\gamma$ -rays and electron beams up to doses of 100 MGy of irradiation [184]. In the presence of oxygen, the physical properties of the aromatic polymers can be dramatically changed. For example, an aromatic polysulfone showed no change in the flexural strength after irradiation with  $\gamma$ -rays to 6 MGy, in vacuo. On the other hand, when the irradiation is carried out in the

**TABLE 52.24.** Crosslinking and scission yields for a series of polystyrenes.

Polymer	<i>G</i> (X)	<i>G</i> (S)
Polystyrene [176]	0.019 – 0.051	0.0094 – 0.019
Poly ( $\alpha$ -methylstyrene) [174]	–	0.25
Poly ( <i>p</i> -Methylstyrene) [44]	0.061	–
Poly ( <i>p</i> -Methoxystyrene) [44]	0.074	–
Poly ( <i>p</i> -Bromostyrene) [44]	3.1	–
Poly ( <i>p</i> -Chlorostyrene) [44]	0.30	–
Poly ( <i>p</i> -Cyanostyrene) [44]	No change in viscosity (200 kGy)	–
Poly ( <i>p</i> -Nitrostyrene) [44]	No change in viscosity (1500 kGy)	–

**TABLE 52.25.** Yields of crosslinking for a series of polysiloxanes.

Polysiloxane	% Phenyl Groups	<i>G</i> (X)
PDMS	0	2.3 [180]
PPMS	50	0.25 [180,181]
PDPS	100	0.07 [180], 0.13 [181]
Dimethyl-/phenyl siloxane copolymer [180]	4.4	2.05
Dimethyl-/phenyl siloxane copolymer [180]	8.7	1.73
Dimethyl-/phenyl siloxane copolymer [180]	21.5	1.09
Dimethyl-/phenyl siloxane copolymer [180]	36	0.53
Dimethyl-/diphenyl siloxane copolymer [180]	17	1.44
Dimethyl-/diphenyl siloxane copolymer [181]	42	0.87

presence of air, the flexural strength dropped to about half its initial value at relatively low doses of between 0.2 and 4 MGy [185].

The radiation resistance for a series of polyimides(PI), poly(aryl ether ether ketone) (PEEK), poly(aryl ether sulphone) (PES), bisphenol A type Udel™ poly(aryl sulphone) (U-PS), and a poly(aryl ester) (U-Polymer) is shown to be excellent when compared to the related aliphatic polymers.  $G$  values for the evolution of gases were lower by factors of between 0.01 and 0.001 of the  $G$  values for the corresponding aliphatic polymers. From the study of gas evolution, the order of radiation resistance to  $\gamma$ -irradiation is [186]:

Upilex™-R(PI) > Kapton™ (PI) > PEEK > PES > Upilex™-S(PI) {  $\gg$  } U-PS > U-Polymer

The order of resistance for electron beam irradiation is slightly different [187]:

Upilex™-R(PI) = Upilex™-S(PI) > Kapton™ (PI) > PEEK > PES {  $\gg$  } U-PS > U-Polymer

The polyimides and PEEK show high radiation resistance to attenuation of physical properties.

The major component gases are: H<sub>2</sub> and N<sub>2</sub> for polyimides; CO<sub>2</sub> and CO for PEEK; CO<sub>2</sub>, CO, and SO<sub>2</sub> for polysulphones; and CO<sub>2</sub> and CO for U-Polymer. The yields for gaseous evolution are very low and are given in Table 52.26 for electron beam and Table 52.27 for  $\gamma$ -irradiation.

An increase in the glass transition temperature  $T_g$  occurs when PEEK, either in the crystalline form PEEK-c or the amorphous form PEEK-a, is irradiated with  $\gamma$ -irradiation. This is indicative that a crosslinking process is occurring [188].

The irradiation of both amorphous and semicrystalline poly(phenylene sulfide) (PPS) with an electron beam in the presence of nitrogen shows no noticeable change in the

mechanical or thermal properties at least to 10<sup>4</sup> kGy [189]. On the other hand, irradiation in air instead of nitrogen showed a change in both mechanical and thermal properties. At very high doses, 4 × 10<sup>4</sup> kGy, the amorphous PPS loses about 62% of its original tensile strength while the semi-crystalline PPS loses about 57%. The  $T_m$  also changes, decreasing by about 10–271°C.

### 52.3.16 Other Polymers

Table 52.28 gives the  $G(X)$  and the  $G(S)$  values for a list of different polymers which will not be discussed in detail. The polyoxymethylene, cellulose, and polyisobutylene are all readily degraded upon irradiation.

The irradiation of some composite materials such as epoxy/graphite, polyimide/graphite, and polysulfone/graphite fibers have shown that the effects for irradiation up to 5 × 10<sup>4</sup> kGy for electron radiation and up to 3,500 kGy for  $\gamma$ -radiation are negligible provided the irradiation is carried out in the absence of oxygen [196,197].

Polycarbonates, although they tend to strongly discolor for unstabilized grades, are relatively resistant to irradiation showing retention of elongation at yield and tensile modulus after irradiation up to 1,000 kGy [198].

### Polymer Blends

The effect of electron beam irradiation on the miscible poly(styrene) and poly(vinyl methyl ether) (PVME) blend has been studied. The poly(styrene), being much more resistant to effects of irradiation, does not offer any protection to the poly(vinyl methyl ether). Gel content studies indicated significant crosslinking [199]. Further studies of this

**TABLE 52.26.** Yields for gas evolution  $G(\text{Gas})(10^{-4})$  for electron beam irradiation.

Polymer	$G(\text{H}_2)$	$G(\text{N}_2)$	$G(\text{CO})$	$G(\text{CO}_2)$	$G(\text{CH}_4)$	Dose (MGy)
Kapton™	4.8	0.15	3.5	11	0.89	6.0
PEEK-c	7.5	–	3.4	11.3	0.16	5.8
PEEK-a	12	–	5.2	16	0.22	6.0
Upilex™-R	1.3	0.10	2.1	3.4	0.07	5.0
Upilex™-S	2.3	2.9	1.9	8.2	0.27	5.0

**TABLE 52.27.** Yields for gas evolution  $G(\text{Gas})(10^{-4})$  for  $\gamma$ - irradiation under vacuum.

Polymer	$G(\text{H}_2)$	$G(\text{N}_2)$	$G(\text{CO})$	$G(\text{CO}_2)$	$G(\text{CH}_4)$	Dose (MGy)
Kapton™	2.1	3.6	3.9	7.4	0.89	7.4
PEEK-c	6.3	–	12	5.5	0.14	8.1
PEEK-a	12	–	6.5	12	0.20	7.4
Upilex™-R	0.38	9.8	2.5	5.2	0.08	5.7
Upilex™-S	8.4	13	1.8	15	0.30	8.1

**TABLE 52.28.** Yields of crosslinking  $G(X)$  and scission  $G(S)$  for polymeric materials.

Polymer	$G(X)$	$G(S)$	Reference
Polyoxymethylene	6.5	11.1	[190]
Polyisobutylene	–	5	[191]
Cellulose	–	11	[192]
Polyvinylacetate ( $O_2$ )	0.3	0.07	[26]
Polyvinylacetate ( $N_2$ )	0.15	0.06	[193]
Poly(vinyl ether)	5.8	–	[194]
Polypropylene oxide (atactic)	0.15	0.22	[195]
Polypropylene oxide (isotactic)	0.31	0.51	[195]

polymer blend with gamma irradiation and deuterated PS showed that a significant amount of grafting between the blend components occurred [200].

The gamma irradiation of a PS and PMMA blends showed that the polystyrene did not offer radiation protection for the PMMA. However, in the copolymer, poly(styrene-*co*-methylmethacrylate), a protective effect from the polystyrene was observed [201]. Some radiation (electron beam and gamma) crosslinking in PS/PMMA has also been reported [202]. A more recent study has shown the effect of gamma irradiation on the glass transition temperature ( $T_g$ ) of the miscible blend [203].

Gamma irradiation of the highly miscible poly(vinyl alcohol)/polyacrylamide blends up to 100 kGy has been shown to increase the thermal stability of the blend [204].

Recent irradiation studies with blends of PVC and modifiers such as flexible polymers (EVA [205] or ENR –epoxidized natural rubber [206]) or PFMs (polyfunctional monomers) have shown that the irradiation achieves more crosslinking and less degradation (chlorine loss) at lower doses. Seven PFMs, used at 10 parts per hundred rubber (phr), were compared for effectiveness for increasing softening temperature, gel yield and swelling ratio in PVC wire formulations [207].

EVA blends with PE (usually LDPE) have been studied and found to be more sensitive in achieving property improvements at lower doses [208,209]. In one case, a thermoplastic elastomer (TPE) with lower set was formed at < 50 kGy [210,211].

## 52.4 ADDITIVES

The above review of the effects of high energy irradiation on polymeric materials has covered the effects on the “pure” polymer, that is, the materials without the addition of additives except the ones added by the manufacturer, such as antioxidants.

With many of the materials discussed above, the effect of high energy irradiation can be dramatically changed by the addition of additives. For example, more efficient crosslink-

ing can be induced in irradiated polyvinyl chloride by the addition of polyfunctional materials [212]; atactic polypropylene crosslinking is enhanced when irradiated, in vacuo, in the presence of nitrous oxide [213]. Many of the materials can be readily crosslinked at relatively low irradiation doses using crosslinking promoters, “prorads” [214–216]. The use of prorads, as well as increasing the crosslinking efficiency can reduce the other effects of irradiation, such as oxidation or gas evolution, because of the low doses that are used. In some cases, the need to retard crosslinking may be required. For example, with a highly efficient crosslinking polymer such as natural rubber the addition of “antirads” can reduce the yield of crosslinking [217,218].

The addition of fillers to a polymer will increase the back scattering of the incident radiation if the filler has a higher electron density than the polymer. The deposition of energy will in this case increase and will lead to an increase in crosslinking or scission, depending on which is the more dominant process.

All the processes of irradiation lead to the production of radicals. In the presence of monomers these radicals can initiate grafting on to the polymer chain. This review will not cover this aspect but an excellent introductory review is available [219].

## 52.5 SUMMARY

The effect of high energy irradiation on the properties of polymeric materials is complex and is dependent on the polymer structure, molecular weight, polymeric state, and the crystallinity level. The rate of irradiation and atmosphere during irradiation are major factors. Crosslinking, degradation, and evolution of gases are the major processes. These processes will lead to property changes in the polymer.

## REFERENCES

1. A. Chapiro, “Radiation Chemistry of Polymeric Systems,” Interscience, New York, 1962.
2. A. Charlesby, “Atomic Radiation and Polymers,” Pergamon Press, London, 1960.
3. “The Radiation Chemistry of Macromolecules. Volume I,” edited by M. Dole, Academic Press, New York, 1972.
4. “The Radiation Chemistry of Macromolecules. Volume II,” edited by M. Dole, Academic Press, New York, 1973.
5. “Radiation Processing of Polymers,” edited by A. Singh and J. Silverman, Hanser, Munich, 1992.
6. “Irradiation of Polymeric Materials,” edited by E. Reichmanis, C. W. Frank and J. H. O’Donnell, American Chemical Society, 1993.
7. W. L. McLaughlin, Conference on National and International Standardization of Radiation Dosimetry Part I, p. 89, (1978).
8. R. A. Harrod, *Radiat. Phys. Chem.* **9**, 91, (1977).
9. A. Brynjolfsson, “Sterilization By Ionizing Radiation,” p. 145, Multiscience, Montreal, 1974.
10. R. Eymery, “Sterilization by Ionizing Radiation,” p. 84, Multiscience, Montreal, 1974.
11. M. R. Cleland, “Radiation Processing of Polymers,” Chapter 3, edited by A. Singh and J. Silverman, 1992.
12. K. Tomita and S. Sugimoto, *Radiat. Phys. Chem.* **9**, 576, (1977).

13. A. Charlesby, "Atomic Radiation and Polymers," Chapter 6, p. 96, Pergamon Press, London, 1960.
14. P. W. Moore, "Irradiation of Polymeric Materials," Chapter 2, p. 9, edited by E. Reichmanis, C. W. Frank and J. H. O'Donnell, American Chemical Society, 1993.
15. B. J. Lyons and W. C. Johnson, "Irradiation of Polymeric Materials," Chapter 5, p. 62, edited by E. Reichmanis, C. W. Frank and J. H. O'Donnell, American Chemical Society, 1993.
16. M. Burton, *Discuss. Faraday Soc.* **12**, 317, (1952).
17. B. J. Lyons and A. S. Fox, *J. Polym. Sci.: Part C*, **21**, 159, (1968).
18. A. Charlesby, *Proc. R. Soc. London*, **A222**, 60, (1954).
19. A. Charlesby, *Proc. R. Soc. London*, **A222**, 542, (1954).
20. A. Charlesby, *Proc. R. Soc. London*, **A224**, 120, (1954).
21. O. Saito, *J. Phys. Soc. Jpn.* **13**, 198, (1958).
22. O. Saito, *J. Phys. Soc. Jpn.* **13**, 1451, (1958).
23. O. Saito, *J. Phys. Soc. Jpn.* **13**, 1465, (1958).
24. O. Saito, *J. Phys. Soc. Jpn.* **13**, 798, (1959).
25. O. Saito, "The Radiation Chemistry of Macromolecules. Volume I," Chapter 11, p.223, edited by M. Dole, Academic Press, New York, 1972.
26. A. Charlesby and S. H. Pinner, *Proc. R. Soc.* **A249**, 367, (1959).
27. M. Inokuti, *J. Chem. Phys.* **18**, 2999, (1963).
28. B. J. Lyons, *J. Polym. Sci.: Part A*, **3**, 777, (1965).
29. A. Charlesby, "Atomic Radiation and Polymers," Chapter 9, p. 147, Pergamon Press, London, 1960.
30. D. I. C. Kells and J. E. Guillet, *J. Polym. Sci.: Part A-2*, **7**, 1895, (1969).
31. J. H. O'Donnell, N. P. Rahman, C. A. Smith and D. J. Winzor, *Macromolecules*, **12**, 113, (1979).
32. J. H. O'Donnell, N. P. Rahman, C. A. Smith and D. J. Winzor, *J. Polym. Sci.: Polym. Phys. Ed.* **16**, 1515, (1978).
33. B. J. Lyons, *Radiat. Phys. Chem.* **22**, 135, (1983).
34. O. Saito, H. Y. Kang and M. Dole, *J. Chem. Phys.* **46**, 3607, (1967).
35. A. Charlesby, in "Irradiation Effects on Polymers", p. 39, editors D. W. Clegg and A. A. Collyer, Elsevier Applied Science, Amsterdam, 1991.
36. A. Charlesby, "Atomic Radiation and Polymers," Chapter 9, p.142, Pergamon Press, London, 1960.
37. A. R. Shultz and F. A. Bovey, *J. Polym. Sci.* **22**, 485, (1956).
38. L. A. Wall and D. W. Brown, *J. Phys. Chem.* **61**, 129, (1957).
39. D. T. Turner, *J. Polym. Sci.* **35**, 541, (1959).
40. H. Kaufmann and H. Heusinger, *Makromol. Chem.* **177**, 871, (1976).
41. H. Katzer and H. Heusinger, *Makromol. Chem.* **163**, 195, (1973).
42. A. Charlesby, *Plastics*, **18**, 142, (1953).
43. A. A. Miller, *J. Phys. Chem.* **63**, 1755, (1959).
44. W. Burlant, J. Neerman and V. Serment, *J. Polym. Sci.* **58**, 491, (1962).
45. L. A. Wall and R. E. Florin, *J. Appl. Polym. Sci.* **2**, 251, (1959).
46. R. M. Keyser, K. Tsuji and F. Williams, *Macromolecules*, **1**, 289, (1968).
47. R. M. Keyser and F. Williams, *J. Phys. Chem.* **73**, 1623, (1969).
48. R. M. Keyser, K. Tsuji and F. Williams, "The Radiation Chemistry of Macromolecules. Volume I," Chapter 9, p. 145, edited by M. Dole, Academic Press, New York, 1972.
49. G. H. Bowers and E. R. Lovejoy, *Ind. Eng. Chem. Prod. Res. Dev.* **1**, 89, (1962).
50. E. R. Lovejoy, M. I. Bro and G. H. Bowers, *J. Appl. Polym. Sci.* **9**, 401, (1965).
51. R. P. Kusy and D. T. Turner, *Macromolecules*, **4**, 337, (1971).
52. S. K. Bhateja, E. H. Andrews and R. J. Young, *J. Polym. Sci.: Polym. Phys. Ed.* **21**, 523, (1983).
53. G. G. A. Bohm and J. O. Tveekrem, *Rubber Chem. Technol.* **55**, 575, (1982).
54. K. Arakawa, T. Seguchi and K. Yoshida, *Radiat. Phys. Chem.* **27**, 157, (1986).
55. F. A. Makhliis, L. Y. Nikitin, A. K. Volkova and M. N. Tikhonova, *Vysokomol. Soedin. A13*, 596, (1971).
56. L. Mullins and D. T. Turner, *Nature*, **183**, 1547, (1959).
57. L. Mullins and D. T. Turner, *J. Polym. Sci.* **43**, 35, (1960).
58. A. Charlesby and E. von Arnim, *J. Polym. Sci.* **25**, 151, (1957).
59. V. T. Kozlov, A. G. Yevseyev and P. I. Zubov, *Vysokomol. Soed. A11*, 2230, (1969).
60. A. Von Raven and H. Heusinger, *J. Polym. Sci.: Polym. Chem. Ed.* **12**, 2255, (1974).
61. E. Witt, *J. Polym. Sci.* **41**, 507, (1959).
62. D. J. T. Hill, J. H. O'Donnell, M. C. S. Perera and P. J. Pomery, *ACS Symp. Ser.* **527**, "Irradiation of Polymeric Materials," Chapter 6, p. 74, edited by E. Reichmanis, C. W. Frank and J. H. O'Donnell, American Chemical Society, 1993.
63. G. Odian, D. Lamparella and J. Canamare, *J. Polym. Sci.: Part C*, **16**, 3619, (1968).
64. W. Geissler, H. Zott and H. Heusinger, *Makromol. Chem.* **179**, 697, (1978).
65. R. J. Elred, *Rubber Chem. Technol.* **47**, 924, (1974).
66. M. Aoshima, T. Jinno and T. Sassa, *Cell. Polym.* **10**, 359, (1991).
67. H. Kanbara, S. J. Huang and J. F. Johnson, *Polym. Eng. Sci.* **34**, 691, (1994).
68. G. L. Grune, V. T. Stannett, R. T. Chern and J. Harada, *Polym. Adv. Technol.* **4**, 341, (1993).
69. B. J. Lyons, *Nature*, **195**, 690, (1962).
70. L. Mandelkern, "The Radiation Chemistry of Macromolecules. Volume II," Chapter 13, p. 302, edited by M. Dole, Academic Press, New York, 1973.
71. Y. Sakai, K. Umetsu and K. Miyasaka, *Polymer*, **34**, 3362, (1993).
72. D. J. Dijkstra, W. Hoogsteen and A. J. Pennings, *Polymer*, **30**, 866, (1989).
73. S. K. Bhateja, *J. Appl. Polym. Sci.* **28**, 861, (1983).
74. M. Dole, D. C. Milner and T. F. Williams, *J. Am. Chem. Soc.* **80**, 1580, (1958).
75. B. J. Lyons and M. A. Crook, *Trans. F. Soc.* **59**, 2334, (1963).
76. M. Dole, "The Radiation Chemistry of Macromolecules. Volume II," Chapter 14, p. 339, edited by M. Dole, Academic Press, New York, 1973.
77. D. C. Waterman and M. Dole, *J. Phys. Chem.* **74**, 1906, (1970).
78. L. Mandelkern, "The Radiation Chemistry of Macromolecules. Volume II," Chapter 13, p. 322, edited by M. Dole, Academic Press, New York, 1973.
79. B. J. Lyons, *Radiat. Phys. Chem.* **28**, 149, (1986).
80. L. Mandelkern, "The Radiation Chemistry of Macromolecules. Volume II," Chapter 13, edited by M. Dole, Academic Press, New York, 1973.
81. M. Dole, "The Radiation Chemistry of Macromolecules. Volume II," Chapter 14, edited by M. Dole, Academic Press, New York, 1973.
82. B. J. Lyons and F. E. Weir, "The Radiation Chemistry of Macromolecules. Volume II," Chapter 7, edited by M. Dole, Academic Press, New York, 1973.
83. D. J. Dijkstra, W. Hoogsteen and A. J. Pennings, *Polymer*, **30**, 866, (1989).
84. G. Heirich *et al.*, *Kunststoffe*, **57**, 156, (2004).
85. C. F. Coote, J. V. Hamilton, W. G. McGimpsey and R. W. Thompson, *J. Appl. Polym. Sci.* **77**, 2525, (2000).
86. E. A. Reeves, D. C. Barton, D. P. Fitzpatrick and J. Fisher, *Proc. Inst. Mach. Eng., Part H: J. Eng. Med.* **214**, 249, (2000).
87. Y. Luisetto, B. Wesslen, F. Maurer and L. Lidgren, *J. Med. Mater. Res. Part A*, **67**, 908, (2000).
88. N. M. Burns, *Radiat. Phys. Chem.* **14**, 797, (1979).
89. P. E. Jacobs, *Polym.-Plast. Technol. Eng.* **17**, 69, (1981).
90. B. J. Lyons and C. R. Vaughn, in "Irradiation of Polymers", *Adv. Chem. Ser.* **66**, 139, (1967), American Chemical Society Publications.
91. R. M. Black and B. J. Lyons, *Nature*, **180**, 55, (1957).
92. R. M. Black and B. J. Lyons, *Proc. R. Soc.* **A253**, 322, (1959).
93. T. S. Dunn, B. J. Epperson, H. W. Sugg, V. T. Stannett and J. L. Williams, *Radiat. Phys. Chem.* **14**, 625, (1979).
94. D. E. Gavrilina and B. Gosse, *J. Radioanal. Nucl. Chem. Art.* **185**, 311, (1994).
95. E. A. Hegazy, T. Seguchi, K. Arakawa and S. Machi, *J. Appl. Polym. Sci.* **26**, 1361, (1981).
96. W. Snabel and M. Dole, *J. Phys. Chem.* **67**, 295, (1963).
97. B. J. Lyons, *J. Polym. Sci.* **A3**, 777, (1965).
98. J. N. Tomlinson and D. E. Kline, *J. Appl. Polym. Sci.* **11**, 1931, (1967).
99. B. J. Lyons, *Radiat. Phys. Chem.* **45**, 159, (1995).
100. Y. Rosenberg, A. Siegmann, M. Narkis and S. Shkolnik, *J. Appl. Polym. Sci.* **45**, 783, (1992).
101. E. Katan, M. Narkis and A. Siegmann, *J. Appl. Polym. Sci.* **70**, 1471, (1998).
102. R. E. Uscold, *J. Appl. Polym. Sci.* **29**, 1335, (1984).
103. L. A. Wall and R. E. Florin, *J. Appl. Polym. Sci.* **2**, 251, (1959).

104. R. E. Florin, "Fluoropolymers", Chapter 11, p. 321, edited by L. A. Wall, Wiley Interscience, New York, 1972.
105. P. Hedvig, *J. Polym. Sci., Part A-1*, **7**, 1145, (1969).
106. A. Nishioka, A. K. Matsumae, M. Watanabe, M. Tajima and M. Owaki, *J. Appl. Polym. Sci.* **2**, 114, (1959).
107. D. E. Kline and J. A. Sauer, *J. Polym. Sci. Part A*, **1**, 1621, (1963).
108. W. R. Licht and D. E. Kline, *J. Polym. Sci. Part A*, **2**, 4673, (1964).
109. J. Sun, Y. Zhang, X. Zhong and X. Zhu, *Radiat. Phys. Chem.* **44**, 655, (1994).
110. J. Sun, Y. Zhang and X. Zhong, *Polymer*, **35**, 2881, (1994).
111. E. R. Lovejoy, M. I. Bro and G. H. Bowers, *J. Appl. Polym. Sci.* **9**, 401, (1965).
112. D. M. Pinkerton and B. T. Sach, *Austral. J. Chem.* **23**, 1947, (1970).
113. Y. Rosenberg, A. Siegmann, M. Narkis and S. Shkolnik, *J. Appl. Polym. Sci.* **45**, 783, (1992).
114. P. Barnaba, D. Cordischi, A. Dell Site and A. Mele, *J. Chem. Phys.* **44**, 3672, (1966).
115. J. Pacansky and R. J. Waltman, *J. Chem. Phys.* **95**, 1512, (1991).
116. J. Pacansky and R. J. Waltman, *Chem. Mater.* **5**, 486 and 1526, (1993).
117. J. Pacansky, R. J. Waltman and G. Pacansky, *Chem. Mater.* **5**, 1526, (1993).
118. D. P. Carlson and N. E. West, *US Patent No.* 3, 378, 923, (1973).
119. B. J. Lyons, *Rad. Proc. Plastics Rubber II*, University of Kent at Canterbury, The Chameleon Press, London, (1984).
120. Y. X. Luo, F. C. Pang and J. X. Sun, *Radiat. Phys. Chem.* **18**, 445, (1981).
121. T. Yoshida, R. E. Florin and L. A. Wall, *J. Polym. Sci.: Part A*, **3**, 1685, (1965).
122. I. Klier and A. Vokal, *Radiat. Phys. Chem.* **38**, 457, (1991).
123. V. S. Ivanov, I. I. Migunova and A. I. Mikhailov, *Radiat. Phys. Chem.* **37**, 119, (1991).
124. J. L. Suther and J. R. Laghari, *J. Mater. Sci. Lett.* **10**, 786, (1991).
125. E. Adem, G. Burillo, E. Munoz, J. Rickards, L. Cota and M. Avalos-Borja, *Polym. Degrad. Stab.* **81**, 75, (2003).
126. N. Betz, E. Petersohn and A. le Moël, *Radiat. Phys. Chem.* **46**, 411, (1996).
127. A. le Moël, J. P. Duraud, I. Lemaire, E. Balanzat, J. M. Ramillon and C. Darnez, *NUC. Instr. Methods Phys. Res.* **B105**, 71, (1987).
128. T. Seguchi, K. Makuuchi, T. Suwa, N. Tamura, T. Abe and M. Takehisa, *Nippon Kagaku Kaishi*, **7**, 686, (1975).
129. L. A. Wall, S. Straus and R. E. Florin, *J. Polym. Sci.: Part A-1*, **4**, 349, (1966).
130. A. J. Lovinger, *Macromolecules*, **18**, 910, (1985).
131. K. Makucchi, M. Asano and T. Abe, *Nippon Kagaku Kaishi*, 686, (1976).
132. R. E. Florin and L. A. Wall, *J. Res. NBS*, **65A**, 375, (1961).
133. M. M. Nasef, H. Saidi and Z. M. Dahlen, *Polym. Degrad. Stab.* **75**, 85, (2002).
134. K. D. Pae, S. K. Bhateja and J. R. Gilbert, *J. Polym. Sci.: Part B: Polym. Phys.* **25**, 717, (1987).
135. Z. Zhao, X. Chen and W. Yu, *Radiat. Phys. Chem.* **65**, 173, (2002).
136. H. Kawai, *Jpn. J. Appl. Phys.* **8**, 975, (1969).
137. P. Harnischfeger and B. J. Jungnickel, *Appl. Phys. A* **50**, 523, (1990).
138. T. T. Wang, *Ferroelectrics*, **41**, 213, (1982).
139. M. M. Nasef and Z. M. Dahlen, *Nuclear Inst. Methods Phys. Res.: Section B*, **201**, 604, (2003).
140. A. J. Lovinger, T. Furukawa, G. T. Davies and M. G. Broadhurst, *Polymer*, **24**, 1225 and 1233, (1983).
141. A. J. Lovinger, *ACS Symp. Ser.* **475**, "Radiation Effects on Polymers", edited by R. Clough and S. W. Shalaby, American Chemical Society, 1991.
142. R. Timmerman and W. Greyson, *J. Appl. Polym. Sci.* **22**, 456, (1962).
143. J. Byrne, T. W. Costikyan, C. B. Hanford, D. L. Johnson and W. L. Mann, *Ind. Eng. Chem.* **45**, 2549, (1953).
144. J. C. Bresee, J. R. Flanary, J. H. Goode, C. D. Watson and J. S. Watson, *Nucleonics*, **14**, 75, (1956).
145. J. Goodman and J. H. Coleman, *J. Polym. Sci.* **25**, 253, (1957).
146. G. J. Atchison, *J. Polym. Sci.* **49**, 385, (1961).
147. G. J. Atchison, *J. Appl. Polym. Sci.* **7**, 1471, (1963).
148. B. R. Joy, *J. Polym. Sci.* **50**, 245, (1961).
149. A. H. Zahran, E. A. Hegazy and F. M. Ezz Eldin, *Radiat. Phys. Chem.* **26**, 25, (1985).
150. L. Cota, M. Avalos-Borja, E. Adem and G. Burillo, *Radiat. Phys. Chem.* **44**, 579, (1994).
151. E. Adem, M. Avalos-Borja, L. Cota and G. Borillo, *Radiat. Phys. Chem.* **39**, 397, (1992).
152. K. Harada, O. Kogure and K. Murase, *IEEE Trans. Elect. on. Dev.* **29**, 518, (1982).
153. W. Burlant, J. Hirsch and C. Taylor, *J. Polym. Sci.: Part A*, **2**, 57, (1964).
154. K. Ishigure, S. Egusa, S. Tagawa and Y. Tabata, *Radiat. Phys. Chem.* **14**, 585, (1979).
155. I. Gitsov and O. G. Todorova, *J. Appl. Polym. Sci.* **46**, 1631, (1992).
156. R. G. Jones, R. H. Cragg, R. D. P. Davies and D. R. Brambley, *J. Mater. Sci.* **2**, 371, (1992).
157. A. Masayuki and U. Toshiyuki, *Radiat. Phys. Chem.* **33**, 461, (1989).
158. N. A. Slovokhotova, G. K. Sadovskaya and V. A. Kargin, *J. Polym. Sci.* **58**, 1293, (1962).
159. Z. Yiquin, J. Danliang, C. Xinfang, C. Zhanchen, L. Yuxia and L. S. Hua, *Radiat. Phys. Chem.* **43**, 459, (1994).
160. T. Memetea and V. Stannett, *Polym. Prepr.* **18**, 777, (1977).
161. V. H. Ritz, *Radiat. Res.* **15**, 460, (1961).
162. S. D. Burow, D. T. Turner, G. F. Pezdirtz and G. D. Sands, *J. Polym. Sci. Part A-1*, **4**, 613, (1966).
163. D. T. Turner, "The Radiation Chemistry of Macromolecules. Volume II," Chapter 8, p. 137, edited by M. Dole, Academic Press, New York, 1973.
164. J. Kroh and M. Pietrzak, *Khim. Vys. Energ.* **4**, 246, (1970).
165. M. Pietrzak, *Radiochem. Radioanal. Lett.* **54**, 67, (1982).
166. B. J. Lyons and L. C. Glover, *Radiat. Phys. Chem.* **35**, 139, (1990).
167. B. J. Lyons and L. C. Glover, *Radiat. Phys. Chem.* **37**, 93, (1991).
168. J. Zimmerman, *J. Appl. Poly. Sci.* **2**, 181, (1959).
169. J. Zimmerman "The Radiation Chemistry of Macromolecules. Volume II," Chapter 7, p. 129, edited by M. Dole, Academic Press, New York, 1973.
170. L. K. McCune, *Textile Res.* **32**, 262, (1962).
171. A. Charlesby, *J. Polym. Sci.* **11**, 513 and 521, (1953).
172. J. C. Spiro and C. A. Winkler, *J. Appl. Polym. Sci.* **8**, 1709, (1964).
173. J. Wilske and H. Heusinger, *J. Polym. Sci. Part A-1*, **7**, 995, (1969).
174. R. M. Keyser, W. K. Kirkland and W. W. Parkinson, *Oak Ridge Nat. Lab. Reactor Chem. Div. Ann. Prog. Rep. ORNL-3591*, 224, (1964).
175. A. M. Kotliar, *J. Appl. Polym. Sci.* **2**, 134, (1959).
176. W. W. Parkinson and R. M. Keyser, "The Radiation Chemistry of Macromolecules. Volume II," Chapter 5, p. 72, edited by M. Dole, Academic Press, New York, 1973.
177. O. Sisman and C. D. Bopp, *Physical Properties of Irradiated Plastics, ORNL-928, Nat. Tech. Info. Ser., Operations Div.* Springfield, Virginia, (1951).
178. M. Baccaredda, E. Butta and V. Frosini, *J. Appl. Polym. Sci.* **10**, 399, (1966).
179. A. A. Miller, *J. Amer. Chem. Soc.* **82**, 3519, (1960).
180. W. Schnabel, *Makromol. Chem.* **104**, 1, (1967).
181. A. A. Miller, *Ind. Eng. Chem. (Prod. Res. Dev.)*, **3**, 252, (1964).
182. A. Charlesby, "Atomic Radiation and Polymers," Chapter 16, p. 307, Pergamon Press, London, 1960.
183. A. A. Miller, *J. Polym. Sci.* **42**, 441, (1960).
184. C. L. Hanks and D. J. Hamman "Radiation Effects Design Handbook", NASA-CR-1787, Sec 3, (1971).
185. J. R. Brown, J. H. O'Donnell, *J. Appl. Polym. Sci.* **23**, 2763, (1979).
186. E. A. Hegazy, T. Sasuga, M. Nishii and T. Seguchi, *Polymer*, **33**, 2897, (1992).
187. E. A. Hegazy, T. Sasuga, M. Nishii and T. Seguchi, *Polymer*, **33**, 2904, (1992).
188. E. A. Hegazy, T. Sasuga and T. Seguchi, *Polymer*, **33**, 2911, (1992).
189. A. M. El-Naggar, H. C. Kim, L. C. Lopez and G. L. Wilkes, *J. Appl. Polym. Sci.* **37**, 1655, (1989).
190. H. Fischer and W. Langbein, *Kolloid-Z.* **216-217**, 329, (1967).
191. P. Alexander, R. M. Black and A. Charlesby, *Proc. R. Soc. A* **232**, 31, (1955).
192. A. Charlesby, *J. Polym. Sci.* **15**, 263, (1955).
193. S. Miller, M. W. Spindler and R. L. Vale, *Polym. Sci. Part A*, **1**, 2537, (1963).
194. X. Liu, R. M. Briber and B. J. Bauer, *J. Polym. Sci.: Part B: Polym. Phys.* **32**, 811, (1994).

195. G. P. Roberts, M. Budzol and M. Dole, *J. Polym. Sci. Part A-2*, **9**, 1729, (1971).
196. R. E. Fornes, J. D. Memory and N. Naranong, *J. Appl. Polym. Sci.* **26**, 2061, (1981).
197. J. D. Memory, R. E. Fornes and R. D. Gilbert, *J. Reinf. Plast. Compos.* **7**, 33, (1988).
198. R. E. Weyers, P. R. Blankenhorn, L. R. Stover and D. E. Kline, *J. Appl. Polym. Sci.* **22**, 2019, (1978).
199. D. C. McHerron and G. L. Wilkes, *Polymer*, **34**, 3976, (1993).
200. R. M. Briber and B. J. Baure, *Macromolecules*, **21**, 3296, (1988).
201. T. Ayoko, H. Ken-ichi, H. Nobutomo and M. Takuya, *Radiat. Phys. Chem.* **43**, 493, (1994).
202. R. Katare, R. Bajpai and S. C. Datt, *Polym. Testing*, **13**, 107, (1994).
203. K. El-Salmawi, M. M. Abu Zeid, A. M. El-Naggar and M. Mamdouh, *J. Appl. Polym. Sci.* **72**, 509, (1999).
204. H. M. N. El-din, A. M. El-Naggar and F. I. Ali, *Polym. Int.* **52**, 225, (2003).
205. S. Wang, Y. Zhang, C. Zhang and E. Li, *J. Appl. Polym. Sci.* **91**, 1571, (2004).
206. C. T. Ratnam, M. Nasir, A. Baharin and K. Zaman, *J. Appl. Polym. Sci.* **81**, 1926, (2001).
207. H. A. Youssef, Z. I. Ali and A. H. Zahran, *Polym. Degrad. Stab.* **74**, 213, (2001).
208. J. Sharif, S. H. S. A. Aziz and K. Hashim, *Radiat. Phys. Chem.* **58**, 191 (2000).
209. S. M. A. Salehi, G. Mirjalili and J. Amrollahi, *J. Appl. Polym. Sci.* **92**, 1049, (2004).
210. S. Chattopadhyay, T. K. Chaki and A. K. Bhowmick, *J. Appl. Polym. Sci.* **79**, 1877, (2001).
211. S. Chattopadhyay, T. K. Chaki and A. K. Bhowmick, *J. Appl. Polym. Sci.* **81**, 1936, (2001).
212. K. Posselt, *Kolloid-Z. Z. Polym.* **223**, 104, (1968).
213. Y. Okada, *Adv. Chem. Ser.* **66**, 44, (1967).
214. B. J. Lyons, *Nature*, **185**, 604, (1960).
215. A. A. Miller, *J. Appl. Polym. Sci.* **5**, 388, (1961).
216. B. J. Lyons and P. E. Cross, *Trans. F. Soc.* **59**, 2350, (1963).
217. R. G. Bauman, *J. Appl. Polym. Sci.* **2**, 328, (1959).
218. R. G. Bauman and J. W. Born, *J. Appl. Polym. Sci.* **1**, 351, (1959).
219. A. Chapiro, "Radiation Chemistry of Polymeric Systems," Chapter 12, p. 596, Interscience, New York, 1962.

# CHAPTER 53

## Flammability

Archibald Tewarson

*FM Global Research, 1151 Boston-Providence Turnpike, Norwood, MA 02062*

---

<b>53.1</b>	Introduction .....	889
<b>53.2</b>	Fire properties Associated with the Pyrolysis of the Polymer: Heat of Gasification and Surface Re-radiation Loss .....	890
<b>53.3</b>	Fire Properties Associated with Ignition of the Polymer: Critical Heat Flux and Thermal Response Parameter .....	892
<b>53.4</b>	Fire Properties Associated with Combustion of the Polymer: Flame Heat Flux, Heat of Gasification, and Surface Re-Radiation Loss .....	893
<b>53.5</b>	Fire Properties Associated with Flame Propagation: Limiting Oxygen Index and Fire Propagation Index .....	897
<b>53.6</b>	Testing Methods for Flame Propagation .....	898
<b>53.7</b>	Fire Properties Associated with the Generation of Products: Yields of Products .....	902
<b>53.8</b>	Fire Properties Associated with the Generation of Heat .....	907
<b>53.9</b>	Fire Properties Associated with Corrosion and Smoke Damage .....	909
<b>53.10</b>	Fire Properties Associated with Fire Suppression/Extinguishment .....	910
<b>53.11</b>	Standards and Testing of Polymer Products and Materials .....	913
<b>53.12</b>	Appendix .....	923
	References .....	924

---

### 53.1 INTRODUCTION

The flammability of a polymer is an interaction of pyrolysis, ignition, combustion, flame propagation, and flame extinction processes. The processes are brought about by the heat exposure of the polymer. Pyrolysis is an endothermic process and involves softening, melting, discoloration, cracking, decomposition, vaporization, etc. of the polymer and release of pyrolysis products. The boundary of the pyrolysis process on the surface of the polymer is defined as the pyrolysis front. Pyrolysis process is also defined as the gasification of the polymer.

Ignition is a process in which the gasified polymer mixes with air, forms a combustible mixture and the mixture ignites by itself (auto-ignition) or is ignited by a flame, a hot object, an electrical spark, etc., (piloted-ignition).

Combustion is a process in which the solid surface of the polymer or the gasified polymer reacts with the oxygen from air with a visible flame (flaming combustion) or without a visible flame (nonflaming combustion).

Flame propagation is a process in which the pyrolysis front accompanied by flaming- or nonflaming combustion moves with time beyond the point of origin.

Flame extinction is a process where the pyrolysis, ignition, combustion, and fire propagation processes are interrupted by applying agents such as water, inert or chemically active gases, liquids or solids, or reducing the oxygen concentration.

Heat and products are generated in pyrolysis, ignition, combustion, and flame propagation processes, presenting hazards to life and property. Hazard due to release of heat (high temperature and radiation) is defined as thermal hazard [1]. Hazard due to release of products is defined as



nonthermal hazard [2]. Nonthermal hazard is due to toxic and corrosive products which interfere in light transmission (reducing visibility) and in electrical operations of delicate electrical components and equipment, and impart discolor and malodor.

For the assessment of thermal and nonthermal hazards, fire prevention and protection, several types of models have been developed. All these models use fire properties of polymers associated with pyrolysis, ignition, combustion, and flame propagation as inputs [2,3]. These properties are listed in Table 53.1 and are discussed in this chapter.

### 53.2 FIRE PROPERTIES ASSOCIATED WITH THE PYROLYSIS OF THE POLYMER: HEAT OF GASIFICATION AND SURFACE RE-RADIATION LOSS

The steady state polymer gasification rate is expressed as [2,3]:

$$\dot{m}_f'' = \frac{\dot{q}_e'' - \dot{q}_{rr}''}{\Delta H_g}, \quad (53.1)$$

where  $\dot{m}_f''$  is the polymer gasification rate or the mass loss rate in pyrolysis ( $\text{kg}/\text{m}^2 - \text{s}$ ),  $\dot{q}_e''$  is the external heat flux

**TABLE 53.1.** Fire properties associated with pyrolysis, ignition, combustion, and fire propagation processes.

Fire property	Fire property description
<b>Pyrolysis process</b>	
Heat of gasification ( $\Delta H_g$ ) in MJ/kg	Energy required to vaporize a unit mass of the polymer originally at ambient temperature.
Surface re-radiation Loss ( $\dot{q}_{rr}''$ ) in kW/m <sup>2</sup>	Heat lost to the environment from the hot surface of the polymer.
Yield of a product ( $y_j$ ) in kg/kg	Amount of a product generated per unit mass of the polymer gasified.
Product generation parameter (PGP)	Defines product generation rate in non-flaming combustion for a specified heat flux exposure.
<b>Ignition process</b>	
Critical Heat Flux, CHF, ( $\dot{q}_{cr}''$ ) in kW/m <sup>2</sup>	Minimum heat flux at or below which a flammable vapor-air mixture is not created. It is related to the fire point or ignition temperature.
Thermal Response Parameter (TRP) in kJ/m <sup>2</sup> for thermally thin polymer and in kW-s <sup>1/2</sup> m <sup>2</sup> for thermally thick polymer	Resistance to ignition and fire propagation.
<b>Combustion process</b>	
Flame heat flux ( $\dot{q}_f''$ ) in kW/m <sup>2</sup>	Heat flux transferred from the flame back to the surface of the burning polymer.
Net Heat of Complete Combustion ( $\Delta H_T$ ) in MJ/kg	Amount of energy released in the complete combustion of a unit mass of the polymer with water as a gas.
Chemical Heat of Combustion ( $\Delta H_{ch}$ ) in MJ/kg	Amount of energy actually released in the flaming combustion of a unit mass of the polymer.
Convective heat of combustion ( $\Delta H_{con}$ ) in MJ/kg	Component of the chemical heat of combustion carried away from the flame by combustion product-air mixture.
Radiative heat of combustion ( $\Delta H_{rad}$ ) in MJ/kg	Component of the chemical heat of combustion transmitted away from the flame by radiation.
Yield of a product ( $y_j$ ) in kg/kg	Amount of a product generated per unit mass of the polymer gasified.
Heat release parameter (HRP)	Defines heat release rate in the combustion process for a specified heat flux exposure.
Product generation parameter (PGP)	Defines product generation rate in the combustion process for a specified heat flux exposure.
<b>Fire propagation</b>	
Limiting oxygen index (LOI)	Defines propagating and non-propagating fire behavior.
Flame propagation rate	
Fire propagation index (FPI)	

(kW/m<sup>2</sup>),  $\dot{q}_{rr}''$  is the surface re-radiation loss (kW/m<sup>2</sup>), and  $\Delta H_g$  is the heat of gasification (MJ/kg). Pyrolysis experiments are performed where the polymer is heated in an inert environment and various measurements are made. The most widely used techniques are: (1) differential scanning calorimetry, and (2) mass pyrolysis technique.

In the differential scanning calorimetry, measurements are made for the specific heat, heats of melting, vaporization, decomposition, etc., in a differential scanning calorimeter and the data are used in the following equation to calculate the heat of gasification, such as for a melting polymer [2]:

$$\Delta H_g = \int_{T_a}^{T_m} c_{p,s} dT + \Delta H_m + \int_{T_m}^{T_v} c_{p,l} dT + \Delta H_v, \quad (53.2)$$

where  $\Delta H_m$  and  $\Delta H_v$  are the heats of melting and vaporization at the respective melting and vaporization temperatures in MJ/kg,  $c_{p,s}$  and  $c_{p,l}$  are the specific heats of the polymer in the solid and molten states in MJ/kg respectively, and  $T_a$ ,  $T_m$ , and  $T_v$  are the ambient, melting, and vaporization temperatures in K, respectively. For polymers which do not melt, but sublime, decompose or char, Eq. (53.2) is modified accordingly. The values of the heat of gasification calculated from the differential scanning calorimetry in our laboratory are listed in Table 53.2 [4].

In the mass pyrolysis technique, the mass loss rate is measured as a function of external heat flux in the presence of co-flowing nitrogen or air with an oxygen concentration of 10% by volume, and the data are used in Eq. (53.1). The heat of gasification is determined from the linear regression

**TABLE 53.2.** Surface re-radiation loss and heat of gasification of polymers.<sup>a</sup>

Polymer <sup>b</sup>	Surface reradiation loss (kW/m <sup>2</sup> )	Heat of gasification (MJ/kg)	
		ASTM E 2058 FPA	DSC
<b>Natural polymers</b>			
Filter paper	10	3.6	—
Corrugated paper	10	2.2	—
Wood (Douglas fir)	10	1.8	—
Plywood/FR	10	1.0	—
Particle board	—	3.9	—
<b>Synthetic polymers</b>			
Epoxy resin	—	2.4	—
Polypropylene	15	2.0	2.0
Polyethylene (low density)	15	1.8	1.9
Polyethylene (high density)	15	2.3	2.2
Polyethylene foams	12	1.4–1.7	—
Polyethylene/25% Chlorine	12	2.1	—
Polyethylene/36% Chlorine	12	3.0	—
Polyethylene/48% Chlorine	10	3.1	—
Rigid polyvinylchloride (PVC)	15	2.5	—
PVC/plasticizer	10	1.7	—
Plasticized PVC, LOI = 0.20	10	2.5	—
Plasticized PVC, LOI = 0.25	—	2.4	—
Plasticized PVC, LOI = 0.30	—	2.1	2.1
Plasticized PVC, LOI = 0.35	—	2.4	2.4
Rigid PVC, LOI = 0.50	—	2.3	2.3
Polyisoprene	10	2.0	—
PVC panel	17	3.1	—
Nylon 6/6	15	2.4	—
Polyoxymethylene	13	2.4	2.4
Polymethylmethacrylate	11	1.6	1.6
Polycarbonate	11	2.1	—
Polycarbonate panel	16	2.3	—
Isophthalic polyester	—	3.4	—
Polyvinyl ester	—	1.7	—
Acrylonitrile-Butadiene-Styrene	10	3.2	—
Styrene-Butadiene	10	2.7	—
Expanded Polystyrene	10–13	1.3–1.9	—
Polystyrene (granular)	13	1.7	1.8

TABLE 53.2. Continued.

Polymer <sup>b</sup>	Surface reradiation loss (kW/m <sup>2</sup> )	Heat of gasification (MJ/kg)	
		ASTM E 2058 FPA	DSC
Expanded polyurethane (flexible)	16–19	1.2–2.7	1.4
Expanded polyurethane (Rigid)	14–22	1.2–5.3	—
Expanded polyisocyanurate	14–37	1.2–6.4	—
Expanded phenolic	20	1.6	—
Expanded phenolic/FR	20	3.7	—
Tefzel® (ETFE)	27	0.9	—
Teflon® (FEP)	38	2.4	—
Teflon® (TFE)	48	0.8;1.8	—
Teflon® (PFA)	37	1.0	—
PEEK-30% fiber glass	—	7.9	—
Polyethersulfone-30% fiber glass	—	1.8	—
Polyester1-fiber glass	—	2.5	—
Polyester2-fiber glass	10	1.4	—
Polyester3-fiber glass	10	6.4	—
Polyester4-fiber glass	15	5.1	—
Polyester5-fiber glass	10	2.9	—
Phenolic-fiber glass (thick sheet)	20	7.3	—
Phenolic-Kevlar (thick sheet)	15	7.8	—

<sup>a</sup>Data are from the Flammability Laboratory of the FM Global using the ASTM E 2058 FPA shown in Fig. 53.1 and a differential scanning calorimeter.

<sup>b</sup>Abbreviations listed in the nomenclature.

analysis of the data. An external heat flux value at which there is no measurable mass loss rate for 15 min of heat flux exposure is taken as the value for the surface re-radiation loss. The mass pyrolysis technique is used in the ASTM E 2058 FPA, shown in Fig. 53.1, originally designed in our laboratory for this application [4]. Table 53.2 lists the values of the heat of gasification and surface re-radiation loss using the mass pyrolysis technique in our laboratory [4].

The interruption of pyrolysis by passive and/or active fire protection techniques would prevent fires to propagate beyond the ignition zone resulting in reduced fire hazards. The passive fire protection technique involves changes in the polymer to increase the values of the surface re-radiation loss and heat of gasification.

### 53.3 FIRE PROPERTIES ASSOCIATED WITH IGNITION OF THE POLYMER: CRITICAL HEAT FLUX AND THERMAL RESPONSE PARAMETER

Ignition of a polymer involves formation of a flammable vapor air mixture and initiation of combustion on its own (auto-ignition) or assisted by a small heat source (piloted ignition). Minimum heat flux at or below which there is no ignition is defined as the critical heat flux (CHF).

The surface of a polymer exposed to heat flux is at a higher temperature than the interior. A polymer with a steep temperature gradient between the surface and the interior is defined as thermally thick. If there is no temperature gradi-

ent between the surface and the interior, the polymer is defined as thermally thin. Thermally thick and thin conditions depend on the actual thickness of the polymer, heating rates, chemical structures of the polymers and additives. The time to ignition and external heat flux satisfy the following relationships [2,3]:

$$\frac{1}{t_{ig}} = \frac{\pi}{4} \frac{\dot{q}_e''}{K_{thin}}, \quad (53.3)$$

for thermally thin polymers where  $K_{thin} = \rho c_p \delta \Delta T_{ig}$  is defined as the thermal response parameter (TRP) for thermally thin polymers (kJ/m<sup>2</sup>),  $\rho$  is the density of the polymer (kg/m<sup>3</sup>),  $c_p$  is the specific heat of the polymer (MJ/kg-K),  $\delta$  is the actual thickness of the polymer (m), and  $T_{ig}$  is the ignition temperature above ambient (K); and

$$\sqrt{\frac{1}{t_{ig}}} = \sqrt{\frac{\pi}{4} \frac{\dot{q}_e''}{K_{thick}}}, \quad (53.4)$$

for thermally thick polymers where  $K_{thick} = \Delta T_{ig} \sqrt{k \rho c_p}$  is defined as the TRP for thermally thick polymers (kW - s<sup>1/2</sup>/m<sup>2</sup>), and  $k$  is the thermal conductivity of the polymer (kW.m-K).

The TRP represents resistance of a polymer to generate flammable vapor-air mixture. The CHF and TRP values of the polymers are obtained by using the ignition technique [3,4]. External heat flux at which there is no ignition for 15 min is taken as the CHF. The CHF value is generally close to the value for the surface re-radiation loss. In the ignition technique, time to ignition is measured at various external

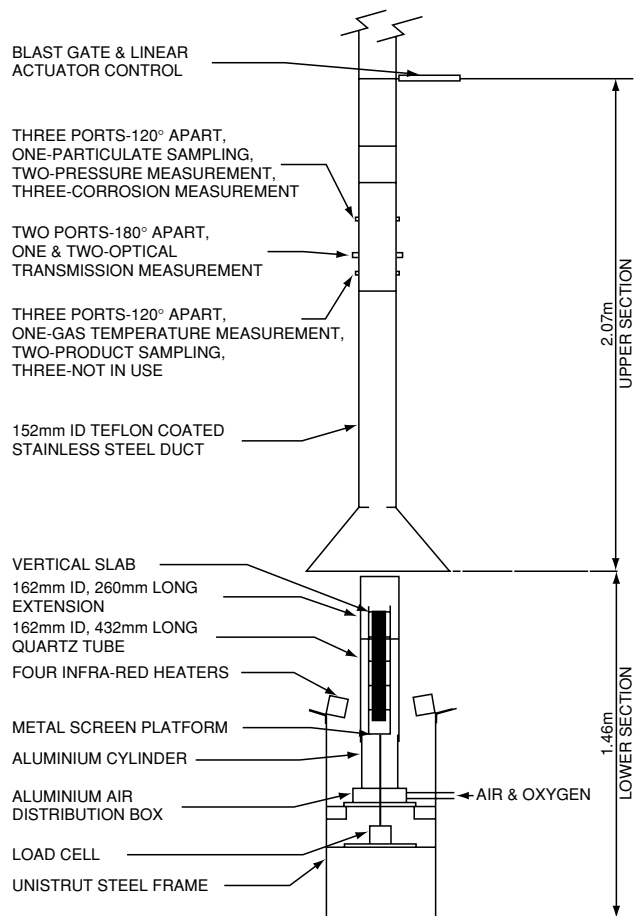


**FIGURE 53.1.** The ASTM E 2058 Fire Propagation Apparatus (FPA).

heat flux values and the data are used in Eqs. 53.3 and 53.4. A linear relationship between the time to ignition or square root of time to ignition and external heat flux, away from the CHF value [Eqs. (53.3) or (53.4), respectively], is indicative of the thermally thin or thick behavior, such as shown in Fig. 53.2 for a silicone polymer, which behaves as a thermally thick polymer. The TRP value is obtained from the linear regression analysis of the data in the linear portion of the curve, away from the CHF value.

The ASTM E 2058 FPA, shown in Fig. 53.1, has been designed to use this technique. The TRP values from the ignition technique are listed in Table 53.3. The values of the ignition temperature, thermal conductivity, and specific heat, which are individual components of TRP, taken from Tewason *et al.* [7,8] are listed in Table 53.4.

The CHF and TRP values depend on the physical and chemical characteristics of the polymers. Increasing the CHF and TRP values of the polymers by various passive protection techniques would delay initiation of combustion and flame would propagate at lower rate or there would be no fire propagation beyond the ignition zone.

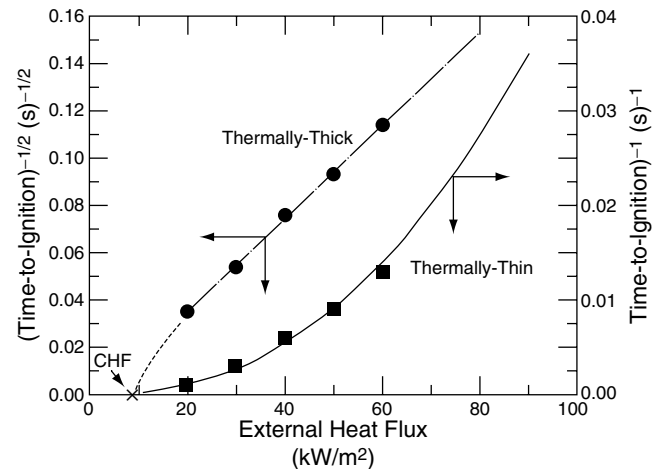


**FIGURE 53.2.** Time to ignition versus external heat flux for a 100×100 mm×10 mm thick silicone based polymer. Data were measured in the ASTM E 2058 FPA. Data satisfy the thermally-thick behavior away from the critical heat flux value.

#### 53.4 FIRE PROPERTIES ASSOCIATED WITH COMBUSTION OF THE POLYMER: FLAME HEAT FLUX, HEAT OF GASIFICATION, AND SURFACE RE-RADIATION LOSS

The steady state relationship for polymer gasification rate or mass loss rate is similar to the relationship for the pyrolysis condition [Eq. (53.1)], except for an additional term for the flame heat flux [2,3]:

$$\dot{m}_f'' = \frac{\dot{q}_e'' + \dot{q}_f'' - \dot{q}_{rr}''}{\Delta H_g}, \quad (53.5)$$

where  $\dot{m}_f''$  is the mass loss rate in combustion ( $\text{kg}/\text{m}^2 - \text{s}$ ) and  $\dot{q}_f''$  is the flame heat flux transferred back.

The values of the heat of gasification and surface re-radiation loss determined in pyrolysis are used. The flame heat flux is determined from the flame radiation scaling technique [2,3,13]. This technique utilizes the knowledge that in small-scale fires, flame radiative heat flux increases with increase in the oxygen mass fraction ( $Y_0$ ) [2,3,13]. For  $Y_0 \geq 0.30$ , the flame radiative heat flux reaches an asymptotic limit comparable to the limit for large-scale fires burning in the open [2,3,13].

In the flame radiation scaling technique, mass loss rate is measured with co-flowing air having various oxygen mass fractions. Flame heat flux is calculated by using the mass loss rate data in Eq. (53.5), along with the values of the heat of gasification and surface radiation loss measured in pyrolysis [13]. The convective component of the flame heat flux is determined from the combustion of methanol dominated by convective heat transfer [13]. The flammability

**TABLE 53.3.** Critical heat flux and thermal response parameter.<sup>a</sup>

Polymer	Critical heat flux (kW/m <sup>2</sup> )	Thermal response parameter	
		Thermally thick (kW-s <sup>1/2</sup> /m <sup>2</sup> )	Thermally thin (kJ/m <sup>2</sup> )
<b>Natural polymers</b>			
100% cellulose	13	—	159
Tissue paper	13	—	130
News paper	11	—	175
Wood (red oak)	10	134	—
Wood (Douglas fir)	10	138	—
Wood (Douglas fir/FR)	10	251	—
Wood (hemlock)	—	175	—
Corrugated paper	13	—	385
Wool 100%	—	252	—
<b>Nonhalogenated synthetic polymers</b>			
Epoxy resin	15	457	—
Polystyrene	13	162	—
Polypropylene	15	193	—
Styrene-butadiene	10	198	—
Crosslinked polyethylenes	15	224–301	—
Polyvinyl ester	—	263	—
Polyoxymethylene	13	269	—
Nylon	15	270	—
Polymethylmethacrylate	11	274	—
Isophthalic polyester	—	296	—
Acrylonitrile-butadiene-styrene	13	317	—
Polyethylene (high density)	15	321	—
Polyethylene/NH- FR	15	652–705	—
Polycarbonate	15	331	—
<b>Halogenated synthetic polymers</b>			
Isoprene	10	174	—
Plasticized PVC, LOI = 0.20	10	285	—
Plasticized PVC, LOI = 0.25	10	401	—
Plasticized PVC, LOI = 0.30	10	397	—
Plasticized PVC, LOI = 0.35	10	345	—
Rigid PVC, LOI = 0.50	10	388	—
Rigid PVC	15	406	—
Tefzel® (ETFE)	27	356	—
Teflon® (FEP)	38	682	—
<b>Composite systems</b>			
Polyester-0% fiber glass	—	296	—
Polyester1-30% fiber glass	—	256	—
Polyester2-70% fiber glass	10	275	—
Polyester3-70% fiber glass	10	382	—
Polyester4-70% fiber glass	15	406	—
Polyester5-70% fiber glass	10	338	—
Polyester-77% fiber glass	—	426	—
Epoxy-0% fiber glass	—	257	—
Epoxy-fiber glass (thin sheet)	10	156	—
Epoxy-65% fiber glass	10	420	—
Epoxy-76% fiber glass	15	667	—
Vinyl ester-0% fiber glass	—	263	—
Vinyl ester-62% fiber glass	—	312	—
Vinyl ester-69% fiber glass	—	444	—
Polyimide-fiber glass	—	833	—
PPS-fiber glass	—	588	—
PPS-84% fiber glass	20	909	—
Bismaleimide-fiber glass	—	625	—

TABLE 53.3. Continued.

Polymer	Critical heat flux (kW/m <sup>2</sup> )	Thermal response parameter	
		Thermally thick (kW-s <sup>1/2</sup> /m <sup>2</sup> )	Thermally thin (kJ/m <sup>2</sup> )
Phenolic-fiber glass (thin sheet)	33	105	—
Phenolic-80% fiber glass	20	610	—
Phenolic-fiber glass	—	345–769	—
Epoxy/phenolic-fiber glass	20	1250	—
PEEK-30% fiber glass	—	301	—
Polyethersulfone-30% FG	—	256	—
Phenolic-kevlar (thin sheet)	20	185	—
Phenolic-84% kevlar	15	403	—
Cyanate-73% graphite	20	1000	—
Epoxy-71% graphite	24	667	—
Epoxy-graphite	—	476–667	—
Bismaleimide-graphite	—	526–588	—
PPS-graphite	—	333	—
PEEK-graphite	—	526	—
Phenolic-graphite	—	400–714	—
<b>Expanded synthetic polymers</b>			
Polyurethanes	13–40	55–221	—
Polystyrenes	10–15	111–317	—
Phenolics	20	610	—
Neoprenes	16	113–172	—
<b>Polymers with fiberweb, net-like and multiplex structures</b>			
Polypropylenes	8–15	—	278–385
Polyester-polypropylene	10	—	139
Wood pulp-polypropylene	8	—	130
Polyesters	8–18	—	161–303
Rayon	14–17	—	161–227
Polyester-rayon	13–17	—	119–286
Wool-nylon	15	—	293
Nylon	15	—	264
Cellulose	13	—	159
Cellulose/polyester	13–16	—	149–217
<b>Polymers as electrical power cable insulation and jackets</b>			
PVC/PVC	13–25	156–341	—
PE/PVC	15	221–244	—
Silicone/PVC	19	212	—
Silicone/XLPO	25–30	435–457	—
EPR/EPR	20–23	467–567	—
EPR,FR/EPR,FR	14–28	289–448	—
XLPE/XLPE	20–25	273–386	—
XLPE/EVA	12–22	442–503	—
XLPE/Neoprene	15	291	—
XLPO/XLPO	16–25	461–535	—
XLPO,PVF/XLPO	14–17	413–639	—
EPR/CLS-PE	14–19	283–416	—
<b>Polymers as communications cable insulation and jackets</b>			
PVC/PVC	15	131	—
PE/PVC	20	183	—
XLPE/XLPO	20	461–535	—
Si/XLPO	20	457	—
EPR-FR	19	295	—
Chlorinated PE	12	217	—
ETFE/EVA	22	454	—
PVC/PVF	30	264	—

<sup>a</sup>Data from the ASTM E 2058 FPA at FMRC [2,3,5–8] or calculated from the data reported in Refs. 9 and 10.

**TABLE 53.4.** Ignition temperature, thermal conductivity, and specific heats of polymers.<sup>a</sup>

Polymers	Ignition temperature (K) <sup>b</sup>	Specific heat (kJ/kg-K)	Thermal conductivity (kW/m-K) × 10 <sup>4</sup>
<b>Natural polymers</b>			
Cotton	527	—	—
News paper	503	—	—
White pine, shavings	533	—	—
<b>Nonhalogenated synthetic polymers</b>			
ABS	527	1.26–1.67	1.88–3.35
Acetal homopolymer	—	1.46	2.30
Acrylics	—	1.46	1.67–2.51
Cellulose acetate	—	1.26–2.09	1.67–3.35
Epoxy	—	1.05	1.67–2.09
Epoxy/silica	—	0.84–1.13	4.18–8.37
Nylon 6/6	785	1.67	2.43
Nylon 6/6/33% glass	—	1.26	2.13
Nylon 6	—	1.67	2.43
Nylon 6/30–35% glass	—	2.09	2.43
Polymethylmethacrylate	651	2.09	2.68
Polyethylene			
Low density	622	2.30	3.35
Medium density	—	2.30	3.35–4.18
High density	—	2.30	4.60–5.19
Polypropylene	736	1.92	1.17
Polystyrene	675	1.34	1.00–1.38
Polycarbonate	651	1.17–1.26	1.92
Polyester	—	1.17–2.30	1.76–2.89
Polyester/premix chopped glass	—	1.05	4.18–6.69
Polyaryl ether	—	1.46	2.98
Polyether sulfone	—	1.09	1.34–1.84
Phenol-formaldehyde	—	1.59–1.76	1.26–2.51
Polyphenylene oxide	—	1.34	1.88
Polyurethane	—	1.67–1.88	0.63–3.10
Styrene-acrylonitrile (SAN)	—	1.34–1.42	1.21–1.26
Styrene-butadiene (SB)	645	1.88–2.09	1.51
<b>Halogenated synthetic polymers</b>			
PVC	675	1.34	1.25–2.93
PVC <sub>2</sub>	—	1.34	1.26
PTFE	767	1.05	2.51
FEP	900	1.17	2.51
PVF <sub>2</sub>	—	1.38	1.26
PCTFE	—	0.92	1.97–2.22
<b>Inert fibers for composite systems</b>			
Kevlar	—	—	2.00
Glass	—	—	10.5
Quartz	—	—	17.2
Graphite	—	—	50.2
Sapphire (aluminum oxide)	—	—	240
Silicone carbide	—	—	850

<sup>a</sup>Data taken from Refs. 11 and 12.<sup>b</sup>Estimated from the CHF value in Table 53.3.

apparatus, shown in Fig. 53.1, has been designed to use this technique.

The asymptotic values for the mass loss rate in combustion and flame heat flux determined from the radiation

scaling technique in the ASTM E 2058 FPA are listed in Table 53.5. The measured asymptotic values of the mass loss rate in combustion in large-scale fires reported in the literature are also listed in Table 53.5. The asymptotic flame

**TABLE 53.5.** Asymptotic mass loss rate and flame heat flux.

Polymers/Liquids <sup>a</sup>	Mass loss rate (kg/m <sup>2</sup> -s) × 10 <sup>3</sup>		Flame heat flux (kW/m <sup>2</sup> )	
	Flame rad. Scaling tech <sup>b</sup>	Largescale	Flame rad. scaling tech <sup>b</sup>	Largescale
<b>Aliphatic carbon-hydrogen atoms</b>				
Polyethylene	26	—	61	—
Polypropylene	24	—	67	—
Heavy fuel oil (2.6–23 m)	—	36 <sup>c</sup>	—	29
Kerosene (30–80 m)	—	65 <sup>c</sup>	—	29
Crude oil (6.5–31 m)	—	56 <sup>c</sup>	—	44
<i>n</i> -Dodecane (0.94 m)	—	36 <sup>c</sup>	—	30
Gasoline (1.5–223 m)	—	62 <sup>c</sup>	—	30
JP-4 (1.0–5.3 m)	—	67 <sup>c</sup>	—	40
JP-5 (0.60–17 m)	—	55 <sup>c</sup>	—	39
<i>n</i> -Heptane (1.2–10 m)	~66	75 <sup>c</sup>	32	37
<i>n</i> -Hexane (0.75–10 m)	—	77 <sup>c</sup>	—	37
Transformer fluids (2.37 m)	27–30	25–29	23–25	22–25
<b>Aromatic carbon-hydrogen atoms</b>				
Polystyrene (0.93 m)	36	34	75	71
Xylene (1.22 m)	—	67 <sup>c</sup>	—	37
Benzene (0.75–6.0 m)	—	81 <sup>c</sup>	—	44
<b>Aliphatic carbon-hydrogen-oxygen atoms</b>				
Polyoxymethylene	16	—	50	—
Polymethylmethacrylate (2.37 m)	28	30	57	60
Methanol (1.2–2.4 m)	20	25	22	27
Acetone (1.52 m)	—	38 <sup>c</sup>	—	24
<b>Aliphatic carbon-hydrogen-oxygen-nitrogen atoms</b>				
Expanded Polyurethanes (flexible)	21–27	—	64–76	—
Expanded Polyurethanes Rigid	22–25	—	49–53	—
<b>Aliphatic carbon-hydrogen-halogen atoms</b>				
Polyvinylchloride	16	—	50	—
Tefzel® (ETFE)	14	—	50	—
Teflon® (FEP)	7	—	52	—

<sup>a</sup>Numbers in parentheses are the pool diameters in meters.<sup>b</sup>Flame radiation scaling technique: pool diameter fixed at 0.10 m,  $Y_0 \geq 0.30$ . ASTM E 2058 FPA.<sup>c</sup>Taken from various references in the literature.

heat flux values, determined in the ASTM E 2058 FPA are in good agreement with the values derived from the mass loss rate in large-scale fires.

The asymptotic flame heat flux values vary from 22 to 77 kW/m<sup>2</sup>, dependent primarily on the pyrolysis mode rather than on the chemical structures. For examples, for the liquids, which vaporize primarily as monomers or as very low molecular weight oligomer, the asymptotic flame heat flux values are in the range of 22–44 kW/m<sup>2</sup>, irrespective of their chemical structures. For polymers, which vaporize as high molecular weight oligomer, the asymptotic flame heat flux values increase substantially to the range of 49 to 71 kW/m<sup>2</sup>, irrespective of their chemical structures. The independence of the asymptotic flame heat value from the chemical structure is consistent with the dependence of

the flame radiation on optical thickness, soot concentration and flame temperature.

Decrease in the flame heat flux and increase in the heat of gasification and surface re-radiation loss through various passive fire protection techniques would prevent the fire to grow and propagate beyond the ignition zone and the thermal and nonthermal hazards would be reduced and/or eliminated.

### 53.5 FIRE PROPERTIES ASSOCIATED WITH FLAME PROPAGATION: LIMITING OXYGEN INDEX AND FIRE PROPAGATION INDEX

Flame propagation is a process where the pyrolysis front moves beyond the ignition zone over the polymer surface,



accompanied by the sustained combustion process. The rate of the movement of the pyrolysis front, accompanied by the sustained combustion process, is defined as the flame propagation rate. For a sustained fire propagation process, flame or external heat sources need to transfer heat flux ahead of the pyrolysis front to satisfy the CHF and TRP values. Flame propagation can occur in the downward, upward, and horizontal directions.

Three test apparatuses and methods have been developed to determine the fire properties associated with flame propagation: (1) the ASTM D 2863 oxygen index test method for downward flame propagation for small samples [14]; (2) the ASTM E 1321-90 lateral ignition and flame spread (LIFT) test method for horizontal and lateral flame propagation [15,16]; and (3) the fire propagation index (FPI) test method for vertical flame propagation [2,3,17,18].

In the LIFT and FPI test methods, the following definition of the flame propagation velocity for thermally thick polymers is utilized [2,3,7,15]:

$$u = \frac{\text{funct}(\dot{q}_f'')}{[\Delta T_{\text{ig}}^2 k \rho c_p]}, \quad (53.6)$$

where  $u$  is the flame propagation rate in m/s,  $\text{funct}(\dot{q}_f'')$  is a function representing the flame heat flux transferred to the surface of the polymer ahead of the pyrolysis front ( $\text{kW}^2/\text{m}^3$ ),  $\rho$  is the density of the polymer ( $\text{kg}/\text{m}^3$ ),  $c_p$  is the specific heat of the polymer ( $\text{MJ}/\text{kg}\cdot\text{K}$ ),  $k$  is the thermal conductivity of the polymer ( $\text{kW}/\text{m}\cdot\text{K}$ ) and  $\Delta T_{\text{ig}}$  is the ignition temperature above ambient ( $\text{K}$ ) [see the definition of the TRP for thermally thick polymer in Eq. (53.4)].

## 53.6 TESTING METHODS FOR FLAME PROPAGATION

### 53.6.1 The ASTM D 2863 Oxygen Index Test

In this test, downward flame propagation for small vertical sheets (6.5-mm wide, 70–150-mm long, 3-mm thick) is examined, in air flowing in the opposite direction with variable oxygen concentration [14]. Minimum oxygen concentration (volume percent) at or below which the downward flame propagation cannot be sustained, defined as the limiting oxygen index (LOI), is determined [14]. The LOI values reported in the literature [8,19] are compiled in Table 53.6.

For PMMA, LOI=17.3 in Table 53.6 which is higher than the oxygen concentration of 16.0% required for flame extinction for larger PMMA slabs [6]. The difference is probably due to differences in the flame radiation and flow characteristics. For example, for larger PMMA slabs exposed to external heat flux values of 40, 60, and 65  $\text{kW}/\text{m}^2$  in the ASTM E 2058 FPA, flame extinction occurs at oxygen concentrations of 13.0%, 12.0%, and 11.5%, respectively [6]. The LOI value decreases with in-

crease in the gas temperature as indicated by the LOI values of the composite systems in Table 53.6.

The oxygen index test utilizes the flame radiation scaling technique for small samples and indirectly assesses heat flux from the flame through LOI. At or below the LOI value of a polymer, the heat flux requirements for CHF and TRP values for fire propagation are not satisfied. The higher is the LOI of a polymer, higher are its CHF and TRP values and/or lower is the heat flux provided by its flame, and the polymer is considered as fire hardened.

The oxygen index test is used for molded polymers, fabrics, expanded polymers, thin films, polymers which form char, drip, or soften, and for liquids. The data are reproducible. The test is used to study polymer combustion chemistry, fire retardant treatment of the polymers and for screening the polymers. No relationships have been established between LOI and the flame heat flux, CHF, TRP, and fire propagation rate. The application of the oxygen index test data to predict the fire propagation behavior of polymers expected in actual fires is thus uncertain.

### 53.6.2 The ASTM E 1321-90 Lateral Ignition and Flame Spread (LIFT) Test

Equation (53.6) is expressed as [15]:

$$u = \frac{\Psi}{\text{TRP}^2}, \quad (53.7)$$

where  $\Psi$  is defined as the flame heating parameter ( $\text{kW}^2/\text{m}^3$ ). The ignition and flame spread tests are performed in normal air at various external heat flux values [15,16]. In the ignition tests, 155- $\times$ 155-mm samples are exposed to various external heat flux values and times to flame attachment are measured [15,16]. The values of  $k$ ,  $\rho$ ,  $c_p$ ,  $\Delta T_{\text{ig}}$  are determined from the relationship between the time to flame attachment and external heat flux [15,16]. These values can be used to calculate the TRP value [Eq. (53.4)].

In the flame spread tests, 155-mm wide and 800-mm long horizontal samples in a lateral configuration are used [15,16]. The samples are exposed to an external heat flux which is 5  $\text{kW}/\text{m}^2$  higher than the CHF value in the ignition zone [15,16]. Beyond the ignition zone, the external heat flux decreases gradually and is significantly lower than the CHF value at the end of the sample [15,16]. The sample is preheated to thermal equilibrium and ignited with a pilot flame in the ignition zone. The pyrolysis front is tracked as a function of time and is used to determine the flame heating parameter and used in Eq. (53.7) along with the TRP value to calculate the flame propagation rate. The flame propagation rate calculated from the data reported in Refs. 15 and 19 are listed in Table 53.7. The relative flame propagation rate is also listed in Table 53.7.

In the LIFT Apparatus, most of the common polymers and carpets have faster lateral flame propagation than

**TABLE 53.6.** Limiting oxygen indices for polymers.<sup>a</sup>

Polymer	LOI	Polymer	LOI
Cotton	16–17	Polyethylene1	17.4
Cotton (loosely woven)	18.5	Polyethylene2	17.4
Filter paper	18.2	Polyethylene-50% Al <sub>2</sub> O <sub>3</sub>	19.6
Wood (birch)	20.5	Polypropylene	17.4
Wood (red oak)	23.0	Polypropylene-30% FG	18.5
Wood (plywood)	23.0	Polystyrene1	17.8
Cellulose	19.0	Polystyrene2	17.6–18.3
Cellulose acetate (dry)	16.8	Polymethylmethacrylate(Plexiglas®)	17.3
Cellulose acetate (4.9% water)	18.1	Polycarbonate1	22.5
Cellulose butyrate (0.06% water)	18.8	Polycarbonate2	24.9
Cellulose butyrate (2.8% water)	19.9	Polycarbonate3	26.0–28.0
Cellulose acetate-butyrates	19.6	ABS-1	18.3–18.8
Rayon	18.7–18.9	ABS-2	18.8
Wool (loosely woven)	23.8	ABS-20% FG	21.6
Wool fiber (dry cleaned)	25.2	SBR foam	16.9
Leather (chrome based)	34.8	Nylon fiber	20.1
Natural rubber foam	17.2	Nylon-6,6	24.3
Polyacetal (Celcon®)	14.9	Nylon-6,6	24.0–29.0
Polyacetal-30% FG	15.6	Nylon-6,12	25.0
Polyformaldehyde	15.0	Nylon-6	25.0–26.0
Poly(ethylene oxide)	15.0	Polyacrylonitrile	18.0
Polyoxymethylene (Delrin®)	14.9	Polyimide (Kapton®)	36.5
Polyphenylene oxide	29.9	Silicon rubber	30.0
Polyurethane foam	16.5	Polyester2–70% fiber glass, °C	
Polyvinyl alcohol	22.5	25	28.0
Polysulfone	30.0–32.0	100	28.0
PVC fiber	37.1	200	13.0
PVC (rigid)	45.0–49.0	300	<10
PVC (chlorinated)	45.0–60.0	Polyester3–70% fiber glass, °C	
Poly(vinyl fluoride) (Tedlar®)	22.6	25	52.0
Polyethylene (20% chlorine)	24.5	100	95.0
Neoprene	40.0	200	77.0
Neoprene rubber	26.3	300	41.0
Polyisoprene	18.5	Epoxy resin	19.8
Poly(vinylidene chloride) (Saran®)	60.0	Epoxy1–65% fiber glass, °C	
Polytrichlorofluoroethylene	95.0	25	38.0
Teflon® (TFE)	95.0	100	43.0
Nomex®	28.5	200	34.0
Polyester fabric	20.6	300	16.0
Polyester	41.5	Epoxy2–65% fiber glass, °C	
Polyester-70% fiber glass; (heated to °C)		25	50.0
25	23.0	100	59.0
100	23.0	200	49.0
200	<10	300	24.0
300	<10		
Epoxy3–65% fiber glass, (heated to °C)		Phenolic-80% fiber glass, °C	
25	43.0	200	94.0
100	54.0	300	80.0
200	47.0	Phenolic-84% Kevlar, °C	
300	27.0	25	28.0
Phenolic resin	21.0	100	30.0
Phenol-formaldehyde resin	35.0	200	29.0
Phenolic-80% fiber glass, (heated to °C)		300	26.0
25	53.0		
100	98.0		

<sup>a</sup>Data taken from Refs. 8 and 19.

**TABLE 53.7.** Lateral flame propagation rate in the LIFT apparatus.<sup>a</sup>

Polymers	Thickness (mm)	Flame propagation rate (mm/s)	Relative flame propagation rate
<b>Natural polymers</b>			
Hardboard	3	10	1.0
Hardboard (gloss paint)	3	5	0.5
Hardboard	6	6	0.6
Plywood plain	6	11	1.1
Plywood plain	13	13	1.3
Particle board	13	5	0.5
Douglas fir particle board	12	10	1.0
Fiber insulation board	—	7	0.7
Gypsum board, wall paper	—	3	0.3
Gypsum board	13	10	1.0
Asphalt shingle	—	9	0.9
Fiberglass shingle	—	10	1.0
<b>Synthetic polymers</b>			
Polyisocyanurate foam	51	37	3.7
Rigid polyurethane foam	25	28	2.8
Flexible polyurethane foam	25	16	1.6
Polymethylmethacrylate	2	11	1.1
Polymethylmethacrylate	13	11	1.1
Polycarbonate	2	7	0.7
<b>Carpets</b>			
Acrylic	—	17	1.7
Nylon/wool blend	—	15	1.5
Wool, Untreated	—	13	1.3
Wool, Treated	—	4	0.4
<b>Aircraft panel materials</b>			
Phenolic fiberglass	—	14	1.4
Phenolic kevlar	—	13	1.3
Epoxy kevlar	—	11	1.1
Phenolic graphite	—	9	0.9
Epoxy fiberglass	—	6	0.6

<sup>a</sup>Calculated from the data reported in Refs. 15 and 20.

Douglas fir. Three out of five aircraft panel materials also have faster lateral flame propagation than a Douglas fir. For most of the ordinary polymers, the lateral flame propagation rate is either comparable to or lower than the rate for a Douglas fir.

### 53.6.3 The Fire Propagation Index (FPI) Test for Vertical Flame Propagation

The fire propagation test is performed in the ASTM E 2058 FPA (Fig. 53.1) using the flame radiation scaling technique with the TRP value determined from the ignition test. The test can be considered as a larger version of the ASTM D 2863 oxygen index test, with an ignition zone provided by four external heaters. In the test, upward fire propagation is examined under co-flowing air with an oxygen concentration of 40% [2,3]. Polymers as vertical slabs and cylinders of

up to 600 mm in length and up to about 25 mm in thickness, 100 mm in width or diameter are used. The chemical heat release rate is measured during flame propagation and is used in the following relationship [modified Eq. (53.6)]:

$$\sqrt{u} \propto \frac{(0.42\dot{Q}'_{ch})^{1/3}}{[\Delta T_{ig}(k\rho c_p)^{1/2}]} \quad (53.8)$$

where  $\dot{Q}'_{ch}$  is the chemical heat release rate per unit width or circumference (kW/m). The fire propagation index (FPI) is calculated from Eq. (53.8) with a proportionality constant of  $1000 \text{ kW}^{2/3} - \text{s}^{1/2}/\text{m}^{5/3}$  and TRP from Eq. (53.4):

$$\text{FPI} = 1000 \frac{(0.42\dot{Q}'_{ch})^{1/3}}{\text{TRP}} \quad (53.9)$$

The FPI values determined in this fashion are listed in Table 53.8 for selected polymers and shown in Fig. 53.3 for a fire

**TABLE 53.8.** Fire propagation index for polymers.

Polymers	Diameter/ thickness (mm)	FPI	Group	Fire propagation <sup>a</sup>
<b>Synthetic polymers</b>				
PMMA	25	30	3	P
PP-FR	25	≥ 10	3	P
<b>Polymers as electrical cable insulation and jacket</b>				
PVC/PVC (power)	4–13	11–28	2–3	P
PVC/PVC (communications)	4	36	3	P
PE/PVC (power)	11	16–23	3	P
PE/PVC (communications)	4	28	3	P
PVC/PE (power)	34	13	2	P
PVC/PVF (communications)	5	7	1	NP
Silicone/PVC (power)	16	17	2	P
Silicone/XLPO (power)	55	6–8	1	NP; DP
Si/XLPO (communications)	28	8	1	DP
EP/EP (power)	10–25	6–8	1	NP; DP
XLPE/XLPE (power)	10–12	9–17	1–2	DP; P
XLPE/XLPO (communications)	22–23	6–9	1	NP; DP
XLPE/EVA (power)	12–22	8–9	1	DP
XLPE/Neoprene (power)	15	9	1	DP
XLPO/XLPO (power)	16–25	8–9	1	DP
XLPO, PVF/XLPO (power)	14–17	6–8	1	NP; DP
EP/CLP (power)	4–19	8–13	1–2	DP; P
EP, FR/None (power)	4–28	9	1	DP
EP-FR/none (communications)	28	12	2	P
ETFE/EVA (communications)	10	8	1	DP
FEP/FEP (communications)	8–10	4–5	1	NP
<b>Composite systems</b>				
Polyester1-70% fiber glass	4.8	13	2	P
Polyester2-70% fiber glass	4.8	10	2	P
	19	8	1	DP
	45	7	1	NP
Epoxy1-65% fiber glass	4.4	9	1	DP
Epoxy2-65% fiber glass	4.8	11	2	P
Epoxy3-65% fiber glass	4.4	10	2	P
Epoxy4-76% fiber glass	4.4	5	1	NP
Phenolic-80% fiber glass	3.2	3	1	NP
Epoxy-82% fiber glass-phenolic	—	2	1	NP
Phenolic-84% kevlar	4.8	8	1	DP
Cyanate-73% graphite	4.4	4	1	NP
PPS-84% fiber glass	4.4	2	1	NP
Epoxy-71% fiber glass	4.4	5	1	NP
<b>Polymers as conveyor belts<sup>b</sup></b>				
SBR	—	8–11	1–2	DP; P
CR	—	5	1	NP
CR/SBR	—	8	1	DP
PVC	—	4–10	1–2	NP; DP

<sup>a</sup>P: propagating; DP: decelerating propagation; NP: nonpropagating.

<sup>b</sup>3–25 mm thick.

retarded polypropylene slab. The FPI values show the following flame propagation behavior in large-scale fires:

1.  $FPI \leq 7$ : there is no flame propagation beyond the ignition zone, defined as nonpropagating (NP). Polymers

showing this type of behavior are defined as Group 1-NP polymers. Flame is at a critical extinction condition.

2.  $7 < FPI < 10$ : there is decelerating flame propagation beyond the ignition zone, defined as decelerating

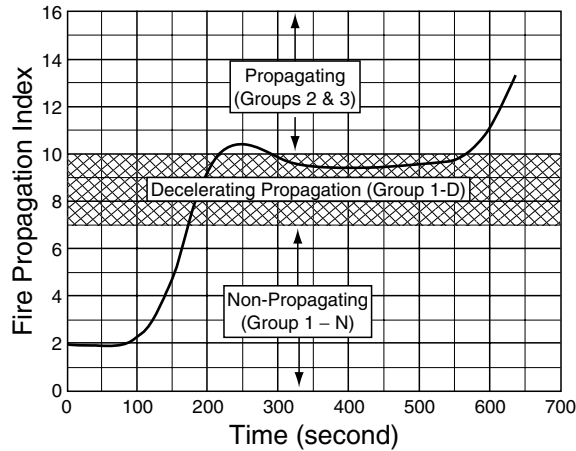


**FIGURE 53.3.** Fire propagation index versus time for a 10 mm thick, 100 mm wide, and 600 mm long vertical slab of fire retarded polypropylene in co-flowing air with 40% oxygen concentration. The sides and back of the slab were covered tightly with ceramic paper and heavy duty aluminum foil. The data were measured in the ASTM E 2058 FPA.

propagation (DP). Flame propagation beyond the ignition zone is limited. Polymers showing this type of behavior are defined as Group 1-*DP* polymers.

3.  $10 \leq \text{FPI} < 20$ : there is slow flame propagation beyond the ignition zone. Polymers showing this type of behavior are defined as Group 2 polymers.
4.  $\text{FPI} \geq 20$ : there is a rapid flame propagation beyond the ignition zone. Polymers showing this type of behavior are defined as Group 3 polymers.

The FPI is one of the most important fire properties to assess fire hazard and protection requirements. Increasing the TRP value and decreasing the heat release rate for polymers by various passive fire protection techniques would decrease the FPI value and change the fire propagation behavior from propagating to decelerating to non-propagating. Passive fire protection techniques could involve modifications of chemical structures, incorporation of fire retardants, and changes in the shape, size, and arrangements of the polymers, use of coatings, and inert barriers. The heat release rate could also be reduced by the application of active fire protection agents such as water, Halon and alternates, etc.

### 53.7 FIRE PROPERTIES ASSOCIATED WITH THE GENERATION OF PRODUCTS: YIELDS OF PRODUCTS

The mass generation rate of a product is directly proportional to the mass loss rate, the proportionality constant is defined as the yield of the product [3,4]:

$$\dot{G}_j'' = y_j \dot{m}_f'' \quad (53.10)$$

where  $\dot{G}_j''$  is the mass generation rate of product  $j$  ( $\text{kg}/\text{m}^2 - \text{s}$ ) and  $y_j$  is the yield of product  $j$  ( $\text{kg}/\text{kg}$ ). The average yield of a product is determined from the ratio of the total mass of the product generated,  $W_j$ , obtained by the summation of the mass generation rate of the products to the total mass of the polymer gasified,  $W_f$ , obtained by the summation of the mass loss rate:

$$y_j = \frac{W_j}{W_f} \quad (53.11)$$

The average yields of products obtained in this fashion are listed in Table 53.9.

#### 53.7.1 Generation Rates of Products at Various Heat Fluxes

The generation rates of products can be predicted at various heat flux values from the following relationship obtained from Eqs. (53.5) and (53.10):

$$\dot{G}_j'' = \left( \frac{y_j}{\Delta H_g} \right) (\dot{q}_e'' + \dot{q}_f'' - \dot{q}_{\text{tr}}''), \quad (53.12)$$

where  $y_j/\Delta H_g$  is defined as the product generation parameter (PGP) ( $\text{kg}/\text{kJ}$ ). PGP values of the products are independent of the fire size, but depend on the ventilation and can be calculated from the data such as listed in Tables 53.2, 53.5, and 53.9, from the slopes of the lines obtained by plotting the generation rates of the products against the external heat flux for various fire scenarios with specified external and flame heat flux values.

#### 53.7.2 Generation of Products and Ventilation

The concentrations of products generated at various ventilation conditions are predicted by the following equations [21]:

$$c_{j,v} = (y_{j,\infty}/S)(\rho_a/\rho_j)[1 + \{\alpha/\exp(\beta\Phi^{-\xi})\}]\Phi, \quad (53.13)$$

where  $c_{j,v}$  is the concentration for the ventilation controlled combustion;  $y_{j,\infty}/S$  is the yield of product  $j$  per unit mass of air consumed ( $\text{kg}/\text{kg}$ ) for well-ventilated combustion (values are listed in Table 53.10),  $\rho_a$  and  $\rho_j$  are the densities of air and product  $j$  respectively ( $\text{kg}/\text{m}^3$ ) ( $\rho_a/\rho_j$  values for  $\text{O}_2$ ,  $\text{CO}$ ,  $\text{CO}_2$ , hydrocarbons (methane) and smoke (carbon) are 0.905, 0.654, 1.034, 1.804, and 2.333, respectively);  $\Phi$  is the equivalence ratio (ratio of the amount of gasified polymer (fuel) to the amount of air, normalized by the stoichiometric air-to-fuel ratio; for well-ventilated combustion,  $\Phi < 1.0$  and for ventilation controlled combustion,  $\Phi > 1.0$ );  $\alpha$ ,  $\beta$ , and  $\xi$  are the ventilation correlation coefficients. Values for the coefficients for  $\text{CO}$ , hydrocarbons, and smoke listed in Table 53.11. For  $\text{O}_2$  and  $\text{CO}_2$ , the values of the coefficients are same and are independent of the chemical structures within the halogenated and nonhalogenated polymers (for

**TABLE 53.9.** Yields of products and heats of combustion for well ventilated combustion.<sup>a</sup>

Polymers <sup>b</sup>	Yield (kg/kg)				Heat of Combustion (MJ/kg) <sup>d</sup>			
	CO <sub>2</sub>	CO	Hyd <sup>c</sup>	Smoke	Comp	Chem	Con	Rad
<b>Natural polymers</b>								
Tissue paper	1.05	—	—	—	—	11.4	6.7	4.7
News paper	1.32	—	—	—	—	14.4	—	—
Wood (red oak)	1.27	0.004	0.001	0.015	17.1	12.4	7.8	4.6
Wood (Douglas fir)	1.31	0.004	0.001	—	16.4	13.0	8.1	4.9
Wood (pine)	1.33	0.005	0.001	—	17.9	12.4	8.7	3.7
Corrugated paper	1.22	—	—	—	—	13.2	—	—
Wood (hemlock) <sup>e</sup>	1.22	—	—	0.015	—	13.3	—	—
Wool 100% <sup>e</sup>	1.79	—	—	0.008	—	19.5	—	—
<b>Synthetic polymers</b>								
ABS <sup>e</sup>	—	—	—	0.105	—	30.0	—	—
POM	1.40	0.001	0.001	—	15.4	14.4	11.2	3.2
PMMA	2.12	0.010	0.001	0.022	25.2	24.2	16.6	7.6
PE	2.76	0.024	0.007	0.060	43.6	38.4	21.8	16.6
PP	2.79	0.024	0.006	0.059	43.4	38.6	22.6	16.0
PS	2.33	0.060	0.014	0.164	39.2	27.0	11.0	16.0
Silicon	0.96	0.021	0.006	0.065	21.7	10.6	7.3	3.3
Polyester-1	1.65	0.070	0.020	0.091	32.5	20.6	10.8	9.8
Polyester-2	1.56	0.080	0.029	0.089	32.5	19.5	—	—
Epoxy-1	1.59	0.080	0.030	—	28.8	17.1	8.5	8.6
Epoxy-2	1.16	0.086	0.026	0.098	28.8	12.3	—	—
Nylon	2.06	0.038	0.016	0.075	30.8	27.1	16.3	10.8
Polyamide-6 <sup>e</sup>	2.64	—	—	0.011	—	28.8	—	—
Silicon	0.96	0.21	0.005	0.078	21.7	10.9	—	—
<b>Expanded polyurethanes (flexible)</b>								
GM21	1.55	0.010	0.002	0.131	26.2	17.8	8.6	9.2
GM23	1.51	0.031	0.005	0.227	27.2	19.0	10.3	8.7
GM25	1.50	0.028	0.005	0.194	24.6	17.0	7.2	9.8
GM27	1.57	0.042	0.004	0.198	23.2	16.4	7.6	8.8
<b>Expanded polyurethanes (rigid)</b>								
GM29	1.52	0.031	0.003	0.130	26.0	16.4	6.8	9.6
GM31	1.53	0.038	0.002	0.125	25.0	15.8	7.1	8.8
GM35	1.58	0.025	0.001	0.104	28.0	17.6	7.8	9.8
GM37	1.63	0.024	0.001	0.113	28.0	17.9	8.7	9.2
GM41	1.18	0.046	0.004	—	26.2	15.7	5.7	10.0
GM43	1.11	0.051	0.004	—	22.2	14.8	6.4	8.4
<b>Expanded polystyrenes</b>								
GM47	2.30	0.060	0.014	0.180	38.1	25.9	11.4	14.5
GM49	2.30	0.065	0.016	0.210	38.2	25.6	9.9	15.7
GM51	2.34	0.058	0.013	0.185	35.6	24.6	10.4	14.2
GM53	2.34	0.060	0.015	0.200	37.6	25.9	11.2	14.7
<b>Expanded polyethylenes</b>								
1	2.62	0.020	0.004	0.056	41.2	34.4	20.2	14.2
2	2.78	0.026	0.008	0.102	40.8	36.1	20.6	15.5
3	2.60	0.020	0.004	0.076	40.8	33.8	18.2	15.6
4	2.51	0.015	0.005	0.071	40.8	32.6	19.1	13.5
<b>Expanded phenolics</b>								
1 <sup>e</sup>	0.92	—	—	0.002	—	10.0	—	—
2 <sup>e</sup>	0.92	—	—	—	—	10.0	—	—
<b>Halogenated polymers</b>								
PE + 25% chlorine	1.71	0.042	0.016	0.115	31.6	22.6	10.0	12.6
PE + 36% chlorine	0.83	0.051	0.017	0.139	26.3	10.6	6.4	4.2
PE + 48% chlorine	0.59	0.049	0.015	0.134	20.6	7.2	3.9	3.3

TABLE 53.9. *Continued.*

Polymers <sup>b</sup>	Yield (kg/kg)				Heat of Combustion (MJ/kg) <sup>d</sup>			
	CO <sub>2</sub>	CO	Hyd <sup>c</sup>	Smoke	Comp	Chem	Con	Rad
PVC	0.46	0.063	0.023	0.172	16.4	5.7	3.1	2.6
PVC-1 <sup>e</sup> (LOI = 0.50)	0.64	—	—	0.098	—	7.7	—	—
PVC-2 <sup>e</sup> (LOI = 0.50)	0.69	—	—	0.076	—	8.3	—	—
PVC <sup>e</sup> (LOI = 0.20)	0.93	—	—	0.099	—	11.3	—	—
PVC <sup>e</sup> (LOI = 0.25)	0.81	—	—	0.078	—	9.8	—	—
PVC <sup>e</sup> (LOI = 0.30)	0.85	—	—	0.098	—	10.3	—	—
PVC <sup>e</sup> (LOI = 0.35)	0.89	—	—	0.088	—	10.8	—	—
ETFE	0.54	0.060	0.020	0.042	12.6	5.4	—	—
PFA	0.37	0.097	—	0.002	5.0	4.7	—	—
FEP	0.25	0.116	—	0.003	4.8	4.1	—	—
TFE	0.38	0.092	—	0.003	6.2	4.2	—	—
<b>Polymers as building products<sup>e</sup></b>								
Particle board (PB)	1.28	0.004	—	—	—	14.0	—	—
Fiber board (FB)	1.28	0.015	—	—	—	14.0	—	—
Medium density FB	1.28	0.002	—	—	—	14.0	—	—
Wood panel	1.38	0.002	—	—	—	15.0	—	—
Melamine faced	0.98	0.025	—	—	—	10.7	—	—
Gypsum board (GB)	0.39	0.027	—	—	—	4.3	—	—
Paper on GB	0.49	0.028	—	—	—	5.6	—	—
Plastic on GB	1.31	0.028	—	—	—	14.3	—	—
Textile on GB	1.19	0.025	—	—	—	13.0	—	—
Textile on rock wool	2.29	0.091	—	—	—	25.0	—	—
Paper on PB	1.15	0.003	—	—	—	12.5	—	—
Rigid polyurethane	1.19	0.200	—	—	—	13.0	—	—
Expanded PS	2.60	1.9	0.054	—	—	28.0	—	—
<b>Composite systems</b>								
PEEK-fiber glass <sup>e</sup>	1.88	—	—	0.042	—	20.5	—	—
IPST-fiber glass <sup>e</sup>	2.48	—	—	0.032	—	27.0	—	—
Polyester1-fiber glass <sup>e</sup>	2.52	—	—	0.049	—	27.5	—	—
Polyester2-fiber glass <sup>e</sup>	1.47	—	—	—	—	16.0	—	—
Polyester3-fiber glass <sup>e</sup>	1.18	—	—	—	—	12.9	—	—
Polyester4-fiber glass	1.74	—	—	—	—	19.0	—	—
Polyester5-fiber glass	1.28	—	—	—	—	13.9	—	—
Polyester6-fiber glass	1.47	0.055	0.007	0.070	—	17.9	10.7	7.2
Polyester7-fiber glass	1.24	0.039	0.004	0.054	—	16.0	9.9	6.1
Polyester8-fiber glass	0.71	0.102	0.019	0.068	—	9.3	6.5	2.8
Epoxy1-fiber glass <sup>e</sup>	2.52	—	—	0.056	—	27.5	—	—
Epoxy2-fiber glass	1.10	0.166	—	0.128	—	11.9	—	—
Epoxy3-fiber glass	0.92	0.113	—	0.188	—	10.0	—	—
Epoxy4-fiber glass	0.94	0.132	—	0.094	—	10.2	—	—
Epoxy5-fiber glass	1.71	0.052	—	0.121	—	18.6	—	—
Epoxy-fiber glass-paint	0.83	0.114	0.016	0.166	—	11.3	6.2	5.1
Phenolic1-fiber glass	0.98	0.066	0.003	0.023	—	11.9	—	—
Phenolic2-fiber glass <sup>e</sup>	2.02	—	—	0.016	—	22.0	—	—
Phenolic-fiber glass-paint	1.49	0.027	0.002	0.059	—	22.9	11.5	11.4
Epoxy-fiberglass-phenolic	1.06	0.134	—	0.089	—	11.5	—	—
Vinylester-fiber glass	2.39	—	—	0.079	—	26.0	—	—
PPS-fiber glass	1.56	0.133	—	0.098	—	17.0	—	—
Phenolic-kevlar	1.27	0.025	0.002	0.041	—	14.8	11.1	3.7
Epoxy-kevlar-paint	0.873	0.091	0.016	0.126	—	11.4	6.3	5.1
Phenolic-kevlar-paint	1.67	0.026	0.003	0.062	—	24.6	14.0	10.6
Cyanate-graphite	1.73	0.058	—	0.102	—	18.9	—	—
Epoxy-graphite	1.63	0.046	—	0.107	—	17.8	—	—
Phenolic-graphite-paint	1.67	0.026	0.003	0.062	—	24.6	14.0	10.6

TABLE 53.9. Continued.

Polymers <sup>b</sup>	Yield (kg/kg)				Heat of Combustion (MJ/kg) <sup>d</sup>			
	CO <sub>2</sub>	CO	Hyd <sup>c</sup>	Smoke	Comp	Chem	Con	Rad
<b>Polymers as electrical cable insulation and jackets</b>								
<b>Polyethylene/polyvinylchloride cable</b>								
1	2.08	0.100	0.021	0.076	—	31.3	11.6	19.7
2	1.75	0.050	0.013	0.115	—	25.1	11.1	14.0
3	1.67	0.048	0.012	—	—	24.0	13.0	11.0
4	1.39	0.166	0.038	—	—	22.0	14.0	8.1
5	1.29	0.147	0.042	0.136	—	20.9	10.7	10.2
<b>Polyethylene-polypropylene copolymer/chlorosulfonated polyethylene cable</b>								
1	1.95	0.072	0.014	—	—	29.6	15.8	13.9
2	1.74	0.076	0.022	—	—	26.8	17.0	9.8
3	1.21	0.072	0.014	—	—	19.0	12.3	6.7
4	0.99	0.090	0.085	0.082	—	17.4	6.6	10.8
5	0.95	0.122	0.024	—	—	17.3	7.5	9.8
6	0.89	0.121	0.022	0.164	—	13.9	9.2	4.7
<b>Silicone/silicone cable</b>								
1	1.65	0.011	0.001	—	—	25.0	17.5	7.3
2	1.47	0.029	0.001	—	—	24.0	20.0	4.0
<b>Crosslinked polyethylene/crosslinked polyethylene cable</b>								
1	1.78	0.114	0.029	0.120	—	28.3	12.3	16.0
2	0.83	0.110	0.024	0.120	—	12.5	7.5	5.0
<b>Crosslinked polyethylene/neoprene cable</b>								
1	0.68	0.122	0.031	—	—	12.6	5.9	6.7
2	0.63	0.082	0.014	0.175	—	10.3	4.9	5.5
<b>Silicone/PVC cable</b>								
1	0.76	0.110	0.015	0.111	—	10.0	—	—
2	1.19	0.065	0.005	0.119	—	15.6	—	—
<b>PVC-nylon/PVC-nylon cable</b>								
1	0.63	0.084	0.024	—	—	10.2	5.0	5.2
2	0.49	0.082	0.032	0.115	—	9.2	4.8	4.4
<b>Polytetrafluoroethylene/polytetrafluoroethylene cable</b>								
1	0.180	0.091	0.012	0.011	—	3.2	2.7	0.4
2	0.383	0.103	—	0.005	—	5.7	—	—
<b>Polymers with fiberweb, net-like and multiplex structures</b>								
Olefin	1.49	0.006	—	—	—	16.5	13.3	3.2
PP-1	1.25	0.0029	—	—	—	14.0	10.8	3.2
PP-2	1.56	0.0048	—	—	—	17.2	10.5	6.7
Polyester-1	2.21	0.015	—	—	—	24.6	8.9	15.7
Polyester-2	1.51	0.0079	—	—	—	16.8	9.1	7.7
Polyester-3	2.55	0.020	—	—	—	28.5	22.6	5.9
Polyester-4	1.92	0.014	—	—	—	21.4	12.4	9.0
Rayon-1	1.80	0.043	—	—	—	20.3	14.1	6.2
Rayon-2	1.91	0.043	0.002	—	—	21.5	13.3	8.2
Rayon-3	1.18	0.047	—	—	—	13.5	8.3	5.2
Polyester-Rayon	1.52	0.005	—	—	—	16.8	9.1	7.7
Polyester-polyamide	1.82	0.008	—	—	—	20.2	10.4	9.8
Rayon-PE	1.50	0.027	—	—	—	16.9	8.72	8.2

<sup>a</sup>Data from the ASTM E 2058 FPA (Fig. 53.1). Some of the data are corrected to reflect well-ventilated combustion. All the data are reported for turbulent fires, i.e., polymers exposed to higher external heat flux values. —: either not measured or are less than 0.001.

<sup>b</sup>Abbreviations are listed in the nomenclature.

<sup>c</sup>Hyd: mixture of low molecular weight gaseous hydrocarbons.

<sup>d</sup>Comp: net complete heat of combustion; chem: chemical heat of combustion; con: convective heat of combustion; rad: radiative heat of combustion.

<sup>e</sup>Calculated from the data in Refs. 9, 10 and 23.



**TABLE 53.10.** Mass of O<sub>2</sub> consumed per unit mass of air and mass of products generated per unit mass of air consumed in mg/g.

Polymer	O <sub>2</sub>	CO <sub>2</sub>	CO	Hydrocarbons	Smoke
Polystyrene	200	177	4.55	1.06	12.4
Polypropylene	210	190	1.63	0.408	4.01
Polyethylene	208	188	1.63	0.476	4.08
Nylon	213	184	3.39	1.43	6.70
Polymethylmethacrylate	226	257	1.21	0.121	2.67
Wood	220	219	0.691	0.173	2.59
Polyvinylchloride	92	76	10.3	3.78	28.2

**TABLE 53.11.** Ventilation correlation coefficients for CO, hydrocarbons, and smoke for well ventilated combustion.<sup>a</sup>

Polymer	CO			Hydrocarbons			Smoke		
	$\alpha$	$\beta$	$\xi$	$\alpha$	$\beta$	$\xi$	$\alpha$	$\beta$	$\xi$
Polystyrene	2	2.5	2.5	25	5.0	1.8	2.8	2.5	1.3
Polypropylene	10	2.5	2.8	220	5.0	2.5	2.2	2.5	1.0
Polyethylene	10	2.5	2.8	220	5.0	2.5	2.2	2.5	1.0
Nylon	36	2.5	3.0	1200	5.0	3.2	1.7	2.5	0.8
Polymethylmethacrylate	43	2.5	3.2	1800	5.0	3.5	1.6	2.5	0.6
Wood	44	2.5	3.5	200	5.0	1.9	2.5	2.5	1.2
Polyvinylchloride	6.5	0.001	8.0	0.38	0.001	8.0	0.38	0.001	8.0

<sup>a</sup>From Ref. 21 and the ASTM E 2058 FPA in our laboratory.

the nonhalogenated polymers:  $\alpha = -1$ ,  $\beta = 2.5$ , and  $\xi = 1.2$ ; for the halogenated polymers,  $\alpha = -0.30$ ,  $\beta = 0.001$ , and  $\xi = 11.0$ .

The concentrations of products can be calculated from Eq. (53.13), such as shown in Fig. 53.4 for CO. The predicted concentrations are in good agreement with the concentrations measured in larger-scale fires [22].

For nonhalogenated polymers, the concentration predictions show three regions: (1) flaming combustion region for well ventilated combustion ( $\Phi < 1.0$ ), where a sufficient amount of oxygen is present and the concentrations of products of incomplete combustion are small; (2) transition combustion region for  $\Phi$  values between 1.0 and 3.5, where oxygen concentration is close to zero and concentrations of products of incomplete combustion are high; and (3) non-flaming combustion region for  $\Phi \geq 3.5$ , where pyrolysis becomes the dominant process. For halogenated polymers, only flaming combustion region ( $\Phi < 1.0$ ) and nonflaming combustion region ( $\Phi \geq 1.0$ ) are present.

The concentration variations with the equivalence ratio depends on the generic nature of the polymer. The increase in the concentration of hydrocarbons with the equivalence ratio follows the order:

1. Hydrocarbon: nylon > PMMA > PE and PP > wood and PS > PVC,
2. CO<sub>2</sub>: the concentrations for polymers with oxygen atom in the structure (PMMA and wood) are higher

than the concentrations for polymers with only carbon and hydrogen atoms (PS, PE, PE, and natural gas).

3. CO: the concentrations are high for oxygen containing polymers (PMMA, wood, and PU) and lower for non-

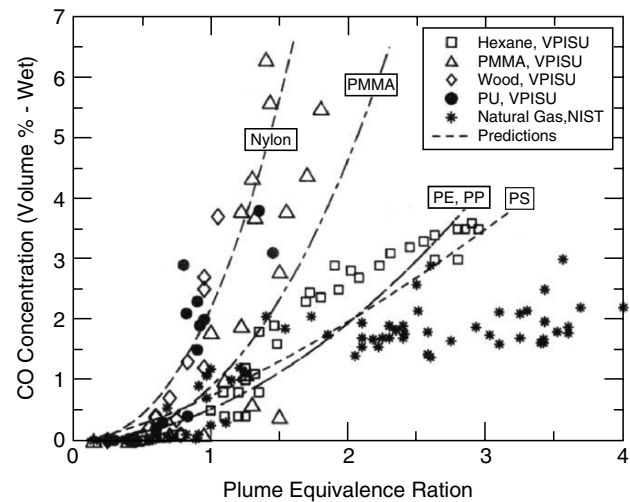


**FIGURE 53.4.** Carbon monoxide concentration versus the equivalence ratio. Symbols are the experimental concentrations measured in larger-scale fires by the Virginia Polytechnic Institute and State University (VPISU) and by the National Institute of Standards and Technology (NIST) [22]. Lines are the predicted concentrations from Eq. (53.13) using the data from Tables 53.10 and 53.11 and density ratio of 0.654.

oxygenated polymers (PE, PP, PS). The CO concentration increases with the molecular weight as predicted [2]. For example, within the carbon-hydrogen atom containing materials (PE, PP, PS, hexane, and natural gas), the CO concentration is lower for the lower molecular weight natural gas (mostly methane) than for the higher molecular weight hexane, PP, PE, and PS.

4. Smoke: the smoke concentration follows the order: PS (carbon-hydrogen atom aromatic bonds) > nylon (carbon-hydrogen-oxygen-nitrogen atom aliphatic bonds) > PE and PP (carbon-hydrogen atom aliphatic bonds) > wood (carbon-hydrogen-oxygen atom aliphatic bonds) > PMMA (carbon-hydrogen-oxygen atom aliphatic bonds). This order is opposite to the order for CO, but is expected on the basis of the fundamental understanding of the smoke formation in the combustion of the polymeric materials.

The concentration predictions can be used to define the experimental conditions in various toxicity, corrosion, and smoke damage evaluation tests. The correlations for the concentration predictions can be combined with various toxicity, corrosion, and smoke damage relationships, as inputs to the hazard assessment models.

### 53.8 FIRE PROPERTIES ASSOCIATED WITH THE GENERATION OF HEAT

The heat release rate is directly proportional to the mass loss rate and the proportionality constant is defined as the heat of combustion:

$$\dot{Q}_i'' = \Delta H_i \dot{m}_f'' \quad (53.14)$$

where  $\dot{Q}_i''$  is the heat release rate (kW/m<sup>2</sup>),  $\Delta H_i$  is the heat of combustion (kJ/kg), and  $\dot{m}_f''$  is the mass loss rate (kg/m<sup>2</sup>-s). The rate of heat release in a combustion process, within the flame, is defined as the chemical heat release rate. The chemical heat released within the flame is carried away from the flame by flowing product-air mixture and is emitted to the environment as radiation. The component of the chemical heat release rate carried away by the flowing products-air mixture is defined as the convective heat release rate. The component of the chemical heat release rate emitted to the environment is defined as the radiative heat release rate. The heat of combustion is defined respectively as the chemical, convective, and radiative heat of combustion.

The chemical heat release rate is determined from the carbon dioxide generation (CDG) and oxygen consumption (OC) calorimetries [2,3]. In the CDG calorimetry, the chemical heat release rate is determined from the mass generation rate of CO<sub>2</sub> corrected for CO [2,3]. In the OC calorimetry, the chemical heat release rate is determined from the mass consumption rate of O<sub>2</sub> [2,3,24]. The convective heat release rate is determined from the gas temperature rise

(GTR) calorimetry [2,3,25]. The radiative heat release rate is determined from the difference between the chemical and convective heat release rates [2,3].

#### 53.8.1 The CDG Calorimetry

The chemical heat release rate is determined from the following relationships:

$$\dot{Q}_{ch}'' = \Delta H_{co_2}^* \dot{G}_{co_2}'' + \Delta H_{co}^* \dot{G}_{co}'', \quad (53.15)$$

$$\Delta H_{co_2}^* = \frac{\Delta H_T}{\Psi_{co_2}}, \quad (53.16)$$

$$\Delta H_{co}^* = \left[ \frac{\Delta H_T - \Delta H_{co} \Psi_{co}}{\Psi_{co}} \right], \quad (53.17)$$

where  $\dot{Q}_{ch}''$  is the chemical heat release rate (kW/m<sup>2</sup>),  $\Delta H_{co_2}^*$  is the net heat of complete combustion per unit mass of CO<sub>2</sub> generated (MJ/kg),  $\Delta H_{co}^*$  is the net heat of complete combustion per unit mass of CO generated (MJ/kg),  $\Delta H_T$  is the net heat of complete combustion per unit mass of fuel consumed (kJ/g),  $\Psi_{co_2}$  is the stoichiometric yield of CO<sub>2</sub> (kg/kg),  $\Psi_{co}$  is the stoichiometric yield of CO (kg/kg),  $\dot{G}_{co_2}''$  is the generation rate of CO<sub>2</sub> (kg/m<sup>2</sup>-s) and  $\dot{G}_{co}''$  is the generation rate of CO (kg/m<sup>2</sup>-s).

The values of  $\Delta H_{co_2}^*$  and  $\Delta H_{co}^*$  for over 200 fuels are tabulated in Tewarson [2]. The values depend on the chemical structures of the fuels. With some exceptions, the values remain approximately constant within each generic group of fuels. For approximate calculations, the average values can be used, which are:  $\Delta H_{co_2}^* = 13.3 \text{ kJ/g} \pm 11\%$ , and  $\Delta H_{co}^* = 11.1 \text{ kJ/g} \pm 18\%$ .

In the CDG calorimetry, the CO correction for well-ventilated combustion is very small, because of the small amounts of the CO generated. The variations of 11% and 18% in the  $\Delta H_{co_2}^*$  and  $\Delta H_{co}^*$  values, respectively, would reduce significantly if values for low molecular weight hydrocarbons with small amounts of O, N, and halogen were used in averaging.

For the determination of the chemical heat release rate, mass generation rates of CO<sub>2</sub> and CO are measured and actual values of  $\Delta H_{co_2}^*$  and  $\Delta H_{co}^*$  are used for accuracy or the average values for approximate results. The CO<sub>2</sub> and CO measurement details are described in Tewarson [2].

#### 53.8.2 The OC Calorimetry

The chemical heat release rate is determined from the following relationship:

$$\dot{Q}_{ch}'' = \Delta H_0^* \dot{C}_0'', \quad (53.18)$$

$$\Delta H_0^* = \frac{\Delta H_T}{\Psi_0}, \quad (53.19)$$

where  $\Delta H_0^*$  is the net heat of complete combustion per unit mass of oxygen consumed (MJ/kg),  $\dot{C}_0''$  is the mass consumption rate of oxygen (kg/m<sup>2</sup>-s) and  $\Psi_0$  is the stoichiometric mass-oxygen-to-fuel ratio (kg/kg).

The values of  $\Delta H_0^*$  for over 200 fuels are tabulated in Tewarson [2]. The values depend on the chemical structures of the fuels. With some exceptions, the values remain approximately constant within each generic group of fuels. For approximate calculations, the average value can be used, which is:  $\Delta H_0^* = 12.8 \text{ kJ/g} \pm 7\%$ . The variation of  $\pm 7\%$  would reduce significantly if values for low molecular weight hydrocarbons with small amounts of O, N, and halogen were used in averaging.

For the determination of the chemical heat release rate, mass consumption rate of O<sub>2</sub> is measured and the actual value of  $\Delta H_0^*$  is used for accuracy or the average value for approximate results. The O<sub>2</sub> measurement details are described in Tewarson [2].

The chemical heat release rates determined from the CDG and OC calorimetries are very similar.

### 53.8.3 The GTR Calorimetry

The convective heat release rate is determined from the following relationship:

$$\dot{Q}_{\text{con}}'' = \frac{\dot{W}c_p(T_g - T_a)}{A}, \quad (53.20)$$

where  $\dot{Q}_{\text{con}}''$  is the convective heat release rate (kW/m<sup>2</sup>),  $c_p$  is the specific heat of the combustion product-air mixture at the gas temperature (MJ/kg-K),  $T_g$  is the gas temperature (K),  $T_a$  is ambient temperature (K),  $\dot{W}$  is the total mass flow rate of the fire product-air mixture (kg/s), and  $A$  is the total exposed surface (m<sup>2</sup>).

For the determination of the convective heat release rate, temperature and total mass flow rate of the fire-products air mixture are measured. The literature value of the specific heat of air at the gas temperature is used as the fire products are diluted by fresh air by about 20 times their volume. The temperature and mass flow rate measurement details are described in Tewarson [2].

### 53.8.4 Heat of Combustion

The average heat of combustion is determined from the ratio of the energy,  $E_i$ , obtained from the summation of the chemical, convective, and radiative heat release rates and the total mass of gasified polymer,  $W_f$ , obtained from the summation of the mass loss rate:

$$\Delta H_i = \frac{E_i}{W_f}, \quad (53.21)$$

where  $\Delta H_i$  is the average chemical, convective, or radiative heat of combustion (MJ/kg). The values of the average heat

of combustion obtained in this fashion are listed in Table 53.9. The radiative heat of combustion is obtained from the difference between the chemical and convective heats of combustion, as heat losses are negligibly small in the ASTM E 2058 FPA.

### 53.8.5 Heat Release Rate at Various Heat Fluxes

The heat release rate can be predicted at various heat flux values from the following relationship obtained from Eqs. (53.5) and (53.14):

$$\dot{Q}_i'' = \left( \frac{\Delta H_i}{\Delta H_g} \right) (\dot{q}_e'' + \dot{q}_f'' - \dot{q}_{rr}''), \quad (53.22)$$

where  $\Delta H_i/\Delta H_g$  is defined as the heat release parameter (HRP) (kJ/kJ). HRP values are independent of the fire size, but depend on the ventilation and can be calculated from the data such as listed in Tables 53.2 and 53.9 or from the slopes of the lines obtained by plotting the heat release rates against the external heat flux. The heat release rate can be calculated from the HRP and  $\dot{q}_{rr}''$  values for the fire scenario for specified external and flame heat flux values.

### 53.8.6 Generation of Heat and Ventilation

The relationship between heat release rate or heat of combustion and the equivalence ratio is expressed as [21]:

$$\dot{Q}_{i,v}'' = \dot{Q}_{i,\infty}'' \left[ 1 - \frac{\alpha}{\exp \beta \Phi^{-\xi}} \right], \quad (53.23)$$

$$\Delta H_{i,v} = \Delta H_{i,\infty} \left[ 1 - \frac{\alpha}{\exp \beta \Phi^{-\xi}} \right], \quad (53.24)$$

$$\chi_v = \chi_\infty \left[ 1 - \frac{\alpha}{\exp \beta \Phi^{-\xi}} \right], \quad (53.25)$$

where  $\dot{Q}_{i,v}''$  is the heat release rate,  $\Delta H_{i,v}$  is the heat of combustion, and  $\chi_v$  is the combustion efficiency for the ventilation-controlled combustion (kW/m<sup>2</sup>),  $\dot{Q}_{i,\infty}''$  is the heat release,  $\Delta H_{i,\infty}$  is the heat of combustion, and  $\chi_\infty$  is the combustion efficiency for the well-ventilated combustion (kW/m<sup>2</sup>), and  $\alpha$ ,  $\beta$  and  $\xi$  are the ventilation correlation coefficients. Combustion efficiency is the ratio of the chemical heat release rate or chemical heat of combustion to the heat release rate for complete combustion or net heat of complete combustion. For the nonhalogenated polymers,  $\alpha = 0.97$ ,  $\beta = 2.5$ , and  $\xi = 1.2$  for the chemical heat release rate or the chemical heat of combustion and  $\alpha = 1.0$ ,  $\beta = 2.5$ , and  $\xi = 2.8$  for the convective heat release rate or the convective heat of combustion. For the halogenated polymers,  $\alpha = 0.30$ ,  $\beta = 0.001$ , and  $\xi = 11$  for the chemical heat release rate or the chemical heat of combustion. Chemical heat release rate, chemical heat

of combustion, and combustion efficiency decrease with ventilation restriction or increase in the equivalence ratio.

Figure 53.5 shows the combustion efficiency calculated from Eq. (53.25). As expected, combustion efficiency decreases with increase in the equivalence ratio due to limitation in the availability of air. For the nonhalogenated polymers, flame extinction occurs for combustion efficiency between about 0.20 and 0.40. The halogenated polymer burns with a low combustion efficiency; a slight decrease in the combustion efficiency (below about 0.30) results in flame extinction, although combustion remains well ventilated. The combustion efficiency decreases rapidly with increase in the equivalence ratio for the low molecular fuel (natural gas, methane) compared to the polymers, which gasify as higher molecular weight oligomer.

### 53.9 FIRE PROPERTIES ASSOCIATED WITH CORROSION AND SMOKE DAMAGE

#### 53.9.1 Corrosion Damage

The fire property associated with corrosion damage is defined as corrosion index (CI), which is the corrosion rate per unit mass concentration of the products  $[(\text{\AA}/\text{min})/(\text{g of polymer gasified}/\text{m}^3 \text{ of air flow})]$  [2,3]:

$$CI = \{ \delta_{\text{loss}} / \Delta t_{\text{exposure}} \} / \{ W_f / \dot{V}_T \Delta t_{\text{test}} \}, \quad (53.26)$$

where CI is in  $(\text{\AA}/\text{min})/(\text{mg}/\text{g})$ ,  $\delta_{\text{loss}}$  is the metal loss due to corrosion ( $\text{\AA}$ ),  $\Delta t_{\text{exposure}}$  is the time the corrosive product deposit is left on the surface of the metal (min),  $W_f$  is the total mass of the polymer lost in the experiment (g),  $\dot{V}_T$  is the total volumetric flow rate of the mixture of fire products and air ( $\text{m}^3/\text{s}$ ) and  $\Delta t_{\text{test}}$  is the combustion duration (s).

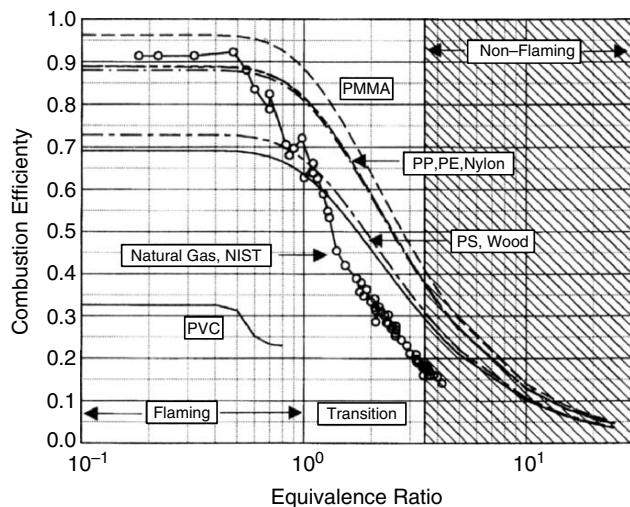


**FIGURE 53.5.** Calculated combustion efficiency versus the equivalence ratio. For the calculations, Eq. (53.25) and data from Table 53.9 and [2] were used. For natural gas, the data measured at the National Institute of Standards and Technology (NIST) as reported in [22] were used.

Corrosion is measured by exposing metal surfaces to the flowing fire products in the sampling duct of the ASTM E 2058 FPA. The change in resistance due to corrosion is measured as a function of time such as shown in Fig. 53.6. The slopes of the lines represent corrosion rates, ( $\text{\AA}/\text{min}$ ). In Fig. 53.6, corrosion rate is faster for the polyester-PVC-fiber glass sample than it is for the fire-retarded (FR) polypropylene (PP) sample. PP polymer sample shows negligible corrosion as it does not contain halogen atoms.

The total mass loss of the polymer lost (g), total volumetric flow rate of the mixture of fire products and air mixture ( $\text{m}^3/\text{s}$ ) and combustion duration (s) are measured in the experiments.

The CI values for various polymers have been determined in the flammability apparatus; Table 53.12 lists values for some selected polymers, as examples. The CI values for nonhalogenated polypropylene and wood are negligibly small. For the highly halogenated polymers, the CI value is

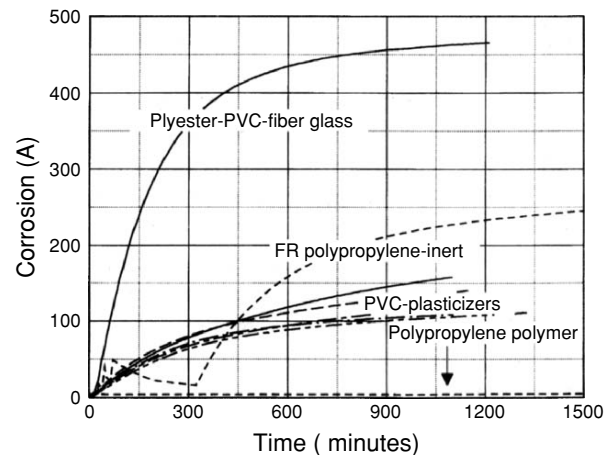


**FIGURE 53.6.** Corrosion of thin copper strip on a fiber glass polyester plate by the flowing combustion products-air mixture in the sampling duct of the ASTM E 2058 FPA.

**TABLE 53.12.** Corrosion index for selected polymers.<sup>a</sup>

Materials	Corrosion index [( $\text{\AA}/\text{min}$ )/(g polymer gasified/ $\text{m}^3$ of air)]
Polyvinylchloride (PVC) <sup>b-1</sup>	1.8
PVC-2	0.78
PVC-3	0.60
PVC-4	0.36
Polypropylene	0.074
Polypropylene/fire retardant	1.7
Teflon <sup>®</sup> (TFE)	0.28
Wood	0.088

<sup>a</sup>Determined in the ASTM E 2058 FPA at the Factory Mutual Research Corporation.

<sup>b</sup>Amount of nonhalogenated additive increasing from 1 to 4.

high if hydrogen atoms are present in the structure (PVC) or halogenated fire-retardant additive is present (PP/FR), and is low if there are no hydrogen atoms in the structure (Teflon<sup>®</sup> TFE). The difference in the CI values indicate the importance of water as a combustion product to generation acids for PVC and PP/FR. Teflon<sup>®</sup> (TFE) does not generate water as a product of combustion and thus the formation of an acid (HF) would depend on the efficiency of the hydrolysis process between the ambient water from air and Teflon<sup>®</sup> (TFE) vapors. The hydrolysis process appears to be inefficient. The CI value decreases with increase in the amount of non-halogenated additive (PVC-1 to -4).

### 53.9.2 Smoke Damage

The fire property associated with smoke damage is the ratio of the yield of smoke-to-the yield of CO<sub>2</sub>. The ratio increases with increase in the equivalence ratio or ventilation restriction. The yield of smoke is proportional to the smoke generation rate and the yield of CO<sub>2</sub> is proportional to the chemical heat release rate. The higher the ratio of the yield of smoke to the yield of CO<sub>2</sub>, higher the damage due to smoke relative to the damage due to heat.

Smoke is a mixture of black carbon (soot) and aerosol [26,27]. It has been suggested that soot nucleation and growth occur near the highly ionized regions of the flames in combustion processes, and that some of the charges are transferred to smoke particles. Multimodal distributions show that the soot particle radii belong to three “modes” [26]:

1. “Nuclei mode” has a geometric mean radius between 0.0025 and 0.020  $\mu$  and probably results from the condensation of gaseous carbon moieties.
2. “Accumulation mode” encompasses particles in the size range 0.075–0.25  $\mu$  and apparently results from the coagulation and condensation of the “nuclei mode” particles.
3. “Coarse mode” at several microns that is attributed to the precipitation of fine particles on the walls of vehicle exhaust systems and a subsequent entrainment in the issuing gases.

In fires, large variations in smoke particle size are due to coagulation and condensation. Data from various fires show that initially the smoke particles are in the coarse mode. As the smoke moves away from the fire origin, large particles settle down to the floor, leaving small particles having radii of 0.04–0.09  $\mu$  (accumulation mode). It thus appears that smoke damage in the room of fire origin is expected to be due to particles of several microns in radius in the coarse mode, whereas smoke damage downstream of the fire is expected to be due to particles with radius less than 0.1  $\mu$  in the lower end of the accumulation mode. Soot is an efficient absorber of HCl. In the combustion of 79.5%

PVC-20.5% PE, 19 mg of HCl/g of smoke is loosely bound and 27 mg of HCl/gm of smoke is tightly bound to soot [28].

Smoke damage in industrial and commercial occupancies is considered in terms of discoloration and odor of the property exposed to smoke, interference in the electric conduction path and corrosion of the parts exposed to smoke is a carrier of the corrosive products.

## 53.10 FIRE PROPERTIES ASSOCIATED WITH FIRE SUPPRESSION/EXTINGUISHMENT

Several fire properties are associated with fire suppression/extinguishment by active and passive fire protection techniques. Changes in the values of the properties are used to assess the effectiveness of the techniques. Passive fire protection techniques enhance resistance to: (1) pyrolysis, ignition, combustion, and fire propagation processes, and (2) generation of heat and products. Active fire protection techniques provide hinderance to the growth of the fire by: (1) interacting with the burning polymer in the solid phase (mainly removal of heat) [29]; (2) reducing the availability of the oxygen to the fire (creation of nonflammable mixture); and (3) removal of heat from the flame and interference with the chemical reactions within the flame [30].

### 53.10.1 Passive Fire Protection

Passive fire protection is provided by various chemical and physical means.

#### *Increasing the Resistance to Ignition and Fire Propagation by Increasing the Values of CHF and TRP*

The CHF and TRP values can be increased by modifying the pertinent parameters such as the chemical bond dissociation energy and thermal diffusion (combination of the density, specific heat and thermal conductivity).

#### *Decreasing the Values of the HRP and the Flame Heat Flux*

The heat release rate is equal to the Heat Release Parameter (HRP) times the net heat flux [Eq. (53.22)]. Decrease in the HRP value would decrease the heat release rate. The HRP value can be decreased by decreasing the heat of combustion and/or increasing the heat of gasification by various chemical and physical means. An examination of the data in Table 53.9 for heat of combustion show that introduction of oxygen, nitrogen, sulfur, halogen, and other atoms into the chemical structures of the polymers reduces the heat of combustion. For example, the heat of combustion decreases when the hydrogen atoms attached to

carbon atoms in polyethylene are replaced by the halogen atoms, such as by fluorine in TFE. The chemical heat of combustion decreases from 38.4 MJ/kg to 4.2 MJ/kg and the HRP value decreases from 17 to 2 (Table 53.9).

The HRP values can also be reduced by increasing the heat of gasification and decreasing the heat of combustion by retaining the major fraction of the carbon atoms in the solid phase, a process defined as charring. Several passive fire protection agents are commercially available to enhance the charring characteristics of materials.

The effect on flame heat flux by passive fire protection is determined by using the radiation scaling technique, where combustion experiments are performed in oxygen concentration higher than the ambient values. As discussed previously, liquids which vaporize primarily as monomers or as very low molecular weight oligomer, the flame heat flux values are in the range of 22–44 kW/m<sup>2</sup>, irrespective of their chemical structures. For solid polymers, which vaporize as high molecular weight oligomer, the flame heat flux values increase substantially to the range of 49–71 kW/m<sup>2</sup>, irrespective of their chemical structures. Passive fire protection agents which can reduce the molecular weight of the pyrolysis products of the polymers would be effective in reducing the flame heat flux and complement the active fire protection agents.

#### *Changing the Melting Behavior of Materials*

The chemical heat release rate increases very rapidly as a polymer changes from a solid to a boiling liquid pool, creating dangerous conditions and presenting a serious challenge to the active fire protection agents. Inert passive fire protection agents added to the polymer which would eliminate the boiling liquid pool would be effective in complementing the active fire protection agents.

#### *Decreasing the Value of the Product Generation Parameter (PGP)*

Nonhalogenated passive fire protection agents which reduce or eliminate the release of halogenated and highly aromatic products and enhance release of aliphatic products, rich in hydrogen and oxygen atoms but poor in carbon atoms, would be effective in reducing the nonthermal damage due to smoke and corrosion. Some of the passive fire protection agents, available commercially, interact with the polymers in the solid as well as in the gas phase during pyrolysis and combustion.

The critical parameter that needs to be examined in the presence and absence of the passive fire protection agents is the ratio of PGP (smoke, CO, corrosive and toxic products) to HRP. The effectiveness of the passive fire protection agent would be reflected in the small values of the ratios at fire control, suppression, and/or extinguishment stage.

### **53.10.2 Active Fire Protection**

Active fire protection is provided by applying agents as liquids, gases, solid powders, or foams to the flame and/or to the surface of the burning polymers.

#### *Flame Suppression/Extinguishment by Liquid Vapors and Gaseous Agents*

A flame will extinguish when the time required for the chain reaction which sustains the combustion process exceeds the time it takes to replenish the necessary heat and reactants [30]. The most commonly used liquid and gaseous chemical inhibition agents at the present time are: Halon<sup>1</sup> - 1211 (CBrClF<sub>2</sub>), 1301 (CBrF<sub>3</sub>), and 2402 (CBrF<sub>2</sub>CBrF<sub>2</sub>). Because of the contribution of Halons to depletion of the stratospheric ozone layer, they will, however, not be used in the future [30]. There is thus an intense effort underway to develop alternative fire suppressants to replace ozone layer depleting Halons. The Halon alternatives belong to one of the following classes: (1) Hydrobromofluorocarbons (HBFC); (2) Chlorofluorocarbons (CFC); (3) Hydrochlorofluorocarbons (HCFC); (4) Perfluorocarbons (FC); (5) Hydrofluorocarbons (HFC); and (6) Inert gases and vapors.

The most common test to screen the Halon alternates is the “cup burner” test, where concentration of Halons or alternates required for extinction of a small laminar diffusion flame are determined. Table 53.13 lists the concentrations of Halon 1301 and alternates required for heptane flame extinction in the “cup burner” test. Acceptable total flooding agents in normally occupied areas are indicated by bold letters and numbers.

When the amount of an agent applied to a burning polymer is close to the amount required for flame extinction, first flame instability sets in, followed by flame liftoff from the surface and finally the flame is extinguished, as indicated in Fig. 53.7 for the flame extinction of PMMA by Halon 1301. Initially there is a rapid decrease in the chemical heat release rate as Halon is added to the flame. There is a gradual increase in the chemical heat release rate between 5.40% and 6.25% of Halon unto flame extinction. The increase in the chemical heat release rate appears to be due to increase in the flame luminosity (increase in the flame radiative heat flux transferred back to the fuel surface).

Figure 53.8 shows that the generation efficiencies of CO, mixture of hydrocarbons, and smoke increase significantly with increase in the Halon concentration. The effect of Halon on the generation efficiencies is strong for CO and the mixture of hydrocarbons and weak for smoke. This type of combustion behavior of PMMA is similar to one found with the ventilation controlled combustion, i.e., increasing preference of fuel carbon atom to convert to CO and the mixture of hydrocarbons rather than to smoke. It thus appears that the chemical interruption processes for flame extinction by Halon and reduced oxygen are very similar.

**TABLE 53.13.** Concentrations of halon 1301 and alternates required for flame extinction in the heptane “cup burner” test.<sup>a</sup>

Agent Name	Formula	Concentration (volume %)	Relative concentration
Inert Agents			
Nitrogen	N <sub>2</sub>	32	11.0
Carbon dioxide	CO <sub>2</sub>	23	7.9
Helium	He	31	10.7
Argon	Ar	41	14.1
Silicone Containing Agent			
Silicone tetrafluoride	SiF <sub>4</sub>	36	12.4
Sodium Containing Agent			
Sodium bicarbonate (10–20 μm)	NaHCO <sub>3</sub>	3.0 <sup>b</sup>	—
Halon			
Halon 1301	CF <sub>3</sub> Br	2.9	1.0
HFC			
HCFC-22 (Du Pont FE 232)	CHClF <sub>2</sub>	11.6	4.00 <sup>b</sup>
HBFC-22B1 (Great Lakes FM 100)	CHBrF <sub>2</sub>	4.4	1.52
HFC-23 (Du Pont FE13)	CHF <sub>3</sub>	12.4	4.28
HFC-32	CH <sub>2</sub> F <sub>2</sub>	8.8	3.03
HCFC-124	CHClFCF <sub>3</sub>	8.2	2.83
HBFC-124B1	CF <sub>3</sub> CHBrF <sub>3</sub>	2.8	0.97
HFC-125 (Du Pont FE 25)	CF <sub>3</sub> CHF <sub>2</sub>	9.40	3.24
HFC-134	CHF <sub>2</sub> CHF <sub>2</sub>	11.2	3.86
HFC-134a	CF <sub>3</sub> CH <sub>2</sub> F	10.5	3.62
HFC-142b	CClF <sub>2</sub> CH <sub>3</sub>	11.0 (calc)	3.79
HFC-152a	CHF <sub>2</sub> CH <sub>3</sub>	27.0 (calc)	9.31
HFC-218	CF <sub>3</sub> CF <sub>2</sub> CF <sub>3</sub>	6.1	2.10
HFC-227ea (Great Lakes FM 200)	CF <sub>3</sub> CHFCF <sub>3</sub>	6.1	2.10 <sup>b</sup>
Trifluoromethyl iodide 1311	CF <sub>3</sub> I	3.0	1.03
FC-14	CF <sub>4</sub>	13.8	4.76
FC-116	CF <sub>3</sub> CF <sub>3</sub>	7.8	2.69
C318	C <sub>4</sub> F <sub>8</sub>	7.3	2.52
FC-5-1-14 (3M PFC 614)	C <sub>4</sub> F <sub>10</sub>	5.5	1.90 <sup>b</sup>

<sup>a</sup>From Refs. 30 and 31.

<sup>b</sup>Acceptable total flooding agents in normally occupied areas [32].

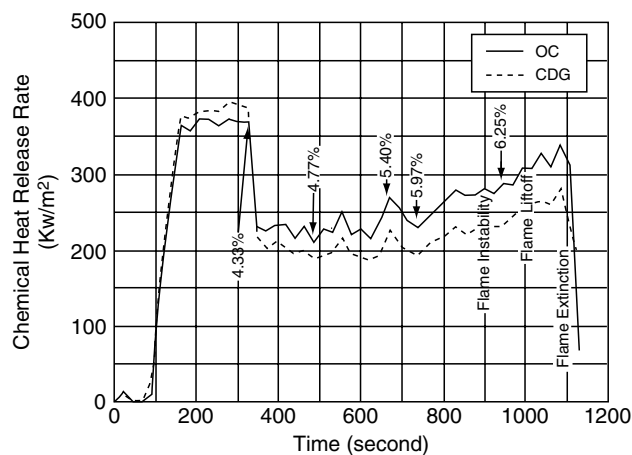


**FIGURE 53.7.** Chemical heat release rate versus time for the combustion of 100 mm × 100 mm × 25 mm thick horizontal slab of polymethylmethacrylate exposed to 40 kw/m<sup>2</sup> in co-air flow with varying Halon 1301 concentration at a velocity of 90 mm/s in the ASTM E 2058 FPA. Numbers and their locations represent Halon 1301 concentrations in volume percents and application times. Times for flame instability, liftoff, and extinction are also indicated.

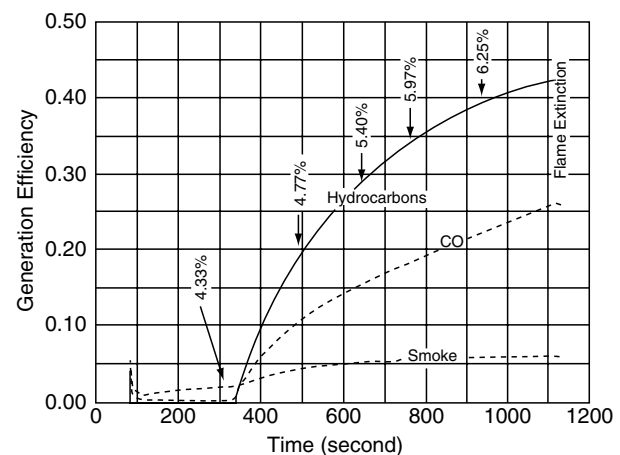


**FIGURE 53.8.** Generation efficiencies of CO, mixture of hydrocarbons, and smoke versus time for the combustion of 100 mm × 100 mm × 25 mm thick horizontal slab of polymethylmethacrylate exposed to 40 kw/m<sup>2</sup> in co-air flow with varying Halon 1301 concentration at a velocity of 90 mm/s in the ASTM E 2058 FPA. Numbers and their locations represent Halon 1301 concentrations in volume percents and application times. Times for flame instability, liftoff, and extinction are also indicated.

This experimental finding is consistent with the concept that a critical value of the Damkohler number for flame extinction [30].

The existence of the critical conditions at flame extinction has also been postulated by the “Fire Point Theory” [29] and supported by the experimental data for the critical mass pyrolysis and heat release rates [2].

The fire property associated with flame extinction by gaseous agents thus would be the critical value of the HRP.

### Flame Suppression/Extinguishment by Liquids

At the flame extinction condition, the critical mass pyrolysis and heat release rates can be expressed as:

$$\dot{m}_{\text{cr}}'' = \frac{\dot{q}_e'' + \dot{q}_f'' - \dot{q}_{\text{tr}}'' - \dot{q}_w''}{\Delta H_g}, \quad (53.27)$$

$$\dot{Q}_{\text{cr}}'' = \left[ \frac{\Delta H_{\text{ch}}}{\Delta H_g} \right] (\dot{q}_e'' + \dot{q}_f'' - \dot{q}_{\text{tr}}'' - \dot{q}_w''), \quad (53.28)$$

where  $\dot{m}_{\text{cr}}''$  is the critical mass pyrolysis rate for flame extinction ( $\text{kg}/\text{m}^2\text{-s}$ ),  $\dot{q}_e''$  is the external heat flux ( $\text{kW}/\text{m}^2$ ),  $\dot{q}_f''$  is the flame heat flux transferred back to the surface ( $\text{kW}/\text{m}^2$ ),  $\dot{q}_{\text{tr}}''$  is the surface re-radiation loss ( $\text{kW}/\text{m}^2$ ),  $\Delta H_g$  is the heat of gasification ( $\text{kJ}/\text{kg}$ ),  $\dot{Q}_{\text{cr}}''$  is the critical value of the chemical heat release rate for flame extinction ( $\text{kW}/\text{m}^2$ ),  $\Delta H_{\text{ch}}$  is the chemical heat of combustion ( $\text{kJ}/\text{kg}$ ),  $\Delta H_{\text{ch}}/\Delta H_g$  is the HRP, and  $\dot{q}_w''$  is the heat flux removed from the surface of a burning polymer by a liquid such as water, as a result of vaporization expressed as:

$$\dot{q}_w'' = \varepsilon_w \dot{m}_w'' \Delta H_w, \quad (53.29)$$

where  $\varepsilon_w$  is the water application efficiency,  $\dot{m}_w''$  is the water application rate per unit surface area of the polymer ( $\text{kg}/\text{m}^2\text{-s}$ ), and  $\Delta H_w$  is the heat of gasification of water (2.58 MJ/kg). If only part of the water applied to a hot surface evaporates and the other part forms a puddle, such as on a horizontal surface, blockage of flame heat flux to the surface and escape of the fuel from the polymer surface are expected. Eq. 53.27 thus is modified as:

$$\dot{q}_w'' = \dot{m}_w'' (\varepsilon_w \Delta H_w + \delta_w), \quad (53.30)$$

where  $\delta_w$  is the energy associated with the blockage of flame heat flux to the surface and escape of the fuel vapors per unit mass of the fuel (MJ/kg).

From Eqs. 53.27 and 53.30, with no external heat flux:

$$\dot{m}_w'' = \frac{\dot{q}_f'' - \dot{q}_{\text{tr}}''}{\varepsilon_w \Delta H_w + \delta_w} - \frac{\dot{m}_{\text{cr}}'' \Delta H_g}{\varepsilon_w \Delta H_w + \delta_w}. \quad (53.31)$$

The first term on the right-hand side takes into account the effects of the physical differences on flame extinction such as the fire size and polymer shape, size, and arrangement. The second term on the right-hand side takes into account

the effects of the chemical differences on flame extinction such as the chemical structures of the polymers and additives. In large-scale fires, the second term is negligibly small and water application rate required for flame extinction depends mainly on the flame heat flux, surface re-radiation loss, and mode of water application.

The critical values of the mass pyrolysis rate, heat release rates, and water application rates for flame extinction for polymers, are listed in Table 53.14. For the polymers listed in the table, the critical values of the heat release rates do not depend on the generic natures of the polymers. The average critical values of the chemical, convective, and radiative heat release rates are  $100 \pm 7$ ,  $53 \pm 9$ , and  $47 \pm 10 \text{ kW}/\text{m}^2$ , respectively. The critical water application rate required for flame extinction is: polyoxymethylene, polymethylmethacrylate and polyethylene with 25% chlorine ( $2.1\text{--}2.5 \text{ g}/\text{m}^2\text{-s}$ ) < polyethylene and polypropylene ( $3.5\text{--}4.1 \text{ g}/\text{m}^2\text{-s}$ ) < polystyrene ( $5.1 \text{ g}/\text{m}^2\text{-s}$ ).

### 53.11 STANDARDS AND TESTING OF POLYMER PRODUCTS AND MATERIALS

Polymer products are used in a variety of applications in residential, private, government, industrial, transportation, and manufacturing occupancies. Consequently, for the assessment of the fire hazards of polymer products large numbers of fire scenarios need to be considered for testing. To avoid this problem of large number of fire scenarios to be considered for testing, two types of standard test methods have been developed:

1. *Test methods to comply with specific regulations or voluntary agreements*: these types of test methods are usually larger than laboratory-scale tests and are included in the prescriptive (specification)-based fire codes<sup>1</sup>. Generally, products in their end-use configurations are tested under a defined fire condition.
2. *Small-scale standard test methods*: these types of test methods have been developed based on qualitative experiences as well as on the understanding of fire stages and associated hazards. Relatively simple types of measurements are made for various fire properties of the polymeric materials for each fire stage. These types of standard test methods are useful for the performance-based fire codes which are being considered to augment or replace the prescriptive-based fire codes<sup>2</sup> [33–35].

Both types of standard test methods for products in their end-use configurations and polymeric materials used for the construction of products are promulgated by various

<sup>1</sup> The codes reflect expectations for the level of fire protection.

<sup>2</sup> An example of the prescriptive-based code for passive fire protection is the specified fire resistance rating for an interior wall, whereas for the performance-based code it would be a prediction for the desired passive fire protection based on the engineering standards, practices, tools, and methodologies.



**TABLE 53.14.** Critical mass pyrolysis, heat release, and water application rate.<sup>a</sup>

Polymers	Critical values for flame extinction				
	$\dot{m}''_{cr}(\text{kg}/\text{m}^2\text{-s}) \times 10^3$	$\dot{Q}''_{ch}(\text{kW}/\text{m}^2)$	$\dot{Q}''_{con}(\text{kW}/\text{m}^2)$	$\dot{Q}''_{rad}(\text{kW}/\text{m}^2)$	$\dot{W}''_w(\text{kg}/\text{m}^2\text{-s}) \times 10^3$
Polyoxymethylene	4.5	(65)	50	(14)	2.3
Polymethylmethacrylate	3.2	77	53	24	2.5
Polyethylene	2.5	96	55	42	3.8
Polypropylene	2.7	104	61	43	3.0
Polystyrene	4.0	108	44	64	5.1
<b>Polyethylene foams</b>					
1	2.6	—	—	—	—
2	2.6	—	—	—	—
3	2.5	—	—	—	—
4	2.6	—	—	—	—
Average	2.6	88	51	38	3.8
<b>Chlorinated polyethylenes</b>					
25% chlorine	6.6	95	48	47	2.1
36% chlorine	7.5	—	—	—	—
48% chlorine	7.6	—	—	—	—
<b>Expanded polystyrene</b>					
GM47	6.3	—	—	—	—
GM49	4.9	—	—	—	—
GM51	6.3	—	—	—	—
GM53	5.7	—	—	—	—
Average	5.8	108	44	64	5.1
<b>Polyurethane foams (flexible)</b>					
GM21	5.6	—	—	—	—
GM23	5.3	—	—	—	—
GM25	5.7	—	—	—	—
GM27	6.5	—	—	—	—
1/CaCO <sub>3</sub>	7.2	—	—	—	—
Average	6.1	101	48	53	—
<b>Polyurethane foams (rigid)</b>					
GM29	7.9	—	—	—	—
GM31	8.4	—	—	—	—
GM35	6.9	—	—	—	—
Average	7.7	102	44	58	—
<b>Polyisocyanurate foams (rigid)</b>					
GM41	6.8	—	—	—	—
GM43	5.5	—	—	—	—
Phenolic foam	5.5	—	—	—	—

<sup>a</sup>From the data measured in the ASTM E 2058 FPA at FMRC; -: no data or considered in the average data.

national and international standards organizations and government and private agencies, for example the following [36,37].

1. Australia (Standards Australia, SA);
2. Canada (Canadian General Standards Board, CGSB);
3. China-People's Republic (China Standards Information Center, CSIC);
4. China-Republic of China-Taiwan-(Bureau of Standards, Metrology and Inspection, BSMI);
5. Europe (International Electrotechnical Commission, IEC; European Committee for Electrotechnical Standardization, CENELEC; European Committee for Standardization, CEN, International Standards Organization, ISO);
6. Finland (Finnish Standards Association, SFS);
7. France (Association Europeene Des Constructeurs De Materiel Aerospatial, AECMA; Association Francaise De Normalisation, AFNOR);

8. Germany (Deutsches Institut Fur Normung, DIN);
9. India (Indian Standards Institution, ISI);
10. Israel (Standards Institution of Israel, SII);
11. Italy (Ente Nazionale Italiano Di Unificazione, UNI);
12. Japan (Japanese Standards Association, JSA);
13. Korea (Korean Standards Association, KSA);
14. New Zealand (Standards New Zealand, SNZ);
15. Nordic Countries (Nordtest: Denmark, Finland, Greenland, Iceland, Norway, and Sweden);
16. Russia (Gosudarstvennye Standarty State Standard, GOST);
17. South Africa (South African Bureau of Standards, SABS);
18. United Kingdom (British Standards Institution, BSI; Civil Aviation Authority, CAA);
19. USA (examples of government agencies: department of transportation, DOT; military-MIL; National Aeronautical and Space Administration, NASA. Examples of private agencies: American National Standards Institute, ANSI, American Society for Testing and Materials, ASTM; Building Officials & Code Administrators International Inc., BOCA; Electronic Industries Alliance, EIA; FM Approvals; Institute of Electrical and Electronics Engineers, IEEE; National Fire Protection Association, NFPA; Underwriters Laboratories, UL).

Each national and international standards organization, government, and private industries from each country, listed above and others, use their own standard test methods for the evaluation of the products and materials. Consequently, there are literally thousands of standard test methods used on a worldwide basis [37–41]. The national and international standards organizations list their test methods in catalogues for standards such as: the European Committee for Standardization, CEN [42], FM Approvals [43], Underwriter’s Laboratories (UL) [44], International Standards Organization (ISO) [45], American Society of Testing and Materials (ASTM) [46] and others.

Because of the use of thousands of standard testing methods, products accepted in one country may be unacceptable in the other, creating confusion and serious problems for the manufacturers and fire safety regulator. Vigorous efforts are thus being made, especially in Europe, to harmonize the standard test methods<sup>3</sup>. Recently the European Commission’s, single burning item (SBI) and reaction to fire classification [42] is the best example of harmonizing hundreds of

<sup>3</sup> ISO, IEC, Nordtest, CEN, US Federal Aviation Administration’s (FAA) standards criteria are internationally acceptable for regulations, and others.

European standard testing methods for building products into a single standard test method. The single burning item test method (EN 13823) for testing the fire safety of construction products will be widely used by the manufacturers to allow for the affixing of “C” marking that will indicate compliance with the “Essential Requirements of the Union Directive 89/106/EEC”. In addition, new regulations, Euroclasses<sup>4</sup>, and test methods designated EN ISO, are in a process of being introduced that will be used throughout Europe [47,48].

Further harmonization is expected as many regulatory agencies are considering augmenting or replacing the prescriptive-based fire codes (currently in use) by the performance-based fire codes. In the performance-based fire codes, engineering methods are used that need data for the fire properties [33–35]. The data for the fire properties can be obtained from many standard test methods currently in use worldwide by modifying the test procedures and data acquisition methodology. Since fire properties will be measured quantitatively, the standard test methods will be automatically harmonized worldwide and the assessment for the fire resistance of materials and products will become reliable, as it will be subject to quantitative verification. Following sections describe some commonly used standard test methods:

### 53.11.1 Standard Tests for the Ignition Behavior of Polymer Materials

Standard test methods have been developed for examining the ignition behavior of polymeric materials. Some test methods provide qualitative data, while others provide partial or complete quantitative data for the ignition resistance of materials (Section 53.3, Tables 53.3 and 53.4). The following are examples of the common standard test methods used for examining the ignition resistance of materials:

1. ISO 871 ( $T_{ig}$ , ignition temperature in the hot oven) [45];
2. ASTM D 1929 ( $T_{flash}$ , flash ignition temperature) and  $T_{ig}$  (spontaneous) [46];
3. ASTM E 1352 (qualitative-cigarette ignition of upholstered furniture) [46];
4. ASTM E 1353 (qualitative-cigarette ignition resistance of components of upholstered furniture) [46];
5. ASTM F 1358 (qualitative-effects of flame impingement on materials used in protective clothing not designed primarily for flame resistance) [46];
6. ASTM C 1485 (CHF value of exposed attic floor insulation using an electric radiant heat energy source) [46];

<sup>4</sup> There are seven main Euroclasses for building materials for walls, ceiling, and floors: A1, A2, B, C, D, E, and F [47,48]. A1 and A2 represent different degrees of limited combustibility. B to E represent products that may go to flashover in a room within certain times [47,48]. F means that no performance is determined [47,48]. Thus there are seven classes for linings and seven class for floor coverings [47,48]. There are additional classes of smoke and any occurrence of burning droplets [47,48].

7. ASTM E 648 (CHF value of floor covering systems using a radiant heat energy source) [46];
8. ASTM E 1321 and ISO 5658 (CHF and TRP values) [45,46];
9. ASTM E 1354 and ISO 5660 (CHF and TRP values) [45,46];
10. ASTM D 1929 ( $T_{ig}$  values) [46];
11. ASTM E 2058 (CHF and TRP values) [46].

Tests performed in the apparatuses specified in the three standards listed above, i.e., ASTM E 1321/ISO 5658 (LIFT apparatus), ASTM E 1354/ISO 5660 (cone calorimeter), and ASTM E 2058 (fire propagation apparatus) provide complete set of fire properties for the assessment of ignition behavior of polymer products. These apparatuses also provide data in a format that is useful for the engineering methods in the performance-based fire codes.

Examples of the data for CHF and TRP values are listed in Table 53.3. Polymer products with high CHF and TRP values have high resistance to ignition.

### 53.11.2 Standard Tests for the Combustion Behavior of Polymer Materials

The burning behaviors of polymeric materials are examined by measuring the release rates of material vapors, heat, and chemical compounds including smoke in the apparatuses specified in the standard test methods. From these measurements, the following fire properties are derived:

1. Heat of gasification and heat losses (Table 53.2);
2. Chemical, convective, and radiative heats of combustion (ratio of the summation of the heat release rate to the summation of the release rate of material vapors) (Table 53.9);
3. Yields of various chemical compounds (ratio of the summation of the release rate of each compound to the summation of the release rate of material vapors, Table 53.9).
4. Combustion efficiency (ratio of the heat of combustion to the net heat of complete combustion);
5. Generation efficiency of chemical compounds (ratio of the yield of a compound to the maximum possible stoichiometric yield of the compounds based on the elemental composition of the material).

The heat of complete combustion is measured according to ASTM D 5865/ISO 1716 test methods [45,46]. The release rates of material vapors, heat, and various chemical compounds (including smoke) are measured according to ASTM E 906 (the Ohio State University Heat Release Rate, OSU-HRR, Apparatus), ASTM E 2058 (fire propagation apparatus) and ASTM E 1354/ISO 5660 (cone calorimeter) [45,46]. Smoke released in flaming and nonflaming fires of materials is also characterized

following these standard test methods as well by the ASTM E 662 (smoke density Chamber) [46].

### *ASTM D 5865/ISO 1716: Test Method for Gross Heat of Complete Combustion [45,46]*

This standard test method incorporates the fundamental principles for the energy associated with the complete combustion of materials and thus is independent of fire scenarios [49]. Gross and net of complete combustion of materials are used in the performance-based fire codes for the assessment of fire hazards associated with the use of products and protection needs. The gross heat of complete combustion is measured in the oxygen bomb calorimeter.

In Europe, gross heat of complete combustion (gross calorific potential, PCS), measured by following the ISO 1716 standard test method is used for the classification of reaction to fire performance for construction products (prEN 13501-1) [42]:

#### 1. Construction products excluding floorings:

- Class A1:  $PCS \leq 1.4\text{--}2.0$  MJ/kg.
- Class A2:  $PCS \leq 3.0\text{--}4.0$  MJ/kg.

#### 2. Floorings:

- Class A1<sub>f1</sub>:  $PCS \leq 1.4\text{--}2.0$  MJ/kg.
- Class A2<sub>f1</sub>:  $PCS \leq 3.0\text{--}4.0$  MJ/kg.

The gross heat of complete combustion is used to determine the net heat of complete combustion<sup>5</sup> defined as the quantity of energy released when a unit mass of specimen is burned at constant pressure, with all the combustion products, including water, being gaseous.

### *ASTM E 136/ISO 1182: Standard Test Method for Behavior of Materials in a Vertical Tube Furnace at 750 °C [45,46]*

This standard test method specifies the use of a small-scale apparatus to assess the noncombustibility behavior of building construction materials under the test conditions. The standard test apparatus consists of two concentric, vertical refractory tubes, 76-mm and 102-mm (3 and 4-in.) in inside diameter and 210 to 250-mm (8.5–10-in.) in length. Electric heating coils outside the larger tube are used to apply heat. A controlled flow of air is admitted tangentially near the top of the annular space between the tubes and passes to the bottom of the inner tube. The top of the inner tube is covered. Temperatures are measured by thermocouples at the center: (1) between the two concentric tubes, (2) close to specimen location, and (3) sample surface.

<sup>5</sup> If the percentage of hydrogen atoms in the sample is known: net heat of complete combustion in kJ/g = gross heat of complete combustion in kJ/g – 0.2122 × mass percent of hydrogen atoms, where heats of combustion are in kJ/g [46]. If the percentage of hydrogen atoms is not known: net heat complete of complete combustion in kJ/g = 10.025 + (0.7195) gross heat of combustion in kJ/g [46].

Test specimens are used in granular or powdered form contained in a 38-mm × 38-mm × 51-mm holder. The specimen in the holder is placed in the center of the inside vertical refractory tube after the temperature at the specimen location is maintained at  $750 \pm 5.5^\circ\text{C}$  for 15 min. The test is continued until all the temperatures have reached their maximum values. Visual observations are made throughout the test on the specimen behavior, combustion intensity, smoke formation, melting, charring, etc. The specimen is weighed before and after the test. The data measured in the test are used to assess the following specimen behaviors:

1. Weight loss,  $\Delta m \leq 50\%$ ;
2. Surface and interior temperature,  $\Delta T \leq 30^\circ\text{C}$ ;
3. There is either no flaming, i.e., flaming duration,  $t_f = 0$ , or there is no flaming after the first 20 seconds,  $t_f \leq 20$  s.

In Europe, data from ISO 1182 are used for the classification of reaction to fire performance for construction products (prEN 13501-1) [42]:

1. *Construction products excluding floorings:*
  - Class A1:  $\Delta T \leq 30^\circ\text{C}$ ,  $\Delta m \leq 50\%$ , and  $t_f = 0$ .
  - Class A2:  $\Delta T \leq 30^\circ\text{C}$ ,  $\Delta m \leq 50\%$ , and  $t_f \leq 20$  s.
2. *Floorings:*
  - Class A1<sub>f1</sub>:  $\Delta T \leq 30^\circ\text{C}$ ,  $\Delta m \leq 50\%$ , and  $t_f = 0$ .
  - Class A2<sub>f1</sub>:  $\Delta T \leq 30^\circ\text{C}$ ,  $\Delta m \leq 50\%$ , and  $t_f \leq 20$  s.

**ASTM E 906, ASTM E 2058, and ASTM E 1354/ISO 5660: Standard Test Methods for Release Rates of Material Vapors, Heat, and Chemical Compounds [45,46]**

These standard test methods specify the use of small-scale apparatus to quantify the fire properties of materials. The apparatuses specified are:

1. ASTM E 906 (the OSU-HRR Apparatus);
2. ASTM E 2058 (the fire propagation apparatus, FPA);
3. ASTM E 1354/ISO 5660 (cone calorimeter).

One of the standard test apparatuses (the FPA is shown in Figs. 53.1).

**ASTM E 119: Standard Test Methods for Fire Tests of Building Construction and Materials-The Fire Endurance Test [46]**

This standard test method specifies use of large-scale furnace for testing of walls, columns, floors, and other building members, under high fire exposure conditions. Fire resistance is expressed in terms of time to reach critical point, i.e., “1/2-h (hour)”, “2-h”, “6-h”, and other ratings of building materials and assemblies as they are exposed to heat. The building materials and assemblies are exposed

to heat in a natural gas or propane fueled furnace with temperature increasing in the following fashion:

5 min	538 °C	10 min	704 °C	30 min	843 °C
1 h	927 °C	2 h	1,010 °C	4 h	1,093 °C
≥ 8 h	1,260 °C				

The standard test method has been designed to test the following building materials and assemblies in the furnace<sup>6</sup>:

1. *Bearing and nonbearing walls and partitions:* the area exposed to fire is  $\geq 9\text{-m}^2(100\text{-ft}^2)$  with neither dimension less than 2.7-m (9-ft);
2. *Columns:* the length of the column exposed to fire is  $\geq 2.7\text{-m}$  (9-ft);
3. *Protection for structural steel columns:* the length of the protected column is  $\geq 2.4\text{-m}$  (8-ft) held in a vertical orientation. The column is exposed to heat on all sides;
4. *Floors and roofs:* the area exposed to fire is  $\geq 16\text{-m}^2(180\text{-ft}^2)$  with neither dimension  $\geq 3.7\text{-m}$  (12-ft);
5. *Loaded restrained and unrestrained beams:* the length of the beam exposed to fire  $\geq 3.7\text{-m}$  (12-ft) and tested in a horizontal position;
6. *Protection for solid structural steel beams and girders:* the length of beam or girder exposed to the fire is  $\geq 3.7\text{-m}$  (12-ft) tested in a horizontal position;
7. *Protective members in walls, partition, floor, or roof assemblies:* the sizes used are same as above for the respective specimens.

Various criteria are used for the acceptance of the specimens:

1. Sustains itself or with the applied load without passage of flame or gases hot enough to ignite cotton waste or the hose assembly for a period equal to that for which classification is desired;
2. There is no opening that projects water from the stream beyond the unexposed surface during the time of water hose stream test;
3. Rise in the temperature on the unexposed surface remains  $\leq 139^\circ\text{C}$  above its initial temperature;
4. Transmission of heat through the protection during the period of fire exposure for which classification is desired maintains the average steel temperature  $\leq 538^\circ\text{C}$  (measured temperature  $\leq 649^\circ\text{C}$ );
5. For steel structural members (beams, open-web steel joists, etc), spaced more than 1.2-m (4-ft), the average temperature of steel  $\leq 593^\circ\text{C}$  (measured temperature  $\leq 704^\circ\text{C}$ ) during the classification period.

<sup>6</sup> As needed, load is applied to the specimens throughout the test to simulate a maximum load condition in their end use application.

***ASTM E 1529: Standard Test Methods for Determining Effects of Large Hydrocarbon Pool Fires<sup>7</sup> on Structural Members and Assemblies [46]***

The standard test method specifies large-scale test, similar to ASTM E 119, except that exposure of specimens consist of rapidly increasing heat flux. In the test, specimen surface is exposed to an average heat flux exposure of  $158 \text{ kW/m}^2 \pm 8 \text{ kW/m}^2$  attained within the first 5-min and maintained for the duration of the test. The temperature of the environment reaches  $\geq 815 \text{ }^\circ\text{C}$  after the first 3-min of the test and remains between  $1010 \text{ }^\circ\text{C}$  and  $1180 \text{ }^\circ\text{C}$  at all times after the first 5-min.

This standard test method is used to determine the response of columns, girders, beams or structural members, and fire-containment walls, or either homogeneous or complete construction exposed to rapidly increasing heat flux. In this standard test method, combination of heat flux and temperature for the control is specified compared to ASTM E 119, where only temperature is specified. Performance is defined as the period during which structural members or assemblies will continue to perform their intended function when subjected to fire exposure. The results are reported in terms of time increments such as 1/2-h (hour), 3/4-h, 1-h, 1.5-h, and others.

The tests are performed in a fashion similar to that in the ASTM E 119, except for the heat flux and temperature profiles. For example, in this standard test method, a heat flux exposure of  $158 \text{ kW/m}^2$  to the specimen surface is specified within first 5-min of the test. In the ASTM E 119, a heat flux exposure of  $35 \text{ kW/m}^2$  at 5-min and  $118 \text{ kW/m}^2$  at 60-min to the specimen surface is specified.

In this standard test method, conditions are simulated to test the performance of structural members and assemblies exposed to fire conditions resulting from large, free-burning (outdoors), fluid-hydrocarbon-fueled pool fires. This information is needed for the design of facilities for the hydrocarbon processing industry (oil refineries, petrochemical plants, offshore oil production platforms, and others) and chemical plants. In the future, this information may also be used in the design of high rise buildings because of the extreme terrorist act that occurred in New York City on September 11, 2001. There was a complete collapse of the World Trade Center Towers due to exposure to very hot pool fires from the large spillage of aviation gasoline.

<sup>7</sup> A large pool fire is defined as that resulting from hundreds (or thousands) of gallons of liquid hydrocarbon fuel burning over a large area (several hundred to thousand square meters) with relatively unrestricted airflow and release of chemical compounds. A range of temperatures, velocities, heat fluxes, and chemical conditions exist and vary dramatically with time and spatial location.

**53.11.3 Standard Tests for the Flame Spread Behavior of Polymer Materials**

In the standard test methods, specifications are made for making visual observations for movement of flame and char during the test and measurements for the surface temperature and release rates of material vapors, heat, and chemical compounds, including smoke. Both small-scale and large-scale flame spread and fire growth tests are performed using materials and products. Following are some of the popular standard test methods for characterizing flame spread and fire growth behaviors of materials and products. The following are some of the popular standard test methods for the flame spread behaviors of the polymeric materials.

***prEN ISO/FDIS 11925-2: Reaction to Fire Tests for Building Products-Part 2: Ignitability When Subjected to Direct Impingement of Flame [42,45]***

The apparatus consists of a stainless steel 800-mm high, 700-mm long, and 400-mm wide chamber with an exhaust duct attached at the top of the chamber. In the test, 250-mm long and 180-mm wide specimen with thickness  $\leq 60$ -mm is used. The specimen is placed in a holder consisting of a double U-shaped frame made from 15-mm wide and 5-mm thick stainless steel sheets hanging vertically inside the stainless steel chamber. The holder is 370-mm long and 110-mm wide with a 80-mm wide open mouth.

The specimen is placed between two halves of the holder that are held together by screws or clamps. The holder can move closer to or away from a  $45^\circ$ -propane gas burner (similar to a Bunsen burner). A 100-mm  $\times$  50-mm  $\times$  10-mm deep aluminum foil tray containing filter paper is placed beneath the specimen holder and replaced between the tests.

The flame from the burner is applied for 15 or 30 s and the burner is retracted smoothly. For 15 s flame application, the test duration is 20 s after flame application. For 30 s flame application time, the test duration is 60 s after flame application. The following observations are made in the test:

1. Ignition of the specimen;
2.  $F_s$ : Flame spread up to 150-mm and time taken;
3. Presence of flaming droplets;
4. Ignition of the filter paper below the specimen.

In Europe, data from ISO 11925-2 are used for the classification of reaction to fire performance for construction products (prEN 13501-1) [42]:

1. *Construction products excluding floorings:*
  - Class B:  $F_s \leq 150$ -mm within 60 s for 30-s exposure.
  - Class C:  $F_s \leq 150$ -mm within 60 s for 30-s exposure.

- Class D:  $F_s \leq 150$ -mm within 60 s for 30-second exposure.
- Class E:  $F_s \leq 150$ -mm within 20 s for 15-s exposure

## 2. Floorings

- Class B<sub>fl</sub>:  $F_s \leq 150$ -mm within 20 s for 15-s exposure.
- Class C<sub>fl</sub>:  $F_s \leq 150$ -mm within 20 s for 15-s exposure.
- Class D<sub>fl</sub>:  $F_s \leq 150$ -mm within 20 s for 15-s exposure.
- Class E<sub>fl</sub>:  $F_s \leq 150$ -mm within 20 s for 15-s exposure.

### **UL 94: Standard Test Methodology for Flammability of Plastic Materials for Parts in Devices and Appliances [44]**

This standard test method is similar to prEN ISO/FDIS 11925-2 test. In the test, both horizontal burning (HB) and vertical burning (V) behaviors of 127-mm (5-in) long, 13-mm (0.5-in) wide, and up to 13-mm (0.5-in) thick material samples are examined. Horizontal burning test is performed for 94HB classification of materials. The sample used is placed on top of a wire gauge and ignited by a 30-s exposure to a Bunsen burner at one end.

The material is classified as 94HB if over 76-mm (3.0-in) length of sample: (1) flame spread rate  $< 38.1$  mm/min for 3–13-mm thick sample and  $< 76$ -mm/min for 3-mm thick sample or flame spread is  $< 102$ -mm (4.0-in.).

Vertical burning test is performed for the 94V-0, 94V-1, or 94V-2 classification of materials. The bottom edge of the sample is ignited by a 5-s exposure to a Bunsen burner with a 5-s delay and repeated five times until the sample ignites. The 94V-0, 94V-1, and 94V-2 material classification criteria are listed in Table 53.10.

The relative resistance of materials to flame spread and burning according to UL94 is HB  $<$  V-2  $<$  V-1  $<$  V-0. The ordinary polymeric materials, which generally have low fire resistance, are classified as HB. Most of the high temperature and halogenated polymeric materials, that generally have high fire resistance, are classified as V-0.

### **ASTM D 2863 (ISO 4589): Test Methodology for Limited Oxygen Index [46]**

The test is described in Section 53.6.1. The LOI values and UL 94 classification of materials are interrelated. The LOI values for V-0 materials are  $\geq 35$ , whereas the LOI values are  $< 30$  for materials classified as V-1, V-2, and HB.

The standard test method has not been developed to predict the fire behavior of materials expected in actual fires, but rather to screen materials for low and high resistance to fire propagation. For the majority of high temperature and highly halogenated materials, the LOI values are  $\geq 40$ . These polymers have high resistance to ignition, combustion, as well as fire spread, independent of fire size and ignition source strength.

### **ASTM E 162 (D 3675): Standard Test Method for Surface Flammability Using a Radiant Energy Source [46]**

In this small-scale test method, 460-mm (18-in.)  $\times$  150-mm (6-in.) wide and up to 25-mm (1-in.) thick vertical sample is used. The sample is exposed to a temperature of  $670 \pm 4$  °C at the top from a 300-mm (18-in.)  $\times$  300-mm (12-in.) inclined radiant heater with top of the heater closest to and the bottom farthest away from the sample surface. The sample is ignited at the top and flame spreads in the downward direction. In the test, measurements are made for the arrival time of flame at each of the 75-mm (3-in.) marks on the sample holder and the maximum temperature rise of the stack thermocouples. The test is completed when the flame reaches the full length of the sample or after an exposure time of 15-min, whichever occurs earlier, provided the maximum temperature of the stack thermocouples is reached. Flame spread index ( $I_s$ ) is calculated from the measured data, defined as the product of flame spread factor,  $F_s$ , and the heat evolution factor,  $Q$ .

Many polymeric materials and products have been tested using this standard test method. The  $I_s$  values vary from 0 to 2,220, suggesting large variations in the fire spread behavior of materials.

Many regulations and codes specify the  $I_s$  value as an acceptance criterion of materials and products. For example, for structural composites inside naval submarines and for passenger cars and locomotive cabs [50,51], the following  $I_s$  values are specified for the acceptance of the materials:

1.  $I_s < 20$  for structural composites inside naval submarines;
2.  $I_s \leq 25$  for cushions, mattresses, and vehicle components made of flexible cellular foams for passenger cars and locomotive cabs and thermal and acoustic insulation for buses and vans;
3.  $I_s \leq 35$  for all vehicle components in passenger cars and locomotive cabs and for seating frame, seating shroud, panel walls, ceiling, partition, windscreen, HVAC ducting, light diffuser, and exterior shells in buses and vans;
4.  $I_s \leq 100$  for vehicle light transmitting polymers in passenger cars and locomotive cabs.

The above listed criteria for the  $I_s$  values ( $< 20$ ) suggest that structural composites for inside naval submarines are expected to have high resistance to flame spread and heat release if exposed to heat flux values similar to those used in the ASTM E 162. Also, materials used in passenger cars, locomotive cabs, buses, and vans with  $I_s$  values  $\leq 25$  as well as  $\leq 35$  are expected to have relatively higher resistance to fire spread and heat release rate compared to the ordinary materials with  $I_s$  values  $\leq 100$  under low heat exposure conditions.

**ASTM E 1321 (ISO 5658): Standard Test Method for Determining Material Ignition and Flame Spread Properties (Lateral Ignition and Flame Spread Test, LIFT) [45,46]**

This standard test method is discussed in Section 53.6.2. The test has been developed to provide pertinent data needed by the prescriptive-based and performance-based fire codes for the fire hazard analyses and protection needs for residential, private, government and industrial occupancies, transport and manufacturing, and others.

**ASTM E 648 (ISO 9239-1): Standard Test Method for Critical Radiant Flux of Floor-Covering Systems Using a Radiant Heat Energy Source [45,46]**

This standard test method specifies the use of an intermediate-scale test method for testing, similar in principle to ASTM E 1321 (ISO 5658). A 1.0-m (39.4-in.) long and 0.20-m (7.9-in.) wide horizontal sample is exposed to radiant heat flux in the range of 1–11 kW/m<sup>2</sup> from a 30°-inclined radiant panel all contained inside a chamber. The heat flux is at 11 kW/m<sup>2</sup> at the sample surface that is closer to the radiant heater. The radiant flux decreases as the distance between the sample surface and the radiant heater increases to the lowest value of 1 kW/m<sup>2</sup>.

A pilot flame ignites the sample surface exposed to 11 kW/m<sup>2</sup>, and flame spread is observed until the flame is extinguished at some downstream distance due to decrease in the radiant flux. The radiant flux at this distance is defined as the critical radiant flux (CRF) of the sample:

$$\text{CRF} = \dot{q}_{\text{cr}}'' - \dot{q}_f''(x) \quad (53.32)$$

where  $\dot{q}_f''(x)$  is the flame heat flux at distance  $x$  where flame is extinguished (kW/m<sup>2</sup>). Thus, materials and products for which radiant fraction of the flame heat flux is higher would have lower CRF values. Materials with higher radiant fraction of the flame heat flux have lower resistance to flame spread due to efficient heat transfer ahead of the flame front.

This test method was developed as a result of need for flammability standard for carpets and rugs to protect the public against fire hazards [52]. Consequently, several carpet systems were tested by this standard [52–54]. This standard test method (ASTM E 648) is specified for the classification of the interior floor finish in buildings in the NFPA 101 Life Safety Code [55]:

1. *Class I*: interior floor finish: CRF > 4.5 kW/m<sup>2</sup>;
2. *Class II*: interior floor finish: 2.2 kW/m<sup>2</sup> < CRF < 4.5 kW/m<sup>2</sup>.

And ISO 9293-1 with a test duration of 30-min is specified in Europe for the Euroclasses for flooring in prEN 13501-1 [42]:

1. *Class A<sub>2fl</sub>*: CRF ≥ 8 kW/m<sup>2</sup>
2. *Class B<sub>fl</sub>*: CRF ≥ 8 kW/m<sup>2</sup>
3. *Class C<sub>fl</sub>*: CRF ≥ 4.5 kW/m<sup>2</sup>
4. *Class D<sub>fl</sub>*: CRF ≥ 3 kW/m<sup>2</sup>

**ASTM E 84: Standard Test Method for Surface Burning Characteristics of Building Materials [46]**

This standard test method specifies the use of a larger-scale apparatus for testing. It is one of the most widely specified methods. In this 10-min test, a 7.3-m (24-ft) long and 0.51-m (20-in.) wide horizontal sample is used inside a 7.6-m (25-ft) long, 0.45-m (17-in.) wide and 0.31-m (12-in.) deep tunnel. Two gas burners, located 0.19-m (7-in.) below the specimen surface and 0.31-m (12-in.) from one end of the tunnel are used as ignition sources. The two burners release 88 kW of heat creating a gas temperature of 900 °C near the specimen surface. The flames from the burners cover 1.37-m (4.5-ft) of the length and entire width or 0.63-m<sup>2</sup> (7-ft<sup>2</sup>) area of the specimen. Air enters the tunnel at 1.4-m (54-in.) upstream of the burner at a velocity of 73-m (240-ft)/min. The test conditions are set such that for red oak flooring control material, flame spreads to the end of the 7.3-m (24-ft) long sample in 5.5 min or a flame spread rate is 22 mm/s.

In the test, measurements are made for the percent light obscuration by smoke flowing through the exhaust duct, gas temperature (7.0-m/23-ft from the burner) and location of the leading edge of the flame (visual measurement) as functions of time. The measured data are used to calculate the flame spread index (FSI) and smoke developed index (SDI) from the flame spread distance-time and percent light absorption-time areas, respectively. Some typical FSI values are listed in Table 53.16 taken from Ref. 46.

The NFPA 101 Life Safety Code uses the ASTM E 84 test data for the following classification of building products (Table 53.17 lists the interior finish classification limitations) [55]:

1. *Class A interior wall and ceiling finish*: FSI- 0 to 25, SDI- 0 to 450;
2. *Class B interior wall and ceiling finish*: FSI- 26 to 75, SDI- 0 to 450;
3. *Class C interior wall and ceiling finish*: FSI- 76 to 200, SDI- 0 to 450.

**FM Global Approval Class 4910 [43] (NFPA 318 [56]): Standard Test Methods for Clean Room Materials for the Semiconductor Industry**

This standard test method is discussed in Section 53.6.3.

### ASTM E 603: Standard Guide for Room Fire Experiments [46]

One major reason for performing room fire tests is to learn about various fire stages in the room so that results of standard fire test methods can be related to the performance of the products in full-scale room fires. In addition, some of the tests or their reduced versions are used for the acceptance of building products as they are specified in the prescriptive-based fire codes.

The ASTM E 603 is a guide written to assist in conducting full-scale compartment fire tests dealing with any or all stages of fire in a compartment. Whether it is a single- or multi-room test, observations can be made from ignition to flashover or beyond full-room involvement. Examples of the full-scale room fire tests are:

1. FM approval class no. 4880 for building wall and ceiling panels and coatings and interior finish materials [43];
2. ISO 9705: full scale fire test for surface products [45];
3. EN 13823: single burning item (SBI) [42,47,48].

### FM Approval Class No. 4880: Test for Building Wall and Ceiling Panels and Coatings and Interior Finish Materials [43]

This standard test method specifies use of a larger-scale test, identified as the “25-ft Corner Test”, to evaluate flame spread characteristics of building walls and ceiling panels and coatings. The test is performed in a 7.6-m (25-ft) high, 15.2-m (50-ft) long, and 11.6-m (38-ft) wide walls and ceiling forming a corner of a building. The products tested are typically panels with a metal skin over the insulation core material. The panels installed on the walls and ceiling are subjected to a growing exposure fire at the base of the corner. The growing exposure fire consists of a burning 340 kg (750 lb.), 1.2-m (4-ft) × 1.2-m (4-ft) oak crib pallets, stacked 1.5-m (5-ft) high with a peak heat release rate of about 3 MW.

In the test, measurements are made for the surface temperatures (at 100 equidistant locations on the walls and ceiling) and length of flame on the wall (under the ceiling) visually. After the test, visual measurements are made for the flame spread by the extent of charring on the walls and ceiling. The product is considered to have failed the test if within 15 min either:

1. Flame spread on the wall and ceiling extends to the limits of the structure or
2. Flame extends outside the limits of the structure through the ceiling smoke layer.

The fire environment within the “25-ft Corner Test” has been characterized by heat flux and temperature measure-

ments [57]. It has been shown that the flame spread boundary (measured visually by the extent of surface charring) is very close to the CHF boundary for the material, very similar to the flame spread behavior in the ASTM E 1321 (ISO 5658). A good correlation has been developed between the extent of flame spread and the ratio of the convective heat release rate to  $\Delta T_{ig} \sqrt{k\rho c}$ , measured in the ASTM E 2058 apparatus.

This test has been instrumental in encouraging the development of other larger-scale and intermediate-scale standard corner tests such as ISO 9705 [45] and prEN 13823 (single burning item) [42].

### ISO 9705: Room/Corner Test Method for Surface Products [45]

This standard test method specifies the use of a larger-scale test to simulate a well-ventilated fire, starting at the corner of a 3.6-m long, 2.4-m high, and 2.4-m wide room with a 0.8-m wide and 2.0-m high doorway. Figure 53.12 shows the sketch of the room. The walls and ceiling with a total surface area of 32 m<sup>2</sup> (344 ft<sup>2</sup>) are covered with the specimen. The ignition source, located in the corner of the room, consists of a propane-fuelled 0.17-m square sandbox burner set to produce a heat release rate of 100-kW<sup>8</sup> for the first 10 min. If the flashover does not occur, then the sandbox burner output is increased to produce a heat release rate of 300-kW<sup>16</sup> for another 10 min. The test is ended after 20 min or as soon as the flashover is observed.

A hood attached to a sampling duct is used to capture heat and chemical compounds that are released during the test. In the sampling duct measurements are made for gas temperature, concentrations of chemical compounds released in the fire and oxygen, light obscuration by smoke, total flow of the mixture of air and chemical compounds and heat flux values at various locations in the room. Two parameters are used for ranking the products [47,48,58]:

1. *FIGRA index (fire growth rate index)*: defined as the peak heat release rate in kW during the period from ignition to flashover (excluding the contribution from the ignition source) divided by the time at which the peak occurs (kW/s);
2. *SMOGRA index (smoke release index)*: defined as the 60 s average of the peak smoke production rate (SPR in m<sup>2</sup>/s) divided by the time at which this occurs and the value is multiplied by 1,000 (m<sup>2</sup>/s<sup>2</sup>). SPR is defined as  $[\ln(I_0/I)/\ell]\dot{V}$ , where  $I/I_0$  is the fraction of light transmitted through smoke,  $\ell$  is the optical path length (m), and  $\dot{V}$  is the volumetric flow rate of the mixture of smoke and other compounds and air (m<sup>3</sup>/s). SPR can

<sup>8</sup> 100 kW diffusion flame is used to simulate a burning large waste paper basket and the 300 kW diffusion flame is used to simulate a burning small upholstered chair [47,48].



also be expressed in terms of gm of smoke released per second as  $[\ln(I_0/I)/\ell]\dot{V}(\lambda\rho_s \times 10^{-6}/\Omega)$ , where  $\lambda$  is the wavelength of light (0.6328  $\mu\text{m}$  used in the Cone),  $\rho_s$  is the density of smoke ( $1.1 \times 10^6 \text{g/m}^3$  [59]), and  $\Omega$  is the coefficient of particulate extinction (7.0 [59]). Thus, SPR in  $\text{m}^2/\text{s}$  multiplied by 0.0994 changes the unit to  $\text{g/s}$  (for  $\lambda = 0.6328 \mu\text{m}$ ).

Numerous products have been tested during the last 10 years following the ISO 9705 Room/Corner test method [58,60].

Under similar burning conditions, the combustion chemistry responsible for release of heat and smoke are conserved and thus release rates of heat and smoke are interrelated:

$$\text{SMOGR}/\text{FIGRA} = y_s/\Delta H_{\text{ch}}. \quad (53.33)$$

This interrelationship was found to be satisfied by the data from the ISO 9705 tests.

#### *prEN 13823: The Single Burning Item [42]*

This standard test method specifies use of an intermediate-scale apparatus. The apparatus consists of a trolley with two 1.5-m high, 1.0-m wide, and 0.5-m wide vertical noncombustible boards mounted at  $90^\circ$  to each other. The test specimen (wall and ceiling materials) are mounted and fixed onto the noncombustible boards in a manner representative of “end-use”. The ignition source consists of a 31 kW propane right-angled triangular sandbox burner (each side: 250-mm and 80-mm high), placed at the bottom of the vertical corner. The test is performed inside a 2.4-m high and 3.0-m square room with top attached to a hood connected to a sampling duct to exhaust heat and chemical compounds released during the fire test. Evenly distributed airflow along the floor of the test room is achieved by introduced the air under the floor of the trolley through perforated plates.

In the sampling duct measurements are made for the gas temperature, concentrations of chemical compounds released in the fire and oxygen, light obscuration by smoke, and total flow of the mixture of air and chemical compounds. The parameters used for the assessment of fire performance of specimens are:

1. Heat release rate obtained from the measurements for oxygen depletion in the sampling duct;
2. Smoke release from the light obscuration by smoke in the sampling duct;
3. Horizontal flame spread observed visually, i.e., time taken to reach the extreme edge of the main 1.5-m  $\times$  1.0-m sample panel;
4. Falling molten droplets and particles.

The performance of the specimen is evaluated over a period of 20 min. However, the test is terminated earlier if any of the following conditions occur:

1. Heat release rate  $>350 \text{ kW}$  at any instant or  $>280 \text{ kW}$  over a period of 30 s;
2. Sampling duct temperature  $>400^\circ\text{C}$  at any instant or  $>300^\circ\text{C}$  over a period of 30 s;
3. Material falling onto the sandbox burner substantially disturbs the flame of the burner or extinguishes the burner by choking.

The test data are used to obtain the following parameters to rank the fire performance of the specimens:

1. FIGRA index,
2. SMOGRA index<sup>9</sup>,
3. THR<sub>600s</sub>: total heat released within 600 s,
4. TSP<sub>600s</sub>: total smoke released within 600 s,
5. LFS: lateral flame spread,
6. Flaming/nonflaming droplets/particles and ignition of the paper<sup>10</sup> (prEN ISO 11925–2).

In Europe, data from prEN 13823 are used for the classification of reaction to fire performance for construction products (prEN 13501–1) [42]:

1. *Construction products excluding floorings:*
  - *Class A2:* FIGRA  $\leq 120 \text{ W/s}$ ; LFS  $<$  edge of specimen, THR<sub>600s</sub>  $\leq 7.5 \text{ MJ}$ , smoke production and melting/burning drops.
  - *Class B:* FIGRA  $\leq 120 \text{ W/s}$ ; LFS  $<$  edge of specimen, THR<sub>600s</sub>  $\leq 7.5 \text{ MJ}$ , smoke production and melting/burning drops.
  - *Class C:* FIGRA  $\leq 250 \text{ W/s}$ ; LFS  $<$  edge of specimen, THR<sub>600s</sub>  $\leq 15 \text{ MJ}$ , smoke production and melting/burning drops
  - *Class D:* FIGRA  $\leq 750 \text{ W/s}$ , smoke production and melting/burning drops.

The use of this standard test method for regulatory purposes is very similar to that of the ASTM E 84 standard test method. The intent of this standard test method is to separate materials and products with higher flame spread resistance from those with lower resistance. It has not been designed to predict the flame spread behavior of materials and products in actual fires.

<sup>9</sup> s1 = SMOGRA  $\leq 30 \text{ m}^2/\text{s}^2$  and TSP<sub>600s</sub>  $\leq 50 \text{ m}^2$ ; s2 = SMOGRA  $\leq 180 \text{ m}^2/\text{s}^2$  and TSP<sub>600s</sub>  $\leq 200 \text{ m}^2$ ; s3: neither s1 nor s2.

<sup>10</sup> d0 = no flaming droplets/particles in prEN 13823 within 600s; d1 = no flaming droplets/particles persisting longer than 10 s in prEN 13823 within 600 s; d2 = neither d0 nor d1 (ignition of paper in prEN ISO 11925–2 results in a d2 classification).

53.12 APPENDIX

53.12.1 Nomenclature

$A$	total exposed surface area of the material ( $m^2$ )
CHF	critical heat flux ( $kW/m^2$ )
CI	corrosion index ( $\dot{A}/min$ )/( $g/m^3$ )
$c_p$	specific heat ( $MJ/kg-K$ )
CDG	carbon dioxide generation calorimetry
FPI	fire propagation index
$\dot{G}_j''$	mass generation rate of product $j$ ( $kg/m^2-s$ )
GTR	gas temperature rise calorimetry
$\Delta H_i$	heat of combustion per unit mass of fuel pyrolyzed ( $MJ/kg$ )
$\Delta H_{co}$	heat of complete combustion of CO ( $MJ/kg$ )
$\Delta H_g$	heat of gasification of the polymer ( $MJ/kg$ )
$\Delta H_w$	heat of gasification of water (2.58 $MJ/kg$ )
$\Delta H_{co}^*$	net heat of complete combustion per unit mass of CO generated ( $MJ/kg$ )
$\Delta H_{co2}^*$	net heat of complete combustion per unit mass of CO <sub>2</sub> generated ( $MJ/kg$ )
$\Delta H_o^*$	net heat of complete combustion per unit mass of oxygen consumed ( $MJ/kg$ )
HRP	heat release parameter ( $\Delta H_{ch}/\Delta H_g$ )
$K_{thick}$	thermal response parameter for thermally thick polymers ( $kW-s^{1/2}/m^2$ )
$K_{thin}$	thermal response parameter for thermally thin polymers ( $kJ/m^2$ )
$\dot{m}_a$	mass flow rate of air ( $kg/s$ )
$\dot{m}_f''$	gasification rate of the polymer or the mass loss rate ( $kg/m^2-s$ )
$\dot{m}_w''$	water application rate per unit surface area of the material ( $kg/m^2-s$ )
OC	oxygen consumption calorimetry
PGP	product generation parameter $\{y_j/\Delta H_g\}$ ( $kg/MJ$ )
$\dot{q}_e''$	external heat flux ( $kW/m^2$ )
$\dot{q}_f''$	flame heat flux ( $kW/m^2$ )
$\dot{q}_{rr}''$	surface re-radiation loss ( $kW/m^2$ )
$\dot{Q}_i''$	heat release rate per unit sample surface area ( $\dot{m}'' \Delta H_{ch}$ ) ( $kW/m^2$ )
$\dot{Q}_i'$	heat release rate per unit sample width ( $kW/m$ )
$S$	stoichiometric mass air-to-fuel ratio ( $-$ )
$\Delta T_{ig}$	ignition temperature above ambient ( $K$ )
TRP	Thermal Response Parameter
$u$	fire propagation rate ( $mm/s$ )
$\dot{V}_T$	total mass flow rate of the fire product-air mixture ( $m^3/s$ ) volumetric
$W_f$	total mass pyrolyzed in the pyrolysis or combustion of the polymer ( $kg$ )
$W_j$	total mass of product $j$ generated in the pyrolysis or combustion of the polymer ( $kg$ )
$y_j$	yield of product $j$ ( $W_j/W_f$ ) ( $kg/kg$ )
$Y_o$	mass fraction of oxygen ( $-$ )

Greek

$\alpha$	ventilation correlation coefficient for nonflaming region ( $-$ )
$\beta$	ventilation correlation coefficient for transition region ( $-$ )
$\xi$	ventilation correlation coefficient for the equivalence ratio ( $-$ )
$\Phi$	equivalence ratio ( $S\dot{m}_p'' A/\dot{m}_{air}$ )
$\delta$	thickness or depth ( $m$ )
$\delta_w$	energy associated with the blockage of flame heat flux to the surface and escape of the fuel vapors per unit mass of the fuel ( $MJ/kg$ )
$\epsilon_w$	water application efficiency ( $-$ )
$\chi$	combustion efficiency [ $\dot{Q}_{ch}''/\dot{m}'' \Delta H_T$ ]
$\rho$	density ( $kg/m^3$ )
$\psi_j$	stoichiometric yield for the maximum conversion of fuel to product $j$ ( $-$ )

Subscript

a	air or ambient
ch	chemical
con	convective
corr	corrosion
cr	critical
e	external
ex	flame extinction
f	flame or fuel
fc	flame convective
fr	flame radiative
g	gas or gasification
i	chemical, convective, radiative
ig	ignition
j	fire product
m	melting
n	net
o	initial
rad	radiation
stoich	stoichiometric for the maximum possible conversion of the fuel to the product
rr	surface re-radiation
s	surface
v	ventilation-controlled fire
w	water
$\infty$	well-ventilated

Superscripts

.	per unit time ( $s^{-1}$ )
'	per unit width ( $m^{-1}$ )
''	per unit area ( $m^{-2}$ )

Abbreviations

ABS	acrylonitrile-butadiene-styrene
CPVC	chlorinated polyvinylchloride

CR	neoprene or chloroprene rubber
CSP, CSM,	
CLS-PE	chlorosulfonated polyethylene rubber (Hypalon)
CTFE	chlorotrifluoroethylene (Kel-F) <sup>®</sup>
E-CTFE	ethylene-chlorotrifluoroethylene (Halar) <sup>®</sup>
EPR	ethylene propylene rubber
ETFE	ethylenetetrafluoroethylene (Tefzel) <sup>®</sup>
EVA	ethylvinyl acetate
FG	fiber glass reinforced
FR	fire retarded
FEP	fluorinated polyethylene-polypropylene (Teflon <sup>®</sup> )
IPST	isophthalic polyester
PAN	polyacrylonitrile
PC	polycarbonate
PE	polyethylene
PEEK	polyether ether ketone
PES	polyethersulphone
PEST	polyester
PET	polyethyleneterephthalate (Melinex <sup>®</sup> , Mylar <sup>®</sup> )
PFA	perfluoroalkoxy (Teflon <sup>®</sup> )
PMMA	polymethylmethacrylate
PO	polyolefin
PP	polypropylene
PPS	polyphenylene sulfide
PS	polystyrene
PTFE	polytetrafluoroethylene (Teflon <sup>®</sup> )
PU	polyurethane
PVEST	polyvinylester
PVCl <sub>2</sub>	polyvinylidene chloride (Saran <sup>®</sup> )
PVF	polyvinyl fluoride (Tedlar <sup>®</sup> )
PVF <sub>2</sub>	polyvinylidene fluoride (Kynar <sup>®</sup> , Dyflor <sup>®</sup> )
PVC	polyvinylchloride
Si	silicone
SBR	styrene-butadiene rubber
TFE	tetrafluoroethylene (Teflon <sup>®</sup> )
XLPE	crosslinked polyethylene
XLPO	crosslinked polyolefin

Related information can be found in Chapter 43.

## REFERENCES

1. A. Tewarson, *J. Fire Science* **10**, 188 (1992).
2. A. Tewarson, *SFPE Handbook of Fire Protection Engineering*, (The National Fire Protection Association Press, Quincy, MA, 1995) pp. 3-53-3-124.
3. A. Tewarson, *J. Fire Science* **12**, 329 (1994).
4. A. Tewarson and R. F. Pion, *Combustion and Flame*, **26**, 85 (1976).
5. A. Tewarson, "Fire Hardening Assessment (FHA) Technology for Composite Systems", Technical Report ARL-CR-178, Contract DAAL01-93-M-S403, prepared by the Factory Mutual Research Corporation, Norwood, MA for the U.S. Army Research Laboratory, Watertown, MA., November 1994.
6. A. Tewarson and S. D. Ogden, *Combustion and Flame*, **89**, 237 (1992).
7. A. Tewarson and M. M. Khan, "Flame Propagation for Polymers in Cylindrical Configuration and Vertical Orientation," Twenty-Second Symposium (International) on Combustion, (The Combustion Institute, Pittsburgh, PA, 1988) pp. 1231-1240.
8. A. Tewarson and D. Macaione, *J. Fire Sciences*, **11**, 421 (1993).
9. M. J. Scudamore, P. J. Briggs, and F. H. Prager, *Fire and Materials*, **15**, 65 (1991).
10. M. M. Hirschler, *J. Fire Sciences*, **5**, 289 (1987).
11. *Handbook of Plastics and Elastomers*, edited by C. A. Harper (McGraw-Hill, New York, 1975).
12. C. J. Hilado, *Flammability Handbook for Plastics*, (Technomic Publications, Stamford, CT, 1969).
13. A. Tewarson, J. L. Lee, and R. F. Pion, "The Influence of Oxygen Concentration on Fuel Parameters for Fire Modeling," Eighteenth Symposium (International) on Combustion, (The Combustion Institute, Pittsburgh, PA, 1981) pp. 563-570.
14. ASTM D 2863-70, *Flammability of Plastics Using the Oxygen Index Method*, (The American Society for Testing and Materials, Philadelphia, PA, 1970).
15. J. G. Quintiere, *The SFPE Handbook of Fire Protection Engineering*, (The National Fire Protection Association Press, Quincy, MA, 1988) pp. 1-360-1-367.
16. ASTM E 1321-90 "Standard Test Method for Determining Material Ignition and Flame Spread Properties" (The American Society for Testing and Materials, Philadelphia, PA., 1990).
17. *Specification Standard for Cable Fire Propagation*, Class No. 3972, (Factory Mutual Research Corporation, Norwood, MA, 1989).
18. Approval Standard Class I for Conveyor Belting, Class No. 4998, (Factory Mutual Research Corporation, Norwood, MA, 1995).
19. C. F. Cullis and M. M. Hirschler, *The Combustion of Organic Polymers*, (Clarendon Press, Oxford, U.K., 1981).
20. J. G. Quintiere, V. Barbrauskas, L. Cooper, *et al.* "The Role of Aircraft Panel Materials in Cabin Fires and Their Properties", Final Report DOT/FAA/CT-84/30, (The Federal Aviation Administration, Atlantic City Airport, NJ, 1985).
21. A. Tewarson, F. H. Jiang, and T. Morikawa, *Combustion and Flame*, **95**, 151 (1993).
22. W. M. Pitts, "The Global Equivalence Ratio Concept and the Prediction of Carbon Monoxide Formation in Enclosure Fires", Monograph 179, (National Institute of Standards and Technology, Gaithersburgh, MD, 1994).
23. L. Tsantarides and B. Ostman, "Smoke, Gas, and Heat Release Data for Building Products in the Cone Calorimeter", Technical Report I 8903013, (Swedish Institute for Wood Technology Research, Stockholm, Sweden, 1989).
24. ASTM E 1354-90, "Standard Test Method for Heat and Visible Smoke Release Rates for Materials and Products Using Oxygen Consumption Calorimeter", (The American Society for Testing and Materials, Philadelphia, PA, 1990).
25. ASTM E 906-83, "Standard Test Method for Heat and Visible Smoke Release Rates for Materials and Products" (The American Society for Testing and Materials, Philadelphia, PA., 1984).
26. E. D. Goldberg, "Black Carbon in the Environment-Properties and Distribution", (John Wiley & Sons, New York, 1985).
27. *Particulate Carbon Formation During Combustion*, edited by D. C. Siegla and G. W. Smith, (Plenum Press, New York, 1981).
28. J. P. Stone, R. N. Hazlett, J. E. Johnson, *et al.* *J. Fire and Flammability*, **4**, 42 (1973).
29. D. J. Rasbash, "The Extinction of Fire with Plain Water: A Review", *Fire Safety Science-Proceedings of the First International Symposium*, (Hemisphere Publishing Co., New York, 1986) pp. 1145-1163.
30. "Evaluation of Alternative In-Flight Fire Suppressants for Full-Scale Testing in Simulated Aircraft Engine Nacelles and Dry Bays", edited by W. L. Grosshandler, R. G. Gann, W. M. Pitt, (National Institute of Standard and Technology, Gaithersburgh, MD., 1994), Superintendent of Documents, U.S. Government Printing Office, Washington, D.C.
31. E. W. Heinonen and S. R. Skaggs, "Fire Suppression and Inertion Testing of Halon 1301 Replacement Agents", *Proceedings -Halon Alternates Technical Working Conference 1992*, pp. 213-223. The University of New Mexico, New Mexico Engineering Research Institute, (Center for Global Environmental Technologies, Albuquerque, NM, 1992).
32. K. Metchis, "The Regulation of Halon and Halon Substitutes", *Proceedings of the Halon Options Technical Working Conference 1994*, pp. 7-30, The University of New Mexico, New Mexico Engineering

- Research Institute, (Center for Global Environmental Technologies, Albuquerque, NM, 1994).
33. V. Beck, "Performance-Based Fire Engineering Design and Its Application in Australia", *Fire Safety Science, Fifth International Symposium*, pp. 23–40, International Association for Fire Safety Science, edited by Y. Hasemi, Japan, 1997.
  34. B.J. Meacham, "Concepts of a Performance-Based Building Regulatory System for the United States", *Fifth International Symposium*, pp. 701–712, International Association for Fire Safety Science, edited by Y. Hasemi, Japan, 1997.
  35. ASTM's Role in Performance-Based Fire Codes and Standards, edited by J.R. Hall, ASTM STP 1377, The American Society for Testing and Materials, West Conshohocken, PA, 1999.
  36. Worldwide Standards Service for Windows, HIS, Englewood, CO, 2002.
  37. J. Troitzsch, "International Plastics Flammability Handbook--Principles, Regulations, Testing and Approval", (Macmillan Publishing Co., Inc., New York, NY 1983).
  38. A.H. Landrock, "Handbook of Plastics Flammability and Combustion Toxicology-Principles, Materials, Testing, Safety, and Smoke Inhalation Effects", (Noyes Publications, Park Ridge, NJ, 1983).
  39. "Flammability Testing of Building Materials-An International Survey", Document NO. TH 42126, British Standards Institution, London, UK, 2000.
  40. A.D. Makower, "Fire Tests-Buildings Products, and Materials", British Standards Institution, London, UK.
  41. C.J. Hilado, "Flammability Test Methods Handbook", Technomic Publication, Westport, Conn, 1973.
  42. European Committee for Standardization (CEN) (<http://www.cenorm.be/>).
  43. FM Approval Standards ([http://www.fmglobal.com/research\\_standard\\_testing/product\\_certification/approval\\_standards.html](http://www.fmglobal.com/research_standard_testing/product_certification/approval_standards.html)).
  44. UL Standards (<http://ulstandardsinfonet.ul.com/catalog/>).
  45. ISO Standards (<http://www.iso.ch/iso/en/isonline.frontpage>).
  46. ASTM Standards (<http://www.astm.org>).
  47. B. Sundstrom, "European Classification of Building Products", Interflam '99, 8th International, Fire Science & Engineering Conference, 2, pp. 769- Interscience Communications, London, UK, 1999.
  48. B. Sundstrom, and S.D. Christian, "What are the New Regulations, Euroclasses, and Test Methods Shortly to be Used Throughout Europe", Conference Papers, Fire and Materials, pp. 117–127, January 22–24, 2001, Interscience Communications, London, UK, 1999.
  49. F.B. Clarke, "Issues Associated with Combustibility Classification: Alternate Test Concepts", *Fire Safety Science, Proceedings of the Fifth International Symposium*, pp. 165–175, International Association for Fire Safety Science, edited by Y. Hasemi, Japan, 1997.
  50. "Test Procedures and Performance Criteria for the Flammability and Smoke Emission Characteristics of Materials Used in Passenger Cars and Locomotive Cabs", Federal Register, Rules and Regulations, 64(91), Wednesday, May 12, 1999.
  51. Department of Transportation, Federal Transit Administration, Docket 90-A "Recommended Fire Safety Practices for Transit Bus and Van Materials Selection", Federal Register, 58(201), Wednesday, October 20, 1993.
  52. I.A. Benjamin, and C.H. Adams, "The Flooring Radiant Panel Test and Proposed Criteria", *Fire Journal*, 70 (2), 63–70, March 1976.
  53. S. Davis, J.R. Lawson, and W.J. Parker, "Examination of the Variability of the ASTM E 648 Standard with Respect to Carpets", Technical Report NISTIR 89-4191, National Institute of Standards and Technology, Gaithersburg, MD, October 1989.
  54. K. Tu, and S. Davis, "Flame Spread of Carpet Systems Involved in Room Fires", Technical Report NBSIR 76-1013, National B.
  55. NFPA 101 Life Safety Code, Chapter 10 Annex, National Fire Codes-A Compilation of NFPA Codes, Standards, Recommended Practices and Guides, 5, pp. 101–306 to 101–307, National Fire Protection Association, Quincy, MA 2000.
  56. NFPA 318 "Standard for the Protection of Cleanrooms", National Fire Codes, 6, pp. 318-1 to 318-22, National Fire Protection Association, Quincy, MA, 2000;
  57. J.S. Newman, and A. Tewarson, "Flame Spread Behavior of Char-Forming Wall/Ceiling Insulation", *Fire Safety Science, Third International Symposium*, pp. 679–688, International Association for Fire Safety Science, edited by G. Cox and B. Langford, (Elsevier Applied Science, New York, NY, 1991).
  58. B. Sundstrom, P.V. Hees, and P. Thureson, "Results and Analysis from Fire Tests of Building Products in ISO 9705, the Room/Corner Test; The SBI Research Program", Technical report SP-RAAPP, 1998:11, Swedish National Testing and Research Institute, Fire Technology, Boras, Sweden 1998.
  59. J.S. Newman, and J. Steciak, "Characterization of Particulates from Diffusion Flames", *Combustion and Flame*, 67, 55–64, 1987.
  60. S.E. Dillon, "Analysis of the ISO 9705 Room/Corner Test: Simulation, Correlations, and Heat Flux Measurements", NIST-GCR-98-756, National Institute of Standards and Technology, Gaithersburg, MD, August 1998.

## CHAPTER 54

# Thermal-Oxidative Stability and Degradation of Polymers

Vladyslav Kholodovych and William J. Welsh

*Department of Pharmacology, University of Medicine & Dentistry of New Jersey (UMDNJ) – Robert Wood Johnson Medical School (RWJMS) and the UMDNJ Informatics Institute, Piscataway, NJ 08854*

---

54.1	Basic Definitions and Modes of Degradation.....	927
54.2	Structure–Property Relationships .....	928
54.3	Degradation Reaction Mechanisms .....	929
54.4	Specific Examples .....	930
54.5	Additives for Enhanced Thermal-Oxidative Stability.....	933
54.6	Experimental Methods of Analysis.....	933
54.7	Tabulated Data .....	934
54.8	Material Science Tools on the World Wide Web .....	936
	References .....	938

---

### 54.1 BASIC DEFINITIONS AND MODES OF DEGRADATION

Thermal stability refers to the ability of a material to maintain desirable mechanical properties such as strength, toughness, or elasticity at a given temperature. At the other extreme, thermal degradation can be defined functionally as the deterioration of those properties of polymers which make them useful commercially as rubbers, plastics, and fibers. Degradation reactions are most important in two phases of the life of a synthetic polymer: (1) during fabrication when both thermal and oxidative reactions can occur, and (2) during service life under prolonged exposure to light and oxidation. Symptoms of polymer degradation include hardening, brittleness, softening, cracking, discoloration, as well as alteration of specific polymer properties, e.g., mechanical and thermodynamic properties. In cases where molecular weight decreases, such molecular weight-sensitive properties as mechanical strength, elasticity, solution viscosity, and softening point will suffer most dramatically. Thermal degradation of organic polymers typically begins around 150–200 °C, and the rate of degradation increases as the temperature increases. The types of polymer degradation can be divided into three general categories: chain depolymerization, random scission, and substituent reactions [1–11].

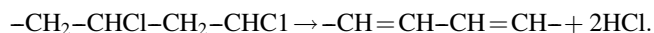
In chain depolymerization (also known as chain depropagation or “unzipping”), a given main chain is reduced in length by the sequential removal of monomer units from chain termini or at “weak links”. A “weak link” may be a chain defect, such as an initiator fragment, peroxide, or an ether linkage arising as impurities from polymerization in the presence of oxygen. The slightly higher activity of a tertiary H atom may also provide a site for the initiation of the degradation process. Chain depolymerization exhibits three characteristic features: (1) the major product (volatile or not) is monomer, (2) the decrease in bulk-polymer molecular weight is initially negligible, and (3) the rate of conversion gradually decreases. Chain depolymerization can be regarded as the opposite of addition (chain-growth) polymerization. A specific example is poly(methyl methacrylate) (PMMA).

In random scission, chain breaking occurs at random points along the chain. Random scission exhibits the following characteristic features: (1) the major products are typically fragments of monomer, dimer, trimer, etc., up to molecular weights of several hundred; (2) the decrease in molecular weight is initially appreciable; and (3) the rate of degradation is initially rapid and approaches a maximum. Random scission, as exemplified by polyethylene (PE) and polypropylene (PP), can be viewed as the reverse of

condensation (step-growth) polymerization. In random scission, the polymer radical is both highly reactive and surrounded by an abundance of secondary hydrogens. This type of thermal degradation will therefore be favored if transfer is significant. Transfer reactions, in which a long-chain radical attacks another chain (intermolecular) or itself (intramolecular), produce fragments larger than monomer and promote random chain scission.

In both chain depolymerization and random scission, thermal degradation is a free-radical chain reaction. Initiation, which is the splitting of the chain to form radicals, may occur at chain ends, at “weak links”, or at random points along the chain structure. Radical degradation often leads to crosslinking which can be visualized as resulting from the combination of radical sites on adjacent chains. Chain cleavage can occur either by primary homolytic skeletal cleavage or by an intramolecular attack by a terminal radical unit on its own chain. It is possible to differentiate between chain depolymerization and random scission in some cases by following the molecular weight of the residue as a function of the extent of reaction. Specifically, the ultimate product of random scission is likely to be a disperse mixture of fragments of molecular weight up to several hundred, whereas chain depolymerization yields large quantities of monomer.

In degradation by substituent reactions, the substituents attached to the polymer-chain backbone are modified or eliminated. Any volatile products evolved will therefore be chemically unlike monomer. The most prominent example of degradation via substituent reaction is poly(vinyl chloride) (PVC). Like all thermoplastics, PVC is processed at about 200 °C at which temperature it loses HCl quite rapidly and is converted to a deeply colored polyene polymer, i.e.,



The actual degradation mechanism is more complex than implied by this simple reaction. If substituent reactions occur, they generally ensue at temperatures ( $T < 150$  °C) below that of degradation reactions in which the backbone bonds are broken. Consequently, the reactivity of the substituents relative to that of the polymer backbone will largely dictate whether a particular polymer undergoes thermal degradation by substituent reactions or by reactions involving the backbone (e.g., chain depolymerization and random scission) [1–11].

## 54.2 STRUCTURE-PROPERTY RELATIONSHIPS

Polymers decompose at significantly lower temperatures than model compounds, perhaps by as much as 200 °C. The main reasons are twofold: (1) polymer molecules often incorporate reactive structural abnormalities (“weak links”) absent in the model compound; and (2) polymer degradation can lead to chain processes, not accessible to

model compounds, which accelerate the degradation reaction. The limited thermal stability of organic high polymers is due to several factors, including: (1) C–C bonds are relatively weak and oxidatively unstable; (2) fragmentation of the polymer during degradation is entropy favored; and (3) the presence of terminal catalytic sites, reactive atoms (e.g., tertiary H atoms), and “weak links” (e.g., branch points) along the chain which initiate decomposition [1–11].

The thermal stability and mode of decomposition of a polymer are determined by both physical and chemical factors [1–11]. In many cases, the maximum service temperature of polymers is limited not by the breaking of chemical bonds but rather by changes in physical characteristics at elevated temperatures. While retaining their chemical structures, they become weak, soft, and eventually fluid. The physical requirement of a thermally stable polymer is that it has high melting or softening temperature. The same factors that raise  $T_g$  and  $T_m$ , namely, chain rigidity and strong interchain forces, also raise thermal stability. Chain rigidity can be conferred by ring structures linked by collinear or *para* chain-extending bonds, while strong interchain attractions are attained by (intermolecular) dipolar and hydrogen-bonding interactions. The introduction of polar groups (e.g., CN, Cl, F) and hydrogen-bonding groups (e.g., –OH, –C(O)NH–) will often raise the melting and softening points appreciably. Stereoregularity in a vinyl-type polymer can produce a dramatic positive effect on thermal stability. For example, atactic polystyrene is amorphous with a  $T_g$  of about 80 °C while isotactic polystyrene is crystalline with a  $T_m$  of about 230 °C. The regular structure of the latter fits more readily into a crystalline lattice, and intermolecular forces are more difficult to overcome. Short bulky sidegroups (e.g., –CH<sub>3</sub> in polypropylene) can actually increase the melting point by reducing chain mobility, but long bulky sidegroups tend to reduce the melting point by disrupting the efficiency of chain packing. Crystalline forms of polymers are more resistant to oxidation than amorphous forms due to oxygen-permeability differences. For amorphous polymers, polymers oxidize more rapidly above than below their  $T_g$  due to the faster rate of diffusion of oxygen. Surface regions are particularly susceptible to oxidative degradation.

The chemical factors which influence thermal stability are more diverse than the physical factors. Of primary importance, heat-resistant polymers require bonds of high dissociation energy. For example, poly(tetrafluoroethylene) (PTFE) is superior to PE and many other polymers in terms of thermal stability. The stability conferred by fluorine substitution is clearly associated with the relatively high value for the dissociation energy of C–F bonds. In fact, PTFE [–CF<sub>2</sub>CF<sub>2</sub>–] is the most stable and most widely applied of the fluorinated polymers. Since the strong C–F bond renders transfer unlikely, chain depolymerization of PTFE gives high yields of monomer.

Van Krevelen [12] found a reasonably linear correlation between the half-decomposition temperature  $T_{1/2}$  and the

**TABLE 54.1.** Typical bond dissociation energies (kJ/mol).

Bond	Aromatic or heterocyclic	Aliphatic	Reference
C–C	410	284–368	[1,22,23]
C=C	—	615	[22]
C≡C	—	812	[22]
C–H	427–435	381–410	[1,22,23]
C–Cl	—	326	[22]
C–F	—	452	[23]
C–O	448	350–389	[22]
C–N	460	293–343	[22]
C=N	—	615	[22]
N–H	—	390	[22]
ROO–H	—	377	[1]
CH <sub>3</sub> C(O)–H	—	368	[1]

bond dissociation energy  $E_{\text{diss}}$  of vinyl polymers, i.e.,  $T_{1/2} = 1.6E_{\text{diss}}$  (in kJ/mol)+140. The bond dissociation energy (Table 54.1) of the bond in question depends on its bond order (i.e., single, double, triple), on resonance effects, on steric strain induced by bulky neighboring groups, and on the rigidity of their own or adjacent valence structures. Steric strain from crowded methyl groups, for example, makes polyisobutylene less stable to heat than PE. Most heat-resistant polymers, other than some inorganic and fluorinated polymers, have wholly aromatic chains like poly(*p*-phenylene). A rigid crosslinked network will also improve thermal stability. Crosslinked thermosets, such as phenolic, melamine, and epoxy plastics, are more resistant to heat than general purpose thermoplastics. Whereas thermoplastics are limited in use by the temperatures at which they soften, thermoset materials are limited by temperatures at which bonds begin to break [13].

Two additional chemical factors that are important in determining thermal stability are the reactivity of the depropagating radical and the availability of reactive hydrogen atoms for transfer. Reactive tertiary H atoms are important for the production of oligomers, whereas methylene or benzene H atoms are relatively inert. In 1,1-disubstituted vinyl polymers (e.g., poly(vinylidene cyanide):  $[-\text{CH}_2-\text{C}(\text{CN})_2-]$ ), the degrading radical is relatively unreactive by virtue of being trisubstituted. Since there are no reactive hydrogen atoms, transfer is suppressed and monomer production is dominant. The influence of radical stability is emphasized by a comparison of the behaviors of PE and PP with the polydienes  $[-\text{CH}_2-\text{CR}=\text{CH}-]$ . While PE and PP engage overwhelmingly in transfer (i.e., random scission) due to high radical reactivity, the polydienes engage in chain depolymerization due to the high relative stability the allylic radical. The relative reactivity of C–H bonds in polymers follows the order: allylic > tertiary > secondary > primary. Polystyrene and polyisobutylene are exceptions to this rule in that the benzylic and secondary H atoms, respectively, are shielded by relatively inert phenyl and methyl groups [1–13].

Degradation rates of polymers in air at temperatures below 150 °C depend on the reactivities of the peroxy radicals formed. In polymers most resistant to oxidation, H atoms are either totally absent or appear in unreactive methyl and phenyl groups. Polymers containing unsaturated linkages, such as polyisoprene or polybutadiene rubbers, can be attacked by atmospheric ozone as well as by oxygen. Polarity effects usually dominate in polymers containing heteroatoms, hence the rate of oxidation decreases along the series:  $\text{CH}_2 > \text{CHCl} > \text{C}(\text{H})\text{COOCH}_3 > \text{C}(\text{CH}_3)\text{COOCH}_3 > \text{CH}(\text{CN}) > \text{CF}_2-\text{CF}_2$ . Heteroatoms affect the strength of neighboring C–H bonds mainly by modifying the polar properties of transition states. Since the peroxy radical is electrophilic, the oxidation of ethers, aldehydes, amines, and sulfides occurs through abstraction of H atoms on carbons adjacent to the unshared electron pair on the heteroatom. Conversely, electron-deficient groups tend to stabilize neighboring H atoms.

Few polymers can withstand temperatures above 200 °C in air. Exceptions include aromatic, heterocyclic, and so-called ladder polymers (Fig. 54.1) [13,14–19]. Appropriately named, ladder polymers will degrade into fragments only if two parallel main-chain bonds (the “rungs” of the ladder) break [13]. Since this event is unlikely, ladder polymers like the two benzimidazobenzophenanthrolines designated BBB and BBL [17] (Fig. 54.1) possess exceptional thermal-oxidative stability. Moreover, recombination (“healing”) of the broken bond is facilitated by the remaining intact bond which holds the severed bond in close proximity for recombination. These rigid aromatic and ladder polymers can be “articulated” by linking the rigid units together by ether  $[-\text{O}-]$ , ester  $[-\text{C}(\text{O})\text{O}-]$ , amide  $[-\text{C}(\text{O})\text{NH}-]$ , or sulfone  $[-\text{SO}_2-]$  groups. The insertion of these flexible units between the rings imparts added flexibility but at the cost of reduced thermal stability [13].

In summary, the basic requirements for heat-resistant polymers are: (1) high bond-dissociation energies (i.e., strong primary bonds); (2) chain rigidity supplemented by resonance stabilization; (3) high melting or softening points (i.e., strong secondary bonds); (4) structures resistant to free-radical chain processes; (5) low permeability and chemical reactivity (especially to oxygen) by virtue of crystallinity, crosslinking, and efficient chain packing; and (6) elimination (during synthesis and processing) of “weak links” in the chain where free-radical degradation often initiates.

### 54.3 DEGRADATION REACTION MECHANISMS

The oxidative degradation of polymers involves free-radical chain reactions. For example, degradation of polyolefins such as PE is commonly initiated by hydroperoxide impurities incorporated during synthesis and processing.

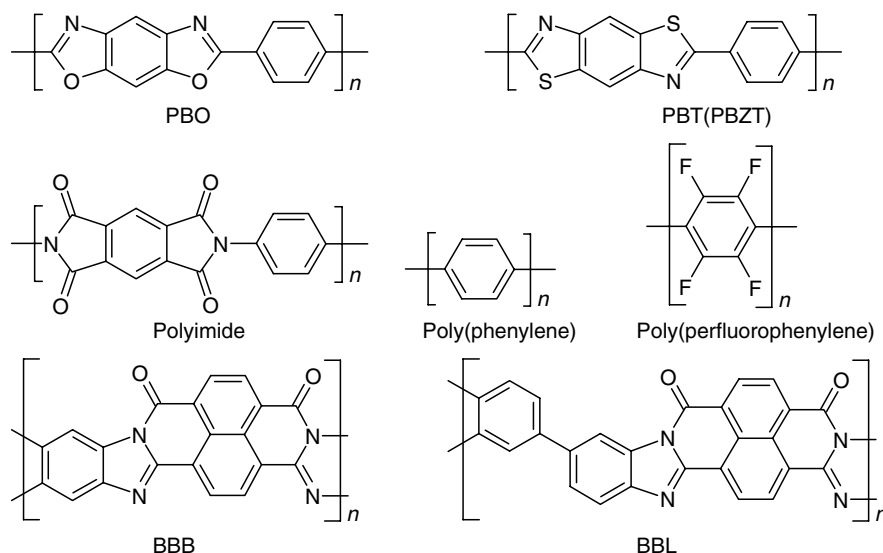
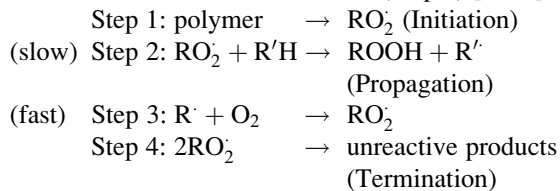


FIGURE 54.1. Examples of aromatic, heterocyclic, and ladder polymers.

Polymers may be attacked by molecular oxygen, ozone, or by indigenous free radicals in the polymer. Thermal-oxidative degradation of polyolefins in air is autocatalytic, i.e., the rate is slow at first but gradually accelerates to a constant value. According to the three-step mechanism outlined below, the  $\text{RO}_2$  peroxy radicals formed (Step 1) are sufficiently reactive to attack some primary CH bonds of the chain  $\text{R}'\text{H}$  (Step 2). The peroxy radical  $\text{RO}_2$  is thus reformed (Step 3) and can attack another CH bond. This chain reaction continues until termination occurs (Step 4) [1–11].



Step 3 is accelerated by the decomposition of the hydroperoxide products  $\text{ROOH}$  to form additional free radicals, i.e.,  $\text{ROOH} \rightarrow \text{RO}' + \text{OH}$ . Degradation is also accelerated by the presence of even a small number of reactive tertiary H atoms but sometimes secondary H atoms. Evidence indicates that a plethora of free-radicals including peroxy  $\text{RO}_2$ , hydroperoxy  $\text{HO}_2$ , oxyradicals  $\text{RO}'$ , hydroxy  $\text{HO}'$ , and alkyl  $\text{R}'$  are capable of formation and thereby initiating thermal-oxidative degradation of the polymer [1–11].

## 54.4 SPECIFIC EXAMPLES

An exhaustive survey of the thermal stabilities and degradation processes of the multitude of polymer families is beyond the scope of this work. Instead, the polymers selected for discussion below are both familiar and representative of the wide range of thermal-oxidative behavior exhibited by polymers [1–13].

### 54.4.1 Polyethylene (PE)

PE is thermally stable to about  $290^\circ\text{C}$ , above which it undergoes a decrease in molecular weight with little volatilization. Above  $360^\circ\text{C}$ , volatilization is rapid. The polymer also undergoes some crosslinking when heated at elevated temperatures. The rate of oxidation is related to the degree of chain branching since this gives rise to susceptible tertiary hydrogens. Small concentrations of  $\text{C}=\text{C}$  and  $\text{C}=\text{O}$  double bonds or peroxides along the chain will activate H atoms on neighboring bonds, thus complete saturation (no double bonds) improves oxidation resistance. The volatile products consist of a continuous spectrum of hydrocarbons ranging from  $\text{C}_1$  to  $\text{C}_{70}$  or higher. This suggests a random-scission degradation mechanism initiated at the weak links followed by inter- and intramolecular chain transfer. Low-density polyethylene (LDPE) contains more chain branching than high-density polyethylene (HDPE). Therefore, the order of increasing oxidation is  $\text{HDPE} < \text{LDPE}$ . Few additives to impart thermal stability are compatible with PE in amounts larger than 1 % or so.

### 54.4.2 Polypropylene (PP)

Thermal degradation of PP starts at about  $230^\circ\text{C}$  by a random scission process which yields virtually no monomer up to about  $300^\circ\text{C}$ . Similar to PE, the degradation products of PP span a range of unsaturated hydrocarbons up to  $\text{C}_{70}$  and higher. PP is much more susceptible than PE to oxidation because PP has branch points on alternate carbon atoms. The greater availability of reactive tertiary H atoms explains why the temperature at which degradation initiates is lower for PP ( $230^\circ\text{C}$ ) than for PE ( $290^\circ\text{C}$ ).



#### 54.4.3 Polystyrene (PS)

PS exhibits a maximum in the rate of degradation and a rapid decrease in molecular weight, both of which are characteristic of a random scission process. Evidence suggests that the decrease in molecular weight is the result of scission of a limited number of “weak links” in the polymer structure. The volatile products of thermal degradation of PS are monomer (42%) with progressively decreasing amounts of dimer, trimer, tetramer, and pentamer. Thermal degradation initiates along the chain at weak links, which might be unsaturated bonds or perhaps  $\text{CH}_2\text{-CHPh-CHPh-CH}_2\text{-}$  (Ph =  $\text{C}_6\text{H}_5$ ) sequences resulting from head-to-head addition of monomer units during polymerization.

#### 54.4.4 Poly(vinylchloride) (PVC)

PVC is relatively unstable to heat above 250 °C, even in the absence of oxygen. The substituent reaction is initiated by scission of the weakest C–Cl bonds, which are characteristically located at the chain ends since double bonds are formed as a result of disproportionation or transfer to monomer during polymerization. The chlorine radical  $\text{Cl}^\cdot$  so formed abstracts an H atom to form HCl. The resulting chain radical then reacts to form a double bond with regeneration of a chlorine radical. The reaction is accompanied by embrittlement and dramatic discoloration of the material, arising from light absorption by the conjugated backbone ( $\text{C=C}^-$ ). The polymer yellows when there are seven conjugated double bonds and discolors through brown to black with increasing extension of the conjugated double-bond system. Stabilizers which are invariably added to improve the heat and light stability include inorganic and organic derivatives of lead as well as organic derivatives of barium, cadmium, zinc, and tin.

#### 54.4.5 Poly(acrylonitrile) (PAN)

Like PVC, PAN discolors thermally at 175 °C due to the linking of nitrile groups to form conjugated carbon–nitrogen sequences. Consistent with degradation by substituent reaction, the color of degrading polymer progresses through the spectrum from yellow to red and the decrease in molecular weight is initially negligible.

#### 54.4.6 Poly(tetrafluoroethylene) (PTFE)

PTFE is a highly crystalline polymer that is devoid of crosslinks and branching. PTFE undergoes nearly 100% conversion to monomer at elevated temperatures. Thermal degradation by chain depolymerization at the chain ends probably starts at low temperatures (250–350 °C), while random-scission cleavage likely becomes more pronounced at higher temperatures. Although PTFE is the most stable of

the vinyl polymers, it cannot withstand prolonged exposure to temperatures above about 350–400 °C. The much greater strength of the C–F bond over the C–H bond explains why transfer processes, which largely control the thermal degradation of PE, are virtually absent in the thermal decomposition of PTFE. The degradation process is more complicated in the presence of air than in vacuum.

#### 54.4.7 Polyamides (PAs)

Degradation of PAs can occur at melt-spinning and molding temperatures. Residual water plays an important role, initiating hydrolysis of peptide linkages followed by decarboxylation of the resulting carboxyl groups. The principal volatile products of thermal degradation are carbon dioxide and water.

#### 54.4.8 Heat-Resistant Polymers

Many of the emerging technologies, particularly in the realm of electronics and aerospace science, require processable polymers endowed with superior mechanical properties and thermal-oxidative stability [13,16]. The structural feature common to such high-performance polymers is an aromatic backbone associated with high-bond dissociation energies, rigidity, and resonance stabilization. The mechanism of polymer degradation is principally oxidative in nature, hence incorporation of heterocyclic units further improves the thermal stability by increasing the char yield at very high temperature. The most successful of the new high-temperature polymers are those containing aromatic units in the chain backbone. For example, the polypyromellitimides (more commonly known as polyimides) (Fig. 54.1) show considerable promise as temperature-resistant plastics. The commercial polyimide Kapton is extremely heat stable, retaining more than 50% of its original tensile strength after 1,000 hours in air at 300 °C. The fluorination of aromatic structures provides additional thermal-oxidative stability. The parent structure, polytetrafluorophenylene, is stable to 500 °C in vacuum [1–11].

The aromatic heterocyclic rodlike polymers poly(*p*-phenylenebenzobisoxazole) (PBO) and poly(*p*-phenylenebenzobisthiazole) (PBZT or PBT) [14–20] possess rigid rodlike structures which provide superior tensile properties and excellent thermal stability. Thermal analysis of PBO and PBT reveals minimal weight loss in air at 316 °C. Thermal decomposition of both polymers begins at 600 °C and reaches a maximum between 660 and 700 °C. The total weight loss for both PBO and PBT is about 28% at 1,000 °C [16].

Unfortunately, wholly aromatic and/or heterocyclic polymers are notoriously difficult to process because they: (1) exhibit low solubilities in common organic solvents and (2) typically start to decompose at a lower temperature than they melt. Attempts to improve the processing characteristics of

these polymers have focused on inserting flexible “spacer” groups (e.g., amides, esters, ethers, sulfones) into the otherwise rigid chain backbone. The incorporation of even a small number of such spacer groups will increase the polymer’s conformational flexibility and entropy and thus improve its tractability by allowing mutual rotation of adjacent chain elements about the flexible moieties. At the same time, these spacer groups will often alter the colinearity of the otherwise rigid chain thereby lowering the melt temperature. In general, the thermal-oxidative stability of these polymers diminishes as the ratio of flexible-to-rigid moieties increases [13].

The so-called “articulated” PBO and PBT, in which 3,3'-biphenyl or 4,4'-(2,2'-bipyridyl) moieties have been incorporated into the otherwise rodlike backbone, are appreciably more stable than those containing diphenoxybenzene (Ph–O–Ph) segments (Fig. 54.2). While PBO and PBT articulated with diphenoxybenzene units experience significant weight losses at 316 °C, those articulated with biphenyl and bipyridyl units are largely unaffected at that temperature and display thermo-oxidative stability comparable to the parent PBO and PBT polymers. While the biphenyl unit appears to give better stability than the dipyrindyl unit, the stability of the articulated PBO and PBT polymers decreases with increased content of the flexible unit in the backbone [14].

A number of techniques, including addition of stabilizers and crosslinking, are used to extend thermal stability. Some polymers, for example PEEK (polyaryletherether ketone) and poly(phenylene sulfide), gain their thermal stability by virtue of their high degree of crystallinity. Other

temperature-resistant polymers contain wholly inorganic backbones with high bond energies, such as the polyphosphazenes  $[-P(RR')=N-]$  and the polysiloxanes  $[SiRR'-O]$  [9]. Some polyorganosilanes  $[-SiRR'-]$  are thermally stable to temperatures above 250 °C (>350 °C under inert conditions). This thermal stability is consistent with the strengths of silicon–silicon (80 kcal/mol) and carbon–silicon (90 kcal/mol) bonds [20].

A clever strategy for imparting thermal-oxidative stability in a polymer is exemplified by the so-called “ladder polymer” (Fig. 54.1) [13,17]. As the name implies, the chain of a ladder polymer can be broken only if at least two bonds on the same ring are severed. The likelihood that this will happen is low. Moreover, the broken bond has a high probability of reconnecting since the other “rung” of the ladder will hold the atoms of the severed bond in close proximity for bond reformation. Owing to these design features, the thermal stability of ladder polymers is often superior to the usual single-stranded types.

Based on the extensive experimental analysis of numerous heat-resistant polymers, Arnold [13] proposed a set of generalizations regarding correlations between polymer structure and thermal stability. Summarizing the more notable points, the highest stabilities were found for ladder-type polymers (e.g., BBB and BBL) and those containing heterocyclic or aromatic conjugated rings (e.g., polyimides, polyphenylenes, perfluoropolyphenylenes, PBO, PBT) (Fig. 54.1). The stability of polymers containing fused rings decreases as the number of fused chain segments increases. With few exceptions, most high-temperature polymers start to decompose at nearly the same temperatures

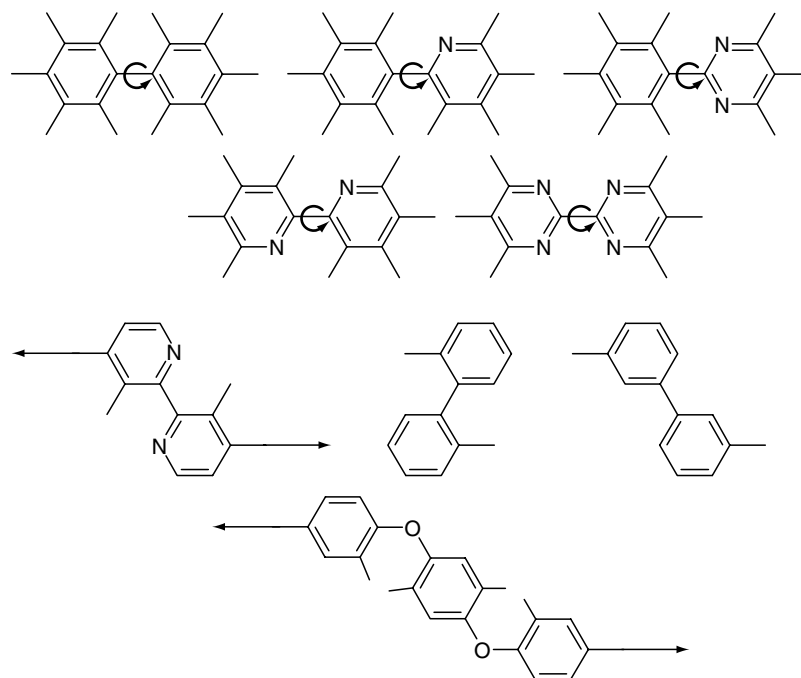
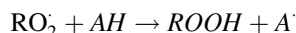


FIGURE 54.2. Examples of flexible spacer groups.

in both air and nitrogen. For polymers containing phenylene groups, the order of stability is *para* > *meta* > *ortho*. Crosslinking generally results in enhanced stability. Copolymerization can yield enhanced thermo-oxidative stability as, for example, imide copolymers of various heterocyclics are oxidatively more stable than the imide homopolymer. In terms of flexible spacer groups, the most stable are perfluoroaliphatics like  $-\text{CF}_2-$  followed by  $-\text{O}-$ ,  $-\text{S}-$ ,  $-\text{CONH}-$ , and  $-\text{CO}-$ . The least stable were alkylene linkages,  $-\text{SO}_2-$ ,  $-\text{NH}-$ , Cl-containing groups, and alkylene groups. However, any flexible spacer unit inserted into the backbone of aromatic or heterocyclic polymers can be expected to diminish both short-term and long-term stability.

#### 54.5 ADDITIVES FOR ENHANCED THERMAL-OXIDATIVE STABILITY

Oxidative degradation of polymers typically follows a free-radical mechanism involving crosslinking and/or chain scission initiated by free radicals from peroxides formed during the initial oxidation step [1–11]. Enhanced stability has been achieved by the use of additives which are frequently called antioxidants or heat stabilizers. One approach employed to reduce the oxidation of polyolefins like PE and PP is to terminate the chain reaction by introducing an antioxidant with a greater affinity than a polyolefin for the peroxy radical  $\text{RO}_2\cdot$ . Such antioxidants (AH) function by reacting with  $\text{RO}_2\cdot$  to form a relatively inactive radical  $\text{A}\cdot$ , i.e.,



While amines and some annular hydrocarbons are suitable chain terminators, hindered phenols such as di-*t*-butyl-*p*-cresol (alias butylated hydroxytoluene or BHT) are most popular because they avoid discolorization and they eliminate two free radicals per BHT molecule (Fig. 54.3). The resonance-stabilized aryloxy radical is protected by the bulky electron-releasing *t*-butyl groups in the 2 and 6 positions, so the hindered phenol can combine with a second peroxy radical but cannot combine readily with molecular oxygen or with another aryloxy radical nor abstract H atoms from the polymer to initiate a new free-radical chain reaction.

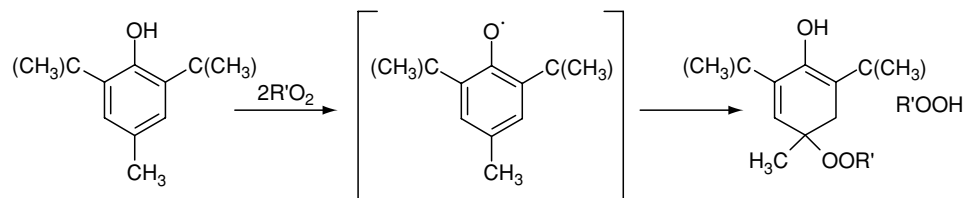
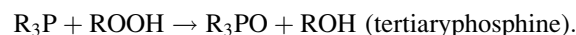


FIGURE 54.3. Illustration of the function of the hindered phenol di-*tert*-butyl-*p*-cresol (BHT).

Oxidative free-radical degradation by hydroperoxides can be catalyzed by certain transition metal ions, especially those of copper, cobalt, and manganese. To reduce the rate of free radical formation, two classes of additives are used: (1) organic phosphines, amines, and sulfides which catalyze the decomposition of the hydroperoxides to nonradical products, and (2) metal-ion chelators (e.g.,  $\text{Ph}-\text{CH}=\text{NNH}-\text{CO}-\text{CO}-\text{NHN}=\text{CH}-\text{Ph}$ ). Tertiary phosphines are thus oxidized to phosphine oxides, tertiary amines to amine oxides, and sulfides to sulfoxides, e.g.,



The inclusion of very small quantities of ethylene or propylene (1–3%) in poly(vinyl chloride) has resulted in copolymers of greatly improved heat stability relative to the parent PVC. Since degradation of PVC involves loss of  $\text{HCl}$ , compounds that react with the  $\text{HCl}$  to form stable products, such as metal oxides, are used as stabilizers.

#### 54.6 EXPERIMENTAL METHODS OF ANALYSIS

Polymer degradation can be monitored by measurement of molecular weight using viscometry, osmometry, light scattering, ultracentrifuge, and gel-permeation chromatography (GPC). GPC (more generally called size-exclusion chromatography) can be used in estimating the effect of degradation on molecular-weight distribution (MWD). Spectroscopic probes of thermal degradation include UV spectroscopy, IR spectroscopy, NMR spectroscopy, electron-spin resonance spectroscopy (ESR, EPR), and mass spectrometry (MS). Multiple internal reflectance infrared spectroscopy (MIRS) allows a very thin surface layer to be examined. Another method is flash pyrolysis in which the polymer's temperature is raised very rapidly to  $500^\circ\text{C}$  or more at which the molecules are broken down into small fragments. The fragment pattern can be analyzed by gas chromatography (pyrolysis-GC) and mass spectrometry (pyrolysis-MS), either separately or in combination (pyrolysis-GC/MS) [2–6,13].

Several thermal techniques are commonly employed to monitor the thermal stabilities of polymers [2–6,13]. In thermogravimetric analysis (TGA), a sensitive balance is used to follow the weight change of the sample in a specified environment (vacuum, air, or inert atmosphere)

as a function of time or temperature. Thermomechanical analysis (TMA) measures the mechanical responses of a polymer as a function of temperature. Typical measurements include: expansion properties, tension properties (elastic modulus), dilatometric properties (specific volume), single-fiber properties (single-fiber modulus), and compression properties. In isothermogravimetric analysis (IGA), weight loss as a function of time is recorded at a specified temperature. At lower temperatures, IGA is a valuable supplement to TGA in obtaining data on long-term stability. Thermal volatilization analysis (TVA) records the evolution of volatile products by measuring the pressure of volatile degradation products continuously in an evacuated system. According to Arnold [13], the preferred method of determining the relative short-term thermal or thermo-oxidative stability of high-temperature polymers is dynamic TGA. Longer-term stabilities are most conveniently defined by IGA if the temperature is properly chosen. Combination of these tests with TMA, which provides data on the  $T_g$  and softening behavior, gives a complete picture of the thermal limitations of most polymers.

Accelerated aging tests, such as the familiar “air-oven test”, have aided the investigation of thermal-oxidative degradation. The air-oven test involves subjecting a polymer sample to temperatures ranging from 70 °C to 150 °C with air flowing over the surface of the sample. The change in stress-strain behavior (e.g., tensile modulus, tensile strength, elongation at break) is measured on samples removed from the oven at intervals until the point of failure is reached. The rationale behind accelerated testing is basically that the results can be extrapolated in time to simulate actual service conditions. In reality, most accelerated aging tests are therefore a compromise between convenience and reliability [2].

In organic polymers, the progress of oxidation reactions can be followed using infrared (IR) spectroscopy. IR absorption bands of interest in PE and related polymers are C–H stretching (3.4  $\mu\text{m}$ ), C–H bending of  $\text{CH}_2$  groups (6.8  $\mu\text{m}$ ) and  $\text{CH}_3$  groups (shoulder at 7.25  $\mu\text{m}$  on an amorphous band at 7.30  $\mu\text{m}$ ), and  $\text{CH}_2$  rocking in sequences of methylene groups (13.9  $\mu\text{m}$ ). Other key absorption bands include C=C in natural rubber (6.1  $\mu\text{m}$ ), C=O and ether in PMMA (5.8 and 8.9  $\mu\text{m}$ , respectively), aromatic structures in PS (6.2, 6.7, 13.3, and 14.4  $\mu\text{m}$ ), C–Cl in PVC (14.5  $\mu\text{m}$ ), peptide groups in nylon (3.0, 6.1, and 6.5  $\mu\text{m}$ ), and  $\text{CF}_2$  in PTFE (8.2–8.3  $\mu\text{m}$ ) [1–11].

## 54.7 TABULATED DATA

There seems to be no accepted standard way of quantifying the thermal-oxidative stability and/or degradation of polymers. Therefore, different sources of data will often provide different criteria for describing the absolute or relative stability of polymers. Tables 54.2–54.5 summarize thermal-stability data extracted from a variety of sources

**TABLE 54.2.** Half-decomposition temperature  $T_{1/2}^a$  and monomer yield for selected polymers.

Polymer	$T_{1/2}(\text{°C})^b$	Monomer yield (%)
Poly(tetrafluoroethylene) (PTFE)	509	> 95
Poly( <i>p</i> -phenylene methylene)	430	0
Polymethylene	414	< 0.1
Polybutadiene	407	< 1
Polyethylene (PE) (branched)	404	< 0.025
Polypropylene	387	< 0.2
Polystyrene (PS)	364	40
Polyisobutylene	348	20
Poly(ethylene oxide)	345	4
Poly(methyl acrylate)	328	0
Poly(methyl methacrylate) (PMMA)	327	> 95
Poly(propylene oxide) (isotactic)	313	1
Poly(propylene oxide) (atactic)	295	1
Poly(vinyl acetate)	269	0
Poly(vinyl alcohol)	268	0
Poly(vinyl chloride) (PVC)	260	0

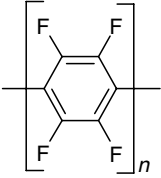
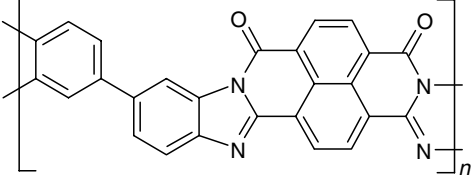
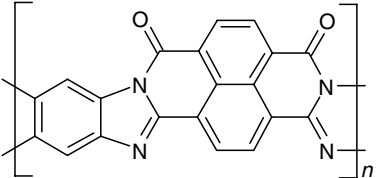
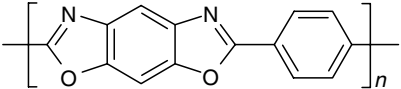
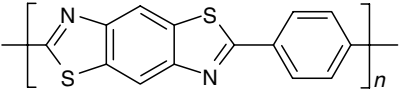
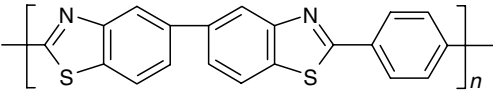
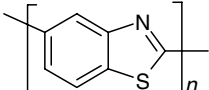
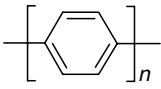
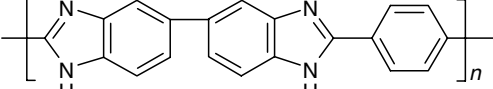
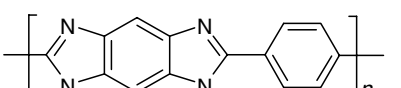
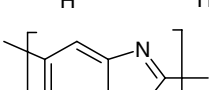
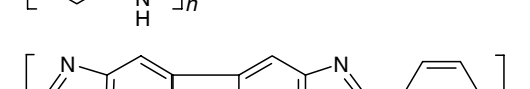
<sup>a</sup>Data taken from [12].

<sup>b</sup>Temperature at which the polymer loses 50% of its weight, if heated in vacuum for 30 min.

**TABLE 54.3.** Typical values of the upper use temperature (°C) for several familiar and commercial polymers.

Polymer	Upper use temperature (°C)	Reference
Natural rubber	80	[11]
SBR	110	[11]
Acrylate	150	[11]
Butyl	100	[11]
Chlorosulfonated polyethylene	120	[11]
EPDM	150	[11]
Epichlorohydrin	120	[11]
Fluorinated rubbers	230	[11]
Neoprene	100	[11]
Nitrile	120	[11]
Polybutadiene ( <i>cis</i> -1,4)	100	[11]
Polyisoprene ( <i>cis</i> -1,4)	60–80	[11, 12]
Polysulfide	80	[11]
Silicone	230	[11]
Poly(vinyl chloride) (PVC)	60	[12]
Polystyrene (PS)	60	[12]
Polymethacrylates	60–80	[12]
Polyolefins	60–90	[12]
Polyamides	80–100	[12]
Epoxy resins	80–110	[12]
Polycarbonate	100–135	[12]
Poly(phenylene oxide) (PPO)	130–150	[12]
Polysulfone	130–150	[12]
Polyfluorocarbons	150–220	[12]
Aromatic polyamides	180–230	[12]
Polyimides	180–250	[12]
Poly(tetrafluoroethylene)	180–250	[12]
Polybenzimidazole (PTFE)	250–300	[12]
Polyurethanes	70–110	[11]

**TABLE 54.4.** Thermal stability of selected heat-resistant aromatic, heterocyclic, and ladder-type polymers in an inert atmosphere.

Polymer	PDT (°C) <sup>a</sup>	Reference
	720	[13]
	690–710	[13]
	690–710	[13]
	660–700	<sup>b</sup>
	700	<sup>b</sup>
	685–700	[13]
	685–700	[13]
	660	[13]
	650	[13]
	650	[13]
	650	[13]
	650	[13]

<sup>a</sup> Polymer decomposition temperature.

<sup>b</sup> A number of relevant articles on PBO and PBT and related rodlike polymers can be found in *Macromolecules*, 14, 891 (1981) and in the Dec. 1980 and March 1981 special issues of the *Brit. Polym. J.*

**TABLE 54.5.** Initial temperature reported for thermal decomposition of selected common polymers.

Polymer	Initial decomposition temperature <sup>a</sup> (°C)
Poly(acetylene)	650
Poly(butadiene)	325
Poly(chloroprene)	170
Natural rubber	287
Poly(ethylene)	264
Poly(propylene)	120
Poly(acrylonitrile)	235
Poly(methacrylic acid)	200
Poly(vinyl acetate)	213
Poly(vinyl alcohol)	240
Poly(vinyl chloride)	200
Poly(styrene)	300
Phenol-formaldehyde resin	250
Cellulose	250
Cellulose triacetate	250
Ethyl cellulose	306

<sup>a</sup>Data taken from [21]. Value given for each polymer represents the lowest decomposition temperature for which decomposition products are given in [21].

in the literature on selected familiar and commercial polymers. Table 54.6 compares the relative stability of several flexible linking groups. For a comprehensive listing of polymers, including a description of the products of thermal degradation, the reader is directed to Grassie [21].

Related information can be found in Chapter 53.

**TABLE 54.6.** Thermal and thermal-oxidative stability of some simple flexible linking groups<sup>a</sup>.

Group	Thermal stability <sup>b</sup> (°C)	Thermal-oxidative stability <sup>c</sup> (°C)
-CO-	500	389
-CONH-	500	431
-(CF <sub>2</sub> ) <sub>3</sub> -	469	— <sup>d</sup>
-COO-	457	447
-S-	436	418
-CH <sub>2</sub> CH <sub>2</sub> -	429	383
-CH <sub>2</sub> -	408	— <sup>d</sup>
-O-	— <sup>d</sup>	368

<sup>a</sup>Data taken from [13].

<sup>b</sup>Temperature for 25% weight loss in 2 hours in inert environment.

<sup>c</sup>Temperature for 25% weight loss in 2 hours in air (oxygen).

<sup>d</sup>Data not available.

#### 54.8 MATERIAL SCIENCE TOOLS ON THE WORLD WIDE WEB

Today more and more information is taken from on-line resources. The World Wide Web has become a popular and reliable tool for research in many disciplines including polymer science. Rather than an exhaustive overview of the available web-based resources for polymer scientists, this section is intended to point the scientist to a few notable Internet portals that were useful in preparing this chapter.

**MatWeb**  
MATERIAL PROPERTY DATA

New! SolidWorks<sup>®</sup>/COSMOSWorks library exports.

Data sheets for over 46,000 metals, plastics, ceramics, and composites.

HOME • SEARCH • TOOLS • FORUM • BASKET • ABOUT US • HELP • LOGIN

Searches: Advanced | Material Type | Property | Composition | Trade Name | Manufacturer

**MatWeb. Your Source for Materials Information**

**What is MatWeb?**

The heart of MatWeb is a **searchable database of material data sheets**, including property information on thermoplastic and thermoset polymers such as ABS, nylon, polycarbonate, polyester, polyethylene and polypropylene; metals such as aluminum, cobalt, copper, lead, magnesium, nickel, steel, superalloys, titanium and zinc alloys; ceramics; plus semiconductors, fibers, and other engineering materials.

**SolidWorks** MatWeb is freely available and does not require registration. You can still access all of the features that have always been available. However, our **advanced features** are only available to our Registered and Premium users, including our new Premium **exports in the SolidWorks COSMOSWorks** library format.

**How to Find Property Data in MatWeb**

**Quantitative Searches:**

- Physical Properties - Metric
- Physical Properties - Common US
- Alloy Composition
- Advanced Search (Registration Required)

**Categorized Searches:**

- Material Type
- Polymer
- Manufacturer
- Polymer Trade Name
- Metal UNS Number

**Text Search:**

- Enter a key word or phrase in the box below (this search is also available at the top of every page).

**Featured Material:**

Windform XT  
Carbon Composite

**GoPolymers INC.**  
BUY/SELL your Scrap, Virgin, and Regrid here!

**FIGURE 54.4.** A screenshot of the main page of the MatWeb portal. Reprinted with permission © (1996-2006) by Automation Creations, Inc.

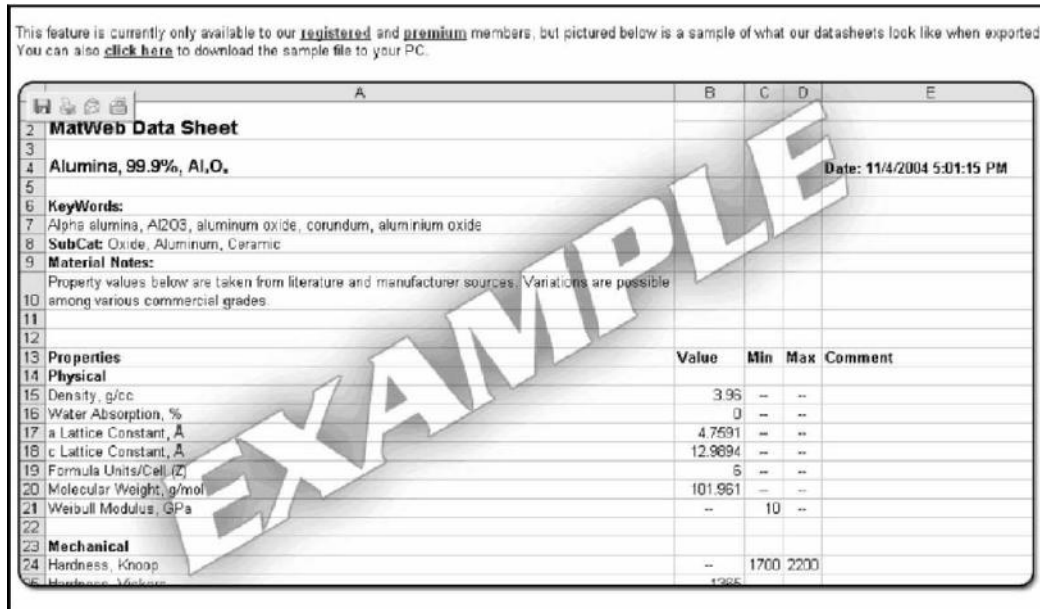


FIGURE 54.5. Example of the Excel spreadsheet generated after MatWeb search. Reprinted with permission © (1996–2006) by Automation Creations, Inc.

MatWeb, <http://www.matweb.com>, is a searchable database of over 46,000 metals, plastics, ceramics, and composite materials. It allows search by material type, trade name, range of values, composition, UNS number (Unified Numbering System for Metals and Alloys) and even system of units (metric, common US units). An example of searchable materials includes thermoplastic and thermoset polymers such as ABS, nylon, polycarbonate, polyester, polyethylene, and polypropylene; metals such as aluminum, cobalt, cop-

per, lead, magnesium, nickel, steel, superalloys, titanium, and zinc alloys; ceramics; plus semiconductors, fibers, and other engineering materials.

For registered users, all data retrieved from searches can be exported to an Excel spreadsheet for further analysis (Fig. 54.4, 54.5).

Another web resource, Omnexus can be found at the following address: <http://www.omnexus.com/index.aspx> (Fig. 54.6).



FIGURE 54.6. A screenshot taken of the front page of the Omnexus website. Reprinted with permission from Omnexus.com.

This site contains very useful information, such as current news in polymer science, information about on-line seminars and scientific conferences, and numerous material databases. Databases are searchable by various criteria, such as physical and chemical properties, molecular weight or density. The search output also contains information about manufacturer and on-line vendors. This site requires registration for full access, but registration is free.

## REFERENCES

1. L. D. Loan and F. H. Winslow, in *Macromolecules: An Introduction to Polymer Science*, edited by F. A. Bovey and F. H. Winslow, (Elsevier Science & Technology, Amsterdam, 1982) p. 576.
2. N. Grassie and G. Scott, *Polymer Degradation & Stabilisation* (Cambridge University Press, Cambridge, 1988) p. 222.
3. L. Reich and S. S. Stivala, *Elements of Polymer Degradation*, (McGraw-Hill Book Company, New York, 1971) p. 361.
4. N. Grassie, in *Encyclopedia of Polymer Science and Technology*, vol.4, (Interscience Publishers, New York, 1966) p. 647.
5. L. I. Nass, in *Encyclopedia of Polymer Science and Technology*, vol.12, (Interscience Publishers, New York, 1966) p. 725.
6. J. E. Mulvaney, in *Encyclopedia of Polymer Science and Technology*, vol. 7, (Interscience Publishers, New York, 1966) p. 478.
7. R. B. Seymour and C. E. Carraher, Jr., *Structure-Property Relationships in Polymers*, (Plenum Press, New York, 1984) p. 246.
8. C. Hall, *Polymer Materials*, (Halsted Press: John Wiley & Sons, New York, 1989) p. 243.
9. H. R. Allcock and F. W. Lampe, *Contemporary Polymer Chemistry*, third edition, (Prentice-Hall, Inc., Upper Saddle River, NJ, 2003) p. 832.
10. H.-G. Elias, *Macromolecules*, second edition, (Plenum Press, New York, 1984), p. 564.
11. F. W. Billmeyer, Jr., *Textbook of Polymer Science*, third edition (Wiley-Interscience: John Wiley & Sons, New York, 1990) p. 578.
12. D. W. van Krevelen, *Properties of Polymers: Their Correlation with Chemical Structure: Their Numerical Estimation and Prediction from Additive Group Contributions*, third edition, (Elsevier Scientific, Amsterdam, 1997), p. 875.
13. C. Arnold, Jr., *J. Polym. Sci.: Macromolecular Rev.* 14, 265 (1979).
14. W. J. Welsh, D. Bhaumik, H. H. Jaffe, *et al. Polym. Eng. Sci.* 24, 218 (1984).
15. R. C. Evers and G. J. Moore, *J. Polym. Sci.: Part A: Polym. Chem.* 24, 1863 (1986).
16. W. J. Welsh, in *Current Topics in Polymer Science*, vol. I, edited by R.M. Ottenbrite, L. A. Utracki, and S. Inoue, (Hanser Publishers, Munich, 1987) p. 217.
17. F. E. Arnold and R. L. Van Deusen, *Macromolecules*, 2, 497 (1969); R.L. Van Deusen, O. K. Goins, and A. J. Sicree, *J. Polym. Sci. A-1*, 6, 1777 (1968).
18. W. J. Welsh, D. Bhaumik, and J. E. Mark, *J. Macromol. Sci. Phys.* 20, 59 (1981).
19. W. J. Welsh and J. E. Mark, in *Computational Modeling of Polymers*, edited by J. Bicerano, (Marcel Dekker, Inc., New York, 1992) p. 648.
20. R. D. Miller and J. Michl, *Chem. Rev.* 89, 1359 (1989).
21. N. Grassie, in the *Polymer Handbook*, fourth ed., edited by J. Brandrup (Editor), Edmund H. Immergut, Eric A. Grulke, Akihiro Abe, Daniel R. Bloch, (Wiley-Interscience: John Wiley & Sons, New York, 2003) p. 2336.
22. J. H. Noggle, *Physical Chemistry*, third ed., (Pearson Education, New York, 2002), p. 1108.
23. B. E. Douglas, D. H. McDaniel, and J. J. Alexander, *Inorganic Chemistry*, 2nd ed., (John Wiley & Sons, Inc., New York, 1993) p. 78.



## CHAPTER 55

# Synthetic Biodegradable Polymers for Medical Applications

Laura J. Suggs\*, Sheila A. Moore†, and Antonios G. Mikos†

\*Department Biomedical Engineering, University of Texas at Austin, Austin, TX 78712

†Department of Bioengineering, Rice University, PO Box 1892, MS-142, Houston, TX 77251-1892

---

55.1	Introduction . . . . .	939
55.2	Biodegradable Polymers . . . . .	939
55.3	Summary . . . . .	947
55.4	Acknowledgments . . . . .	947
55.5	Appendix . . . . .	947
56.6	Chemical Structures . . . . .	948
	References . . . . .	949

---

---

### 55.1 INTRODUCTION

Biodegradability has been the primary consideration in the development of biomedical materials due to problems associated with the biocompatibility of long-term, nondegradable polymer implants. Biodegradable polymers have been formulated for uses such as sutures, drug delivery devices, scaffolds for tissue regeneration, vascular grafts and stents, artificial skin, orthopedic implants, and others. The purpose of this overview is to elucidate the characteristics of several synthetic biodegradable polymers for medical applications, which include degradation modes and rates and their relationship to physicochemical, thermal, and mechanical properties. Polymers mentioned in the chapter are poly( $\alpha$ -hydroxy esters), poly( $\epsilon$ -caprolactone), poly(*ortho* esters), polyanhydrides, poly(3-hydroxybutyrate) polyphosphazenes, polydioxanones, fumarate-based polymer, polyoxalates, poly(amino acids), and pseudopoly(amino acids). The synthesis, medical uses, and processing techniques of these polymers are not discussed in detail, but additional references are given for each polymer as well as several comprehensive review articles [1–8].

### 55.2 BIODEGRADABLE POLYMERS

#### 55.2.1 Poly( $\alpha$ -Hydroxy Esters)

##### *Poly(Glycolic Acid)*

Poly(glycolic acid) (PGA) is a highly crystalline, hydrophilic, linear aliphatic polyester (Structure 1). As such, it has a high melting point and a relatively low solubility in most common organic solvents. At room temperature, PGA is soluble in hexafluoroisopropanol, a highly toxic solvent. It degrades primarily by bulk erosion through random hydrolysis of its ester bonds. Reed and Gilding [9] report that the degradation kinetics is biphasic, with the first phase of degradation occurring by diffusion of water to the amorphous regions and subsequent hydrolysis. The second phase begins as water penetrates and hydrolyzes the more crystalline regions. The molecular weight distributions, which show two degradation phases, are given in Fig. 55.1 [9]. For PGA surgical sutures, mass loss occurs primarily during the second phase, completing the entire process between weeks 4 and 12. The rate of hydrolysis can be controlled

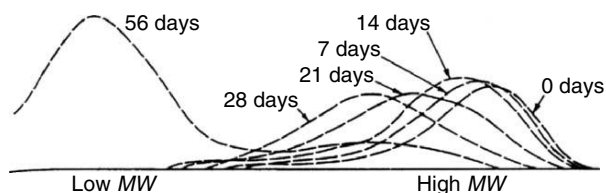


**FIGURE 55.1.** Molecular weight distributions as a function of degradation time for PGA sutures at pH 7 and 37 °C. The formation of a bimodal distribution is evident at large times due to the biphasic degradation of PGA. (Reprinted with permission from [9].)

in vitro by varying the pH [10]. Any large deviation from neutral pH drives hydrolytic cleavage. In addition, the degradation rate can be affected by the degree of crystallinity or “curing time” of PGA, as shown in in vivo studies [11].

The crystallinity of PGA is typically between 46% and 52% [9], the maximum crystallinity during degradation occurring in the time between the two degradation phases. The values of crystallinity are not only influenced by the quenching or “curing” process but also the molecular weight of the polymer [12].

PGA (crystallinity 50%) loses most of its mechanical strength over the first 2–4 weeks of degradation [9]. This is asynchronous with the mass loss which begins at approximately week 4. This is due to the bimodal degradation distribution. The amorphous regions are hydrolyzed first which results in loss of mechanical strength, while the degradation and diffusion of low molecular weight chains later result in significant mass loss. The stress/strain curves showing the effect of degradation on mechanical strength are given in Fig. 55.2 [9].

#### *Poly(Lactic Acid)*

Poly(lactic acid) (PLA) (Structure 2) is also a linear polyester, but the presence of an extra methyl group makes it more hydrophobic than PGA. Its water uptake in thin films is approximately 2% [13]. The methyl group contributes to a more amorphous character as well as increasing its solubility in organic solvents. In addition, this group creates a chiral center which results in two different enantiomeric forms of the polymer, P(D)LA and P(L)LA. The racemic mixture of the two is abbreviated as P(D,L)LA. The most commonly used form is P(L)LA which, like all poly(lactic acids), releases lactic acid upon degradation. PLA is frequently cast from common solvents. These include: chloroform, methylene chloride, methanol, ethanol, benzene, acetone, dioxane, dimethylformamide, and tetrahydrofuran [14–16]. PLA has also been shown to degrade by a homogeneous, hydrolytic erosion [17–19]. For example, P(D,L)LA degrades in a conventional two-stage process where the majority of molecular weight loss occurs in the first stage, and the subsequent loss in mass and tensile strength begins in the second stage at a number average

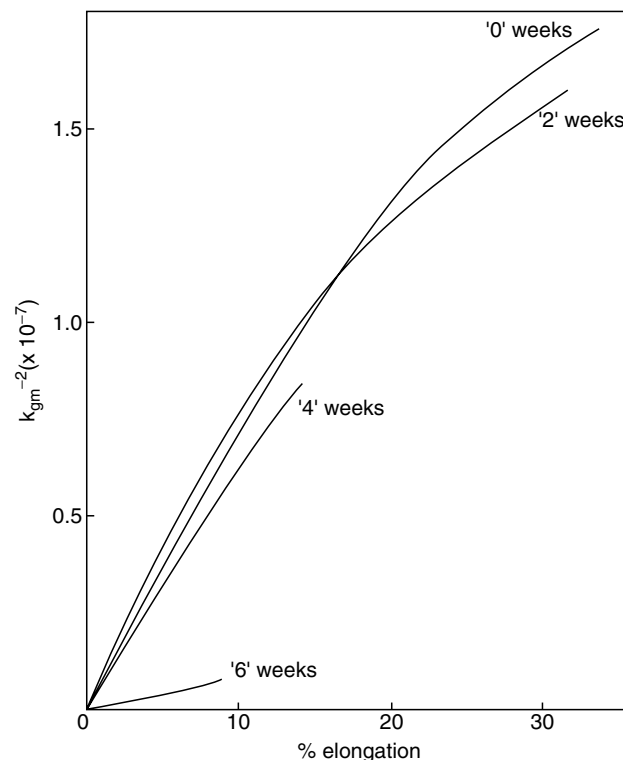


**FIGURE 55.2.** Stress/strain curves showing the loss of mechanical strength with degradation time for PGA sutures at pH 7 and 37 °C. (Reprinted with permission from [9].)

molecular weight of 15,000 [9]. P(L)LA of molecular weight 95,000 degraded in vivo by 56% in 6 months based on peak molecular weight ( $M_p$ ) [20]. For P(D,L)LA between 58,000 and 87,000, 49% degraded in vivo in 1 month, also based on  $M_p$ . A half-life of 6.6 months by mass was reported [11] for P(L)LA of molecular weight 85,000. In vitro studies [9] showed a 50% loss in weight average molecular weight ( $M_w$ ) in 16 weeks with a concurrent loss of 10–15% by mass. The degradation rate of PLA also varies with varying pH [21,22]. The amount of lactic acid released during the course of PLA degradation is very small but increases rapidly as PLA is broken down to low molecular weight oligomers. A sudden rise in the lactic acid concentration in vivo can render the local environment acidic and induce an inflammatory reaction or even tissue necrosis. The use of polydispersed PLA can result in distribution of the lactic acid production over time [23].

Thermal and mechanical properties of both P(L)LA and P(D,L)LA of various molecular weights are given in Table 55.1. Additional thermal properties of PLA are found in Lu *et al.* [24].

#### *Poly(Lactic-co-Glycolic Acid) Copolymers*

The advantage of copolymerizing poly( $\alpha$ -hydroxy esters) is the ability to control physical and mechanical properties;

**TABLE 55.1.** Thermal and mechanical properties of respective synthetic biodegradable polymers [4,24,48,74,75,95,96].

Polymer	Weight average molecular weight	Glass transition temp. (°C)	Melting temp. <sup>a</sup> (°C)	Decomposition temp. (°C)	Heat of fusion <sup>a</sup> (Jg <sup>-1</sup> )	Tensile strength (MPa)	Tensile modulus (MPa)	Flexural modulus (MPa)	Elongation at yield (%)	Elongation at break (%)
<b>Poly(<math>\alpha</math>-Hydroxy Ester)</b>										
PLGA	50,000	35	210	254	71	—	—	—	—	—
P(L)LA	50,000	54	170	242	41	28	1,200	1,400	3.7	6
P(L)LA	100,000	58	159	235	20	50	2,700	3,000	2.6	3.3
P(L)LA	300,000	59	178	255	39	48	3,000	3,250	1.8	2
P(D,L)LA	21,000	50	A	255	A	—	—	—	—	—
P(D,L)LA	107,000	51	A	254	A	29	1,900	1,950	4.0	6
P(D,L)LA	550,000	53	A	255	A	35	2,400	2,350	3.5	5
Poly( $\epsilon$ -Caprolactone)	44,000	-62	57	350	34	16	400	500	7.0	80
<b>Poly(Ortho Esters)</b>										
P(CDM- <i>co</i> -HD) 35:65	99,700	55	A	358	A	20	820	950	4.1	220
P(CDM- <i>co</i> -HD) 70:30	101,000	84	A	362	A	19	800	1,000	4.1	180
P(CDM- <i>co</i> -HD) 90:10	131,000	95	A	338	A	27	1,150	1,250	3.4	7
<b>Polyanhydrides</b>										
PSA	—	60	86	—	153	—	—	—	—	—
P(CPP- <i>co</i> -SA) 22:78	—	47	66	—	64	—	—	—	—	—
P(CPP- <i>co</i> -SA) 41:59	—	4	178	—	8	—	—	—	—	—
P(CPP- <i>co</i> -SA) 60:40	—	0	200	—	25	—	—	—	—	—
P(CPP- <i>co</i> -SA) 80:20	—	15	205	—	34	—	—	—	—	—
PCPP	—	96	240	—	111	—	—	—	—	—
<b>Poly(3-Hydroxybutyrates) Copolymers</b>										
PHB	370,000	1	171	252	51	36	2,500	2,850	2.2	2.5
P(HB- <i>co</i> -HV) 93:7	450,000	-1	160	243	32	24	1,400	1,600	2.3	2.8
P(HB- <i>co</i> -HV) 89:11	529,000	2	145	235	12	20	1,100	1,300	5.5	17
P(HB- <i>co</i> -HV) 78:22	227,000	-5	137	251	7	16	620	750	8.5	36
<b>Polydioxanones</b>										
PTMC	48,000	-15	A	261	A	0.5	3	—	20	160
<b>Pseudopoly(Amino Acids)</b>										
PBPA	105,000	69	A	135	A	50	2,150	2,400	3.5	4
PDTH	101,000	55	A	138	A	40	1,630	—	3.5	7
<b>Poly(Fumarates)</b>										
PPF:PPF-DA 1:2 <sup>b</sup>	2,600	11.2	A	—	A	61	857	3,124	5.6	10.8
PPF:PPF-DA 1:1	2,600	11.2	A	—	A	70	923	2,644	4.3	11.3
PPF:PPF-DA 2:1	2,600	11.2	A	—	A	64	806	2,206	4.3	12.9
P(PF- <i>co</i> -EG) <sup>c</sup> 33:66	8,200	-54.1	26.5	—	17.5	0.23	2.16	0.87	—	—
P(PF- <i>co</i> -EG) 33:66	14,200	-44.6	39.7	—	20.1	0.32	1.9	3.87	—	—
P(PF- <i>co</i> -EG) 66:33	8,050	-43.5	25.0	—	0.2	1.06	11.02	1.69	—	—
P(PF- <i>co</i> -EG) 66:33	13,090	-46.1	27.7	—	9.9	0.91	5.05	2.39	—	—

<sup>a</sup>The symbol A designates amorphous polymer.

<sup>b</sup>PPF:PPF-DA 1:2 refers to the ratio of double bonds present in each monomer.

<sup>c</sup>P(PF-*co*-EG) was crosslinked with poly(*N*-vinyl pyrrolidinone).

however, there is no linear relationship between the physical properties of the constituent homopolymers and their copolymers. Most of these copolymers are amorphous (between approximately 24 and 67 mol% glycolic acid) [13], and therefore, degradation rates are highly dependent on the

relative amount of each comonomer. Copolymers with high or low comonomer ratios are less sensitive to hydrolysis than copolymers with a more equimolar ratio, due to their greater crystallinity. Half-lives for various PLA and PGA ratios are depicted graphically in Fig. 55.3 [11].

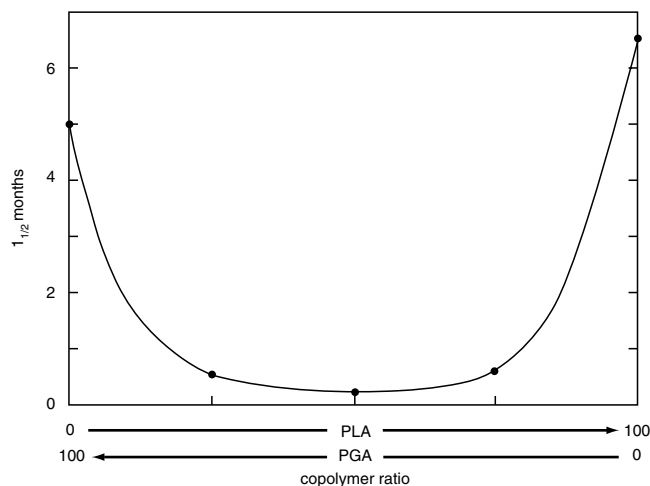


**FIGURE 55.3.** Variation of half-life of PLGA copolymers with the lactic acid and glycolic acid copolymer ratio in vivo. (Reprinted with permission from [11].)

Due to the dependence of the degradation rate of poly(lactic-*co*-glycolic acid) (PLGA) copolymers on pH, a phenomenon known as autocatalysis occurs where the carboxylic acid monomers released during degradation reduce the pH and further induce degradation [22–25]. For large-scale polymers, autocatalysis causes a heterogeneous degradation where the pH decreases in the center of the polymer, and a differential in the degradation rate is created [26].

Multiple uses of poly(lactic acid), poly(glycolic acid), and their copolymers have been described including sutures

[27], vascular grafts [28], drug carriers [29,30], and scaffolds for tissue engineering [31,32]. This is due in part to the FDA approval of these polymers for certain medical applications.

### 55.2.2 Poly( $\epsilon$ -Caprolactone)

Poly( $\epsilon$ -caprolactone) (PCL) is a semicrystalline, aliphatic polyester (Structure 3). It is soluble in tetrahydrofuran, chloroform, methylene chloride, carbon tetrachloride, benzene, toluene, cyclohexanone dihydropyran, and 2-nitropropane; and only partially soluble in acetone, 2-butanone, ethyl acetate, acetonitrile, and dimethyl fumarate [33]. PCL is also capable of forming blends as well as useful copolymers with a wide range of polymers [34].

PCL has been shown to degrade by random hydrolytic scission of its ester groups, and under certain circumstances, by enzymatic degradation [33]. It is similar to P(D,L)LA, in that it degrades in a two-phase process with the molecular weight loss occurring primarily in the first phase, and the major mass and strength loss at the onset of the second at a number average molecular weight of 5,000 [35]. However, PCL degrades almost three times slower than P(D,L)LA [4]. A graph of molecular weight versus time showing the degradation of PCL capsules in vivo is given in Fig. 55.4 [35]. The crystallinity of PCL increases with decreasing molecular weight with polymers of molecular weight above 100,000 being about 40% crystalline. This value increases to about 80% for molecular weights of 5,000 [35]. As a result, PCL behaves like PGA in that the residual crystallinity increases

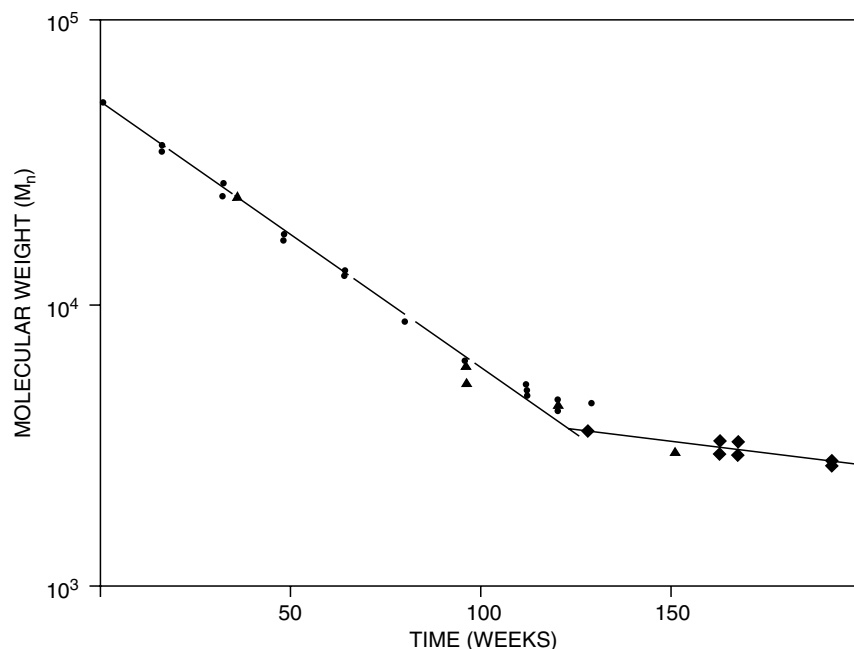


**FIGURE 55.4.** Decrease of molecular weight of PCL with the degradation time for PCL capsules loaded with various drugs in vivo. (Reprinted with permission from [35].)

as the polymer degrades. The degradation rate of PCL can be increased by forming a copolymer with DL-lactide [36]. In addition, PCL is affected by acidic conditions consistent with an autocatalytic degradation mechanism, and it is also influenced by the addition of small molecules such as ethanol, pentanol, oleic acid, decylamine, and tributylamine [37].

PCL has a low glass transition temperature of  $-62\text{ }^{\circ}\text{C}$ , existing always in a rubbery state at room temperature, and a melting temperature of  $57\text{ }^{\circ}\text{C}$ . It has been postulated that these properties lead to a high permeability of PCL for controlled release agents. Other thermal and mechanical properties are listed in Table 55.1.

### 55.2.3 Poly(*Ortho* Esters)

Poly(*ortho* esters) are amorphous, hydrophobic polymers containing hydrolytically labile, acid-sensitive, backbone linkages (Structures 4, 5, 6). Due to their hydrophobicity, they can easily dissolve in organic solvents including: chloroform, methylene chloride, and dioxane. However, it can be difficult to remove the solvent in a situation such as a solvent casting [38]. In addition, these polymers are not inherently susceptible to degradation in the presence of water, although they can be if anhydrides (acid excipients), glycolic acid, or lactic acid are incorporated. They are susceptible to thermal degradation and must be processed accordingly.

Poly(*ortho* esters) are a class of polymers which can degrade heterogeneously by surface erosion [39]. These

polymers lose material from the surface only, while retaining their original geometry. As such, their primary use is in drug delivery [40]. The first class of poly(*ortho* esters), as shown in Structure 4, generates a carboxylic acid upon hydrolysis which then further catalyzes the acid-sensitive cleavage. A basic salt such as  $\text{Na}_2\text{CO}_3$  or  $\text{Mg}(\text{OH})_2$  is usually incorporated to neutralize the acid product, however, this creates a diffusion-limited system which exhibits nonzero-order drug release characteristics.

The second class, represented by Structures 5 and 6, does not produce acidic hydrolysis products, and its degradation can be controlled by the incorporation of either acidic or basic excipients. In the case of acid addition, water penetrates, ionizes the acid, and reduces the pH. This then catalyzes the hydrolysis, resulting in a hydration front and an erosion front. For a basic excipient, water must penetrate, elute, or neutralize the base, and then allow erosion to occur, decreasing the rate of hydrolysis [41]. According to the choice of additive, degradation rates can be varied from several days to years. Acid excipients can also be incorporated into the polymer itself as pendant chains which are solubilized upon cleavage [42]. For example, the degradation rates are enhanced for polymers containing *trans*-cyclohexanedimethanol (CDM) and 1,6-hexanediol (HD) when acidic functionalities, 9,10-dihydroxy-stearic acid (DHSA) [43], are incorporated, as shown in Fig. 55.5. The polymer can also be crosslinked at temperatures as low as  $40\text{ }^{\circ}\text{C}$  with an excipient stabilized interior [44].

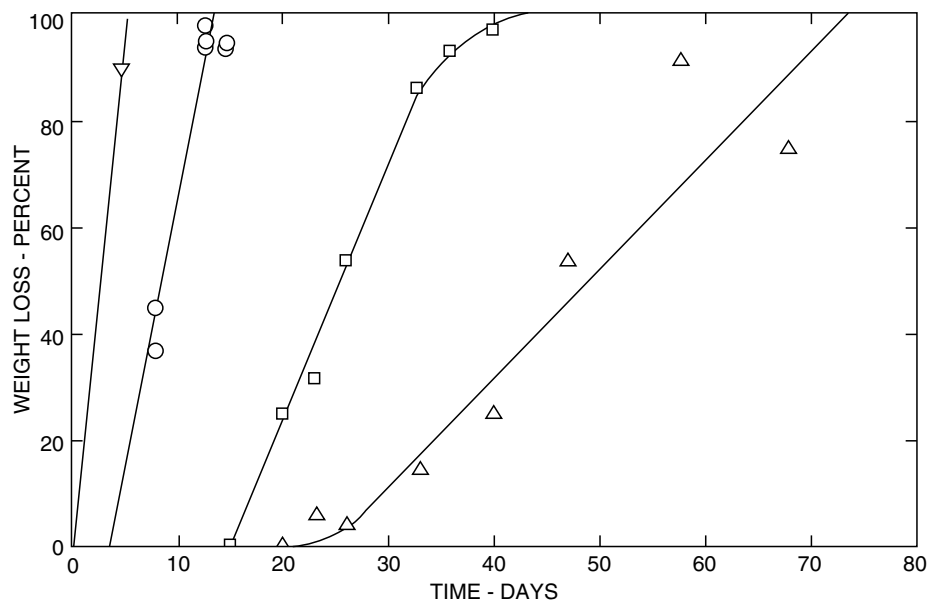


**FIGURE 55.5.** Variation of cumulative weight loss with time for poly(*ortho* esters) containing *trans*-cyclohexanedimethanol (CDM), 1,6-hexanediol (HD), and 9,10-dihydroxy-stearic acid (DHSA) (in the form of  $6 \times 0.5$  mm disks at pH 7 and  $37\text{ }^{\circ}\text{C}$ ). S = 58% CDM, 38% HD, 4% DHSA; E = 59% CDM, 39% HD, 2% DHSA; G = 59.5% CDM, 39.5% HD, 1% DHSA; C = 59.7% CDM, 39.75% HD, 0.5% DHSA. (Reprinted with permission from J. Heller, D. W. H. Penhale, and S. Y. Ng. in *Long-Acting Contraceptive Delivery Systems*, edited by G. I. Zatuchni, A. Goldsmith, J. D. Shelton, and J. J. Sciarra, (Harper and Row, New York, 1984), p. 127.)

Functionalizing the third class with lactic acid or glycolic acid produces an autocatalytic polymer [45,46]. Degradation is mediated by surface and bulk erosion, which is controlled by the concentration of the  $\alpha$ -hydroxy acid segments [47]. There is a linear relationship between weight loss and lactic acid release suggesting surface erosion, also molecular weight decreases signifying bulk erosion. Unlike PLGA and PLA the bulk of the material does not become acidic; the acid products from hydrolysis are concentrated at the surfaces and are easily diffused away [47].

The mechanical and thermal properties of these polymers can also be varied over a wide range by the selection of starting materials with differing compositions and molecular weights. The tripolymerization of 3,9-*bis*(ethylidene 2,4,8,10-tetraoxaspiro[5,5]undecane) with mixtures of the rigid diol CDM and the flexible diol HD allows preparation of polymers with controlled glass transition temperature [40] (Fig. 55.6). Other thermal and mechanical properties for P(CDM-*co*-HD) copolymers are listed in Table 55.1.

### 55.2.4 Polyanhydrides

Polyanhydrides are a class of hydrolytically unstable polymers that are usually either aliphatic, aromatic, or a combination of the two. Two general representations are given in Structures 7 and 8. These polymers dissolve in common organic solvents including chloroform and methylene chloride and are extremely sensitive to aqueous environments. In addition, they are very reactive and can react with amine or other nucleophilic groups that are present in drugs intended for controlled release. This is true especially at elevated temperatures, for example, as occurs during polymer processing [48].

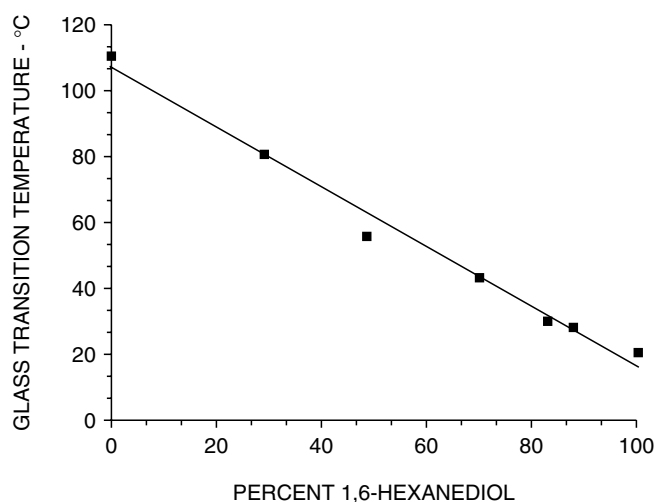


**FIGURE 55.6.** Glass transition temperatures of poly(*ortho* esters) consisting of 3,9-*bis*(ethylidene 2,4,8,10 tetraoxaspiro [5,5]undecane) with *trans*-cyclohexanedimethanol and 1,6-hexanediol as a function of the 1,6-hexanediol content. (Reprinted with permission from [40].)

The degradation of polyanhydrides can be varied from days to years depending on the choice or combination of choices of backbone structure [49,50]. The degradation rate of several different combinations of the aliphatic monomer, sebacic acid (SA), and the aromatic monomer, *bis*-(*p*-carboxyphenoxy)propane (CPP), is given in Fig. 55.7. The polymer primarily degrades by surface erosion [51–53]. As such, it is a candidate for drug delivery, eliminating the need for additional excipients. Its degradation rate is also sensitive to changes in pH, typically increasing with increasing pH as shown in Fig. 55.8 [50].

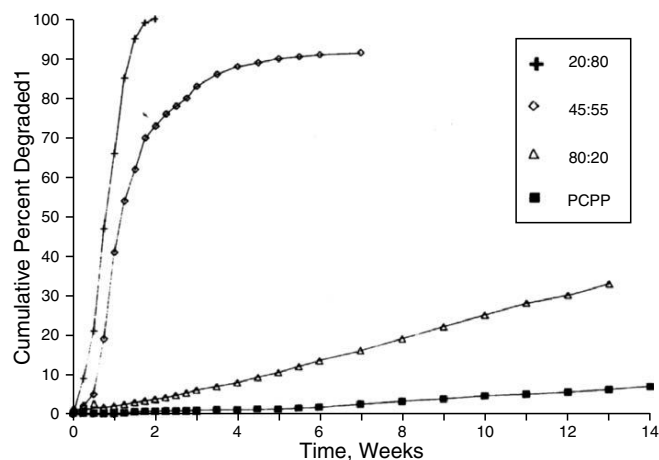


**FIGURE 55.7.** Change of cumulative percent of polymer degraded with degradation time for P(CPP-*co*-SA) copolymers in the form of compression-molded disks of 1.4 cm diameter and 1 mm thickness at pH 7.4 and 37 °C. (Reprinted with permission from K. W. Leong, B. G. Brott, and R. Langer, *J. Biomed. Mater. Res.* 19, 941 (1985).)

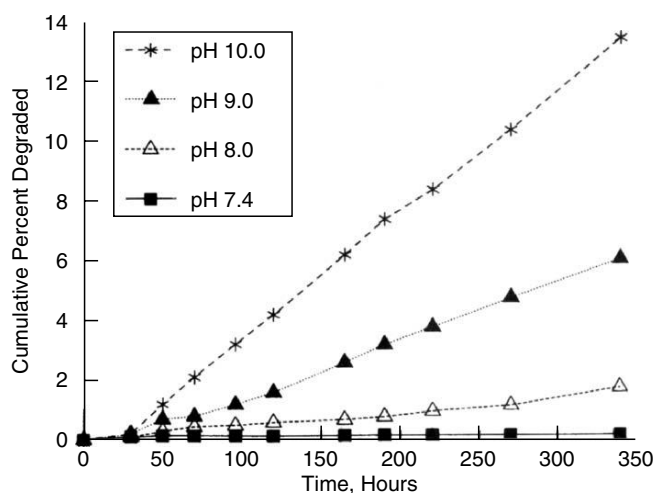


**FIGURE 55.8.** Change of cumulative percent of polymer degraded with degradation time at varying pH levels for PCPP in the form of compression-molded disks of 1.4 cm diameter and 1 mm thickness at 37 °C. (Reprinted with permission from K. W. Leong, B. G. Brott, and R. Langer, *J. Biomed. Mater. Res.* 19, 941 (1985).)

There are a wide variety of processing techniques available for forming polyanhydrides, however, care must be taken in incorporating controlled release agents at high temperatures because of the reactivity of the polymer with the drug and the instability of the polymer itself. The mechanical properties of polyanhydrides are generally poor, tending to be brittle with minimal fiber-forming abilities. Forming copolymers of polyanhydrides increases the mechanical properties, while maintaining their degradation characteristics [54,55]. Copolymers of methacrylated sebacic acid (MSA) and 1,6-bis(carboxyphenoxy) hexane (MCPH) have been shown to have similar mechanical properties of cortical and trabecular bone [56]. These copolymers degrade by surface erosion allowing the scaffold to maintain its structural integrity [56].

In addition, polyanhydrides have been shown to have excellent *in vivo* biocompatibility [57]. The thermal properties of representative P(CPP-*co*-SA) copolymers are given in Table 55.1. A detailed presentation of thermal properties is given in Domb *et al.* and Tamada and Langer [48,58].

### 55.2.5 Poly(3-Hydroxybutyrate) Copolymer

Poly(3-hydroxybutyrate) (PHB) is crystalline, thermoplastic polyester made by micro-organisms as an energy storage molecule (Structure 9). As such, it can be enzymatically degraded by certain bacteria. It is often copolymerized with hydroxyvaleric acid (Structure 10) to create poly(3-hydroxybutyrate-*co*-3-hydroxyvalerate), P(HB-*co*-HV). Solvent casting has been described from solution in chloroform, methylene chloride, and tetrahydrofuran [59,60].

The degradation of PHB produces D-3-hydroxy butyric acid, normally found in human blood, which may contribute to its low toxicity. There is evidence for both enzymatic and hydrolytic degradation *in vivo* [61]. *In vitro* studies [59, 60] suggest that PHB and P(HB-*co*-HV) copolymers degrade by hydrolysis in a multistage process where the majority of the molecular weight loss occurs before any significant mass loss. A graph of weight loss for various P(HB-*co*-HV) copolymers is given in Fig. 55.9 [60]. The copolymerization of hydroxybutyric acid with hydroxyvaleric acid increases the percentage of amorphous regions compared to PHB, which are readily attacked by hydrolytic degradation thereby increasing degradation rates. In addition, elevated temperatures and alkaline conditions have been shown to increase degradation rates.

The crystallinity and mechanical properties of the P(HB-*co*-HV) copolymer can be varied by modification of the percentages of the respective monomers. The higher the percentage of hydroxyvalerate, the less crystalline and the more elastic the polymer becomes. Some thermal and mechanical properties are presented in Table 55.1. A study of thermal characteristics *in vivo* is given in Gogolewski *et al.* [61], and a mechanical evaluation *in vivo* and *in vitro* is found in Miller and Williams [62].

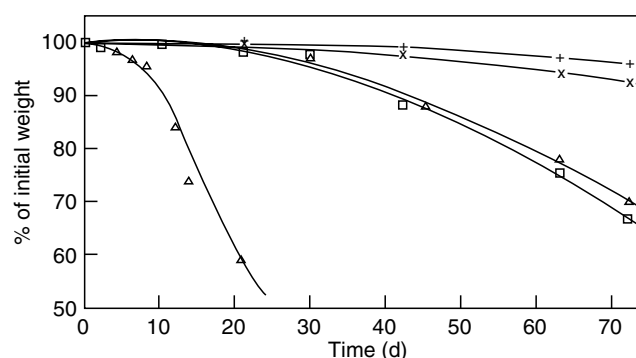


**FIGURE 55.9.** Kinetics of percent of initial weight loss for P(HB-*co*-HV) copolymers of different copolymer ratios and molecular weights in the form of solvent-cast disks of 2 cm diameter and 0.15 mm thickness at 70 °C and pH 7.4.  $D = 10\%$  HV,  $M_w = 750,000$ ;  $I = 20\%$  HV,  $M_w = 300,000$ ;  $C = 12\%$  HV,  $M_w = 170,000$ ;  $G = 12\%$  HV,  $M_w = 100,000$ ;  $C = 20\%$  HV,  $M_w = 36,000$ . (Reprinted with permission from [60].)

### 55.2.6 Polyphosphazenes

Polyphosphazenes consist of a backbone of alternating nitrogen and phosphorus atoms (Structure 11). The R and R' groups on either side of the phosphorus can be widely varied depending on the route of synthesis. The choice of functional groups determines the physical and chemical properties of the polymer [63,64]. Some important types of polyphosphazenes that have been synthesized are nonhydrolyzable, hydrophobic polymers; nonhydrolyzable, hydrophilic polymers; and hydrolyzable polymers. Those in the first class include polymers with side fluoroalkoxy, aryloxy, or organosilicon hybrid groups. These polymers are usually elastomers with water contact angles on the order of poly(tetrafluoroethylene) [65]. The second class consists of polymers with alkylamino, alkylether, alcohol, carboxylic acid, glyceryl, or glucosyl functionalities. These can be quite hydrophilic and are often crosslinked to form hydrogels. The third class of polymers includes those that can be hydrolyzed to form phosphate and ammonia derivatives. Some important side groups include: amino acid esters, steroidal groups, imidazolyl groups, and other bioactive molecules. In addition, the surface can also be activated for use in controlled release.

### 55.2.7 Fumarate-Based Polymers

The following polyesters are based on fumaric acid, a naturally occurring substance found in the Krebs cycle [8]. Three types of fumarate-based polymers are discussed: poly(propylene fumarate) (PPF), poly(propylene fumarate-*co*-ethylene glycol) (P(PF-*co*-EG)), and oligo(poly(ethylene glycol) fumarate) (OPF).

***Poly(Propylene Fumarate)***

Poly(Propylene Fumarate) (PPF) is a linear, unsaturated, hydrophobic polyester (Structure 12) containing hydrolyzable ester bonds along its backbone. PPF is highly viscous at room temperature and is soluble in chloroform, methylene chloride, tetrahydrofuran, acetone, alcohol, and ethyl acetate [66]. The double bonds of PPF can form chemical crosslinks with various monomers, such as *N*-vinyl pyrrolidone, poly(ethylene glycol)-dimethacrylate, PPF-diacrylate (PPF-DA), and diethyl fumarate [67,68]. The choice of monomer and radical initiator directly influence the degradative and mechanical properties of the crosslinked polymer. Once crosslinked, PPF forms a solid material with mechanical properties suitable for a range of bone engineering applications.

PPF crosslinked with either thermal- or photo-initiators exhibits a biphasic degradation at 37 °C. During the initial phase of degradation, PPF's mechanical strength increases, whereas the mechanical strength diminishes in the second phase [69,70]. This phenomenon can be explained by the fact that, at 37 °C, enough energy is provided for the entrapped initiators to sustain the crosslinking reaction [70,71]. To produce a crosslinked polymer of composition similar to that of the uncrosslinked polyester, diethyl fumarate or a derivative of PPF, PPF-diacrylate (PPF-DA) is used as a crosslinker [71,72].

Particulate ceramics such as  $\beta$ -tricalcium phosphate ( $\beta$ -TCP) can also be incorporated within the network to modify the crosslinked polymer's mechanical properties [67]. Hybrid alumoxane nanoparticles can also be incorporated in PPF to provide mechanical reinforcement [73].

***Poly(Propylene Fumarate-co-Ethylene Glycol)***

Poly(propylene fumarate-co-ethylene glycol) (P(PF-co-EG)), (Structure 13), is an amphiphilic block copolymer of PPF and poly(ethylene glycol) (PEG). P(PF-co-EG) is soluble in toluene, *N,N*-dimethylformamide, tetrahydrofuran, and acetone [74]. Similar to PPF, P(PF-co-EG) degrades via hydrolysis of the ester bonds found along its backbone [74]. Unlike PPF, the crosslinked P(PF-co-EG) forms hydrogels. Increasing the amount of PEG within the copolymer increases its hydrophilicity, thus encouraging an influx of water within the network and inducing the material to swell [75]. Similarly, increasing the concentration and/or molecular weight of the PPF block reduces the degree of swelling [75].

The relative amount of the PPF block also affects the mechanical properties of the crosslinked P(PF-co-EG). PPF is the only portion of the copolymer that can form covalent bonds for crosslinking, so more PPF block result in more possible crosslinks, yielding a stronger material [75]. Additionally the hydrophobic PPF moieties can interact with each other, forming secondary interactions that further

strengthen the material. A compilation of thermal and mechanical properties for P(PF-co-EG) are listed in Table 55.1.

***Oligo (Poly(Ethylene Glycol) Fumarate)***

The final type of fumarate-based polymer discussed, oligo (poly(ethylene glycol) fumarate) (OPF) (Structure 14), is a highly hydrophilic, linear, unsaturated polymer, composed of alternating PEG and fumarate moieties [76]. OPF is soluble in aqueous and organic solvents [76]. Like all fumarate-based polymers, crosslinking occurs through the fumarate groups and degradation is mediated by hydrolysis of the ester bonds. Similar to P(PF-co-EG), the PEG block gives OPF its hydrophilicity. In addition, OPF's properties are controlled by the ratio of fumarate to PEG and the molecular weight of the PEG. Increasing the molecular weight of the PEG produces a less crosslinked, and more swollen hydrogel [76,77]. Moreover, increasing the fumarate to PEG ratio increases the number of crosslinks within the network and decreases the swelling of the hydrogel [76]. Due to their high hydrophilicity, OPF hydrogels have been used to encapsulate mesenchymal stem cells for bone engineering applications [78,79].

**55.2.8 Polydioxanones and Polyoxalates**

Four important classes of polymers from dioxane-diones and oxalates are poly(1,4-dioxane-2,5-diones), polyoxalates, poly(1,3-dioxane-2-one) and poly(1,4-dioxane-2,3-dione), and poly(*p*-dioxanone). Representative diagrams are given in structures 15, 16, 17, and 18, respectively.

The first class has been produced with an alternating glycolide/lactide sequence. Both PGA and PLA have been mentioned previously, and the physical properties of the alternating copolymer are a weighted average of the two homopolymers.

Secondly, a polyoxalate has been reported [80] with an ester backbone, which can be hydrolytically cleaved to produce propylene glycol and oxalic acid. The predicted degradation rate is faster than PGA owing to its lower degree of crystallinity and less hydrophobic character.

The third class primarily consists of polymers of 1,3-dioxane-2-one otherwise known as trimethylene carbonate (TMC) and its copolymers with glycolide and lactide. PTMC degrades at a much slower rate than PGA. In addition, it softens between 40 °C and 60 °C, has low mechanical strength [5], and is reported to improve handling properties in copolymers with PGA [4]. Some thermal and mechanical properties of PTMC are shown in Table 55.1.

Lastly, poly(*p*-dioxanone) is thought to degrade by a mechanism similar to PGA [81]. The backbone is hydrolytically cleaved in a bulk erosion process with the major weight loss occurring between weeks 12 and 18 [82]. It has superior strength characteristics compared to PGA as well as high crystallinity up to 37%.



### 55.2.9 Poly(Amino Acids)

Poly(amino acids) as shown in Structure 19 are synthetically derived polymers which can be prepared from a variety of amino acids. The physical and chemical properties depend, in large part, on the functionalities of their respective side chains, however, poly(amino acids) have some common features. Most are highly insoluble in organic solvents, and they tend to swell in aqueous solution. They have poor mechanical properties and are difficult to process. In addition, the hydrolysis of the amide bond has an enzymatic contribution that is difficult to predict or control *in vivo*. The degradation products, amino acids, are natural components of proteins and should not cause a toxic response upon degradation, however, polymers containing three or more amino acids can elicit a strong immunologic response [83]. Additional properties for specific combinations of amino acids are given in Banera et al. [84]. Certain side chain modifications have been made in order to avoid some of these limitations. Poly(L-lysine) [85,86] and poly(L-glutamic acid) [87] have both been modified through their chemically reactive side chains to produce hybrids with bioactive molecules.

### 55.2.10 Pseudopoly(Amino Acids)

Pseudopoly(amino acids) are polymers derived from amino acids with nonamide linkages; these are represented by the wavy line in Structures 20, 21, and 22. This is usually done by the polymerization of trifunctional amino acids by reaction with side chain functional groups. Three important categories include: serine derived polyesters [88] hydroxyproline derived polyesters, and tyrosine-derived polymers. The first has not been widely used as a biomaterial [89]. The second group consists of poly(*N*-acyl-hydroxyproline esters) from *N*-protected hydroxyproline. These polyesters are soluble in benzene, toluene, chloroform, dichloromethane, carbon tetrachloride, tetrahydrofuran, and dimethylformamide. They are thermally stable up to 300 °C, have glass transition temperatures ranging from 71 °C to 157 °C, and are easily processed [89].

The third group consisting primarily of modified polycarbonates [90] can be derived from diphenols such as hydroquinone or Bisphenol A [91] (BPA), or a tyrosine dipeptide such as desaminotyrosyl-tyrosine hexyl ester (DTH). PDTH was found to be relatively strong with good biocompatibility [89,92,91]. The degradation of the tyrosine-derived polycarbonates is controlled by the hydrolysis of the ester and carbonate bonds [93]. Carbonate bonds will hydrolyze at a faster rate than the ester bonds, which leads to an initial reduction of molecular weight without mass loss [93,94]. Its reported half-life is 26 weeks, but it can take up to 4 years before the polymer is completely resorbed [91,93]. Additional thermal and mechanical data is given in Table 55.1

### 55.3 SUMMARY

While the previous list summarizes most of the currently used biodegradable polymers as well as some new materials, and while it describes the state-of-the-art at this time, it is certainly not exhaustive. There are many new products being developed as well as novel modifications of the polymers described within the chapter. Ideally, polymers can be chosen and tailored for a specific application based on their physical and chemical properties. We have shown properties that are crucial to the function of the polymer in question and also give sources where additional information can be found.

### 55.4 ACKNOWLEDGMENTS

We acknowledge support by the National Institutes of Health and the Alliances for Graduate Education and the Professoriate related to synthetic biodegradable polymers for medical applications.

### 55.5 APPENDIX

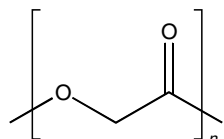
#### Abbreviations

β-TCP	β-tricalcium phosphate
BPA	Bisphenol A
CDM	<i>trans</i> -cyclohexanedimethanol
CPP	<i>bis</i> -( <i>p</i> -carboxyphenoxy)propane
DHSA	9,10-dihydroxy-stearic acid
DTH	desaminotyrosyl-tyrosine hexyl ester
HD	1,6-hexanediol
$M_p$	peak molecular weight
$M_w$	weight average molecular weight
OPF	oligo(poly(ethylene glycol) fumarate)
PBPA	poly(Bisphenol A)
P(CDM- <i>co</i> -HD)	poly( <i>trans</i> -cyclohexanedimethanol- <i>co</i> -1,6-hexanediol)
PCL	poly(ε-caprolactone)
PCPP	poly( <i>bis</i> -( <i>p</i> -carboxyphenoxy)propane)
P(CPP- <i>co</i> -SA)	poly( <i>bis</i> -( <i>p</i> -carboxyphenoxy)propane- <i>co</i> -sebacic acid)
P(D)LA	D enantiomer of poly (lactic acid)
P(D,L)LA	racemic mixture of D and L enantiomers of poly(lactic acid)
PDTH	poly(desaminotyrosyl-tyrosine hexyl ester)
PEG	poly(ethylene glycol)
PGA	poly(glycolic acid)
PHB	poly(3-hydroxybutyrate)
P(HB- <i>co</i> -HV)	poly(3-hydroxybutyrate- <i>co</i> -3-hydroxyvalerate)
PLA	poly(lactic acid)
PLGA	poly(lactic- <i>co</i> -glycolic acid)
P(L)LA	L enantiomer of poly(lactic acid)
PPF	poly(propylene fumarate)
PPF-DA	PPF-diacrylate

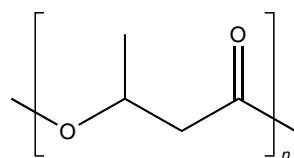
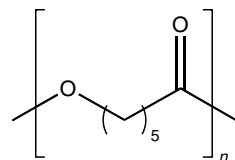
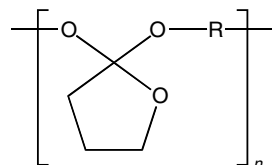
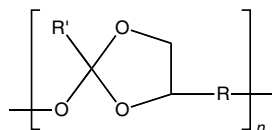
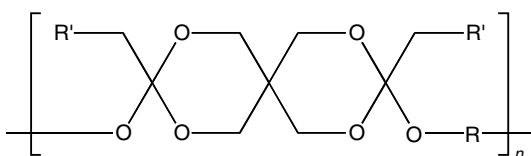
P(PF- <i>co</i> -EG)	poly(propylene fumarate- <i>co</i> -ethylene glycol)
PSA	poly(sebacic acid)
PTMC	poly(trimethylene carbonate)
SA	sebacic acid
TMC	trimethylene carbonate

### 56.6 CHEMICAL STRUCTURES

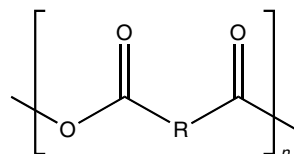
Structure 1: Poly(glycolic acid)



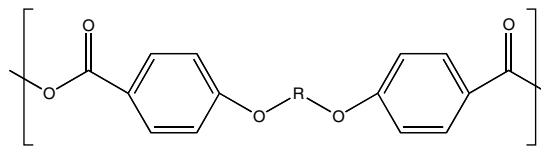
Structure 2: Poly(lactic acid)

Structure 3: Poly( $\epsilon$ -caprolactone)Structure 4: Poly(*ortho* ester)Structure 5: Poly(*ortho* ester)Structure 6: Poly(*ortho* ester)

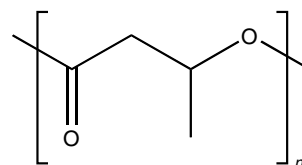
Structure 7: Polyanhydride



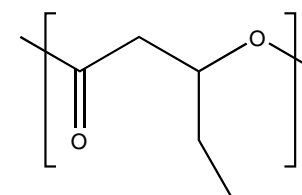
Structure 8: Polyanhydride



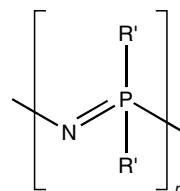
Structure 9: Poly(3-hydroxybutyrate)



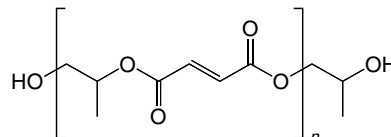
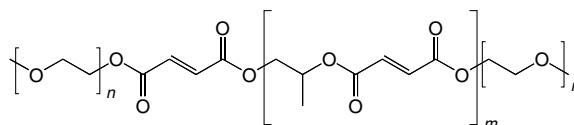
Structure 10: Poly(3-hydroxybutyrate)



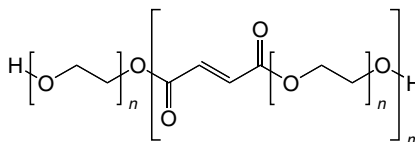
Structure 11: Polyphosphazenes



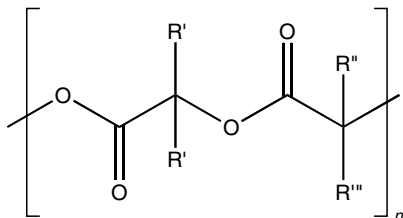
Structure 12: Poly(propylene fumarate)

Structure 13: Poly(propylene fumarate-*co*-ethylene glycol)

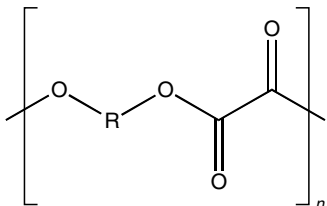
Structure 14: Oligo (poly(ethylene glycol) fumarate)



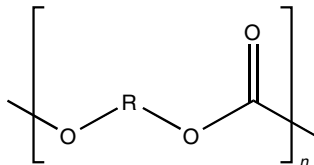
Structure 15: Poly(1,4-dioxane)



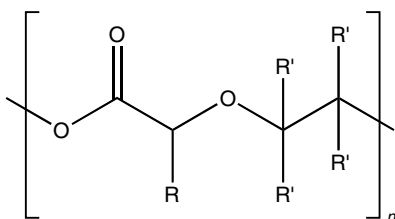
Structure 16: Polyoxalate



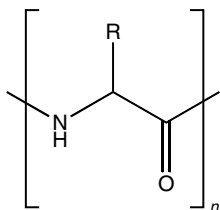
Structure 17: Poly(1,3-dioxane-2-one)



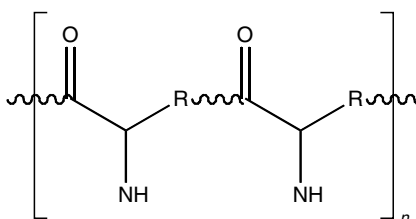
Structure 18: Poly(p-dioxanone)



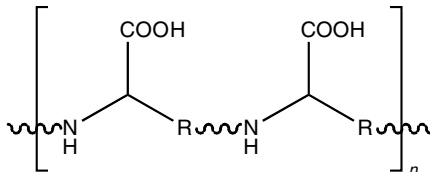
Structure 19: Poly(amino acid)



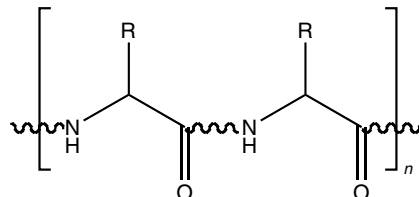
Structure 20: Pseudopoly(amino acid)



Structure 21: Pseudopoly(amino acid)



Structure 22: Pseudopoly(amino acid)



## REFERENCES

- R. C. Thomson, S. L. Ishaug, A. G. Mikos, "Polymer for biological systems," in *Encyclopedia of Molecular Biology: Fundamentals and Applications*, edited by R. A. Meyers (VCH Publishers, New York, 1996) pp 31–44.
- R. C. Thomson, M. C. Wake, M. J. Yaszemski, A. G. Mikos, *Adv. Polym. Sci.* 122, 245 (1995).
- S. Pulapura and J. Kohn, *J. Biomater. Appl.* 6, 216 (1992).
- I. Engelberg and J. Kohn, *Biomaterials* 12, 292 (1991).
- S. J. Holland, B. J. Tighe, P. L. Gould, *J. Control. Release* 4, 155 (1986).
- P. A. Gunatillake and R. Adhikari, *Eur. Cell Mater.* 5, 1 (2003).
- A. Atala and D. J. Mooney, *Synthetic Biodegradable Polymer Scaffolds*. (Birkhauser, Boston, 1997).
- J. S. Temenoff and A. G. Mikos, "Fumarate-based macromers as scaffolds for tissue engineering applications," in *Polymeric Materials Encyclopedia*, edited by J. C. Salamone (CRC Press, Boca Raton, in press).
- A. M. Reed and D. K. Gilding, *Polymer* 22, 494 (1981).
- C. C. Chu, *J. Biomed. Mater. Res.* 15, 19 (1981).
- R. A. Miller, J. M. Brady, D. E. Cutright, *J. Biomed. Mater. Res.* 11, 711 (1977).
- D. Cohn, H. Younes, G. Marom, *Polymer* 28, 2018 (1987).
- D. K. Gilding and A. M. Reed, *Polymer* 20, 1459 (1979).
- H. Younes and D. Cohn, *J. Biomed. Mater. Res.* 21, 1301 (1987).
- S. Gogolewski and A. J. Pennings, *Colloid Polym. Sci.* 261, 477 (1983).
- S. Gogolewski and A. J. Pennings, *Makromol. Chem. Rapid Commun.* 3, 839 (1982).
- A. S. Chawla and T. M. S. Chang, *Biomater. Med. Dev. Art. Org.* 13, 153 (1985).
- H. Pistner, D. R. Bendix, J. Mühling, J. F. Reuther, *Biomaterials* 14, 291 (1993).
- R. K. Kulkarni, E. G. Moore, A. F. Hegyeli, F. Leonard, *J. Biomed. Mater. Res.* 5, 169 (1971).
- G. Spenlehauer, M. Vert, J. P. Benoit, A. Boddart, *Biomaterials* 10, 557 (1989).
- C. C. Chu, *Ann. Surg.* 195, 55 (1982).
- M. Vert, S. Li, H. Garreau, *J. Control. Release* 16, 15 (1991).
- H. A. Von Recum, R. L. Cleek, S. G. Eskin, A. G. Mikos, *Biomaterials* 16, 441 (1995).
- L. Lu and A. G. Mikos, "Poly(lactic acid)," in *Polymer Data Handbook*, edited by J. E. Mark (Oxford University Press, New York, 1999).
- M. Vert, J. Mauduit, S. Li, *Biomaterials* 15, 1209 (1994).
- M. Vert, S. M. Li, H. Garreau, *J. Biomater. Sci. Polym. Ed.* 6, 639 (1994).
- E. Frazza and E. Schmitt, *J. Biomed. Mater. Res.* 5, 43 (1971).
- C. M. Agrawal, K. F. Haas, D. A. Leopold, H. G. Clark, *Biomaterials* 13, 176 (1992).
- L. Lu, M. J. Yaszemski, A. G. Mikos, *J. Bone Joint Surg. Am.* 83-A Suppl 1, S82 (2001).
- D. H. Lewis, "Controlled release of bioactive agents from lactide/glycolide polymer," in *Biodegradable Polymers As Drug Delivery Systems*, edited by M. Chasin, R. Langer (Marcel Dekker, New York, 1990) pp 1–42.
- A. G. Mikos, A. J. Thorsen, L. A. Czerwonka, Y. Bao, R. Langer, D. N. Winslow, J. P. Vacanti, *Polymer* 35, 1068 (1994).
- L. Lu, S. J. Peter, M. D. Lyman, H. L. Lai, S. M. Leite, J. A. Tamada, S. Uyama, J. P. Vacanti, R. Langer, A. G. Mikos, *Biomaterials* 21, 1837 (2000).
- C. G. Pitt, "Poly-ε-caprolactone and its copolymers," in *Biodegradable Polymers As Drug Delivery Systems*, edited by M. Chasin, R. Langer (Marcel Dekker, New York, 1990) pp 71–120.

34. J. R. Koleske, "Blend containing poly( $\epsilon$ -caprolactone) and related polymers," in *Polymer Blends*, vol 2 edited by D. R. Paul, S. Newman (Academic Press, New York, 1978) pp 369–338.
35. C. G. Pitt, F. I. Chasalow, Y. M. Hibionada, D. M. Kilmas, A. Schindler, *J. Appl. Polym. Sci.* 26, 3779 (1981).
36. J. C. Middleton and A. J. Tipton, *Biomaterials* 21, 2335 (2000).
37. C. G. Pitt and G. Zhong-Wei, *J. Control. Release* 4, 283 (1987).
38. J. Heller, R. V. Sparer, G. M. Zentner, "Poly(ortho esters)," in *Biodegradable Polymers As Drug Delivery Systems*, edited by M. Chasin, R. Langer (Marcel Dekker, New York, 1990) pp 121–161.
39. J. Heller, *Adv. Polym. Sci.* 107, 41 (1993).
40. J. Heller, D. W. Penhale, B. K. Fritzingler, J. E. Rose, R. F. Helwing, *Contracept. Deliv. Syst.* 4, 43 (1983).
41. J. Heller, *Biomaterials* 11, 659 (1990).
42. C. Shih, T. Higuchi, K. J. Himmelstein, *Biomaterials* 5, 237 (1984).
43. J. Heller, *J. Control. Release* 2, 167 (1985).
44. J. Heller, B. K. Fritzingler, S. Y. Ng, D. W. H. Pennale, *J. Control. Release* 1, 233 (1985).
45. K. Schwach-Abdellouai, J. Heller, R. Gurn, *Macromolecules* 32, 301 (1999).
46. S. Ng, T. Vandamme, M. Taylor, J. Heller, *Macromolecules* 30, 770 (1997).
47. J. Heller, J. Barr, S. Y. Ng, K. S. Abdellouai, R. Gurny, *Adv. Drug Deliv. Rev.* 54, 1015 (2002).
48. A. Domb, S. Amsalem, J. Shah, M. Maniar, *Adv. Polym. Sci.* 107, 93 (1993).
49. A. Gopferich, *Biomaterials* 17, (1996).
50. M. Chasin, A. Domb, E. Ron, E. Mathiowitz, K. Leong, C. Laurencin, H. Brem, B. Grossman, R. Langer, "Polyanhydrides as drug delivery systems," in *Biodegradable Polymers As Drug Delivery Systems*, edited by M. Chasin, R. Langer (Marcel Dekker, New York, 1990) pp 43–70.
51. A. Gopferich, R. Langer, *J. Polym. Sci. [A1]* 31, 2445 (1993).
52. H. B. Rosen, J. Chang, G. E. Wnek, R. J. Linhardt, R. Langer, *Biomaterials* 4, 131 (1983).
53. J. A. Tamada and R. Langer, *Proc. Natl. Acad. Sci. USA* 90, 552 (1993).
54. K. E. Uhrich, A. Gupta, T. Thomas, C. Laurencin, R. Langer, *Macromolecules* 28, 2184 (1995).
55. K. S. Anseth, V. R. Shastri, R. Langer, *Nat. Biotechnol.* 17, 156 (1999).
56. D. S. Muggli, A. K. Burkoth, K. S. Anseth, *J. Biomed. Mater. Res.* 46, 271 (1999).
57. C. Laurencin, A. Domb, C. Morris, V. Brown, M. Chasin, R. Mcconnell, N. Lange, R. Langer, *J. Biomed. Mater. Res.* 24, 1463 (1990).
58. J. Tamada and R. Langer, *J. Biomater. Sci. Polym. Ed.* 3, 315 (1992).
59. H. T. Wang, H. Palmer, R. J. Linhardt, D. R. Flanagan, E. Schmitt, *Biomaterials* 11, 679 (1990).
60. S. J. Holland, A. M. Jolly, M. Yasin, B. J. Tighe, *Biomaterials* 8, 289 (1987).
61. S. Gogolewski, M. Jovanovic, S. M. Perren, J. G. Dillon, M. K. Hughes, *J. Biomed. Mater. Res.* 27, 1135 (1993).
62. N. D. Miller and D. F. Williams, *Biomaterials* 8, 129 (1987).
63. C. T. Laurencin, M. E. Norman, H. M. Elgendy, S. F. El-Amin, H. R. Allcock, S. R. Pucher, A. A. Ambrosio, *J. Biomed. Mater. Res.* 27, 963 (1993).
64. S. Cohen, M. C. Bano, K. B. Visscher, M. Chow, H. R. Allcock, R. Langer, *J. Am. Chem. Soc.* 112, 7832 (1990).
65. H. R. Allcock, "Polyphosphazenes as new biomedical and bioactive materials," in *Biodegradable Polymers As Drug Delivery Systems*, edited by M. Chasin, R. Langer (Marcel Dekker, New York, 1990) pp 163–194.
66. A. J. Domb, "Poly(propylene glycol fumarate) compositions for biomedical applications." US Patent 4, 888, 413 (1988).
67. S. Peter, P. Kim, A. Yasko, M. J. Yaszemski, A. G. Mikos, *J. Biomed. Mater. Res.* 44, 314 (1999).
68. S. He, M. J. Yaszemski, A. W. Yasko, P. S. Engel, A. G. Mikos, *Biomaterials* 21, 2389 (2000).
69. M. J. Yaszemski, R. G. Payne, W. C. Hayes, R. Langer, A. G. Mikos, *Biomaterials* 17, 2127 (1996).
70. M. D. Timmer, C. G. Ambrose, A. G. Mikos, *Biomaterials* 24, 571 (2003).
71. M. D. Timmer, C. G. Ambrose, A. G. Mikos, *J. Biomed. Mater. Res.* 66A, 811 (2003).
72. J. Fisher, D. Dean, A. G. Mikos, *Biomaterials* 23, 4333 (2002).
73. R. A. Horch, N. Shahid, A. S. Mistry, M. D. Timmer, A. G. Mikos, A. R. Barron, *Biomacromolecules* 5, 1990 (2004).
74. L. J. Suggs, R. G. Payne, M. J. Yaszemski, L. B. Alemany, A. G. Mikos, *Macromolecules* 30, 4318 (1997).
75. L. J. Suggs, E. Y. Kao, L. L. Palombo, R. S. Krishnan, M. S. Widmer, A. G. Mikos, *J. Biomater. Sci. Polym. Ed.* 9, 653 (1998).
76. S. Jo, H. Shin, A. K. Shung, J. P. Fisher, A. Mikos, *Macromolecules* 34, 2839 (2001).
77. J. S. Temenoff, K. A. Athanasiou, R. G. Lebaron, A. G. Mikos, *J. Biomed. Mater. Res.* 59, 429 (2002).
78. J. S. Temenoff, H. Park, E. Jabbari, D. E. Conway, T. L. Sheffield, C. G. Ambrose, A. G. Mikos, *Biomacromolecules* 5, 5 (2004).
79. J. Temenoff, H. Park, E. Jabbari, T. L. Sheffield, R. G. Lebaron, C. G. Ambrose, A. G. Mikos, *J. Biomed. Mater. Res.* 70A, 235 (2004).
80. D. K. Gilding, *Biocomp. Clin. Implant Mater.* 2, 209 (1981).
81. N. Doddi, C. C. Versfelt, D. Wasserman, "Synthetic Absorbable Surgical Devices of Poly-Dioxanone." US Patent 4,052,988. (1976).
82. J. A. Ray, N. Doddi, D. Regula, J. A. Williams, A. Melveger, *Surg. Gynecol. Obstet.* 153, 497 (1981).
83. J. M. Anderson, K. L. Spilizewski, A. Hiltner, "Poly-alpha-amino acids as biomedical polymers," in *Biocompatibility of Tissue Analogs* (CRC Press, Boca Raton, 1985) pp 67–88.
84. D. A. Barrera, E. Zylstra, P. T. Lansbury, R. Langer, *Macromolecules* 28, 425 (1995).
85. P. Campbell, G. I. Glover, J. M. Gunn, *Arch. Biochem. Biophys.* 203, 676 (1980).
86. D. A. Barrera, E. Zylstra, P. T. Lansbury, R. Langer, *J. Am. Chem. Soc.* 115, 11010 (1993).
87. K. R. Sidman, A. D. Schwoppe, W. D. Steber, S. E. Rudolph, S. B. Poulin, *J. Membr. Biol.* 7, 277 (1980).
88. Q. X. Zhou and J. Kohn, *Macromolecules* 23, 3399 (1990).
89. J. Kohn, "Pseudopoly(amino acids)," in *Biodegradable Polymers As Drug Delivery Systems*, edited by M. Chasin, R. Langer (Marcel Dekker, New York, 1990) pp 195–230.
90. S. L. Bourke, J. Kohn, *Adv. Drug. Deliv. Rev.* 55, 447 (2003).
91. A. J. Domb, *Biomaterials* 11, 686 (1990).
92. J. Kohn and R. Langer, *Biomaterials* 7, 176 (1986).
93. V. Tangpasuthadol, S. M. Pendharkar, R. C. Peterson, J. Kohn, *Biomaterials* 21, 2379 (2000).
94. V. Tangpasuthadol, S. M. Pendharkar, J. Kohn, *Biomaterials* 21, 2371 (2000).
95. M. D. Timmer, C. Carter, C. G. Ambrose, A. G. Mikos, *Biomaterials* 24, 4707 (2003).
96. X. Shi and A. G. Mikos, "Poly(propylene fumarate)," in *An Introduction to Biomaterials*, edited by S. A. Guelcher, E. J. Beckman, J. O. Hollinger (Boca Raton, FL, 2005).

## CHAPTER 56

# Biodegradability of Polymers

Anthony L. Andrady

*Engineering & Technology Dirsian, RTI International, Research Triangle Park, NC 27709*

---

<b>56.1</b>	Introduction .....	951
<b>56.2</b>	Environmental Biodegradability of Biopolymers .....	953
<b>56.3</b>	Problem of Assessing Biodegradability of Synthetic Polymers .....	955
<b>56.4</b>	Biodegradability of Synthetic Polymers .....	956
<b>56.5</b>	Chemical Modifications to Enhance Biodegradability of Polymers .....	957
<b>56.6</b>	Conclusions .....	961
	References .....	961

---

### 56.1 INTRODUCTION

Biodegradation might be conveniently defined as “a chemical change in polymer facilitated by living organisms, usually micro-organisms” [1]. This definition is somewhat restricted, however, in that it excludes chemical breakdown processes on polymer substrates mediated by manmade enzymes. In spite of its emphasis on microbial processes, the definition covers both key areas of interest: environmental biodegradability of polymers, and in vivo biodegradability of polymers in mammalian systems. The present discussion is limited to the environmental biodegradation of polymers.

Adopting a definition for practical purposes, particularly to delimit those polymers that are “environmentally biodegradable,” is more complicated and several definitions have been proposed [2]. There is renewed interest in the use of such polymers in disposable packaging materials to ensure their degradation in post-consumer litter and waste streams. All organic materials must invariably biodegrade (despite the extremely slow kinetics in the case of most synthetic polymers) in the environment; however, to be of practical benefit a readily biodegradable polymer must break down due to biotic causes in a reasonable timescale. With no agreed benchmark available to indicate what such a “reasonable” rate of biodegradation might be, the use of natural biopolymers as standard biodegradable materials [3] is a common trend reported in the literature. Because of their rapid breakdown, regenerated cellulose or filter paper [4], wood pulp [5], and

even whole leaves might be used as reference materials in biodegradation studies.

In general, biodegradation of polymers occurs as an extracellular process (because macromolecular dimensions do not permit their transport across cell membranes), catalyzed by enzymes. A number of such enzymes are known and are classified on the basis of the degradation reaction step they catalyze. Thus, hydrolases, esterases, isomerases (or transferases), oxido-reductases, hydrogenases, and ligases can increase the rates of respective reactions by 6–20 orders of magnitude even under ambient temperatures [6]. Enzymes that specifically catalyze the breakdown of naturally occurring polymers such as cellulose, lignin, chitin, and proteins are readily available in nature. For synthetic polymers, with a much shorter history of less than half a century of use, appropriate enzymes are more difficult to find in nature. Given the impressive diversity of microbiota, as yet unknown enzyme systems for synthetic polymers might very well exist. Exceptions to the rule of recalcitrance of synthetic polymers include aliphatic polyesters, polyethers, some polyamides, and poly(vinyl alcohol).

As most of the readily biodegradable polymers are water-insoluble, the degradation reaction must be heterogeneous, initially localized at the surface of the polymer. Close contact between the biota and polymer is generally a prerequisite to ensure the high concentration of enzymes to enable these reactions. With biopolymers, the general process involves both exo- and endo-enzymes. The former yields fragments from chain ends, while the latter causes random

main-chain scission. The fragments, such as cellobiose in the case of cellulose, might then be further biodegraded by specific enzymes.

A distinction needs to be made between true biodegradation and biologically mediated disintegration or volume reduction of polymers, which does not amount to biodegradation. The attack of polyethylene by insects [7,8] for instance, belongs to this latter category. In spite of the 'damage' suffered by the polymer, the predominant change is physical, and the indigestible polymer is merely reduced in particle size at the end of process. The blends of a biologically inert thermoplastic, such as polyethylene, and a readily biodegradable substance, such as starch, also belong to the same class of biodeteriorable materials. On biodegradation of surface starch, a thin film of the composite material disintegrates into small particulates without substantial chemical breakdown of the polymer.

A second class of biodegradable polymers of interest are those used in the human (or animal) body. These polymers include those used in artificial organs, other implants, and controlled release devices for delivery of pharmaceuticals. Being placed in contact with the tissue environment, they can potentially biodegrade. In products such as biodegradable sutures and bioerodible drug-delivery matrices, such breakdown in the body may be undesirable.

Experimental data reported on biodegradation of polymers are somewhat limited. However, from a consideration of the available data and the characteristics of the biodegradation process, several factors that affect the environmental biodegradability of polymers might be identified.

### 56.1.1 Molecular Weight

Long chain-like molecular geometry and high molecular weights do not necessarily preclude biodegradation. Both biopolymers (cellulose, chitin), as well as some synthetic polymers (i.e., polycaprolactone) are readily biodegradable. However, a general relationship does exist between the average molecular weight of polymers and their amenability to biodegradation: the shorter the chains, the higher the likelihood of biodegradation [9–11]. Not only does a lower degree of polymerization yield a higher concentration of chain end groups, but it also discourages the formation of crystalline domains that are generally difficult to biodegrade. High chain-end concentrations [12] promote exotype reactions, and noncrystalline regions are known to be preferentially biodegraded in synthetic polymers [13–16] as well as in the biopolymer lignocellulose [17].

Even with polyethylenes generally regarded as being bioinert, the lower molecular weight fractions biodegrade and yield carbon dioxide product at a measurable rate. Gel permeation chromatography (GPC) was recently used to demonstrate the biodegradability of polyethylene wax exposed to bacteria and fungi. The beta oxidation rates for the low-molecular weight polyethylene exposed to bacterial

consortia were 36 times higher compared to that exposed to *Aspergillus* sp. isolated from soil [150]. Several researchers [151,152] reported the average molecular weight of polyethylenes exposed to biotic environments to slightly increase compared to those incubated in sterile media. The observation is likely a result of the lower molecular weight fraction of the sample with a higher concentration of chain ends being selectively biodegraded. (However, the alternative explanation of the formation of a surface biofilm that limits oxygen availability to the polymer has also been proposed [153].) Even with LDPE exposed to biotic environments (cultured compost microorganisms were used at 95 °C) it is the short chain branches on the chains that are preferentially biodegraded [154]. Observations on common plastics (LDPE, PVC, PS, and urea formaldehyde) subjected to long-term (32 years) soil-burial studies show only the LDPE films to be surface-degraded to any significant extent. The surface molecular weight of these samples decreased to almost 50% of that of the bulk [155,156].

Partially photodegraded polymers contain low-molecular weight fraction of degradation products and therefore biodegrade at a faster rate compared to the virgin material [157,158]. Similarly prethermal degradation of biodegradable polymers such as PHB, PHBV, and PCL copolymer also was reported to increase the rate of biodegradability under compost conditions [159]. The same was also reported for starch/LDPE blends [160]. Degradation of the polymer yields hydrophilic carboxylic acids, susceptible to easy biodegradation, as a major degradation product. These functional groups appear to be preferentially biodegraded under biotic exposure. Unlike with the thermo-oxidative degradation of LDPE where the concentration of carbonyl groups increase with exposure, biodegradation results in a decrease of these hydrophilic groups with the duration of exposure [161,162].

### 56.1.2 Structural Complexity

In most cases, the biodegradability implies the existence of a set of micro-organisms able to utilize the polymer substrate as a carbon and energy source. Since this has to be accomplished with minimum expenditure of energy by the organism, complex polymers requiring numerous enzyme-mediated steps for their breakdown represent a poor substrate [18]. Often, the required ensemble of enzymes is not available from a single species of micro-organism, and the substrate requires several different organisms to act in concert to effect biodegradation. Increased structural complexity of a substrate generally leads to recalcitrance in the environment. Persistence of soil humic acids, naturally occurring biopolymers in soil, are attributed to their structural complexity [19,20].

This assumes that biologically mediated breakdown of organic compounds always involves the use of substrate as a source of energy. Co-metabolism is an important exception in which the biodegradation does not yield any energy

for use by the organism contributing the enzyme. Nevertheless, co-metabolism is common in nature, and is a true biodegradation process to the extent that it depletes the substrate polymer.

### 56.1.3 Hydrophilicity

Water-soluble synthetic polymers such as poly(vinyl alcohol) [21], poly(acrylic acid) [6], and polyethers tend to be more biodegradable than water-insoluble polymers of comparable molecular weight. Increasing the hydrophilicity of a polymer by chemical modification also increases its biodegradability [22]. The functional groups that impart water-solubility may also contribute to ready biodegradability of these systems. From a microbiological standpoint, the presence of a dissolved substrate may induce the production of necessary enzymes within the micro-organisms.

## 56.2 ENVIRONMENTAL BIODEGRADABILITY OF BIOPOLYMERS

Unlike xenobiotic substrates, biopolymers such as cellulose have been in the eco-system for a very long time, allowing the evolution of efficient enzymatic pathways specific for the breakdown of these substrates. Common biopolymers therefore readily undergo biodegradation in a wide variety of environmental conditions ranging from aerobic compost heaps to anoxic deep-sea marine sediments.

### 56.2.1 Cellulose

The average degree of polymerization (DP) of cellulose depends upon the source; values of 153–300 for California cotton [23] and 2000–6000 for *Valonia* sp. [24], have been reported. Pulp and viscose (cellophane) are processed celluloses with drastically reduced DP ranging in the low thousands at best. The lower-DP polymer is generally more readily biodegraded. The common micro-organisms involved in cellulose biodegradation are summarized in Table 56.1. These include both bacteria and fungi; the deleterious effect of white-rot and brown-rot fungi on lignocellulose is well known.

Several enzymes act synergistically in the breakdown of cellulose in a series of hydrolysis reactions [25,26]. Endo-cellulases attacking the amorphous regions of the celluloses cause random chain scission. The exo-cellulases act at terminals of chains splitting off cellobiose units that, in turn, are hydrolyzed by  $\beta$ -glucosidase. Lignin component, often found associated with cellulose, also can biodegrade via oxidative pathways. Relevant enzymes (such as lignases, laccase, alcohol oxidase) have been reported [27,28].

Cellulose fillers [172,173] including some types of wood fibers [174] have been used as a filler with thermoplastics to obtain biodegradable materials with improved film quality. Crude cellulose in the form of surface-modified flax fibers

reinforce biodegradable polyesters [175]. Particularly interesting are cellulose filled composites of biodegradable resins such as poly(propylene carbonate) filled with short lignocellulosic fibers. Cellulose being less hydrophilic compared to biodegradable additives such as starch, yields materials of good mechanical properties [176].

Cellulose is often found in close association with lignin fibers (hence is strictly lignocellulose) in mechanical pulps or flax fiber material. In these, the cellulose component is rapidly biodegradable in the environment while lignin biodegrades but at a much slower rate. However, lignin has also been used in plastic materials to impart some degree of biodegradability. Lignin grafted to PVAc, and PVA enhanced the biodegradability of these materials while that grafted to the readily biodegradable PLC decreased the materials overall its biodegradability [177]. The effect of compatibilizers on cellulose acetate – organoclay was recently reported [178].

### 56.2.2 Chitin and Chitosan

Chitin that occurs in the exoskeleton of invertebrates (such as mollusks and arthropods) is composed of N-acetyl-D-glucosamine residues linked by 1,4  $\beta$ -linkages. A partially deacetylated chitin also occurs naturally as chitosan. Microbial species responsible for the breakdown of chitin and chitosan have not been comprehensively studied. Micro-organisms found in a variety of environments (for instance, in fresh water [29], marine sediment [30], garden soil [31], and even anaerobic environments [32]) are known to produce chitinases and/or chitosanases. Table 56.1 shows a listing of some reported species of bacteria and fungi that yield these enzymes and are therefore, able to biodegrade these polysaccharides.

### 56.2.3 Starch

A polysaccharide made of linear amylose chains and branched amylopectins, starch is well known to be readily biodegradable [33]. The  $\alpha$  1–4 linkages in both components are easily hydrolyzed by amylases while the  $\alpha$  1–6 links at branch points in amylopectin are attacked by glucosidases.

Biodegradable multiphase systems that include starch as one of the phases has been reviewed [163]. (Interestingly, proteins such as crosslinked furfural-soy protein concentrates have also been used in place of carbohydrate polymers for biodegradable polymers [164] or as biodegradable fillers in polyesters [165]. It is important to note that it is only the starch content of the composite that is biodegradable. The biodegradable systems typically include a pro-oxidant additive to facilitate rapid thermooxidative breakdown of the synthetic polymer [166]). To that extent, these systems display not only biodegradation of the starch but concurrent thermooxidative degradation of the synthetic polymer.

Systems where the synthetic polymer matrix is also biodegradable have been reported in recent literature. The morphology and interface properties [167] as well as the biodegradation [168] of starch with poly(lactic acid) was recently reported. A silica filled crosslinked starch/polyacrylamide composite showed superabsorbancy as well as enhanced biodegradability by sewage sludge inoculum as well as specific microorganisms (*Bacillus cereus* and

*E. coli*), (note, however, that polyacrylamide is not an enhanced biodegradable polymer). Starch–poly (propylene carbonate) composites not only yielded a fully biodegradable composite material, but also a composite with improved the mechanical properties [169]. PVA–starch composites were processed into a foam with biodegradable as well as good mechanical properties [170]. PVA is biodegradable, but at a much slower rate compared to PCL or

**TABLE 56.1.** *Microbial biodegradation of cellulose and chitin.*

Substrate	Class	Micro-organism	Reference	
Cellulose	Bacteria	<i>Cellvibro gilvus</i>	[53]	
		<i>Clostridium thermocellum</i>	[54]	
		<i>Bacteroides succinogenus</i>	[55]	
		<i>Ruminococcus albus</i>	[56]	
		<i>Pseudomonas fluorescens var cellulosa</i>	[57]	
	Fungi	<i>Sporocytophaga myxococcides</i>	[58]	
		<i>Coriolus vesicolor</i> [W] <sup>a</sup>	[59,60]	
		<i>Phanerochaete chrysosporium</i> [W] <sup>a</sup>	[61]	
		<i>Irpex lacteus</i> [W] <sup>a</sup>	[62]	
		<i>Schizophyllum commune</i> [W] <sup>a</sup>	[63]	
		<i>Fomes annosus</i> [W] <sup>a</sup>	[64]	
		<i>Stereum sanguinolentum</i> [W] <sup>a</sup>	[65]	
		<i>Peurotus ostreatus</i> [W] <sup>a</sup>	[66]	
		<i>Polyporus schweinitzii</i> [B] <sup>a</sup>	[67]	
		<i>Poria Placenta</i> [B] <sup>a</sup>	[68,69]	
		<i>Poria Vailantii</i> [B] <sup>a</sup>	[70]	
		<i>Coniophora cerebella</i> [B] <sup>a</sup>	[71]	
		<i>Tyromyces palustris</i>	[71,72]	
		<i>Serpula lacrymans</i> [B] <sup>a</sup>	[73]	
		<i>Lentinus lepideus</i> [B] <sup>a</sup>	[74]	
		Ascomycetes and fungi imperfecti	<i>Chaetomium globosum</i>	[75]
			<i>Chaetomium thermophile</i>	[76]
			<i>Trichoderma viride</i>	[77,78]
	<i>Trichoderma reesei</i>		[77,78]	
	<i>Trichoderma koningii</i>		[77,78]	
	<i>Penicillium funiculosum</i>		[79]	
	<i>Fusarium solani</i>		[80]	
	<i>Aspergillus aculeatus</i>		[81]	
	<i>Aspergillus niger</i>		[82]	
	<i>Sporotrichum thermophile</i>		[83]	
	Chitin	Bacteria and fungi	<i>Myrothecium verrucaria</i>	[84]
			<i>Myxobacteria spp.</i>	[85]
			<i>Pseudomonas spp.</i>	
<i>Serratia spp.</i>			[86,87]	
<i>Bacillus spp. Pseudomonas spp.</i>			[88]	
<i>Flavobacterium spp.</i>				
<i>Streptomyces antibioticus</i>			[89]	
<i>Streptomyces griseus</i>			[90]	
<i>Penicillium oxalicum</i>			[91]	
<i>Streptomyces erythaeus</i>			[92]	
<i>Trichoderma harzianum</i>			[93]	
<i>Streptomyces orientalis</i>			[94]	
<i>Aspergillus niger</i>				
Chitosan			<i>Myxobacter</i>	[95]
			<i>Streptomyces griseus</i>	[96]
	<i>Streptomyces spp.</i>	[97]		

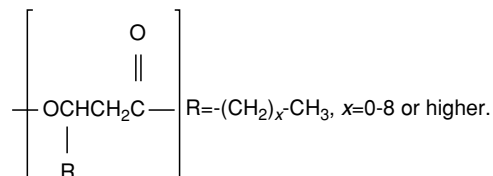
<sup>a</sup>[W] and [B] refer to white-rot and brown-rot fungi, after [98].



cellulose. Lactide fillers have also been successfully used in place of starch with a biodegradable polymer matrix (copolymers of 1,3-trimethylene carbonate) to obtain environmentally biodegradable materials [171].

#### 56.2.4 Polyhydroxyalkanoates (Bacterial polyesters)

These polymers are produced as intracellular storage materials in a variety of bacteria grown under physiologically stressed conditions. Specific species, such as *Alcagenes eutrophus* (cultured under ammonium-limited growth conditions), and *Rhodobacter sphaeroides* (cultured under phosphate or sulfate-limited growth conditions) can yield as much as 80% dry weight of the polyester. The use of mixed organic carbon sources during bacterial fermentation allows the production of a variety of polymers and copolymers of this class. Poly-(hydroxybutyrate), PHB, and the random copolymer of poly(hydroxybutyrate-co-valerate), PHBV, have been the most studied of this class of biopolymers [34]. The structure of the 100% isotactic polymer is given below [6].



Thermal and mechanical properties of several of the copolymers have been reported [35,36]. Biodegradation of these polymers by bacterial esterases yield monomers, dimers and trimers split off from the hydroxyl-terminal of the polymer chain.

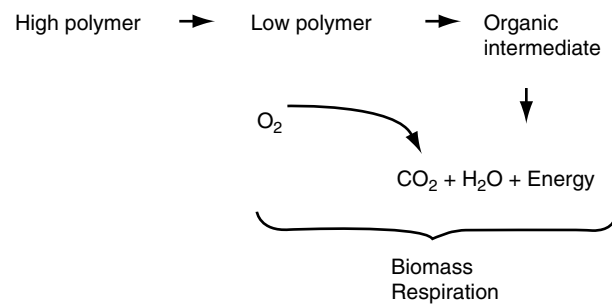
#### 45.2.5 Other Filler Materials

A variety of fillers are used with biodegradable polymer materials to obtain the mechanical properties needed for specific applications. As reported in the literature these additives do not generally alter the biodegradability of the polymer matrix. The effect of the new nanosized filler materials in this regard, however, is interesting and has not been extensively studied. Because of their superior reinforcing characteristics [179] nanofillers such as montmorillonite (nanoclays) and hectile silicates are likely to be a popular additive and its impact on biodegradability needs to be studied. With silica fillers in a range of biodegradable polymers (layered nanocomposites), the general trend was toward increased biodegradability [180]. With nanoclays as well, the same trend was observed for both photo- and biodegradation [181].

### 56.3 PROBLEM OF ASSESSING BIODEGRADABILITY OF SYNTHETIC POLYMERS

Synthetic polymers generally biodegrade very slowly, but several exceptions exist. These exceptions undergo biodegradation in the environment at a measurable rate and are commonly referred to as “biodegradable plastics.” Several experimental approaches to establishing the rates and extents of their biodegradation under specific exposure conditions are available. To quantify the rates of breakdown, it is important to define a criterion for assessment of polymer biodegradability.

With a hypothetical polymer, it is convenient to represent the biodegradation process by the following generalized sequence [1].



The sequence suggests that the criterion for assessment of biodegradation depends upon the particular definition of biodegradation adopted. For instance, the rate of depletion of the polymer substrate might be adopted as the approach; alternatively, the rate of carbon dioxide generation might be used in its place. Under identical conditions, the rates of biodegradation of the same substrate, obtained using these two approaches, will be quite different. The choices of tests available are listed in Table 56.2, along with references on their use to determine the environmental biodegradability of polymers (or organic substrates). Each approach focuses on a different stage of the biodegradation process [37]. Consequently, the results from different tests on the same substrate are not comparable. This is demonstrated in a comparison of the test data on aliphatic polyesters. Lenz [6] compared the data by Potts *et al.* [38] for surface colonization of polymers by micro-organisms (i.e., biomass yield) with data on weight loss in soil burial and on hydrolysis by fungal lipases, for the same polymers. As expected, the rankings of five polyesters in terms of their biodegradability, estimated using two different criteria, were quite different. Recent work by Yakabe *et al.* [39] showed that for PHBV, cellulosics and poly( $\epsilon$ -prolactone) substrates biodegradability as measured by the MITI standard test, and fresh sewage sludge exposure test, showed poor agreement. However, they noted the half-lifetimes for the substrates in sewage sludge exposure, and soil burial exposure to show a moderate degree of correlation.

**TABLE 56.2.** Summary details for six biodegradability tests based on OECD guidelines.

Test method (OECD)	[S]	Units	[I]	Units	Cells/l	Analysis	pH/T °C
Die-away (301 A)	10–40	mg DOC/l	<100	ml/l	10 <sup>7</sup> –10 <sup>8</sup>	Dissolved organic carbon	7.4/22
CO <sub>2</sub> Evolution (301 B)	10–20	mg/l	<100	ml/l	10 <sup>7</sup> –10 <sup>8</sup>	Carbon dioxide evolution	7.4/22
Respirometry (301 F)	100	mg/l	<100	ml/l	10 <sup>7</sup> –10 <sup>8</sup>	Oxygen consumption	7.4/22
Modified screening test (301 E)	10–40	mg DOC/l	0.5	ml/l	10 <sup>5</sup>	Dissolved organic carbon	7.4/22
Closed bottle (301 D)	2–10	mg/l	<5	ml/l	10 <sup>4</sup> –10 <sup>6</sup>	Dissolved oxygen	7.4/22
MITI (1) (301 C)	100	mg/l	30	mg/l <sup>a</sup>	10 <sup>7</sup> –10 <sup>8</sup>	Oxygen consumption	7.0/25

<sup>a</sup>mg of suspended solids per liter. DOC = dissolved organic carbon; [S] = substrate concentration; [I] = inoculum concentration. Based on [1, 39].

Biodegradability of a given polymer can, therefore, be discussed only in relation to the criterion adopted in its assessment and to the nature of microbial environment used for the purpose. Generalization of experimental data (particularly the description of a polymer as being “biodegradable” without qualification) can be misleading and contribute to confusion in the literature.

Several standard test protocols for measurement of polymer biodegradation are presently available. Organizations which have published such tests include the American Society for Testing and Materials (ASTM), Ministry of International Trade and Industry (MITI) (Japan) [40] and the Organization for Economic Cooperation and Development (OECD) [41]. They are, however, for the most part deficient to the extent that they have no control over the nature of microbial inoculum used, or the possible pre-adaptation of the mixed populations to specific substrates, and over the adequate control of particle size of the substrate. The relevance of these factors to laboratory assessment of the biodegradability of synthetic polymers has been recently discussed [1]. Most of these test methods have been derived from tests first used with detergents [42], and are not always well-suited for solid polymer substrates.

The test methods recently published by the ASTM relating to biodegradability of polymers are as follows.

- D 5209-91 Standard Test Method for Determining the Aerobic Biodegradation of Plastic Materials in the Presence of Municipal Sewer Sludge.
- D 5210-92 Standard Test Method for Determining the Anaerobic Biodegradation of Plastic Materials in the Presence of Municipal Sewer Sludge.
- D 5271-92 Standard Test Method for Assessing Aerobic Biodegradation of Plastic Materials in an Activated Sludge - Waste Water System.

D 5338-93 Standard Test Method for Determining the Aerobic Biodegradation of Plastic Materials Under Controlled Composting Conditions.

D 5247-92 Standard Test Method for Determining the Aerobic Biodegradability of Degradable Plastics by Specific Micro-organisms.

G21-90 Standard Practice for Determining the Resistance of Synthetic Polymeric Materials to Fungi.

G22-76 Standard Practice for Determining the Resistance of Synthetic Polymeric Materials to Bacteria.

G29-30 Standard Practice for Determining the Resistance of Synthetic Polymeric Materials to Algae.

OECD, an international organization with 24 member countries, developed guidelines for establishing biodegradability through their Chemical Testing Program [41,43]. Their approach identifies three levels of biodegradability; ready biodegradability, inherent biodegradability, and simulation of environmental compartments. Of these, ready biodegradability or stringent tests that provide limited opportunity for biodegradation and acclimatization to occur are considered screening tests. Yakabe *et al.* [39] recently summarized the test parameters for the six tests used for the purpose. Basic features of the tests are shown in Table 56.2.

## 56.4 BIODEGRADABILITY OF SYNTHETIC POLYMERS

Results from biodegradation studies on numerous synthetic polymers, polymer blends, modified natural polymers and biopolymers have been reported. However, as pointed out earlier, biodegradability of a polymer is a function of several variables, including, but not limited to, the following.

*Material characteristics:* molecular weight, crystallinity, crosslink density, solubility, likelihood of yielding toxic biodegradation products;

*Substrate form:* film, molded specimen, powder, solubility in test medium, swelling in water;

*Biodegradation conditions:* inoculum type, pre-adaptation of organisms, use of single species versus mixed consortia, use of naturally-occurring consortia, use of nutrients or minerals in cultures, aeration levels;

*Test parameters:* concentration of substrate, [substrate]: [inoculum] ratio, test pH, test temperature, agitation, aeration rate; and

*Measurements:* Biochemical oxygen demand, substrate depletion, carbon dioxide generation, biomass estimate, properties of the polymer.

The importance of chain branching and crystallinity of polymer in controlling its biodegradability was already mentioned earlier in the chapter. Substrate geometry affects the surface area available for biotic interaction and is therefore an important factor in controlling biodegradability. During some stage or the other of the biodegradation process shape (specially film versus powder) of the substrate (PLLA, PCL, PBS, PBSA, and PP control) was shown to significantly affect rate of biodegradation [182]. The nature of the inocula is another critical factor in determining the rate of biodegradability. Industrial and municipal sewage inocula were found to be significantly different in this regard when used to biodegrade PCL and cellulose [183]. Test parameters such as temperature also influence the rate of the process and needs to be carefully controlled in biodegradation experiments. PCL and PHB incubated with soil compost inocula the biodegradation rate was found to be higher at 46 °C compared to that at 24 °C [184].

The test method employed to assess biodegradation is a crucial consideration in establishing biodegradability, as different techniques measure different aspects of the degradation process. New test methods are being developed continuously and some of these are later incorporated into standards documents. For instance, Japanese researchers have used the weight gain of CO<sub>2</sub> sorbed in a column charged with sodalime as a modified method for evaluating biodegradability of materials [185]. Under the composting conditions used to demonstrate the method it was found to be a good screening test. Korean workers have reported the biodegradation of plastic-paper laminated or coated composites, by enzymes. Higher degradability compared to the polymer powder was observed for PCL, PLA, PHB, and PBS polymers [186]. A similar result, but using regenerated cellulose films in place of paper, has also been reported recently [187]. The limitations of each test method in quantifying the relevant aspect of the process needs to be taken into account in interpreting test data on polymer biodegradability.

The potential toxicity to soil biota from any products of biodegradation has also received attention in the literature. The presence of deteriorated plastic residue generally does not impair the growth of higher plants; this is an important

consideration in using plastic mulch material in agriculture. In the case of water-soluble polymers such as PVA, however, the situation is less clear. Lee *et. al.* [188] found a significant reduction in the yield of red pepper and tomato cultivars when PVA was blended in with the soil at levels as low as 0.05%. In the cases of lactic acid polymers, however, the oligomers and degradation products were claimed to have a positive effect on plant growth [189].

Thus, biodegradability of a polymer can be discussed only in terms of alone characteristics. At the very least, it is necessary to specify the molecular weight of the polymer, composition in case of a copolymer or a blend, the origin of inoculum, and the criterion (and specific measurements) used to establish biodegradation. Composition of the biotic environment (in the case of laboratory tests, the inoculum) is a key factor in all biodegradation tests; however, there is no convenient way to adequately describe a consortium of micro-organisms in even semi-quantitative terms, for this purpose. Data in Table 56.3 attempt to summarize the recently reported results from various studies on biodegradation of polymers. Unfortunately, not all such reports provide the necessary information. The summarized data is limited to reported polymer biodegradation studies using live cultures or micro-organisms as opposed to those using extracted enzymes.

It is crucial to appreciate that biodegradability under a specific set of conditions as shown in Table 56.3 (particularly where only a single species of micro-organism is involved), does not necessarily imply biodegradability under a different set of conditions. Even when the study used a naturally occurring consortium, the results cannot always be readily extrapolated to natural environments. Even the mere isolation, or “bottling,” of a natural consortium is well known to affect its composition in a relatively short time [44,45].

Published data can rarely be used to compare the “biodegradability” of two materials, except in instances in which both materials were tested under identical conditions. Even in the latter instance, the ranking obtained is solely applicable to biodegradation under that particular test condition. The result cannot be extrapolated to field conditions, to other test conditions, or even to experiments carried out under identical conditions but using a different criterion for biodegradability.

## 56.5 CHEMICAL MODIFICATIONS TO ENHANCE BIODEGRADABILITY OF POLYMERS

High molecular weight polyethylene is virtually nonbiodegradable. Being a commodity thermoplastic widely used in disposable packaging and consequently a very visible component of urban litter, there is interest in rendering the material environmentally biodegradable.

Early attempts to address the problem included the use of biodegradable starch fillers in either polyethylenes,

**TABLE 56.3.** Selected studies on biodegradation of polymeric materials.

Substrate	Example	Method	Inoculum	Reference
Polyethylene/ starch blends	LDPE/EAA/Starch blends	Weight loss FTIR Tensile properties CO <sub>2</sub> evolution	Mixed culture	[99]
	LDPE or HDPE+starch 0–20%	Weight loss and FTIR	Soil culture	[100]
	LDPE+starch (67%, 52%, 29%)	Weight loss and FTIR	Compost culture	[101]
	LLDPE+starch (~6%)	Molecular weight	Soil culture (three types)	[48]
			Soil culture, landfill soil culture, and activated sludge	[46]
		Elongation at break, and CO <sub>2</sub> evolution		
	LDPE+starch (0, 29, 52, 67%)	Weight loss and FTIR	Soil culture Marine sediment	[8]
	LDPE+starch (0, 3, 5.5, 6, 9%)	Starch analysis, elongation at break, and molecular weight	Soil culture, refuse culture, and anaerobic digester culture	[47]
	LDPE+starch (3.85, 5.77, 7.70%)	CO <sub>2</sub> radiotracer studies, chemiluminescence, calorimetry and molecular weight	<i>Verticillium lecanii</i> <i>Verticillium nigrescens</i>	[102]
	LDPE/starch blends	Tensile properties, SEM, spectroscopy	Soil microbes	[160]
Polyethers	Poly(propylene glycol) ( $M_n = 2000-4000$ )	HPLC Analysis	Soil- <i>Corynebacterium sp.</i>	[103]
	Poly(ethylene glycol) ( $M_n = 600-20000$ )	Optical density Biomass and analysis	<i>Alcaligenes denitrificans</i> <i>Sphingomonas parapegl-</i> <i>ytica</i> + <i>Pseudomonas</i> (symbiotic)	[104] <sup>a</sup>
	Poly(tetramethylene glycol) ( $M_n = 200$ and 265)	Analysis	<i>Alcaligenes denitrificans</i> and <i>Xanthomonas maltophilia</i>	[105] <sup>a</sup>
Poly(carboxylic acid)	Poly(acrylic acid salt)-co-(vinyl alcohol)-( $M_n = 7300-12000$ ).	BOD measurements	Activated sludge	[106]
		Optical density and analysis	<i>Pseudomonas sp.</i> and <i>Trichoderma sp.</i>	
Acrylamide polymers	Crosslinked starch graftpolyacrylamide composite	SEM and CO <sub>2</sub> release	Sewage sludge <i>Bacillus</i> <i>cereus</i> and <i>E. coli</i>	[193]
Polyesters	Poly(ethylene adipate) ( $M_n = 3000$ )	Biomass and analysis	<i>Penicillium sp.</i> (soil isolate)	[107]
	Polycaprolactone ( $M_n = 25,000$ )	Biomass and TOC		
	Polycaprolacton ( $M_n = 2000$ and 7000, 19,000, and 35,000)	Molecular weight measurements	<i>Cryptococcus laurenti</i>	[108]
	Polycaprolactone ( $M_w = 40,000$ )	Visual and microscopy	<i>Acinetobacter calcoaceticus</i>	
	Polycaprolactone, PCL. $M_n = 80,000$ . Blends of PCL/LDPE (10%, 80% PCL)	Tensile properties, FTIR spectroscopy, and molecular weight	Soil culture. A mixed culture of: <i>Aspergillus niger</i> <i>Penicillium funiculosum</i> <i>Chaetomium globosum</i> <i>Gliocladium virens</i> <i>Aureobasidium pullulans</i>	[109] [110]
	Polycaprolactone Copolymer (styrene and cyclic ketene acetal) ( $M_n = 13,000-25,000$ )	CO <sub>2</sub> evolution CO <sub>2</sub> evolution	<i>Aspergillus flavus, soil</i> <i>Aspergillus flavus, soil</i>	[49]
	Polycaprolactone ( $M_n = 4000$ and 37,000). Methoxy and hydroxy terminated polymer chains	CO <sub>2</sub> evolution, weight loss, and molecular weight	Compost inoculum	[111]
		Actinomycetes species isolated from compost		

TABLE 56.3. Continued.

Substrate	Example	Method	Inoculum	Reference
Bacterial Polyester	Polycaprolactone	Weight loss, tensile properties and mol. weight	Soil (20 sites) and water (2 marine, 1 fresh water)	[112]
	Polycaprolactone $M_n = 40,000$ and 70,000	Visual substrate loss (clear zone)	Soil culture	[113]
	Polycaprolactone $M_n \sim 25,000$	Weight loss	<i>Penicillium sp.</i>	[114]
	Poly(3 hydroxybutyrate-co-3 hydroxyvalerate) blends with cellulose acetate (25, 50 and 75% CA)	Dynamic mechanical properties, NMR, and FTIR spectroscopy	Activated sludge	[115]
	Poly(3 hydroxy butyrate), PHB, and copolymers PHB, and 3 hydroxy valeric acid, HV. (10% and 20% HV)	Molecular weight Tensile Strength Weight loss	Soil culture (several types) Compost culture Freshwater/sea water	[116] <sup>a</sup>
	Poly(3 hydroxybutyrate-co-3 hydroxyvalerate) 7% HV, plasticized	Weight loss	Compost culture	[117]
	Poly(3 hydroxybutyrate-co-3 hydroxyvalerate) 20% HV	Visual substrate loss (clear zone) CO <sub>2</sub> evolution BOD and weight loss	Bacterial strains (pure culture)	[118]
	Poly(3 hydroxybutyrate-co-3 hydroxyvalerate) HV = 22% $M_w = 400,000-700,000$	Weight loss and microscopy	Activated sludge Soil culture	[39]
	Poly(3 hydroxybutyrate-co-3 hydroxyvalerate) 12.5%, 8.4% HV	Visual substrate loss (clear zone)	Soil culture and compost culture Soil culture	[119]
	Poly(3 hydroxybutyrate), $M_w = 230,000$ . Poly(3 hydroxyvalerate), PHA $M_w = 820,000$ . Copolymer 11% HV $M_w = 150,000$	Visual substrate loss (clear zone)	Soil suspension culture	[113]
	Poly(3 hydroxybutyrate), $M_w = 220,000$ . Crystalline samples	Microscopy and crystallinity	<i>Alcaligenes paradoxus</i> <i>Pseudomonas testosteroni</i> Soil culture isolate	[120]
	Poly(3 hydroxybutyrate) PHB $M_w = 539,000$ blended with cellulose acetate butyrate $M_w = 130,000$ 20, 40, 60, and 80% PHB	Weight loss, differential scanning calorimetry, and wide angle xray scattering	Activated sludge	[121]
	Poly(3 hydroxybutyrate-co-3 hydroxyvalerate) $M_w = 330,000$ 26.5% HV	Tensile properties and molecular weight	Activated sludge	[122]
	Blends of PHBV and PHEMA	CO <sub>2</sub> evolution, mass loss	Penicillium funiculosum and other fungi	[123]
Polyurethane	Polyether-urethane	FTIR or UV spectroscopy	Aspergillus niger and Cladosporium herbarium	[124]
	Polyester-urethane poly-D, L-lactic acid polyurethane	FTIR spectroscopy	Soil culture	[125]
		Weight loss and biochemical oxygen demand	Mixed fungal spore inoculum	[126]
	Polyester-urethane ( $M_n \sim 40,000$ )	Molecular weight measurements	<i>Aspergillus fumigatus</i>	[127,128]
Polyethylenes	(Ethylene-carbon monoxide) copolymer	CO <sub>2</sub> radiotracer studies	<i>Frusarium solanii</i> <i>Cryptococcus laurenti</i> Soil culture and sewage sludge	[129]

TABLE 56.3. Continued.

Substrate	Example	Method	Inoculum	Reference
	LDPE	CO <sub>2</sub> radiotracer studies	Soil culture	[130]
	HDPE ( $M_w = 300,000$ )	CO <sub>2</sub> radiotracer studies	Soil, mixed fungal culture <i>Fusarium redolens</i>	[131,132]
	LDPE ( $M_w = 18,000$ )	CO <sub>2</sub> radiotracer studies	<i>Fusarium redolens</i>	[133]
	HDPE and LDPE 1.5 and 2 mils.	Biomass	Mixed fungal inoculum as per ASTM G21, with <i>Aspergillus versicolor</i> <i>Aspergillus flavus</i>	[134]
	Photo-degraded (partly cross-linked) $M_n = 10,980$ (undegraded)			
	Polyethylene LDPE and HDPE with and without prooxidant	CO <sub>2</sub> , wt. loss, tensile strength, and IR spectroscopy	Municipal solid waste compost	[195]
	LDPE and PP	Tensile properties, turbidity, and BOD changes	<i>Pseudomonas stutzeri</i>	[196]
Nonionic Ethoxylates	Poly(vinyl alcohol) and PVA	CO <sub>2</sub> radiotracer studies	Activated sludge	[135]
Polyalcohols		Weight loss, tensile props, and molecular weight	Soil (20 sites) and water (2 marine, 1 fresh water)	[112]
	Block copolymer of PVA and 1,1 dicarboxylated malonate copolymer. $M_n = 9000-24,000$ VA block content 8-72%	Biochemical oxygen demand, molecular weight, CO <sub>2</sub> evolution, organic carbon analysis	River water culture isolates (aerobic) River sediment or anaerobic activated sludge (anaerobic)	[136]
Cellulose	Cellophane (regenerated cellulose)	Tensile properties and water vapor permeability	Soil culture isolate	[137]
	Cellophane	Crystallinity	Soil culture isolate	[138]
	Cellophane	Weight loss and CO <sub>2</sub> evolution	<i>Aspergillus niger</i> <i>Trichoderma viridi</i> <i>Pseudomonas fluorescens</i> <i>Bacillus subtilis</i>	[4]
	Lignocellulose (plant material from several species)	CO <sub>2</sub> and CH <sub>4</sub> radiotracer studies	Soil culture (swamp soil) for anaerobic species	[139]
	Cellulose acetate. DS = 1.7 and 2.5	Visual, weight loss, and CO <sub>2</sub> evolution	Compost inoculum 1%	[140,141]
	Cellulose acetates with DS = 1.74, 1.86, 2.06, 2.21, 2.52, and 2.97	Weight loss and changes in molecular weight	Simulated compost	[142]
	Cellulose acetate. DS = 1.6, 1.7, 1.85, and 2.5	Analysis for DS, CO <sub>2</sub> radiotracer studies, and molecular weight	Activated sludge	[143]
	Cellulose fabric	XRD, microscopy	Soil microbes	[178]
	Cellulose acetates	Weight loss and mechanical properties	Sewage sludge microbes	[197]
	Chemically modified flax fiber	CO <sub>2</sub> evolution, weight loss	Soil microorganisms <i>Cellvibrio fibrovorans</i>	[198]
Polyuronides	Partially dicarboxylated pectic acid $M_n = 11,900$ 67% carboxylated	Biological oxygen demand	Activated sludge	[144]
Polybutadiene	Cis 1,4 polybutadiene $M_n = 650$ (liquid)	Molecular weight measurements and Biomass	<i>Acenitobacter spp</i>	[145]
Polystyrene	Styrene oligomer $M_n \sim 400$ (liquid)	Molecular weight measurements and Biomass	<i>Alcaligenes spp</i>	[146]
Polyisoprene	$M_n = 990, 1500, 2500$ (liquid)	Molecular weight measurements and Biomass	Soil culture isolates	[147]
Ethylene Copolymer	EVA copolymers and poly (vinyl acetate)	Weight loss	Activated sludge	[148]
	EVA 40/60 copolymer $M_w = 70,000$ EVA: starch = 1:1	Weight loss and FTIR	Soil culture and activated sludge	[149]

polyethylene-containing blends, or copolymers of ethylene. Although several technologies that could blend from about 6%–60% of starch into an extrusion-blown thin film were developed, their biodeteriorability characteristics fell short of expectations. In low-starch formulations, limited accessibility of the starch granules by microbial flora restricted biodegradation, limiting it to only about 10% of the available starch [8,46,47]. In high-starch formulations, the starch domains were sufficiently interconnected to allow a more complete degradation of the starch, but such films often exhibited poor mechanical properties. Adequate connectivity between starch domains to allow biodegradation is expected only at high levels of the additive, around 30 weight percent of starch in the blend [48]. At low starch levels below the percolation threshold only the surface starch can be reasonably be expected to degrade. LDPE with 29 wt% starch, for instance, showed degradation of only about 25% of the starch that was in the surface layers [190]. In starch polyethylene composite materials it is only the starch that biodegrades [191] the same is true in the case of PP [192]. The biodegradation of the starch itself cannot of course, be expected to lead to any significant biodegradation of the polymer matrix.

Copolymerization of ethylene (or other vinyl monomers such as styrene) with a vinyl monomer that undergoes ring-opening to yield a main-chain aliphatic ester group has been reported. For instance, 1,3 dioxepane can be used as a comonomer with styrene, or a ketene acetal might be used with styrene. This approach was shown to increase the biodegradability of polyethylene [49]. The lower molecular weight polyethylenes generated during biodegradation are more likely to undergo faster biodegradation compared to virgin polyethylene.

Biodegradable polymer sequences such as polysaccharides can be block copolymerized with synthetic polymers to obtain a partially biodegradable polymer material. Using a preformed macromolecular block, a ring-opening polymerization of *N*-carboxy anhydride was used to prepare an amylose-poly( $\alpha$ -benzyl-*L*-glutamate) block copolymer. Alternatively, a segmented block copolymer can be made by reacting low molecular weight amylose or cellulose blocks with terminal hydroxy groups with a synthetic prepolymer (such as a polyether) with reactive end groups using an appropriate diisocyanate. Gilbert *et al.* used a five step reaction sequence to produce several such block copolymers [50–52].

## 56.6 CONCLUSIONS

While naturally occurring polymers are readily biodegradable in the environment, most synthetic high polymers biodegrade only very slowly under comparable exposure conditions. There are, however, exceptions to this observation, and several classes of synthetic polymers that undergo ready environmental biodegradation are

known. The ease of biodegradability of these polymers depend on their structural, macromolecular, and morphological characteristics.

Assessment of biodegradability is a key consideration in the development of biodegradable polymers. No strict definitions exist of what constitutes an appropriate biotic environment to carry out such testing and of what criterion is best suited to establish biodegradability of a polymer in the laboratory. The test results are sensitive to a variety of factors, particularly the consortia of micro-organisms used. It is, therefore, often difficult to appreciate the full significance of the reported data and to understand how different test results relate to each other. As more detailed reports of biodegradation assessments are reported, as seen in recent publications, some of these uncertainties and inconsistencies in the reported biodegradability of polymers will be removed.

## REFERENCES

1. A. L. Andrady, *J. Macromol. Sci. Rev. Macromol. Chem. Phys.* **C34**, 25 (1994).
2. R. M. Ottenbrite and A. C. Albertsson, in *Biodegradable Polymers and Plastics*, edited by M. Vert, J. Feijen, A. Albertsson, *et al.* (Royal Soc. Chemistry, Cambridge, England, 1992) p. 73.
3. A. L. Andrady, *ASTM Standardization News*, p. 46, Oct. 1988.
4. V. Coma, Y. Couturier, B. Pascat, *et al.* in *Biodegradable Polymers and Plastics*, edited by M. Vert, J. Feijen, A. Albertsson, G. Scott, and E. Chellini (Royal Society of Chemistry, Cambridge, England, 1992), p. 242.
5. A. L. Andrady, V. R. Parthasarathy, and Ye Song, *Tappi* **75**, April, (1992).
6. R. W. Lenz, *Adv. in Polym. Sci.* **107**, 28 (1993).
7. R. A. Connolly, in *Biodeterioration of Materials*, edited by H. Walters and E. H. Huech-van der Plas (Applied Science Publishers, London, 1972), p. 168.
8. R. P. Wool, J. S. Peanasky, J. M. Long, *et al.* in *Degradable Materials, Perspectives, Issues, and Opportunities*, edited by S. A. Barenberg, J. L. Brash, R. Narayan, *et al.* (CRC Press, Boca Raton, FL 1990), p. 515.
9. Y. Toikawa and T. Suzuki, *Agric. Biol. Chem.* **42**, 1071 (1978).
10. R. D. Fields, F. Rodriguez, and R. K. Finn, *J. Appl. Polym. Sci.* **18**, 3571 (1974).
11. R. D. Fields and F. Rodriguez, in *Proceedings of the Third International Biodegradation Symposium*, edited by J. M. Sharpley and A. M. Kaplan (Applied Science, Barking, England, 1976), p. 775.
12. E. Kuhlwein and F. Demmer, *Kunststoffe* **57**, 183 (1967).
13. L. Kravetz, in *Agricultural and Synthetic Polymers. Biodegradability and Utilization*, Vol. 433, edited by J. E. Glass and G. Swift (ACS Symposium Series, Washington, DC, 1990), p. 96.
14. W. J. Cook, J. A. Cameron, J. T. Bell, *et al.* *J. Polym. Sci., Polym. Lett. Ed.* **19**, 159 (1981).
15. Y. Doi, Y. Kumagai, N. Tanahashi, *et al.* in *Biodegradable Polymers and Plastics*, edited by M. Vert, J. Feijen, A. Albertsson, *et al.* (Royal Society of Chemistry, Cambridge, England, 1992), p. 139.
16. P. Jarrett, C. V. Benedict, J. P. Bell, J. A. Cameron, and S. J. Huang, in *Polymers as Biomaterials*, edited by S. W. Shalaby, A. S. Hoffmann, B. D. Ratner, and T. A. Hobart (Plenum Publishers, New York, 1983), p. 3.
17. K. K. Y. Wong, K. F. Deverell, K. L. Mackie, *et al.*, *Biotechnol Bioeng.* **24**, 447 (1988).
18. R. L. Tate, in *Soil Organic Matter—Biological and Ecological Effects* (John Wiley and Sons, New York, 1987), p. 158.
19. J. P. G. Ballesta and M. Alexander, *J. Bacteriology* **106**, 938 (1971).

20. R. J. Swaby and J. N. Ladd, in *The Use of Isotopes in Soil Organic Matter Studies*, edited by R. A. Silow (Pergamon Press, Oxford, England, 1966), p. 153.
21. M. Shima and N. Kato, in *International Symposium on Biodegradable Polymers*, Abstracts (Biodegradable Plastics Society, Tokyo, Japan, 1990), p. 80.
22. K. W. March, C. R. Widevur, W. L. Sederel, *et al.*, *Biomed. Mater. Res.* **11**, 405 (1977).
23. D. A. I. Goring and T. E. Timell, *Tappi* **45**, 454, (1969).
24. M. Marx-Figini, *Biochim. Biophys. Acta.* **177**, 27 (1969).
25. G. Halliwell and M. Griffin, *Biochem. J.* **128**, 1183 (1973).
26. L. E. R. Berghem and L. G. Petterson, *Eur. J. Biochem.* **37**, 21 (1973).
27. M. Tien and T. K. Kirk, *Science* **221**, 661 (1983).
28. M. Shimada and T. Higuchi, in *Wood and Cellulosic Chemistry*, D. N.-S. Hon and N. Shiraiishi (Marcel Dekker, Inc., New York, 1992), p. 557.
29. L. G. Willoughby, *Hydrobiologica* **34**, 465 (1969).
30. H. Seki and N. Taga, *J. Oceanog. Soc. Japan* **19**, 27 (1963a).
31. N. Okafor, *J. Gen. Microbiol.* **44**, 311 (1966).
32. J. N. Boyer and R. S. Wolfe, *Biological Bull.* **165.N2**, 505, (1983).
33. J. J. Marshall, editor *Mechanism of Saccharide Polymerization and Depolymerization* (Academic Press, New York, 1980), p. 55.
34. Y. Doi, in *Microbial Polyesters* (VCH Publisher, 1990).
35. Zeneca, in *Biopol, Natures Plastic: Properties and Processing* (Zeneca, Billingham, United Kingdom, 1993).
36. A. Schirmer, D. Jendrossek, and H. G. Schlegel, *Appl. Env. Microbiol.* **59**, 1222 (1993).
37. P. Gerike and W. K. Fischer, *Ecotoxicol. Environ. Safety* **3**, 159 (1979).
38. J. E. Potts, in *Encyclopedia of Chemical Technology*, 2nd edition. Suool. Vol. (Wiley Interscience, New York, 1984), p. 626.
39. Y. Yakabe and M. Kitano, in *Biodegradable Plastics and Polymers*, edited by Y. Doi and K. Fukuda (Elsevier Science, 1994), p. 331.
40. Ministry of Trade and Industry, Japan. *The Biodegradability and Bioaccumulation of New and Existing Chemical Substances*, 1983.
41. *OECD Guidelines for Testing Chemicals* (Organization of Economic Corporation and Development, Paris, 1981).
42. Soap and Detergent Association, *J. Am. Oil Chem. Soc.* **42**, 3 (1965).
43. *OECD Expert Group, Determination of the Biodegradability of Anionic Synthetic Surface Active Agents* (Organization for Economic Cooperation and Development, Paris, 1971).
44. R. T. Wright, A. W. Bourquin, and P. H. Pritchards, editors *Microbial Degradation of Pollutants in the Marine Environment* (USEPA, Gulf Breeze, FL, 1979), p. 119.
45. L. H. Stevenson, *Microbiol. Ecol.* **4**, 127 (1978).
46. R. G. Austin, in *Degradable Materials: Perspectives, Issues and Opportunities*, edited by S. A. Barenberg, J. L. Brash, R. Narayan, and A. E. Redpath (CRC Press, Boca Ration, FL, 1990), p. 237.
47. G. Iannotti, N. Fair, M. Tempesta, *et al.* in *Degradable Materials; Perspectives, Issues and Opportunities*, edited by S. A. Barenberg, J. L. Brash, R. Narayan, *et al.* (CRC Press, Boca Raton, FL, 1990), p. 425.
48. S. M. Goheen and R. P. Wool, *J. Appl. Polym. Sci.* **42**, 2691-2701 (1991).
49. W. J. Bailey, V. Kuruganti, and J. S. Angle, in *Agricultural and Synthetic Polymers. Biodegradability and Utilization*, vol. 433, edited by J. E. Glass and G. Swift (ACS Symposium Series, Washington, DC, 1990), p. 149.
50. K.-S. Lee and R. D. Gilbert, *Carbohydr. Res.* **88**, 162 (1981).
51. M. M. Lynn, V. T. Stannett, and R. D. Gilbert, *J. Polym. Sci., Polym. Chem. Ed.* **18**, 1967 (1980).
52. S. L. Kim, V. T. Stannett, and R. D. Gilbert, *J. Macromol. Sci.* **7**, 101 (1979).
53. K. W. King and M. I. Vessal, *Adv. Chem. Ser.* **95**, 7 (1969).
54. T. K. Ng, A. ben-Bessat, and J. G. Zeikus, *Appl. Environ. Microbiol.* **41**, 1337 (1981).
55. D. Groleau and C. W. Forsberg, *Can. J. Microbiol.* **27**, 517 (1981).
56. K. Omiya, K. Nokura, and S. Shimizu, *J. Ferment. Technol.* **61**, 25 (1983).
57. K. Yamane, H. Suzuki, and K. Nisizawa, *J. Biochem.* **67**, 19 (1970).
58. K. Osmundsvag and J. Goksor, *Eur. J. Biochem.* **57**, 405 (1975).
59. D. S. Chahal and W. D. Gray, in *Biodeterioration of Materials*, edited by A. H. Walters and J. J. Elphick (Elsevier, New York, 1968), p. 584.
60. M. P. Levi and E. B. Cowling, in *Biodeterioration of Materials*, edited by A. H. Walters and J. J. Elphick (Elsevier, New York, 1968), p. 575.
61. M. Streamer, K. E. Eriksson, and B. Pettersson, *Eur. J. Biochem.* **51**, 607 (1975).
62. T. Kanda, K. Wakabayashi, and K. Nisizawa, *J. Biochem.* **79**, 977 (1976).
63. M. Paice, M. Desrochers, D. Roh, *et al.* *Biotechnology* **2**, 535 (1984).
64. A. Hutterman and A. Noelle, *Holzforsch.* **36**, 283 (1982).
65. B. Bucht and K. E. Eriksson, *Arch. Biochem. Biophys.* **129**, 416 (1969).
66. T. Hiroi, *Mokuzai Gakkaishi* **27**, 684 (1981).
67. G. Keilich, P. J. Bailey, E. G. Afting, *et al.*, *Biochim. Biophys. Acta.* **185**, 392 (1970).
68. E. B. Cowling and W. Brown, *Adv. Chem. Ser.* **95**, 152 (1969).
69. T. L. Highley, *Wood and Fiber* **5**, 50 (1973).
70. B. C. Sison, W. J. Schubert, and F. F. Nord, *Arch. Biochem. Biophys.* **68**, 502 (1957).
71. N. J. King, in *Biodeterioration of Materials*, edited by A. H. Walters and J. J. Elphick (Elsevier, NY, 1968), p. 558.
72. M. Ishihara and K. Shimizu, *Mokuzai Gakkaishi* **30**, 79 (1984).
73. S. Doi, *Mokuzai Gakkaishi* **31**, 843 (1985).
74. H. Shimazono, *Arch. Biochem. Biophys.* **83**, 206 (1959).
75. G. Keilich, P. Bailey, and W. Liese, *Wood Sci. Technol.* **4**, 273 (1973).
76. J. Eriksen and J. Goksor, *Eur. J. Biochem.* **77**, 445 (1977).
77. T. M. Wood and S. I. McCrae, *Adv. Chem. Ser.* **181**, 181 (1979).
78. R. D. Brown, Jr. and L. Jurasek, *Adv. Chem. Ser.* **181**, 399 (1979).
79. T. M. Wood, S. I. McCrae, and C. C. MacFarlane, *Biochem. J.* **198**, 51 (1980).
80. T. M. Wood and S. I. McCrae, *Carbohydrate Res.* **57**, 117 (1977).
81. S. Murao and R. Sakamoto, *Agric. Biol. Chem.* **43**, 1791 (1979).
82. A. Ikeda, T. Yamamoto, and M. Funatsu, *Agric. Biol. Chem.* **37**, 1169 (1973).
83. M. R. Coudray, G. Canevascini, and H. Meier, *Biochem. J.* **203**, 277 (1982).
84. D. R. Whitaker, *Arch. Biochem. Biophys.* **43**, 253 (1953).
85. C. E. Warnes and C. I. Randles, *Ohio J. Sci.* **77**, 224 (1983).
86. N. G. Aumen, *Microb. Ecol.* **6**, 317, (1981).
87. E. Young, R. L. Bell, and P. A. Carroad, *Biotechnol. and Bioeng.* **27**, 769 (1985).
88. M. Srikantiah and K. C. Mohankumar, *Indian J. Microbiol.* **20**, 216 (1981).
89. C. Jeuniaux, J. C. Bussers, M. F. Voss-Foucart, and M. Poulceek, in *Chitin in Nature and Technology* edited by R. A. Muzarelli, C. Jeuniaux, and G. W. Gooday (Plenum Press, New York, 1986), p. 516.
90. R. A. Smucker, in *Chitin in Nature and Technology*, edited by R. A. Muzarelli, C. Jeuniaux and G. W. Gooday (Plenum Press, New York, 1986), p. 254.
91. J. Rodriguez, M. I. Perez-Leblic, and F. Laborda, in *Chitin in Nature and Technology*, edited by R. A. Muzarelli, C. Jeuniaux, and G. W. Gooday (Plenum Press, New York, 1986), p. 102.
92. S. Hara, Y. Yamamura, Y. Fujii, *et al.*, in *Proc. 2nd Int. Conf. on Chitin and Chitosan*, edited by S. Hirano and S. Tokura, July 12-14, 1982, Sapporo, Japan. The Japanese Soc. of Chitin and Chitosan, p. 125.
93. I. Chet, E. Cohen and I. Elster, in *Chitin in Nature and Technology*, edited by R. A. Muzarelli, C. Jeuniaux, and G. W. Gooday (Plenum Press, New York, 1986), p. 237.
94. A. Ohtakara, H. Ogata, Y. Taketomi, and M. Mitsutomi, in *Chitin, Chitosan, and Related Enzymes*, edited by J. P. Zikakis (Academic Press, Orlando, 1984), p. 147.
95. A. Hedges and R. S. Wolf, *J. Bacteriology* **120-2**, 844 (1974).
96. A. Ohtakara, H. Ogata, Y. Taketomi, *et al.* in *Chitin, Chitosan and Related Enzymes*, edited by J. P. Zikakis (Academic Press, Orlando, 1984), p. 147.
97. J. S. Price and R. Storck, *J. Bacteriology* **124-3**, 1574 (1975).
98. M. Shimada and M. Takahashi, in *Wood and Cellulosic Chemistry*, edited by D. N.-S. Hon and N. Shiraiishi (Marcel Dekker, Inc., New York, 1992), p. 625.
99. J. M. Gould, S. H. Gordon, L. B. Dexter, *et al.* in *Agricultural and Synthetic Polymers Biodegradability and Utilization*, vol. 433, edited by J. E. Glass and G. Swift (ACS Symposium Series, Washington, DC, 1990), p. 65.



100. M. A. Cole, in *Agricultural and Synthetic Polymers. Biodegradability and Utilization*, edited by J. E. Glass and G. Swift (ACS Symposium Series 433. American Chemical Society, Washington DC, 1990), p. 76.
101. A. Corti, G. Vallini, A. Pera, *et al.* in *Biodegradable Polymers and Plastics*, edited by M. Vert, J. Feijen, A. Albertsson, *et al.* (Royal Soc. Chemistry, Cambridge, England, 1992), p. 245.
102. A. C. Albertsson, C. Barnstedt, and S. Karlsson, *J. Environ. Polym. Deg.* **1**, 241 (1993).
103. F. Kawai, in *Agricultural and Synthetic Polymers. Biodegradability and Utilization*, vol. 433, edited by J. E. Glass and G. Swift (ACS Symposium Series, 1989), p. 110.
104. F. Kawai and H. Yamanaka, *Arch. Microbiol.* **146**, 125 (1986).
105. F. Kawai, Japanese patent 208289 (1987a).
106. S. Matsumara, S. Maeda, J. Takahashi, *et al.*, *Kobunshi Ronbunshu*, **45**, 317 (1988).
107. Y. Toikawa, T. Ando, T. Suzuki, *et al.*, in *Agricultural and Synthetic Polymers. Biodegradability and Utilization*, vol. 433, edited by J. E. Glass and G. Swift (ACS Symposium Series, Washington, DC, 1989), p. 136.
108. C. V. Benedict, W. J. Cook, P. Jarrett, *et al.*, *J. Appl. Polym. Sci.* **28**, 327 (1983).
109. M. Kimura, K. Toyota, M. Iwatsuki, *et al.*, in *Biodegradable Plastics and Polymers*, edited by Y. Doi and K. Fukuda (Elsevier Science, New York, 1994), p. 92, 237.
110. L. Tilstra and D. Johnsonbaugh, *J. Environ. Polym. Deg.* **1**, 257 (1993).
111. F. Lefebvre, A. Daro, and C. David, *Macromol. Sci., Pure Appl. Chem.* **A32**, 867 (1995).
112. H. Sawada, in *Biodegradable Plastics and Polymers*, edited by Y. Doi and K. Fukuda (Elsevier Science, New York, 1994), p. 298.
113. M. Tsuji and Y. Omoda, in *Biodegradable Plastics and Polymers*, edited by Y. Doi and K. Fukuda (Elsevier Science, New York, 1994), p. 345; *Engl.* **31**, 1200 (1992).
114. Y. Toikawa, T. Ando, T. Suzuki, and K. Takeda, in *Agricultural and Synthetic Polymers. Biodegradability and Utilization*, Vol. 433, edited by J. E. Glass and G. Swift (ACS Symposium Series, Washington, DC, 1989), p. 136.
115. D. F. Gilmore, R. C. Fuller, B. Schneider, *et al.*, *J. Environ. Polym. Deg.* **2**, 49 (1994).
116. J. Mergaert, A. Wouters, J. Swings, *et al.*, in *Biodegradable Polymers and Plastics*, edited by M. Vert, J. Feijen, A. Albertsson *et al.* (Royal Soc. Chemistry, Cambridge, England, 1992), p. 267.
117. M. Gada, R. A. Gross, and S. P. McCarthy, *Biodegradable Plastics and Polymers*, edited by Y. Doi and K. Fukuda (Elsevier Science, New York, 1994), p. 177; C. Bastioli, V. Bellotti, M. Camia, Del Giudice, and A. Rallis, *ibid.*, p. 204.
118. R. J. Muller, J. Augusta, T. Walter, *et al.* in *Biodegradable Polymers and Plastics*, edited by M. Vert, J. Feijen, A. Albertsson (Royal Soc. Chemistry, Cambridge, England, 1992), p. 149.
119. H. Eya, N. Iwaki, and Y. Otsuji, in *Biodegradable Plastics and Polymers*, edited by Y. Doi and K. Fukuda (Elsevier Science, New York, 1994), p. 337.
120. D. Jendrossek, I. Knoke, R. B. Habibiyan, *et al.*, *J. Environ. Polym. Deg.* **1**, 53 (1993).
121. H. Nishida and Y. Tokiwa, *J. Environ. Polym. Deg.* **1**, 65 (1993).
122. G. Tomasi and M. Scandola, *J. Macromol. Sci., Pure Appl. Chem.* **A32**, 671 (1995).
123. D. F. Gilmore, S. Antoun, R. W. Lenz, *et al.*, *J. Environ. Polym. Deg.* **1**, 269 (1993).
124. Z. Phillip, *Europ. J. Appl. Microbiol. Biotechnol.* **7**, 277 (1979).
125. Z. Phillip, *Europ. J. Appl. Microbiol. Biotechnol.* **5**, 225 (1978).
126. S. Owen, M. Masaoka, R. Kawamura, *et al.*, *J. Macromol. Sci., Pure Appl. Chem.* **A32**, 843 (1995).
127. S. J. Huang, M. S. Roby, C. A. Macri, *et al.* in *Biodegradable Polymers and Plastics*, edited by M. Vert, J. Feijen, A. Albertsson, *et al.* (Royal Soc. Chemistry, Cambridge, England, 1992), p. 149.
128. S. J. Huang, C. Marci, M. Roby, *et al.*, *ACS Symp. Ser.* **172**, 471 (1981).
129. J. E. Guillet, *Adv. Chem. Ser.* **169**, 1 (1978).
130. N. B. Nykvist, in *Proc. of Degradability of Polymers and Plastics Conference* (Inst. Electrical Engineering, London, England, 1973), p. 18.
131. A. C. Albertsson, Z. G. Banhidi, and L. L. Beyer-Ericsson, *J. Appl. Polym. Sci.* **22**, 3434 (1978).
132. A. C. Albertsson and Z. G. Banhidi, *J. Appl. Polym. Sci.* **25**, 1655 (1980).
133. A. C. Albertsson and S. Karlsson, *J. Appl. Polym. Sci.* **35**, 1289 (1988).
134. J. H. Cornell, A. M. Kaplan, and M. R. Rogers, *J. Appl. Polym. Sci.* **29**, 2581 (1984).
135. L. Kravetz, in *Agricultural and Synthetic Polymers. Biodegradability and Utilization*, vol. 433, edited by J. E. Glass and G. Swift (ACS Symposium Series, Washington, DC, 1989), p. 96.
136. S. Matsumara and T. Tanaka, *J. Environ. Polym. Deg.* **2**, 89 (1994).
137. P. Engler and S. H. Carr, *J. Polym. Sci., Polym. Phys. Ed.* **11**, 313 (1973).
138. S. A. Bradley, S. H. Engler, and S. H. Carr, *Polymeric Materials for Unusual Service Conditions*, edited by M. A. Golub and J. A. Parker (Wiley, New York, 1973), p. 269.
139. R. Benner, A. E. Macubbin, and R. E. Hodson, *Appl. Envir. Microbiol.* **47**, 998 (1984).
140. J. Gu, D. Eberiel, S. P. McCarthy, and R. A. Gross, *J. Environ. Polym. Deg.* **1**, 281 (1993).
141. R. A. Gross, J. Gu, D. Eberiel, and S. McCarthy, *J. Macromol. Sci., Pure Appl. Chem.* **A 32**, 613 (1995).
142. C. M. Buchanan, D. Dorschel, R. M. Gardner, R. J. Komarek, and A. W. White, *J. Macromol. Sci. Pure Appl. Chem.* **A 32**, 683 (1995).
143. C. M. Buchanan, R. M. Gardner, and R. J. Komarek, *J. Appl. Polym. Sci.* **47**, 1709 (1993).
144. S. Matsumara, K. Amaya, and S. Yoshikawa, *J. Environ. Polym. Deg.* **1**, 23 (1993).
145. A. Tsuchii, T. Suzuki, and Y. Takahara, *Agri. Biol. Chem.* **42**, 1217 (1978).
146. A. Tsuchii, T. Suzuki, and Y. Takahara, *Agri. Biol. Chem.* **41**, 2417 (1977).
147. A. Tsuchii, T. Suzuki, and Y. Takahara, *Agri. Biol. Chem.* **43**, 2441 (1979).
148. R. T. Darby and A. M. Kaplan, *Appl. Microbiol.* **6**, 900 (1968).
149. C. Bastioli, V. Bellotti, M. Camia, L. Del'Giudice, and A. Rallis, in *Biodegradable Plastics and Polymers*, edited by Y. Doi and K. Fukuda (Elsevier Science, New York, 1994), p. 201.
150. F. Kawai, M. Watanabe, *Polymer Degradation and Stability* **86**, 105–114 (2003).
151. A. L. Pometto, K. E. Johnson, M. Kim, *J. Environ. Polym. Degrad.* **1**, 213 (1993).
152. B. Erlandsson, A.-C. Albertsson, *Acta Polym.* **49**, 363 (1998).
153. A. L. Pometto, K. E. Johnson, *J. Environ. Polym. Degrad.* **1**, 213 (1993).
154. M. Hakkarainen, A. Albertsson, *Adv. Polym. Sci.*, **169**(177) (2004).
155. Y. Otake, T. Kobayashi, *J. Appld. Polym. Sci.*, **56**, 1789 (1995).
156. Y. Otake, T. Kobayashi, *J. Appld. Polym. Sci.*, **70**, 1643 (1998).
157. A.-C. Albertsson, B. Erlandsson, M. Hakkarainen, S. Karlsson, *J. Environ. Polym. Degrad.* **6**, 187 (1998).
158. J. H. Cornell, A. M. Kaplan, *J. Appl. Polym. Sci.*, **29**, 2581 (1984).
159. R. Derval dos Santa, M. R. Callil, C. D. G. F. Guedes, T. C. Rodriguez, *J. Polymers and Environment* **12**(4), 239 (2004).
160. H. A. Abd El-REhim, E. A. Hegazy, *J. Photochem. Photobiol.* **163**(3), 547 (2004).
161. M. Weiland, C. David, *Polymer Degradation and Stability* **48**, 275 (1995).
162. T. Volke-Sepulveda, E. Favela-Torres, *J. Appld. Polym. Sci.* **73**, 1435 (1999).
163. L. Averous, *J. Macromolecular Science, Polymer Reviews* **C44**(3), 231 (2004).
164. D. Graiver, L. H. Waikul, *J. Appld. Polym. Sci.* **92**(5), 3231 (2004).
165. S. N. Swain, K. K. Rao, P. L. Nayak, *J. Appld. Polym. Sci.*, **93**(6), 2590, (2004).
166. G. Vallini, A. Corti, A. Pera, R. Solaro, F. Cioni, E. Chellini, *Gen. Appl. Microbiol.*, **40**, 445 (1994).
167. E. Schwach, L. Averous, *Polymer International*, **53**(12), 2115 (2004).
168. A. Copinet, C. Bertrand, *J. Polym. Environ.* **11**(4), 169 (2003).
169. X. C. Ge, X. H. Li, Q. Zhu, L. Li, Y. Z. Meng, *Polymer Eng. Sci.*, **44**(11), 2134 (2004).
170. D. Preechawong, M. Peesan, *Macromolecular Symposia* **216**, 217 (2004).
171. Z. Zhang, D. W. Grijpma, *Macromolecular Chemistry and Physics*, **205**(7), 867 (2004).

- 172 A. Barclay, 9th Plastics Additives and Modifiers Conference, Vienna, Austria, RAPRA Technologies Ltd., Shrewsbury, UK (2003).
- 173 M. Shibata, S. Oyamada, *J. Appld. Polym. Sci.* **92(6)**, 3857 (2004).
- 174 S. Lee, T. Ohkita, *J. Appld. Polym. Sci.* **90(7)**, 1900 (2003).
- 175 E. Zini, M. Baiardo, *Macromolecular Bioscience* **4(3)**, 286 (2004).
- 176 X. H. Li, Y. Z. Meng, *J. Polym. Sci., Part B: Polymer Physics* **42(4)**, 666 (2004).
- 177 A. Corti, F. Cristiano, 7th World Conference on Biodegradable Polymers and Plastics, Terrenia, Ital, Kluwer Academic/Plenum Publishers (2002).
- 178 H. Park, X. Liang, K. Amar, M. Misra, L. T. Drzai, *Macromolecules*, **37(24)**, 9076 (2004).
- 179 R. Hiroi, S. Suprakas, *Macromolucular Rapid Communications* **25(15)**, 1359 (2004).
- 180 M. J. Okamoto, *Ind. Eng. Chem (Korea)* **10(7)**, 1156 (2004).
- 181 H. Park, X. Liang, K. Amar, M. Misra, L. T. Drzai, *Macromolecules*, **37(24)**, 9076 (2004).
- 182 H. Yang, J. Yoon, *Polymer Degradation and Stability* **87(1)**, 131 (2005).
- 183 V. Mezanotte, R. Bertani, *Polymer Degradation and Stability* **87(1)**, 51 (2004).
- 184 N. T. Lotto, M. R. Calil, *Material Science and Engineering* **C24(5)**, 659 (2004).
- 185 A. Hoshino, M. Tsuji, 7th World Conference on Biodegradable Polymers & Plastics, Terrenia, Italy, Kluwer Academic/Plenum Publishers, New York, NY (2002).
- 186 H. Lim, T. Raku, *Macromolecular Bioscience* **4(9)**, 875 (2004).
- 187 Y. Lu, L. Zhang, *Polymer Degradation and Stability*, **86(1)**, 51 (2004).
- 188 J.-A. Lee, M.-N. Kim, *J. Polym. Environ.*, **9**, 91 (2001).
- 189 A. M. Kinnersley, T. C. Scott III, *Plant Growth Regul.*, 137 (1990).
- 190 S. M. Goheen, R. P. Wool *J. Appld. Polym. Sci.*, **42**, 2691 (1991).
- 191 D. F. Gilmore, S. Antoun, *Ind. Microbiol.*, **10**, 199 (1992).
- 192 X. Ramis, A. Cadenato, *Polymer Degradation and Stability*, **86**, 483–491 (2004).
- 193 P. K. Sahoo, P. K. Rana, A. Sahoo, *Polymer and Polymer Composites*, **12(7)**, 627 (2004).
- 194 J. Gracida, J. Alba, J. Cardoso, F. Perez-Guvera, *Polymer Degradation and Stability*, **83(2)**, 247 (2004).
- 195 Y. Orhan, J. Hrenovic, H. Bueyuekguengier, *Acta Chemica Slovenica*, **513**, 579 (2004).
- 196 A. Sharma, *J. Sci. Ind. Res.*, **63(3)**, 293 (2004).
- 197 K. H. Guruprasad, G. M. Shashidara, *J. Appld. Polym. Sci.*, **91(3)**, 1716 (2004).
- 198 A. Modelli, G. Rondinelli, M. Scandola, J. Mergaert, M. Cnockaert, *Biomacromolecules*, **5(2)**, 596 (2004).

## CHAPTER 57

# Properties of Photoresist Polymers

Qinghuang Lin

*IBM Thomas J. Watson Research Center, 1101 Kitchawan Rd, Route 134 / P.O. Box 218,  
Yorktown Heights, NY 10598*

---

<b>57.1</b>	Introduction .....	965
<b>57.2</b>	Photoresist Materials and Lithographic Patterning Process .....	965
<b>57.3</b>	Optical Properties of Lithographic Polymers and Photoresists .....	967
<b>57.4</b>	Dissolution Properties of Photoresist Polymers .....	968
<b>57.5</b>	Properties of Photoacid Generators .....	975
<b>57.6</b>	Reactive Ion (PLASMA) Etch Resistance of Photoresist Polymers .....	976
	References .....	978

---

### 57.1 INTRODUCTION

The explosive growth of semiconductor industry has been fueled by the relentless pursuit for miniaturization of semiconductor devices. The minimal feature sizes or critical dimensions (CDs) of semiconductor devices in mass production have shrunk from 10 $\mu$ m more than 30 years ago to less than 100 nm in 2005. According to the International Technology Roadmap for Semiconductors, this miniaturization trend is expected to continue unabated with the production of sub-25 nm generations of devices later next decade [1]. The miniaturization of semiconductor devices has made it possible to offer a host of sophisticated devices and equipment, from super computers, personal computers, personal digital assistants, cellular phones to medical devices and household appliances, with ever increasing performance at steadily reduced prices per transistor or bit.

This miniaturization trend has been made possible by advances in a critical device patterning process called photolithography, including constantly improved photosensitive polymeric materials called photoresists, advances in optical lenses, and the use of shorter wavelengths of light for patterning. In 2004, the semiconductor industry quietly ushered in the Nanoelectronics Age with the mass production of sub-100 nm node devices. The current leading-edge semiconductor devices in mass production—the so called 90 nm node devices—have a transistor gate length of less than 50 nm. These leading-edge devices are fabricated using photoresists based on alicyclic polymers at 193 nm wavelength, as well as

Novolak-based mid-ultra violet (MUV) photoresists or poly(4-hydroxystyrene)-based deep UV (DUV) photoresists at wavelengths of 365 and 248 nm, respectively.

### 57.2 PHOTORESIST MATERIALS AND LITHOGRAPHIC PATTERNING PROCESS

In a typical photolithography process, a UV light is projected by a set of sophisticated lenses onto a silicon wafer coated with a thin layer of photoresist through a mask that defines a particular circuitry. Exposure to the UV light, coupled with a subsequent baking, induces photochemical reactions that change the solubility of the exposed regions of the photoresist film. Subsequently an appropriate developer, usually an aqueous base solution, is used to selectively remove the photoresist either in the exposed regions (positive-tone photoresists) or in the unexposed regions (negative-tone photoresists). The pattern thus defined is then imprinted on the wafer by etching away the regions that are not protected by the photoresist with reactive ion (plasma) etching (RIE). Figures 57.1 and 57.2 depict schematic of a typical photolithographic system and a typical device patterning process. Excellent reviews on photoresist materials have been published [2–6].

Advanced photoresists, such as 193 and 248 nm photoresists, are based on chemical amplification concept [7,8]. These chemically amplified photoresists generally consist of a base polymer, a photo-sensitive compound called photoacid generator (PAG), and sometimes a cross-linking

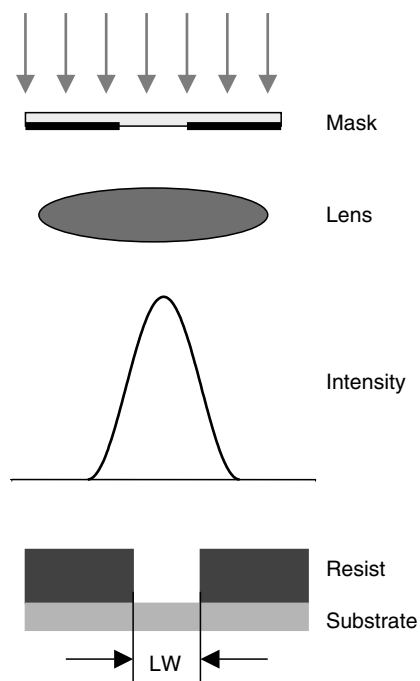


**FIGURE 57.1.** Schematic of a typical photolithographic system.

agent for negative-tone photoresists. When these resists are exposed to UV irradiation, a strong acid is generated in the exposed regions as a result of the photochemistry of the PAG. This strong catalytic acid then induces a cascade of subsequent chemical transformations of the photoresist that alter the solubility of the exposed regions. Thus the quantum efficiency of the photochemistry is amplified by hundreds or even thousands of times through the catalytic chain reactions. This catalytic effects of the chemical amplified resists greatly enhance the sensitivity of a photoresist, thus the efficiency of photolithographic processes. The chemical amplification process of a positive-tone resist is illustrated in Scheme 57.1. The most popular chemical amplification involves the acid catalyzed deprotection poly(4-hydroxy-

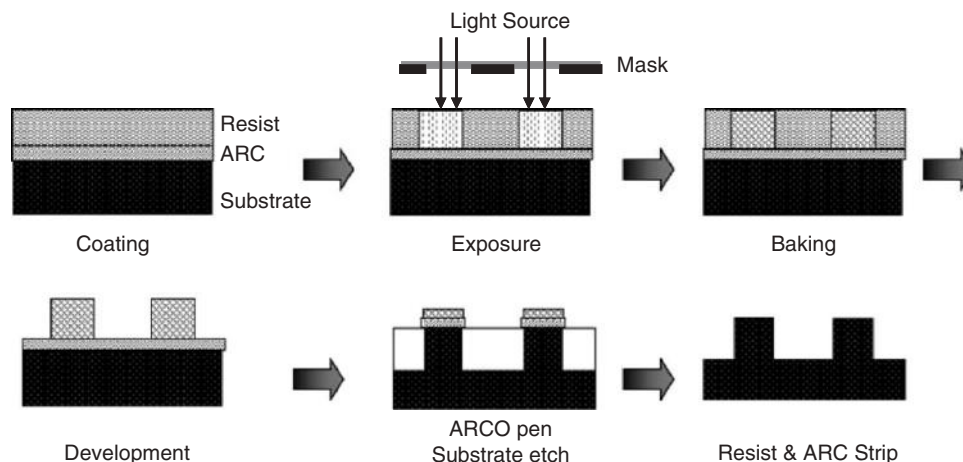
styrene) or poly(acrylic acid) protected by various acid sensitive protecting groups for positive-tone photoresists using a photoacid generator (PAG) [9].

The key figures of merit for a photoresist are resolution, process latitudes (dose and focus), and reactive ion etch resistance. Other important performance parameters include sensitivity, compatibility with industrial standard developer (0.263N aqueous tetramethylammoniumhydroxide (TMAH) solution), adhesion to substrates, environmental stability, and shelf life. These performance characteristics are mainly determined by the base polymer in the photoresist. It should be pointed out, however, that some of these performance parameters, such as resolution, process latitudes and etch resistance, are also tool and process condition dependent.

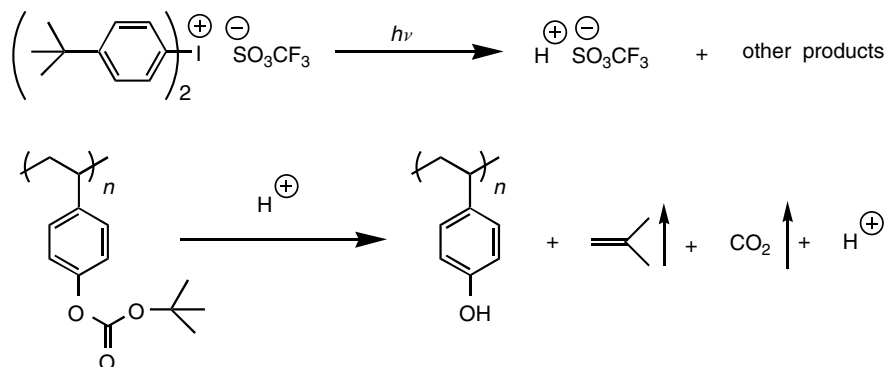
Polymers for advanced photoresists, therefore, need to meet the following requirements in order to deliver the performance necessary for device fabrication: good transparency at the imaging wavelength, etch resistance, optimal dissolution properties, high sensitivity, compatibility with the industrial standard 0.263N TMAH developer, as well as thermal and mechanical properties and shelf life requirements. These stringent requirements led to the design and synthesis of distinct polymer platforms for the evolving lithographic exposure technologies. Table 57.1 summarizes the major polymer platforms for the various exposure technologies.

Photoresists can be classified into three categories based on the lithographic processes: single layer photoresists (SLRs), bilayer photoresists (BLRs), and top surface imaged (TSI) photoresists [5]. Single layer photoresists have traditionally been the work horse for patterning semiconductor devices due to its process simplicity as compared with the bilayer and the TSI processes.

Properties of photoresist polymers were surveyed and reviewed by Kunz [10]. This present chapter is intended to complement, not replace, the review chapter by Kunz. Emphasis in this chapter has been placed on physical property data of photoresist polymers published after Kunz's review.



**FIGURE 57.2.** Schematic of a typical photolithographic patterning process using a positive-tone resist. ARC=antireflective coating.


**SCHEME 57.1.** Chemical amplification in a positive-tone photoresist.

### 57.3 OPTICAL PROPERTIES OF LITHOGRAPHIC POLYMERS AND PHOTORESISTS

Polymers for photoresists must meet stringent transparency requirements at the imaging wavelength in order to deliver superior resolution and image quality. Suitable polymer platforms have been identified for I-line (365 nm) and 248 nm DUV lithography. They are *meta*-cresol novolak

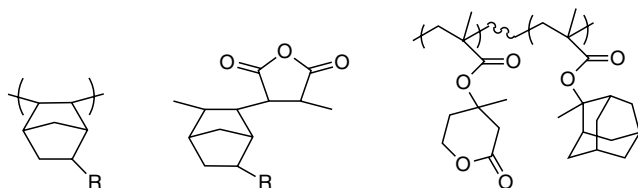
and poly(4-hydroxystyrene), respectively. Novolak and poly(4-hydroxystyrene), however, are not suitable for 193 nm single layer lithography because of their high absorption at 193 nm wavelength as a result of the  $\pi-\pi^*$  transition of the double bonds in these polymers.

The transparency requirements, along with plasma etch resistant requirements, have led to a strategy for designing new polymers for 193 nm lithography, namely, the

**TABLE 57.1.** Major polymer platforms for the evolving exposure technologies.

Technology node	Exposure technology	Polymer platform
0.8–0.35 $\mu\text{m}$	I-Line (365 nm)	
0.25–0.15 $\mu\text{m}$	DUV (248 nm)	
130–65 nm	DUV (193 nm)	
45–32 nm	DUV (157 nm)	
$\leq 25$ nm	EUV (13 nm)	?

incorporation of saturated aliphatic rings to form cycloaliphatic polymers. These saturated aliphatic rings can be incorporated into the polymer side chain [11–14] or in the polymer main chain [15,16], or a combination of both. Some of the most popular alicyclic 193 nm photoresist polymers are depicted below:



**SCHEME 57.2.** Alicyclic polymers for 193 nm lithography.

The absorption of organic polymers at 157 nm is dominated by the C (2p) electrons. An early audition of a large number of both organic and inorganic polymers indicated that fluorinated hydrocarbon polymers and siloxane polymers were the most promising polymer platforms to achieve adequate transparency and plasma etch resistance [17]. This pioneering work has spurred tremendous efforts to develop transparent and etch resistant fluoropolymers for 157 nm lithography.

Tables 57.2–57.4 list the optical constants of some polymers at 157 nm. In these tables,  $M_w$  and  $T_g$  are weight average molecular weight and glass transition temperature, respectively. Both the real ( $n$ ) and imaginary ( $k$ ) parts of the complex refractive indices ( $n+ik$ ) are listed. The absorption coefficient ( $\alpha$ ) is correlated to the imaginary ( $k$ ) part of the refractive index via the following equation:

$$\alpha = 4\pi k/\lambda,$$

where  $\lambda$  is the imaging wavelength.

As can be seen in Tables 57.2–57.4, many of the traditional polymers used for 248 and 193 nm lithography have prohibitively high absorbance at the 157 nm imaging wavelength. So are some of the key functional groups, such as phenol and carboxylic acid employed for solubility in aqueous base solutions. New polymer platforms and functional groups, therefore, must be designed/discovered for the 157 nm lithography.

The world-wide efforts to search for 157 nm transparent and etch resistant polymers for 157 nm lithography have resulted in several promising polymer platforms. They include highly fluorinated polymers as well as aromatic and aliphatic alcohols bearing highly electron withdrawing groups such as hexafluoroisopropanol. These polymers and their copolymers and terpolymers have been explored as possible polymer platforms for 157 nm lithography as well as lithography at longer wavelengths of 193 and 248 nm.

Table 57.5 shows the absorbance of some of these polymers and some reference polymers.

Optical properties of a photoresist are determined by its base polymer as well as additives in the photoresist system, such as photoactive compounds, dissolution inhibitors, etc. Tables 57.6 and 57.7 list optical properties of some commercial I-line (365 nm) and DUV (248 nm) resists.

## 57.4 DISSOLUTION PROPERTIES OF PHOTORESIST POLYMERS

Proper dissolution of photoresist polymers in aqueous base solutions, usually 0.263N aqueous tetramethylammoniumhydroxide (TMAH) solution, is critical to achieving good resist performance. The dissolution rate of photoresist polymers depends on various parameters, including polymer type, molecular weight, copolymer composition, interactions with additives in the polymers, as well as temperature and base strength.

The dissolution rate of a photoresist polymer, like many other physical properties, depends heavily on the molecular weight of the polymer. The dissolution rate generally decreases with increasing molecular weight of the polymer. Figure 57.3 shows the dependence of dissolution rate of novolak with nearly monodisperse molecular weight distribution on its molecular weight [31]. The nearly monodisperse molecular weight distribution was achieved by fractionation with supercritical CO<sub>2</sub> fluids.

Similar dependence of dissolution of poly(4-hydroxystyrene)—the key polymer for 248 nm lithography—have been observed [32] (Fig. 57.4). Again the dissolution rate of poly(4-hydroxystyrene) decreases with increasing molecular weight of the polymer. The relatively narrow molecular weight distribution of poly(4-hydroxystyrene) was achieved by “living” free radical polymerization (Table 57.8).

The dissolution rates (DR) of poly(4-hydroxystyrene) in 0.14N TMAH were found to correlate well with its weight average molecular weight ( $M_w$ ) as described by the following equation [33]:

$$DR = K_1(M_w)^{-1/m}$$

where DR=dissolution rate in Å/s in 0.14N TMAH at room temperature and  $M_w$  = Weight average molecular weight. For poly(4-hydroxystyrene) with a molecular weight range of 3,500–240,000,  $K_1 = 19,100$  and  $m=1.98$

The dissolution rates of photoresist and polymers can also be regulated by making miscible blends of two or more polymers. Tables 57.9 and 57.10 list dissolution rates of binary blends of poly(4-hydroxystyrene) as well as poly(4-hydroxystyrene) and a silicon-containing copolymer [32,34]. This blending method is a convenient way to optimize the dissolution rates of photoresist polymers.

**TABLE 57.2.** Optical constants and other properties of polymers for 157 nm lithography.

Polymer	$M_w$	$n_{157\text{ nm}}$	$k_{157\text{ nm}}$	$\alpha_{157\text{ nm}}$ ( $\mu\text{m}^{-1}$ )	$\lambda_{\text{max}}$ (nm)	$\alpha_{\text{max}}$ ( $\mu\text{m}^{-1}$ )	$T_g$ (°C)	Reference
Poly(methyl methacrylate)				5.69				[17]
Poly(acrylic acid)				11.00				[17]
Poly(norbornene)				6.1				[17]
Poly(vinyl naphthalene)				10.60				[17]
Poly(norbornyl methacrylate)				6.7				[18]
Poly(norbornene- <i>alt</i> -maleic anhydride)				8–9				[18]
Poly(tetrafluoroethylene/norbornene) (49/51)	1,700( $M_n$ )	1.6		1.3			151	[18]
Poly(methyl $\alpha$ -trifluoromethylacrylate)				2.68–3.0				[19–21]
Poly(styrene)	~50,000			6.6	193.0	22.7	~100	[22]
Poly(4-fluorostyrene)	17,500	1.35	0.199	7.0	189.0	24.0	110	[22]
Poly(3-fluorostyrene)	16,000	1.24	0.205	7.08	189.5	29.7		[22]
Poly(pentafluorostyrene)				5.8	177.0	14.4		[22]
Poly(4-trifluoromethyl styrene)	24,900	1.36	0.130	4.33	189.0	14.7	115	[22]
Poly(3,5-bis(trifluoromethyl)styrene)	22,600	1.29	0.096	3.63	185.0	17.2	119	[22]
Poly(4- <i>tert</i> -butyl styrene)	19,600	1.42	0.162	5.67	193.5	22.7	151	[22]
Poly(2-hexafluoroisopropanol styrene)	3,100	1.48	0.094	3.40	191.5	17.8		[22]
Poly(3-hexafluoroisopropanol styrene)	36,700	1.29	0.107	3.80	190.0	17.9	81	[22]
Poly(4-hexafluoroisopropanol styrene)	26,300	1.39	0.099	3.44	190.5	20.5	129	[22]
Poly(4- <i>t</i> -BOC-hexafluoroisopropanol styrene)	6,700	1.52	0.087	2.95	191.0	9.6	62	[22]
Poly(4- <i>t</i> -butylacetate-hexafluoroisopropanol styrene)		1.48	0.111	4.29	191.5	11.2		[22]
Poly( <i>t</i> -butyl acrylate)		1.70	0.147	5.43				[22]
Poly(4-hydroxystyrene)		1.49	0.204	6.70	194.5	28.5		[22]
Poly(norbornene methylene hexafluoro isopropanol)	9,300	13,500		1.67, 1.80	<150	>3.0		[19,23]
Poly(norbornene hexafluoro alcohol- <i>co</i> -norbornene hexafluoro alcohol <i>t</i> -butoxycarbonyl) (20:80)				1.90				[24,25]
Poly(norbornene hexafluoro alcohol- <i>co</i> -norbornene hexafluoro alcohol acetal) (20:80)				1.78				[24,25]
Poly(1,1,2,3,3-pentafluoro, 4-trifluoromethyl-4-hydroxy-1,6-heptadiene) (PFOP)				0.4			152	[26]
Poly( <i>tert</i> -butyl[2,2,2-trifluoro-1-trifluoromethyl-1-(4-vinyl-phenyl)ethoxy]-acetate)	14,500			4.29			55	[27]
Poly(1-(2,2,2-trifluoro-1-methoxymethoxy-1-trifluoromethyl-ethyl)-4-vinyl benzene)	16,200			2.60			69	[27]
Poly(1-[1-( <i>tert</i> -butoxymethoxy)-2,2,2-trifluoro-1-trifluoromethylethyl]-4-vinylbenzene)	16,600						63	[27]
Poly(1-[1-( <i>tert</i> -butoxycarbonyl)-2,2,2-trifluoro-1-trifluoromethylethyl]-4-vinylbenzene)	6,700			2.95			93	[27]
Poly(2-[4-(2-hydroxyhexafluoro isopropyl) cyclohexane] hexafluoroisopropyl acrylate)				1.93				[28]

**TABLE 57.3.** Optical constants and other properties of fluorinated copolymers for 157 nm lithography.

Monomer 1	Monomer 2	Ratio ( $M_1/M_2$ )	$M_n$	$n_{157\text{ nm}}$	$k_{157\text{ nm}}$	$\alpha_{157\text{ nm}}(\mu\text{m}^{-1})$	$T_g(^{\circ}\text{C})$	Reference
4-HFIPS	<i>t</i> -BMA	60/40		1.454	0.112	3.99		[22]
4-HFIPS	<i>t</i> -BMA	50/50		1.496	0.112	4.05		[22]
4-HFIPS	<i>t</i> -BMA	70/30				3.74		[22]
3-HFIPS	<i>t</i> -BMA	60/40		1.476	0.105	3.92		[22]
4-HFIPS	$\alpha$ -CF <sub>3</sub> - <i>t</i> -BMA	75/25		1.382	0.104	3.71		[22]
4-HFIPS	<i>t</i> BOC-pHFIPS	70/30		1.398	0.102	3.58		[22]
4-HFIPS	<i>t</i> BOC-pHFIPS	60/40		1.378	0.097	3.44		[22]
4-HFIPS	<i>t</i> BAcetHFIPS	60/40	61,600	2.354	0.117	3.80	93	[22,27]
4-HS	<i>t</i> BA	50/50				6.5	155	[29]
4-HFIPS	<i>t</i> BA	50/50				3.7	120	[29]
4-HFIPS	<i>t</i> -BMA	50/50				4.0	154	[29]
3-HFIPS	<i>t</i> -BMA	50/50				3.9	111	[29]
4-HFIPS	<i>t</i> BA	60/40	17,600			3.74	124	[27]
4-HFIPS	<i>t</i> BAcetHFIPS	70/30	4,500			3.71	107	[27]
4-HFIPS	<i>t</i> BOC-HFIPS	50/50	16,900			3.39	69	[27]
4-HFIPS	<i>t</i> BOC-HFIPS	60/40	21,800			3.44	73	[27]
4-HFIPS	<i>t</i> BOC-HFIPS	70/30	25,800			5.57	73	[27]
4-HFIPS	MOM-HFIPS	60/40	25,500			3.08	107	[27]
4-HFIPS	MOM-HFIPS	70/30	26,900			3.27	117	[27]
4-HFIPS	BOM-HFIPS	60/40	26,300			2.82	97	[27]
4-HFIPS	BOM-HFIPS	70/30	26,300			3.16	106	[27]
PFOP	MOMPFOP	100/0				0.4	152	[26]
PFOP	MOMPFOP	82/17				0.5	145	[26]
PFOP	MOMPFOP	70/30				0.6	140	[26]
PFOP	MOMPFOP	54/46				0.8	137	[26]
NBHFA	NBC	60/40				2.99		[20]
NBHFA	NBC	80/20				2.28		[20]
NBHFA	TBTFMA	33/67	8,300			2.7		[23]

Note: 4-HFIPS, 4-hexafluoroisopropanol styrene; 3-HFIPS, 3-hexafluoroisopropanol styrene; *t*-BMA, *t*-butyl methacrylate; *t*BA, *t*-butyl acrylate;  $\alpha$ -CF<sub>3</sub>-*t*-BMA,  $\alpha$ -trifluoromethyl *t*-butyl methacrylate; *t*BOC-pHFIPS, *t*-butoxycarbonyl protected 4-hexafluoroisopropanol styrene; *t*BAcetHFIPS, *t*-butyl acetate protected 4-hexafluoroisopropanol styrene; 4-HS, 4-hydroxystyrene; *t*-BuAc HFIPS, *t*-butylacetate protected 4-hexafluoroisopropanol styrene; MOM HFIPS, methoxymethyl protected 4-hexafluoroisopropanol styrene; BOM HFIPS, butoxymethyl protected 4-hexafluoroisopropanol styrene; PFOP, 1,1,2,3,3-pentafluoro, 4-trifluoromethyl-4-hydroxy-1,6-heptadiene; MOMPFP, methoxymethyl protected 1,1,2,3,3-pentafluoro, 4-trifluoromethyl-4-hydroxy-1,6-heptadiene; NBHFA, norbornene-5-methylenehexafluoroisopropanol; BNC, butylnorbornene carboxylate; TBTFMA, methyl 2-trifluoromethylmethacrylate.

Another very effective way to regulate the dissolution rate of photoresist polymers is copolymerization. Table 57.11 lists the physical properties of poly(4-hydroxystyrene-*co*-styrene) [35].

The copolymer architecture of poly(4-hydroxystyrene-*co*-styrene) was found to have insignificant effect on its dissolution rate (Fig. 57.5; Table 57.12) [36]. On the other hand, incorporation of inert styrene unit into poly(4-hydroxystyrene) drastically reduces dissolution rate. This method of incorporating inert unit has been employed to optimize the dissolution of base polymers for advanced DUV photoresists.

The dissolution rates of photoresist polymers can be further modulated by additives, such as photoacid generators or dissolution inhibitors. The photoacid generators are generally hydrophobic due to their usually bulky chromo-

phores. Therefore, they generally act as to slow down the dissolution of photoresist polymers in aqueous base solutions, a phenomenon called dissolution inhibition. Figure 57.6 exhibits the effect of a photoacid generator on the dissolution rates of another key 248 nm photoresist polymer, poly(4-hydroxystyrene-*co*-*t*-butyl acrylate) [37]. It can also be seen that the level of protection, i.e., the fraction of *t*-butyl acrylate monomer in the copolymer, has an even more prominent effect on the dissolution rates. Increasing the protection level sharply reduces dissolution rates in 0.26N TMAH.

Similar dissolution inhibition effect by photoacid generators has also been observed in poly(norbornene-methylenehexafluoroisopropanol) (poly(NBHFA)) system [38]. Table 57.13 lists dissolution rates of poly(NBHFA) in 0.26N TMAH at room temperature with various photoacid



**TABLE 57.4.** Optical constants and other properties of fluorinated terpolymers for 157 nm lithography.

Monomer 1	Monomer 2	Monomer 3	Ratio ( $M_1/M_2/M_3$ )	$M_n$	$n_{157\text{ nm}}$	$k_{157\text{ nm}}$	$\alpha_{157\text{ nm}}(\mu\text{m}^{-1})$	$T_g(^{\circ}\text{C})$	Reference
4-HFIPS	<i>t</i> -BMA	3,5-DiCF <sub>3</sub> -S	60/20/20		1.378	0.112	3.99		[22]
4-HFIPS	<i>t</i> -BMA	4-FHIPyp-S	60/20/20		1.330	0.113	3.89		[22]
4-HFIPS	<i>t</i> -BMA	4-C3F7CO-S	60/20/20		1.350	0.115	4.03		[22]
3-HFIPS	<i>t</i> -BMA	Acrylonitrile	70/20/10		1.397	0.106	3.80		[22]
4-HFIPS	<i>t</i> -BMA	Methacrylonitrile	70/20/10		1.408	0.102	3.72		[22]
PFOP	MOMPFOP	<i>t</i> -BMA	71.5/23.5/5	10,000			0.7	150	[26]
PFOP	MOMPFOP	<i>t</i> -BMA	73/10/17	6,700			1.0	154	[26]
PFOP	MOMPFOP	<i>t</i> -BMA	67/0/33	5,800			1.2	154	[26]
PFOP	MOMPFOP	VP	68/19/13	9,600			0.8	144	[26]
PFOP	MOMPFOP	MA	30/50/20	9,300			1.3		[26]
PFOP	MOMPFOP	PFVE	40/10/50	10,200			0.4		[26]

Note: 4-HFIPS, 4-hexafluoroisopropanol styrene; 3-HFIPS, 3-hexafluoroisopropanol styrene; *t*-BMA, *t*-butyl methacrylate; *t*BA, *t*-butyl acrylate;  $\alpha$ -CF<sub>3</sub>-*t*BMA,  $\alpha$ -trifluoromethyl *t*-butyl methacrylate; *t*BOC-pHFIPS, *t*-butoxycarbonyl protected 4-hexafluoroisopropanol styrene; *t*BAcetHFIPS, *t*-butyl acetate protected 4-hexafluoroisopropanol styrene; 4-HS, 4-hydroxystyrene; *t*-BuAc HFIPS, *t*-butylacetate protected 4-hexafluoroisopropanol styrene; MOM HFIPS, methoxymethyl protected 4-hexafluoroisopropanol styrene; BOM HFIPS, butoxymethyl protected 4-hexafluoroisopropanol styrene; PFOP, 1,1,2,3,3-pentafluoro, 4-trifluoromethyl-4-hydroxy-1,6-heptadiene; MOMPFOP, methoxymethyl protected 1,1,2,3,3-pentafluoro, 4-trifluoromethyl-4-hydroxy-1,6-heptadiene; VP, vinyl pivalate; V4*t*BB, Vinyl-4-*tert*-butyl benzoate; MA, maleic anhydride; PFVE, perfluoro vinyl ether.

**TABLE 57.5.** Absorbance of some cycloolefin polymers, copolymers, and reference polymers [30].

Polymer	$\alpha_{248\text{ nm}}(\mu\text{m}^{-1})$	$\alpha_{193\text{ nm}}(\mu\text{m}^{-1})$	$\alpha_{157\text{ nm}}(\mu\text{m}^{-1})$
Poly(NBHFA)	0.00	0.38	1.76
Poly(BNC)	0.11	0.48	6.41
Poly(BNC- <i>co</i> -MCA) (2:1)	0.04	0.23	5.05
Poly(BNC- <i>co</i> -MCA) (1:1)	0.02	0.38	5.20
Poly(NBHFA- <i>co</i> -MCA) (2:1)	0.10	0.28	3.29
Poly(NB- <i>co</i> -MCA) (2:1)	0.03	0.11	4.98
Poly (MMA)	0.00	0.05	5.60
Poly(MTFA)	0.00	0.00	2.90
Poly(ECA)	0.00	0.00	3.90

Note: NB, norbornene; NBHFA, norbornene-methylenehexafluoroisopropanol; MCA, methyl cyanoacrylate; BNC, butyl norbornene carboxylate; MA, methylacrylate; MMA, methyl methacrylate; MTFA, methyl trifluoromethyl acrylate; ECA, ethyl cyanoacrylate.

**TABLE 57.6.** Optical constants of commercial *I*-line (365 nm) photoresists<sup>a</sup>.

Resist	Supplier	Type	$n_{365\text{ nm}}$	$k_{365\text{ nm}}$	$a_{365\text{ nm}}(\mu\text{m}^{-1})$	$n_{633\text{ nm}}$
IBM7500	IBM	Positive tone	1.701	0.0190	0.65	1.641
IBM7518	IBM	Positive tone	1.694	0.0216	0.74	1.627
Spectralith 5105	IBM	Positive tone	1.693	0.0298	1.03	1.628
Spectralith 5108	IBM	Positive tone	1.683	0.0284	0.98	1.620
IX300	JSR	Positive tone	1.690	0.0177	0.61	1.626
JSR 1010	JSR	Positive tone	1.690	0.0178	0.61	1.622
TMHR 2600	TOK	Positive tone	1.685	0.0209	0.72	1.618
TMHR 3250	TOK	Positive tone	1.687	0.0242	0.83	1.620
THMR 3720	TOK	Positive tone	1.697	0.0277	0.95	1.628
THMR 3780	TOK	Positive tone	1.694	0.0294	1.01	1.625
THMR NP4S	TOK	negative tone	1.654	0.0106	0.36	1.587
TSMR IN008	TOK	negative tone	1.652	0.0063	0.22	1.587
TSMR IN011	TOK	negative tone	1.660	0.0183	0.63	1.588
TSMR IN-TR12	TOK	negative tone	1.641	0.0043	0.15	1.584

<sup>a</sup>Courtesy of Dr. James Bruce, IBM, 2005.

**TABLE 57.7.** Optical constants of commercial DUV (248 nm) photoresists<sup>a</sup>.

Resist	Supplier	Type	$n_{248\text{ nm}}$	$k_{248\text{ nm}}$	$a_{248\text{ nm}}(\mu\text{m}^{-1})$	$n_{365\text{ nm}}$	$k_{365\text{ nm}}$	$a_{365\text{ nm}}(\mu\text{m}^{-1})$	$n_{633\text{ nm}}$
APEX-M	IBM/ Shipley	Positive tone	1.780	0.0076	0.39	1.614	0.0000	0.00	1.562
UVII-HS	Shipley/Rohm Hass	Positive tone	1.730	0.0113	0.57	1.590	0.0000	0.00	1.545
UV4	Shipley/Rohm Hass	Positive tone	1.802	0.0129	0.65	1.631	0.0000	0.00	1.575
UV5	Shipley/Rohm Hass	Positive tone	1.804	0.0109	0.55	1.631	0.0019	0.07	1.577
UV82	Shipley/Rohm Hass	Positive tone	1.762	0.0122	0.62	1.611	0.0000	0.00	1.561
UV110	Shipley/Rohm Hass	Positive tone	1.787	0.0121	0.61	1.626	0.0057	0.20	1.577
UV-113	Shipley/Rohm Hass	Positive tone	1.785	0.0125	0.63	1.628	0.0061	0.21	1.577
UV-N	Shipley/Rohm Hass	Negative tone	1.803	0.0101	0.51	1.640	0.0053	0.18	1.587
CGR 248	Shipley/Rohm Hass	Negative tone	1.813	0.0100	0.51	1.643	0.0003	0.01	1.589
CGR CE	Shipley/Rohm Hass	Negative tone	1.773	0.0077	0.39	1.617	0.0005	0.02	1.567
M20G	JSR	Positive tone	1.779	0.0100	0.51	1.616	0.0002	0.01	1.564
M22G	JSR	Positive tone	1.775	0.0120	0.61	1.616	0.0059	0.20	1.565
M60G	JSR	Positive tone	1.772	0.0133	0.67	1.621	0.0028	0.10	1.574
M92Y	JSR	Positive tone	1.775	0.0074	0.37	1.622	0.0040	0.14	1.574
P015	TOK	Positive tone	1.816	0.0093	0.47	1.641	0.0041	0.14	1.591

<sup>a</sup>Courtesy of Dr. James Bruce, IBM, 2005.

generators and photoacid generator concentrations. As expected, more bulky, hydrophobic photoacid generators effect better dissolution inhibition.

The effects on dissolution inhibitors on the dissolution of a 193 nm terpolymers poly(norbornene-*alt*-maleic anhydride-*co*-acrylic acid) (p(NB/MA-20%AA) are shown in Figure 57.7 [39]. Again the dissolution rate of this 193 nm terpolymer is significantly reduced with the addition of the dissolution inhibitors. The effects of various dissolution inhibitors were attributed to the varied degree of the interactions between the base polymer and the dissolution inhibitors. In these cycloolefin-maleic anhydride terpolymer systems, the position of the base soluble carboxylic group

appeared to have no significant effect on the dissolution of the base polymers. The dissolution rates were very similar whether the carboxylic group is part of norbornene or part of the acrylate [40].

As the resist film thickness shrinks, the interactions of photoresist polymers and substrates become increasingly important. Dissolution rates of photoresist polymers were found to change as the film thickness decreases. Figure 57.8 shows variation of the dissolution rates of poly(4-hydroxystyrene) and poly(norbornene-methylene-hexafluoroisopropanol) as a function film thickness. The dissolution rates of both polymers increase with decreasing initial film thickness [41].

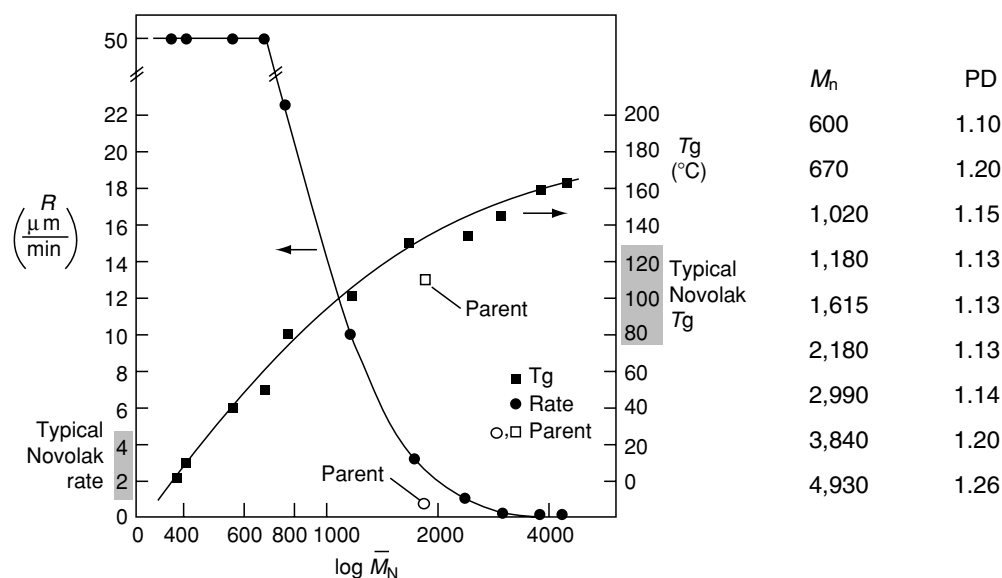


**FIGURE 57.3.** Glass transition temperature and dissolution rate of fractionated novolak in 0.263N TMAH at room temperature [31].

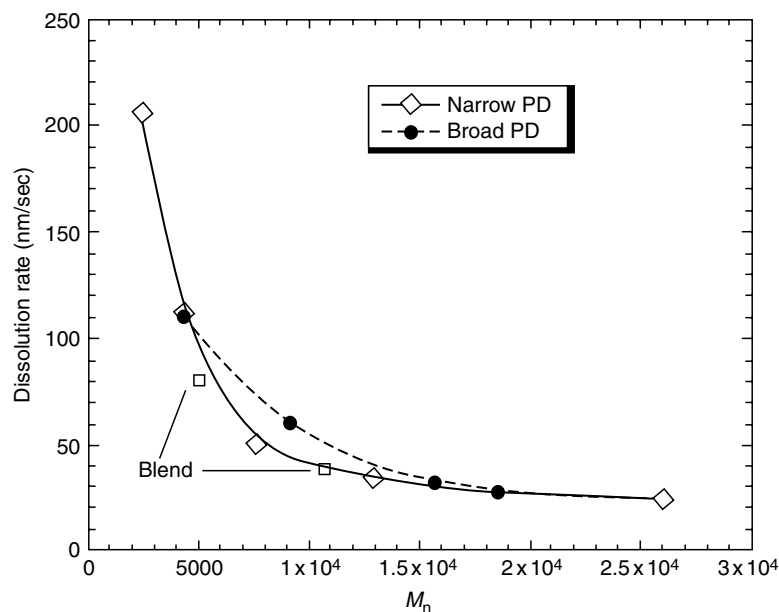


**FIGURE 57.4.** Dissolution rates of narrow polydispersity poly(4-hydroxystyrene) in 0.21 TMAH aqueous solution at room temperature [32].

**TABLE 57.8.** Glass transition temperature of narrow PD of poly(4-hydroxystyrene) synthesized by “living” free radical polymerization [32].

PHOST	$M_n$	$M_w/M_n$	$T_g$ (°C)
PHOST-1	2,304	1.19	149
PHOST-2	3,874	1.18	172
PHOST-3	6,528	1.42	177
PHOST-4	12,726	1.38	185
PHOST-5	24,298	1.43	186

**TABLE 57.9.** Dissolution rates of binary blends of poly(4-hydroxystyrene) in 0.21N TMAH at room temperature [32].

Binary blend (wt/wt)	$M_n$	$M_w/M_n$	Dissolution rate (nm/s)
100/0	2,304	1.19	206
68/32	3,500	4.94	121
50/50	4,400	5.46	81
40/60	4,900	5.49	67
0/100	24,298	1.43	25

**TABLE 57.10.** Dissolution rates of binary blends of P(4-hydroxystyrene) and poly(4-hydroxybenzylsilsesquioxane-co-4-methoxybenzylsilsesquioxane) in 0.26N TMAH at room temperature [34].

PHS wt%	Si conc. (wt%)	Dissolution rate (A/s)	$T_g$ (°C)	Etch selectivity
0	17	5,011	106.8	27.8
10	15.3	4,128	—	—
20	13.6	3,601	115.4	21.6
30	11.9	3,230	121.0	19.0
40	10.2	3,115	130.5	15.6
60	6.8	2,829	139.8	6.6
80	3.4	2,748	150.0	2.5
100	0	2,483	162.4	0.9

Note: etch rate of  $O_2$ -based plasma chemistries vs novolak.

**TABLE 57.11.** Physical properties of poly(4-hydroxystyrene-co-styrene) [35].

Styrene (mol%)	$M_w$	PD	$a_{248\text{ nm}}$ ( $\mu\text{m}^{-1}$ )	$T_g$ (°C)
0	19,400	1.67	0.172	178
5	19,180	1.87	0.165	168
10	11,540	1.56	0.164	166
15	13,650	1.76	0.152	161
20	11,040	1.95	0.156	160
25	14,500	2.00	0.155	158
30	12,570	1.90	0.154	155

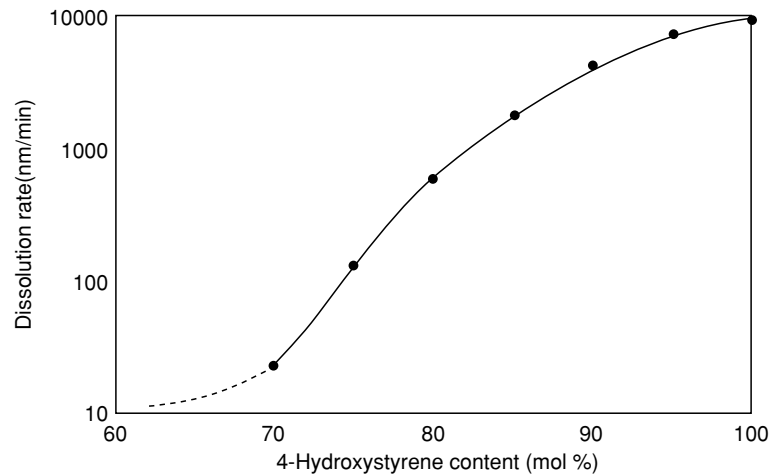


**FIGURE 57.5.** Effect of copolymer composition on the dissolution rates of poly(4-hydroxystyrene -co-styrene) in 0.26N TMAH at room temperature [36].

**TABLE 57.12.** Effect of copolymer architecture and composition on the dissolution rates of poly(4-hydroxystyrene- co-styrene) in 0.26N TMAH at room temperature [36].

4-HOST	Styrene	Architecture	$M_w$	$M_n$	PD	DR (Å/s)
100	0	Homo	9,550	7,958	1.20	2,050
90	10	Random	8,297	6,533	1.27	677
80	20	Random	9,908	8,188	1.21	34
70	30	Random	8,197	7,190	1.14	3
55	45	Random	8,559	6,793	1.26	1
90	10	Block	10,155	8,324	1.22	330
80	20	Block	8,854	7,568	1.17	94
70	30	Block	6,856	6,121	1.12	7
55	45	Block	10,020	8,564	1.17	1

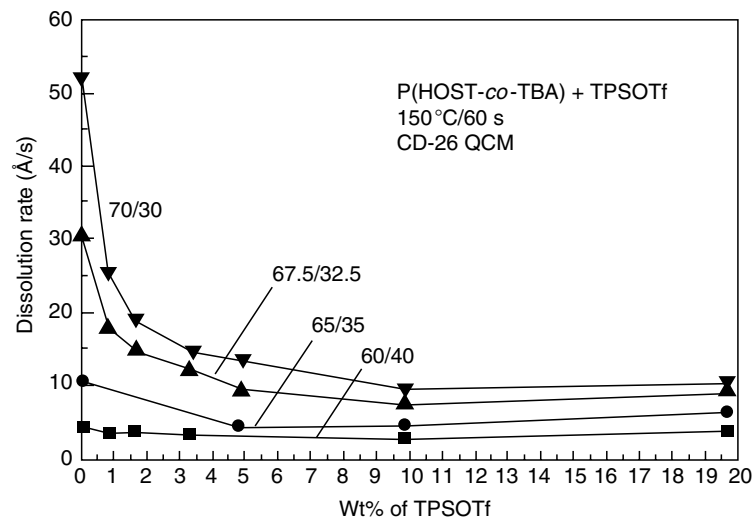


**FIGURE 57.6.** Effects of protection level and photoacid generator on the dissolution of poly(4-hydroxystyrene- co-*t*-butyl acrylate) (P(HOST-*co-t*BA) in 0.26N TMAH at 150 °C. The photoacid generator used is triphenylsulfonium triflate (TPSOTf). The developer is a 0.26N TMAH aqueous solution (CD-26) [37].

**TABLE 57.13.** Effects of photoacid generators (PAGs) on the dissolution rates of poly(NBHFA) in 0.26N TMAH at room temperature [38].

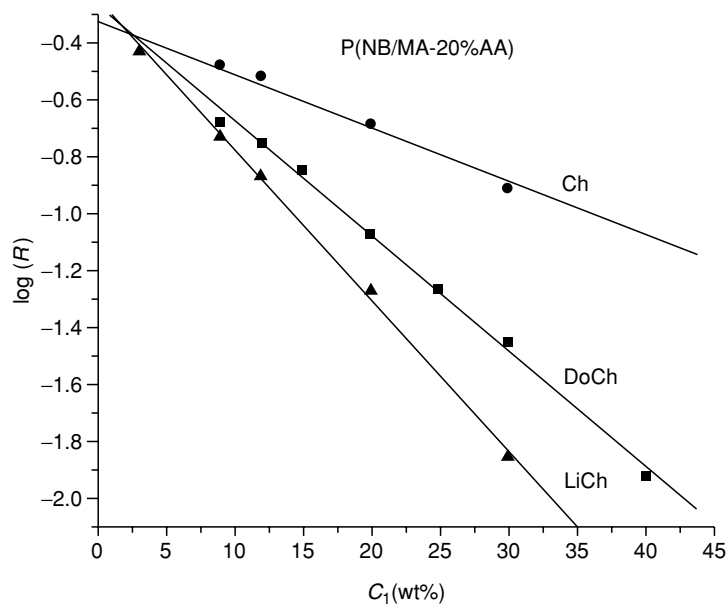
PAG	Wt% of PAG	Mol % of PAG	Dissolution rate (Å/s)
None			3,162.3
1	9.72	4.99	121.4
1	20.50	11.16	44.0
2	7.31	4.98	69.4
3	12.67	4.96	60.3
4	10.06	8.92	400.0
5	2.33	1.24	20.6
5	5.22	2.81	1.5
5	5.94	3.22	0.91
5	10.72	5.95	<0.05
6	8.34	3.60	0.70
7	4.16	1.87	4.84
7	8.00	3.68	0.86
8	4.08	1.73	6.61
8	7.94	3.45	0.64
9	3.13	2.84	503.2

Note: PAG 1, triphenylsulfonium nonaflate; PAG 2, triphenylsulfonium triflate; PAG 3, triphenylsulfonium perfluorooctylsulfonate; PAG 4, *N*-Trifluoromethylsulfonyloxy-1,8-naphthalimide; PAG 5, diphenyl(4-thiophenylphenyl)-sulfonium triflate; PAG 6, diphenyl(4-thiophenylphenyl)-sulfonium nonaflate; PAG 7, 4-methoxy-1-naphthalenyldiphenylsulfonium nonaflate; PAG 8, diphenyliodinium triflate; PAG 9, di-1-naphthalenyldiphenylsulfonium nonaflate.

### 57.5 PROPERTIES OF PHOTOACID GENERATORS

Photoacid generator (PAG) is a critical component of modern chemically amplified resists. It not only determines the sensitivity but also influences the dissolution and the

stability of a chemically amplified photoresist. Major requirements for photoacid generators are sufficient absorption at the imaging wavelength, production of a strong acid to catalyze chemical transformation of the base photoresist polymer. Other considerations include effects on the dissolution of the base photoresist polymer, solubility in


**FIGURE 57.7.** The effects on dissolution inhibitors on the dissolution rate ( $R$ ) of a 193 nm terpolymers poly(norbornene-*alt*-melaic anhydride-*co*-acrylic acid) (p(NB/MA-20%AA) in 0.26N TMAH at room temperature [39]. Ch=*t*-butylcholate, DoCh=*t*-butyldeoxycholate, LiCh=*t*-butyllithocholate.

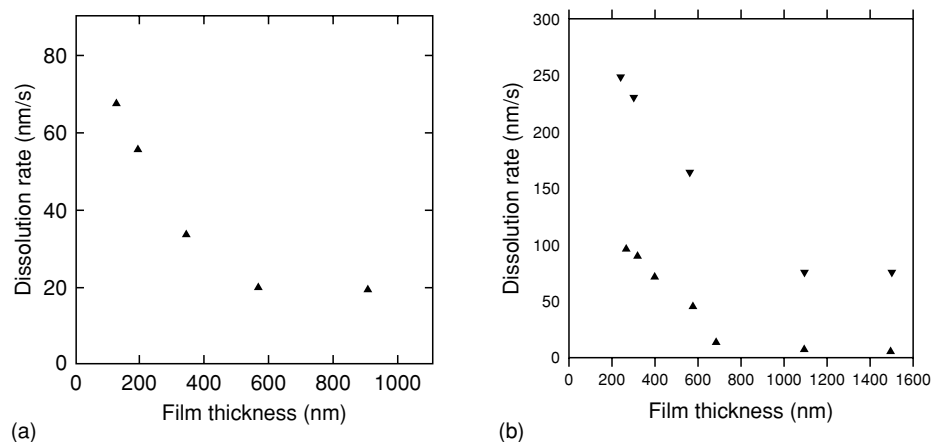


**FIGURE 57.8.** Dissolution rates of poly(norbornene-methylenehexafluoroisopropanol) (poly(NBHFA)) (a) in 0.165N TMAH at room temperature and poly(4-hydroxystyrene) (b) in 0.12 and 0.165N TMAH at room temperature [41].

photoresist solvents, stability of the photoacid generator before exposure to a light source, miscibility with the base photoresist polymer, toxicity, etc. The most popular and efficient photoacid generators are onium salts, such as aryl iodonium and sulfonium salts [42] although some nonionic photoacid generators have also been used in chemically amplified resists. The synthesis, photochemistry, photosensitization of onium salts are reviewed elsewhere [42].

Key performance parameters of photoacid generators are absorbance, quantum efficiency, dissolution inhibition effect, etc. Table 57.14 shows quantum yields for the photolysis of some aryl iodonium and sulfonium salts.

The metal-containing onium salts are generally not preferred in modern photoresists as they will contaminate the device fabrication processes. Instead organic onium salts are preferred in chemically amplified photoresist formulations. Table 57.15 shows extinction coefficients at 248 nm, 254 nm, and the absorption maxima as well as thermal stability of some organic onium salts [43].

Table 57.16 lists the quantum yields of some organic photoacid generators obtained from actual photoresist systems.

## 57.6 REACTIVE ION (PLASMA) ETCH RESISTANCE OF PHOTORESIST POLYMERS

Superior reactive ion (plasma) etch resistance of photoresist polymers is crucial to ensuring faithful transfer of the photoresist images into the appropriate substrates. In general, two types of etch chemistries are of particular interest: One is the  $CF_x$  type of chemistry for patterning silicon oxide type of dielectrics. The other is halogen type of etch chemistry for patterning polysilicon. Phenomenological parameters have been proposed to correlate the etch rates of a photoresist polymer to its composition. One such empirical parameter is Ohnishi parameter [46], the other is ring parameter [47] as expressed below.

$$\text{Ohnishi parameter} = N/(N_c - N_o),$$

$$\text{Ring parameter} = M_{cr}/M_{tot},$$

where  $N$ ,  $N_c$ ,  $N_o$  are the total number of atoms, number of carbon atoms, and number of oxygen atoms in a polymer repeat unit.  $M_{cr}$ ,  $M_{tot}$  are the mass of the resist existing as

**TABLE 57.14.** Quantum yields for the photolysis of some aryl iodonium and sulfonium salts [42]<sup>a</sup>.

Onium salt	Products	Excitation wavelength (nm)	
		313	254
$(C_6H_5)_2I^+AsF_6^-$	$C_6H_5I$	0.34	0.39
	$HAsF_6$	0.7	0.65
$(4-t\text{-Butyl-C}_6\text{H}_4)_2I^+AsF_6^-$	$4-t\text{-Butyl-C}_6\text{H}_4I$	0.2	—
$(4-t\text{-Butyl-C}_6\text{H}_4)_2I^+PF_6^-$	$4-t\text{-Butyl-C}_6\text{H}_4I$	0.22	—
$(4-t\text{-Butyl-C}_6\text{H}_4)_2I^+SbF_6^-$	$4-t\text{-Butyl-C}_6\text{H}_4I$	0.22	—
$(C_6H_5)_3S^+AsF_6^-$	$(C_6H_5)_2S$	0.06	0.26
	$HAsF_6$	0.11	0.74
$(4-CH_3O-C_6H_5)_3S^+AsF_6^-$	$(4-CH_3O-C_6H_5)_2S$	0.17	—

<sup>a</sup>Determined in acetonitrile.

**TABLE 57.15.** Optical properties of sulfonium triflate photoacid generators [43].<sup>a</sup>

PAG	$\epsilon$ 248 nm	$\epsilon$ 254 nm	$\epsilon_{\max}(\lambda_{\text{nm}})$	Thermal stability (°C)
TPSOTf	13,302	8,665	3,925 (267), 2,772 (275)	406
SPTOTf	8,314	6,269	5,042 (265), 5,940 (308)	378
DTSOTf	10,075	8,209	19,832 (302)	408
BDSOTf	24,469	17,080	16,023 (271), 18,077 (278), 18,171 (290), 17,779 (319.5)	406
TASOTf	12,416	9,176	10,801 (9,299)	398

<sup>a</sup>In methanol.

Note: TPSOTf, triphenylsulfonium triflate; SPTOTf, S-phenylthioanthrylsulfonium triflate; DTSOTf, diphenyl-4-thiophenoxyphenylsulfonium triflate; BDSOTf, bis[4-(diphenylsulfonio)phenyl]sulfide triflate; TASOTf, triarylsulfonium triflate.

**TABLE 57.16.** Quantum yields of photoacid generation in resist systems [44,45].

PAG	Polymer matrix	Base additive	Quantum yields	Reference
DTBPICSA	ESCAP	Yes	0.211	[45]
DTBPICSA	ESCAP	No	0.277	[45]
TPSCSA	ESCAP	Yes	0.237	[45]
Methyl-SP	Novolak	No	0.11	[44]
Ethyl-SP	Novolak	No	0.075	[44]
Propyl-SP	Novolak	No	0.071	[44]
Phenyl-SP	Novolak	No	0.035	[44]
Tolyl-SP	Novolak	No	0.029	[44]
Naphthyl-SP	Novolak	No	0.020	[44]

 Note: DTBPICSA, di-(4-*tert*-butylphenyl)iodonium camphoresulfonate; TPSCSA, triphenylsulfonium camphoresulfonate; Methyl-SP, methanesulfonic acid ester of 1,2,3-trihydroxybenzene (pyrogallol); Ethyl-SP, ethylsulfonic acid ester of 1,2,3-trihydroxybenzene (pyrogallol); Propyl-SP, propylsulfonic acid ester of 1,2,3-trihydroxybenzene (pyrogallol); Methyl-SP, phenylsulfonic acid ester of 1,2,3-trihydroxybenzene (pyrogallol); Tolyl-SP, toluenesulfonic acid ester of 1,2,3-trihydroxybenzene (pyrogallol); Naphthyl-SP, naphthalenesulfonic acid ester of 1,2,3-trihydroxybenzene (pyrogallol).

**TABLE 57.17.** Relative etch rates of selected cyclic olefin-based 193 nm photoresist polymers [48].

Polymer	LD PSi	HD PSi	Oxide
IBM V2 Methacrylate	1.98	1.71	2.33
IBM V3 Methacrylate	1.45	1.3	1.94
IBM Cyclic olefin polymer 1	1.48	1.62	1.15
IBM Cyclic olefin polymer 2	1.33	1.46	1.02
IBM Apex-E 248 nm resist	1.35	1.23	1.36
SPR-510L i-Line resist	1	1	1

 Note: LD PSi, low-density polysilicon etch, Cl<sub>2</sub>/HBr etch chemistry (158 m Torr); HD PSi, high-density polysilicon etch, Cl<sub>2</sub>/HBr etch chemistry (10 mTorr); Oxide, high-density oxide etch, C<sub>2</sub>F<sub>6</sub> etch chemistry (5 mTorr).

carbon atoms contained in a ring and total resist mass, respectively. Correlations of these parameters with experiment results suggest that incorporating more carbon atoms, particularly in a ring form, would enhance etch resistance. In Tables 57.17–57.19, the etch rates of photoresist polymers are expressed as ratios to reference polymers/photoresists. The lower the ratio, the higher the etch resistance of the photoresist polymer (Tables 57.20 and 57.21).

**TABLE 57.18.** Relative etch rates of methacrylate-based 193 nm photoresist polymers [49].

Polymer	CF <sub>4</sub>	Ar	Cl <sub>2</sub>	Cl <sub>2</sub> /HBr
Novolak	1	1	1	1
PMMA	1.4	2	2.5	—
MLMA-MAdMA	1.1	1.2	1.3	1.4

Note: MLMA-MAdMA=mevalonic lactone methacrylate (MLMA), 2-methyl-2-adamantane methacrylate (2-MAdMA) copolymer, (51:49).

**TABLE 57.19.** Relative etch rates of 193 nm cyclic olefin-maleic anhydride copolymer [50].

Polymer	Oxide etch (CHF <sub>3</sub> )	Polysilicon etch (Cl <sub>2</sub> )	Metal etch (SF <sub>6</sub> )
i-line resist	1.00	1.00	1.00
248 nm resist	1.13	1.33	1.71
Poly(HNC/BNC/NC/MA)	1.00	1.35	1.07

 Note: Poly (HNC/BNC/NC/MA)=copolymer of 2-hydroxyethyl- 5-norbornene-2-Carboxylate (HNC), *t*-butyl- 5-norbornene-2-Carboxylate (BNC) 5-norbornene-2-carboxylic acid (NC), maleic anhydride (MA).

**TABLE 57.20.** Reactive ion etch rates and selectivity of 157 nm photoresist polymers [27].

Polymer	Oxide etch rate (nm/s)	Oxide etch selectivity	Polysilicon etch rate (nm/s)	Polysilicon etch selectivity
60:40 HOST/TBA	0.86	7.1	0.71	4.0
60:40 HFIP/TBA	1.34	4.5	1.01	2.6
70:30 HFIP/MOM	1.11	5.5	0.72	4.0
70:30 HFIP/BOM	0.89	6.8	0.62	4.6
Thermal oxide	6.05	1.0	0.13	22.6
Amorphous silicon	0.60	10.2	2.85	1.0

**TABLE 57.21.** Relative etch rate of fluorinated polymers [51].

Polymer	$\alpha_{157\text{ nm}}(\mu\text{m}^{-1})$	Cl <sub>2</sub> Etch rate (nm/min)	CF <sub>x</sub> Etch Rate (nm/min)
p(STHFA)	3.6	147	89
ESCAP (69:31)	6.9	132	54
PF-ESCAP	4.0–4.2	165	76
PF2-ESCAP	3.2–3.6	183	75
PF-APEX (50:50)	4.3	—	—
PHOST	—	100	49
SiO <sub>2</sub>	—	22	287

## REFERENCES

1. SIA *International Technology Roadmap for Semiconductors*; International Sematech: Austin, Texas, 2004.
2. Dammel, R. *Diazonaphthoquinone-Based Resists*; SPIE Press: Bellingham, Washington, USA, 1993.
3. Macdonald, S. A.; Willson, C. G.; Frechet, J. M. J. *Accounts of Chemical Research* **1994**, *27*, 151.
4. Reichmanis, E.; Thompson, L. F. *Chem. Rev.* **1989**, *89*, 1273.
5. Willson, C. G. In *Introduction to Microlithography, 2nd ed.*, Thompson, L. F., Willson, C. G., Bowden, M. J., Eds.; American Chemical Society: Washington, DC, 1994, pp. 139–258.
6. Ito, H. *Adv. Polym. Sci.* **2005**, *172*, 37–245.
7. Frechet, J. M. J.; Willson, C. G.; Ito, H. *Proceedings of Microcircuit Engineering* **1982**, 260.
8. Ito, H.; Willson, C. G.; Frechet, J. M. J. *Digest of Technical Papers of 1982 Symposium on VLSI Technology* **1982**, P86.
9. Ito, H. *Advances in Polymer Science* **2005**, *172*, 37–245.
10. Kunz, R. In *Physical Properties of Polymers*; Mark, J. E., Ed.; Springer: New York 1995, pp. 637–642.
11. Allen, R. D.; Wallraff, G. M.; Hinsberg, W. D.; Conley, W. E.; Kunz, R. R. *Solid State Technology* **1993**, *36*, 53.
12. Nozaki, K.; Kaimoto, Y.; Takahashi, M.; Takechi, S.; Abe, N. *Chemistry of Materials* **1994**, *6*, 1492–1498.
13. Nozaki, K.; Watanabe, K.; Namiki, T.; Igarashi, M.; Kuramitsu, Y.; Yano, E. *Japanese Journal of Applied Physics Part 2-Letters* **1996**, *35*, L528–L530.
14. Nozaki, K.; Yano, E. *Journal of Photopolymer Science and Technology* **1998**, *11*(3), 493–498.
15. Okoroanyanwu, U.; Shimokawa, T.; Byers, J.; Medeiros, D.; Willson, C. G.; Niu, Q. J.; Frechet, J. M. J.; Allen, R. *Proceedings of the SPIE—The International Society for Optical Engineering* **1997**, *3049*, 92–103.
16. Wallow, T. I.; Houlihan, F. M.; Nalamasu, O.; Chandross, E. A.; Neenan, T. X.; Reichmanis, E. *Proceedings of the SPIE—The International Society for Optical Engineering* **1996**, *2724*, 355–364.
17. Kunz, R. R.; Bloomstein, T. M.; Hardy, D. E.; Goodman, R. B.; Downs, D. K.; Curtin, J. E. *Journal of Vacuum Science and Technology B* **1999**, *17*, 3267–3272.
18. Crawford, M. K.; Feiring, A. E.; Feldman, J.; French, R.; Periyasamy, M.; Schadt, F. L.; Smalley, R. J.; Zumsteg, F. C.; Kunz, R.; Rao, V.; Liao, L.; Holl, S. In *Proceedings of the SPIE—The International Society for Optical Engineering: Advances in Resist Technology and Processing XVii*; Houle, F., Ed.; SPIE: 2000; Vol. 3999, p. 357.
19. Chiba, T.; Hung, R. J.; Yamada, S.; Trinque, B.; Yamachika, M.; Brodsky, C.; Patterson, K.; Vander Heyden, A.; Jamison, A.; Shang-Ho, L.; Somervell, M.; Byers, J.; Conley, W.; Willson, C. G. *Journal of Photopolymer Science and Technology* **2000**, *13*(4), 657–664.
20. Dammel, R. R.; Sakamuri, R.; Romano, A.; Vicari, R.; Hacker, C.; Conley, W.; Miller, D. *Proceedings of the SPIE—The International Society for Optical Engineering* **2001**, *4345*, pt.1–2, 350–360.
21. Ito, H.; Wallraff, G. M.; Brock, P.; Fender, N.; Truong, H.; Breyta, G.; Miller, D. C.; Sherwood, M. H.; Allen, R. D. *Proceedings of the SPIE—The International Society for Optical Engineering* **2001**, *4345*, pt.1–2, 273–284.
22. Kunz, R. R.; Sinta, R.; Sworin, M.; Mowers, W. A.; Fedynshyn, T. H.; Liberman, V.; Curtin, J. E. *Proceedings of the SPIE—The International Society for Optical Engineering* **2001**, *4345*, pt.1–2, 285–295.
23. Ito, H.; Truong, H. D.; Okazaki, M.; Miller, D. C.; Fender, N.; Breyta, G.; Brock, P. J.; Wallraff, G. M.; Larson, C. E.; Allen, R. D. *Proceedings of the SPIE—The International Society for Optical Engineering* **2002**, *4690*, 18–28.
24. Trinque, B. C.; Chiba, T.; Hung, R. J.; Chambers, C. R.; Pinnow, M. J.; Osburn, B. P.; Tran, H. V.; Wunderlich, J.; Hsieh, Y. T.; Thomas, B. H.; Shafer, G.; DesMarteau, D. D.; Conley, W.; Willson, C. G. *Journal Of Vacuum Science and Technology B* **2002**, *20*, 531–536.
25. Trinque, B. C.; Osborn, B. P.; Chambers, C. R.; Yu-Tsai, H.; Corry, S. B.; Chiba, T.; Hung, R. J.; Tran, H. V.; Zimmerman, P.; Miller, D.; Conley, W.; Willson, C. G. *Proceedings of the SPIE—The International Society for Optical Engineering* **2002**, *4690*, 58–68.
26. Kodama, S.; Kaneko, I.; Takebe, Y.; Okada, S.; Kawaguchi, Y.; Shida, N.; Ishikawa, S.; Toriumi, M.; Itani, T. *Proceedings of the SPIE—The International Society for Optical Engineering* **2002**, *4690*, 76–83.
27. Fedynshyn, T. H.; Mowers, W. A.; Kunz, R.; Sinta, R.; Sworin, M.; Cabral, A.; Curtin, J. E. In *Polymers for Microelectronics and Nanoelectronics*; Lin, Q., Pearson, R. A., Hedrick, J. C., Eds.; American Chemical Society: Washington, DC, 2004; vol. 784, pp. 54–71.
28. Bae, Y. C.; Douki, K.; Yu, T. Y.; Dai, J. Y.; Schmaljohann, D.; Koerner, H.; Ober, C. K. *Chemistry of Materials* **2002**, *14*, 1306–1313.



29. Fedynshyn, T. H.; Kunz, R. R.; Sinta, R. F.; Sworin, M.; Mowers, W. A.; Goodman, R. B.; Doran, S. P. *Proceedings of the SPIE—The International Society for Optical Engineering* **2001**, 4345, pt. 1–2, 296–307.
30. Dammel, R. R.; Sakamuri, R.; Sang-Ho, L.; Rahman, M. D.; Kudo, T.; Romano, A. R.; Rhodes, L. F.; Lipian, J.; Hacker, C.; Barnes, D. A. *Proceedings of the SPIE—The International Society for Optical Engineering* **2002**, 4690, 101–109.
31. Allen, R. D.; Chen, K. J. R.; Gallagher-Wetmore, P. M. *Proceedings of the SPIE—The International Society for Optical Engineering* **1995**, 2438, 250–260.
32. Barclay, G. G.; Hawker, C. J.; Ito, H.; Orellana, A.; Malenfant, P. R. L.; Sinta, R. F. *Macromolecules* **1998**, 31, 1024–1031.
33. Thackeray, J. W.; Orsula, G. W.; Denison, M. *Proceedings of the SPIE—The International Society for Optical Engineering* **1994**, 2195, 152–163.
34. Lin, Q.; Simons, J. P.; Angelopoulos, M.; Sooriyakumaran, R. *Proceedings of the SPIE—The International Society for Optical Engineering* **2002**, 4690, 410–418.
35. Padmanaban, M.; Kinoshita, Y.; Kudo, T.; Lynch, T.; Masuda, S.; Nozaki, Y.; Okazaki, H.; Pawlowski, G.; Przybilla, K. J.; Roeschert, H.; Spiess, W.; Suehiro, N.; Wengenroth, H. *Proceedings of the SPIE—The International Society for Optical Engineering* **1994**, 2195, 61–73.
36. Barclay, G. G.; King, M.; Orellana, A.; Malenfant, P. R. L.; Sinta, R.; Malmstrom, E.; Ito, H.; Hawker, C. J. In *Organic Thin Films* 1998; vol. 695, pp. 360–370.
37. Ito, H. *IBM Journal of Research and Development* **2001**, 45, 683–695.
38. Toukhy, M. A.; Oberlander, J.; Rahman, D.; Houlihan, F. M. *Proceedings of the SPIE—The International Society for Optical Engineering* **2004**, 5376 (1), 384–391.
39. Dabbagh, G.; Houlihan, F. M.; Ruskin, I.; Hutton, R. S.; Nalamasu, O.; Reichmanis, E.; Gabor, A. H.; Medina, A. N. *Proceedings of the SPIE—The International Society for Optical Engineering* **1999**, 3678, pt. 1–2, 86–93.
40. Rushkin, I. L.; Houlihan, F. M.; Kometani, J. M.; Hutton, R. S.; Timko, A. G.; Reichmanis, E.; Nalamasu, O.; Gabor, A. H.; Medina, A. N.; Slater, S. G.; Neisser, M. *Proceedings of the SPIE—The International Society for Optical Engineering* **1999**, 3678, pt. 1–2, 44–50.
41. Singh, L.; Ludovice, P. J.; Henderson, C. L. *Proceedings of the SPIE—The International Society for Optical Engineering* **2005**, 5753, 319.
42. Crivello, J. V. *Advances in Polymer Science* **1984**, 62, 2–48.
43. Cameron, J. F.; Adams, T.; Orellana, A. J.; Rajaratnam, M. M.; Sinta, R. F. *Proceedings of the SPIE—The International Society for Optical Engineering* **1997**, 3049, 473–484.
44. Ueno, T.; Schlegel, L.; Hayashi, N.; Shiraishi, H.; Iwayanagi, T. *Polymer Engineering and Science* **1992**, 32, 1511–1515.
45. Cameron, J.; Fradkin, L.; Moore, K.; Pohlers, G. In *Proceedings of the SPIE—The International Society for Optical Engineering*; Houlihan, F., Ed., 2000; vol. 3999, pt. 1–2, pp. 190–203.
46. Gokan, H.; Esho, S.; Ohnishi, Y. J. *Electrochem. Soc.* **1983**, 130, 143.
47. Kunz, R.; Palmateer, S. C.; Forte, A. R.; Allen, R.; Wallraff, G.; DiPietro, P. A.; Hofer, D. *Proceedings of the SPIE—The International Society for Optical Engineering* **1996**, 2724, 365–376.
48. Wallow, T.; Brock, P.; DiPietro, R.; Allen, R.; Opitz, J.; Sooriyakumaran, R.; Hofer, D.; Meute, J.; Byers, J.; Rich, G.; McCallum, M.; Schuetze, S.; Jayaraman, S.; Hullihen, K.; Vicari, R.; Rhodes, L.; Goodall, B.; Shick, R. *Proceedings of the SPIE—The International Society for Optical Engineering* **1998**, 3333, pt. 1–2, 92–101.
49. Dammel, R. R.; Ficner, S.; Oberlander, J.; Klauck-Jacobs, A.; Padmanaban, M.; Khanna, D. N.; Durham, D. L. *Proceedings of the SPIE—The International Society for Optical Engineering* **1998**, 3333, pt. 1–2, 144–151.
50. Jung, J. C.; Bok, C. K.; Baik, K. H. *Proceedings of the SPIE—The International Society for Optical Engineering* **1998**, vol. 3333, pt. 1–2, 11–25.
51. Fender, N.; Brock, P. J.; Chau, W.; Bangsaruntip, S.; Mahorowala, A.; Wallraff, G. M.; Hinsberg, W. D.; Larson, C. E.; Ito, H.; Breyta, G.; Burnham, K.; Truong, H.; Lawson, P.; Allen, R. D. *Proceedings of the SPIE—The International Society for Optical Engineering* **2001**, vol. 4345, pt. 1–2, 417–427.

## CHAPTER 58

# Pyrolyzability of Preceramic Polymers

Yi Pang<sup>†</sup>, Ke Feng<sup>‡</sup>, and Yitbarek H. Mariam

*Department of Chemistry & Center for High Performance Polymers and Composites, Clark Atlanta University,  
Atlanta, GA 30314*

---

<b>58.1</b>	Introduction .....	981
<b>58.2</b>	Pyrolyzability .....	982
<b>58.3</b>	Latent Reactivity, Ceramic Yield, and Density Changes .....	984
<b>58.4</b>	Silicon Carbide (SiC) and Silicon Nitride (Si <sub>3</sub> N <sub>4</sub> ) .....	984
<b>58.5</b>	Pyrolysis Data on SiC and Si <sub>3</sub> N <sub>4</sub> Precursors .....	985
<b>58.6</b>	Pyrolysis on Some Boron-Containing Precursors .....	999
<b>58.7</b>	Conversion Studies, Uses, and Applications .....	1001
<b>58.8</b>	Summary .....	1001
	Acknowledgments .....	1002
	References .....	1002

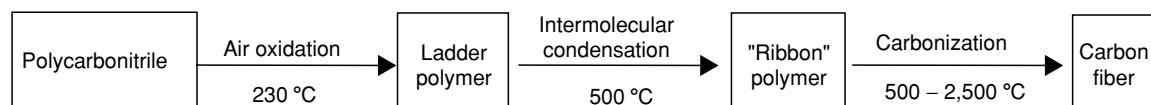
---

### 58.1 INTRODUCTION

Ceramic materials encompass a range of compounds such as silicates, carbides, nitrides, borides, oxides, sulfides, etc. Some of these materials have excellent mechanical properties under heavy stress, outstanding electrical properties, and exceptional resistance to high temperatures and corrosive environments. Such materials are generally known as high-technology ceramics/materials materials and it is because of their potential uses as engineering and structural materials that high-technology ceramics had gained intense interest in industry, government, and academia since early 1970s [1].

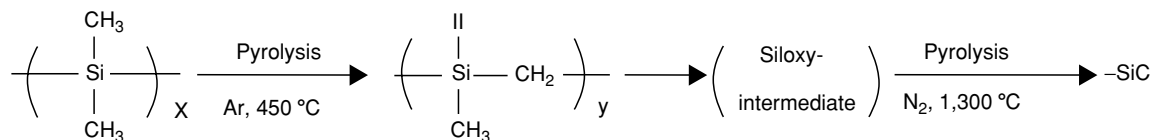
The potential uses cannot be fully realized, however, if the methods of preparation and/or fabrication of the

materials have shortcomings and/or defects and are not economically feasible. This indeed had been true in the case of traditional methods of preparing ceramics which almost invariably required extremely high temperatures [2]. Fortunately, new and unconventional preparative methods have been developed since the mid-1970s as the result of Yajima *et al.*'s work, which led to the fabrication of silicon carbide (SiC) fibers based on the polysilane to polycarbosilane (PCS) transformation technology [3]. In such a transformation, a metalorganic polymer may be converted to a ceramic, and the transformation is not unlike that for the preparation of carbon fibers, which can be summarized as shown below [4,5]



<sup>†</sup>Department of Chemistry, The University of Akron, Akron, OH 44325. <sup>‡</sup>Ticonia, 8040 Dixie Highway, Florence, KY 41042

whereas the Yajima *et al.* technology can be represented as [5]



The Yajima *et al.* process [3] possesses general applicability to the preparation of ceramic materials from polymeric and oligomeric precursors via pyrolysis. In some cases even monomeric units can be used as precursors. Thus, the invention of the Yajima *et al.* process [3] has generated tremendous research activities in the synthesis of precursors and their pyrolytic conversion to ceramic powders and/or fibers, leading to the fields of what generally are known now as “preceramic polymer chemistry” and “polymer pyrolysis technology” [1,6].

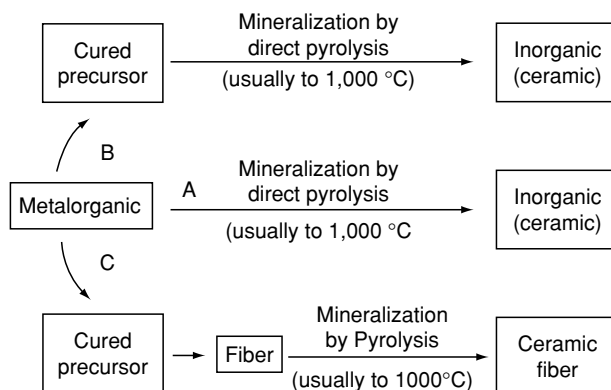
The polymer pyrolysis technology has several advantages over the conventional methods and some of these include the ability to purify precursors at low cost; lower processing temperature; versatility of precursors to form complex shapes, films, fibers, etc; the opportunity to prepare novel materials such as ceramic–ceramic and ceramic–metal composites and modify chemical, physical, optical, mechanical, and electrical properties; and at least some ability to control grain size, microstructure, and crystallinity, thereby allowing densification at temperature lower than traditional processing temperatures.

Early work in the polymer pyrolysis technology area focused on the synthesis of preceramic polymers [7]

with various elemental compositions and their pyrolytic conversion to ceramics. More recent work has, however, focused on the detailed studies of the precursor-to-ceramic conversion processes including amorphous to crystal transitions by several techniques. Despite the tremendous amount of work that has been accomplished in this area, the scope of this review will focus on pyrolyzability of precursors that lead to SiC and Si<sub>3</sub>N<sub>4</sub> ceramics as judged primarily by the amount of ceramic product, but consideration of the extent of impurity such as free carbon, free silicon, and oxygen is also made.

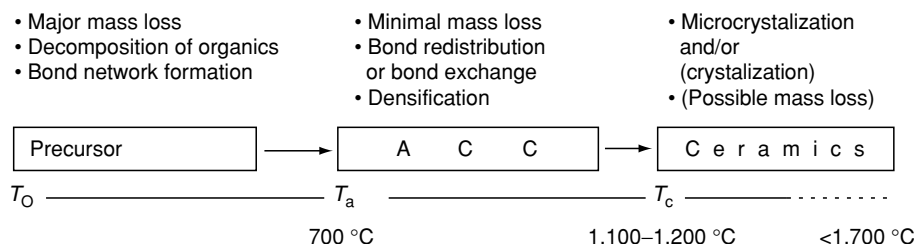
## 58.2 PYROLYZABILITY

For the purposes of this review, pyrolyzability is defined as mineralizability, and the mineralization (from metalorganic to inorganic) can be in one of the three general ways (the term metalorganic will be used in this review as opposed to organometallic, since the latter is usually used to mean M–C (metal–carbon) bond [8]) presented below schematically (Scheme 58.1).



Whatever route is used, one of these three or any other similar ones, the transformation from metalorganic precursors to the final inorganic product can be roughly divided

into three major stages spanning temperature ranges of a few hundred degrees each as shown in the following scheme (Scheme 58.2).



The first stage ( $T_o - T_a$ ) can generally be up to 700 °C. This is a stage where a major mass loss occurs and can roughly be divided into two regions: below 400 °C and 400–700 °C. Below about 400 °C, cleavage of weak bonds such as Si–H, vinylic; Si–Si, N–H, and accompanying reactions will take place. In the range 400–700 °C, strong bonds such as C–C, C–N, Si–N, Si–C, and C–H will be affected. The exact nature of the reaction will depend on the type of functional group constituting the precursors and the method and/or approach of curing used. Typically, oxidative, thermal, and UV curing are undertaken. In some cases catalysts and free-radical initiators are used. Depending on which approach is taken, the type of reaction that is effected may be rather complex. Overall, what takes place in the first stage of the pyrolysis will include, but not be limited to, bond breaking and formation, cross-linking reaction, skeletal bond network formation and bond rearrangement, decomposition/fragmentation, and volatilization of organics. Significant changes in the atomic ratio of the starting material and density changes should also take place.

The second stage ( $T_a - T_c$ ) can cover from roughly 700 °C to about 1,100–1,200 °C. This is a region of minimal mass loss and the material can be described as a disordered

solid. Soraru, Babonneau, and Mackenzie [9] have described the materials in this temperature range as a “new family of noncrystalline solids” and have coined the term “amorphous covalent ceramics (ACC)” to describe the high degree of covalency of carbides and nitrides. As alluded to before, there is minimal mass loss in the range  $T_a - T_c$ . Figure 58.1 shows the thermogravimetric analysis (TGA) curve for a precursor prepared from dichloromethylvinylsilane and ethylenediamine (vide infra, Section 58.5.3). In the TGA experiment, the material was heated to 700 °C, held at 700 °C for 1 h, and then further heated to 1,000 °C (Fig. 58.1). There was only about 2 wt% loss between 700 and 1,000 °C compared to 31 wt% between 400 and 700 °C and about 8 wt% below 400 °C (at least some of which can be accounted for by loss of solvent and low-molecular-weight products) for a total of 39 wt%. The solid-state  $^{29}\text{Si}$ NMR spectra of three samples of the precursor pyrolyzed in a furnace at 400, 700, and 900 °C for 1 h in  $\text{N}_2$  are also shown in the inset. The chemical shifts, assignments, and the percentage composition of each component (determined by NMR) are indicated in Fig. 58.1.

The spectral data clearly show that even though the weight loss is minimal in the 700–1,000 °C range, there

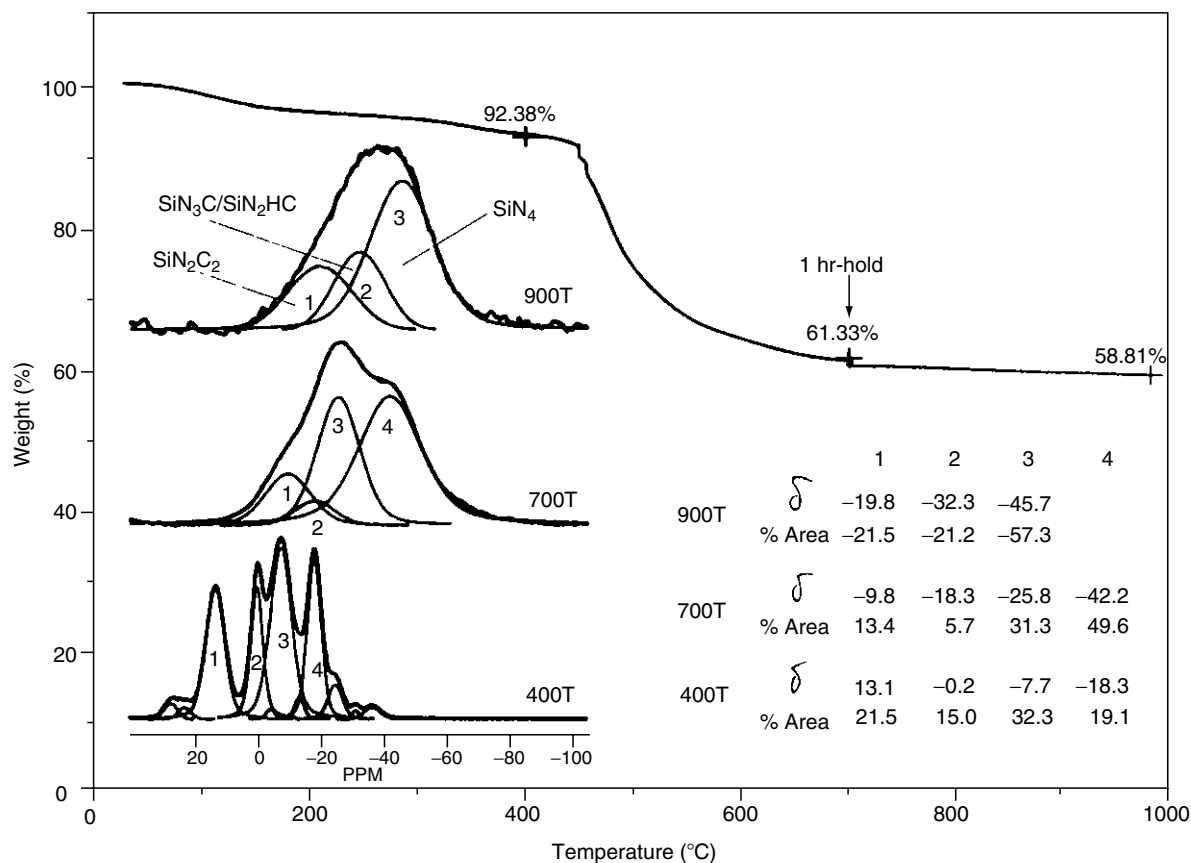


**FIGURE 58.1.** (A) TGA profile (5 °C/min,  $\text{N}_2$ ) of poly(methylvinylsilyl)ethylenediamine (see Ref. [194] for structure). (B) 39.7 MHz  $^{29}\text{Si}$  CP/MAS spectra with simulations of samples 400T, 700T, and 900T. [Heating schedules for samples 400T, 700T, and 900T were 5 °C/min (in  $\text{N}_2$ ) from room temperature (RT) to 400, 700, and 900 °C, respectively, a 1 h-hold at the respective temperature, and furnace cooling (at approx. 100 °C/h) to RT].  $\delta$  (chemical shift) is in ppm relative to external tetramethylsilane.

are clear indications for chemical transformations such as Si–C–N→Si–N–C taking place. While there are not enough data in the literature to ascertain that this kind of chemical transformation does take place in every case, it can be generally assumed that the weight loss is minimal, in most cases, in the  $T_a - T_c$  range.

Finally, above  $T_c$ , a given ceramic product may remain amorphous or in microcrystalline form. In some, and perhaps most, cases crystallization will take place. The final product and its physical characteristics will differ and depend on the nature of the starting material as well as on the processing atmosphere and temperature. For example, Nicalon, which is nearly amorphous, contains 61% SiC, 28% SiO<sub>2</sub>, and 10% free carbon [10]. Some precursors give excess free carbon or free silicon. Such impurities usually hinder crystallization and may bring problems of oxidation at high temperature in wet air [11a], e.g.,  $\text{Si}_3\text{N}_4 + \text{O}_2 \rightarrow \text{SiO}_2 + \text{N}_2$ . Additionally, decomposition reactions are possible in some cases. For example, if Si<sub>3</sub>N<sub>4</sub> is formed along with free carbon, the reaction  $\text{Si}_3\text{N}_4 + 3\text{C} \rightarrow 43\text{SiC} + 2\text{N}_2(\text{gas})$  has been observed above 1,450 °C in Ar [11b]. Similarly, the presence of SiO<sub>2</sub> and excess Si and C along with SiC may lead to reactions such as [12] (i)  $3\text{Si} + 2\text{N}_2 \rightarrow \text{Si}_3\text{N}_4$ ; (ii)  $3\text{SiO}_2 + 6\text{C} + 2\text{N}_2 \rightarrow \text{Si}_3\text{N}_4$ ; (iii)  $\text{SiC} + \text{CO} \rightarrow \text{SiO} + 2\text{C}$ ; and maybe even (iv)  $2\text{CO} \rightarrow \text{CO}_2 + \text{C}$ .

Oxygen impurities are sometimes introduced by inadvertent hydrolysis or during oxidative curing. The presence of oxygen has been shown, experimentally, to lower thermal stability especially when the weight% content of oxygen is greater than about 1.4 [13].

### 58.3 LATENT REACTIVITY, CERAMIC YIELD, AND DENSITY CHANGES

Most Si-containing ceramics have densities between 2.5 and 3.5 g ml<sup>-1</sup>, which are significantly higher than their precursors ( $\sim 1 \text{ g ml}^{-1}$ ). For a pyrolytic process of no mass loss (100% ceramic yield), transformation from a precursor to the densified ceramics will bring about 70% volume change. In reality, the pyrolytic conversion of precursors to ceramic materials involves additional volume changes as extraneous organic ligands are removed as gaseous products. This process may, and often does, create porosity/voids and densification-induced stress [14]. If problems associated with porosity/voids and densification are to be minimized the ceramic yield (=weight of ceramic residue  $\times$  100/weight of pyrolysis charge) should be in an acceptable range of 60–75% or greater. The lower the quantity of gases evolved, the higher the ceramic yield [15]. Cracking and/or rupture of the ceramic product can happen especially if the gases are released in a narrow range of temperatures [15]. The pyrolyzability of a given precursor should then be considered from a practical point of view of

whether the precursor gives the desired composition and with reasonably high yield (low yield can sometimes be tolerated if the ceramic product is pure and the porosity generated during pyrolysis has open porosity so that the pyrolysis gases can escape [15]). A precursor should, therefore, have at least two inherent characteristics: latent reactivity and branched structures. The latent reactivity can provide the opportunity for cross-linking and thereby provide for both maintaining appropriate shape during processing and high ceramic yield. Linear polymers generally give low ceramic yield due to backbone reactions, which lead to volatiles. Branched structures can, however, slow backbone reactions by sterically hindered structures that require multiple bond ruptures [8,15]. The branching should not, however, be too extensive so as to restrict chain mobility that may lead to poor mechanical property. In the case of linear structures, linkages such as Si–Si can lead to cross-linking after UV radiation treatment. The capacity of a given precursor to give the desired product in reasonable yield also depends on the molecular weight of the precursor [16] (at least in some cases), the curing and pyrolysis condition [temperature and atmosphere (inert versus reactive gas)], heating rate, etc.

### 58.4 SILICON CARBIDE (SiC) AND SILICON NITRIDE (Si<sub>3</sub>N<sub>4</sub>)

SiC and Si<sub>3</sub>N<sub>4</sub> are two of the most studied nonoxide ceramic materials derived from metalorganic precursors (others include BN, B<sub>4</sub>C<sub>3</sub>, and AlN). The conventional methods of preparation of Si<sub>3</sub>N<sub>4</sub> powder are [2(a)] (a) nitridation of silicon (at 1,200–1,450 °C),  $3\text{Si} + 2\text{N}_2 \rightarrow \text{Si}_3\text{N}_4$ ; (b) carbothermic reduction of silica (at 1,200–1,450 °C),  $3\text{SiO}_2 + 6\text{C} + 2\text{N}_2 \rightarrow \text{Si}_3\text{N}_4 + 6\text{CO}$ ; (c) gas-phase ammonolysis of silicon tetrachloride,  $3\text{SiCl}_4 + 4\text{NH}_3 \rightarrow \text{Si}_3\text{N}_4 + 12\text{HCl}$ ; (d) thermal decomposition of silicon diimide,  $3\text{Si}(\text{NH})_2 \rightarrow \text{Si}_3\text{N}_4 + 2\text{NH}_3$ . On the other hand, SiC can be prepared by the high-temperature (2,600 °C) reaction between silicon dioxide and graphite [17],  $\text{SiO}_2 + \text{C} \rightarrow \text{SiC} + \text{CO}$ . Both Si<sub>3</sub>N<sub>4</sub> and SiC prepared by the conventional methods are expected to be infusible, intractable, and not applicable for the preparation of fibers and films. The structure of SiC is based on the diamond structure with both Si and C tetrahedral and with alternating Si and C atoms [18]. The basic structural types (polymorphs) are thus hexagonal  $\alpha$ -SiC and cubic  $\beta$ -SiC. As opposed to diamond, SiC has many crystalline  $\alpha$ -SiC modifications called polytypes, and approximately 200 polytypes have been determined [18]. Similarly, Si<sub>3</sub>N<sub>4</sub> is found to have two crystalline forms ( $\alpha$  and  $\beta$  forms), and in both structures each silicon atom is tetrahedrally bonded to four nitrogens [19]. Both SiC [20] and Si<sub>3</sub>N<sub>4</sub> [21] can be used as tough and refractory materials.

### 58.5 PYROLYSIS DATA ON SiC AND Si<sub>3</sub>N<sub>4</sub> PRECURSORS

The pyrolyzability of a fair number of SiC, Si<sub>3</sub>N<sub>4</sub>, and Si<sub>3</sub>N<sub>4</sub>/SiC precursors are examined in various tables below. Data included in the tables are the approximate structures/representations of the precursors, the pyrolysis conditions, and the compositions of the residues. The precursors are grouped together so that direct comparisons can easily be made. Thus, the tables should be, to some extent at least, self-explanatory. In some selected cases, specific curing, and/or other treatments are also indicated in the tables to illustrate the effects of those treatments. In those cases where curing and/or other treatments, ceramic yields, and pyrolysis conditions are not indicated, it generally means either none was done or the relevant information was not available. In all the tables P and Y denote, respectively, pyrolysis conditions (temperature/atmosphere) and ceramic yield (as in Table 58.1). In a number of cases, the compositions of the residues are not given in detail. This is either indicated by NDG (no details given) or left blank and the original publication can be consulted for additional information.

#### 58.5.1 SiC Precursors

Metalorganic precursors for SiC include polysilanes, polycarbosilanes, silicon-acetylene and silicon-olefin poly-

mers, polysiloxanes, polysilsesquioxanes, and polydisilylanes. Polysilanes are generally converted to a polycarbosilane by thermal, oxidative, and UV radiation curing. UV radiation curing is used sometimes to convert polysilanes to SiC directly. Lack of space here does not allow us to cover all the synthetic aspects of SiC precursors. These are, however, excellent reviews that deal with the synthetic aspects, uses, and applications as well as characterization in some cases [1,7,14,22–31]. These and the original publications can thus be consulted for further details. In some cases, the precursors have been modified to incorporate metals such as titanium to prepare precursors such as polytitanocarbosilane [32,33]. These are also not covered here in any detail. There are a number of elegant works dealing with the direct synthesis of polycarbosilanes for which the reviews cited and the original publications can be consulted.

#### Polysilanes

Entries (1)–(6) in Table 58.1 compare polydimethylsilane (PDMS) [5,34,35] with other polysilanes. West and coworkers [35] have actually reported a fairly large number of polysilanes although thermal analysis data are not always reported on them. Abu-eid, King, and Kotliar [41] have investigated polyorganosilanes of the type [R<sub>1</sub>R<sub>2</sub>Si], where R<sub>1</sub>=CH<sub>3</sub> and R<sub>2</sub>=H, C<sub>2</sub>H<sub>5</sub>, etc. The yields were <25% (at 750 °C), except for the case R<sub>2</sub> = H

**TABLE 58.1.** Pyrolysis data on polysilane precursors: Comparison of PDMS with other polysilanes.

Precursors	Pyrolysis condition, yield, and composition			References
	P <sup>a</sup>	Y <sup>b</sup>	Residue and impurities	
(1) Polydimethylsilane (PDMS): —Si(Me) <sub>2</sub> — (T=400 °C) <sup>c</sup>	a		SiC; NDG	[5,34,35]
(2) Polysilastyrene (UV) <sup>d</sup>	a	30	SiC; NDG	[35–37]
(3) Polysilastyrene (T=500 °C) <sup>c</sup>	b	68	SiC; C (30°)	[36,37]
(4) —(SiMe <sub>2</sub> )—	c	1	SiC; C	[38,39]
(5) —(PhSiMe)—	c	24.6	SiC; C	[39]
(6) —[(C <sub>6</sub> H <sub>13</sub> )SiMe]—	c	5.8	SiC; C	[39]
(7) PDMS + B(OR) <sub>3</sub> (cat., 380–400 °C) <sup>e</sup>	d	63–80		[40]
(8) PDMS+PBDBS (cat., 340 °C) <sup>e</sup>			NDG	[44]
(9) PDMS→“SiC” fiber			SiC; <2%O	[46]
(10) PDMS→PCS fiber→SiC fiber	e	60–65	SiC	[47]
(11) PDMS→PCS	e	58–87	SiC, O	[48]
(12) PDMS (T=4000 °C) <sup>c</sup>	e	60	β-SiC; C, O?	[34]
(13) Yajima <i>et al.</i> 's PCS	f	42	SiC (83%); C (14.5%), SiO <sub>2</sub> (2%)	[49]
(14) Yajima <i>et al.</i> 's PCS	g	54	Si <sub>3</sub> N <sub>4</sub> ; C (4.5%), SiO <sub>2</sub> (8.4%),	[49]
(15) Nicalon SiC-based fibers, NG 100		NI <sup>f</sup>	SiC, SiC <sub>2</sub> O <sub>2</sub> , SiO <sub>4</sub> C <sub>graph</sub> <sup>g</sup> (35%)	[50]
(16) Nicalon SiC-based fibers, NG 200		NI	SiC, SiC <sub>2</sub> O <sub>2</sub> , SiCO <sub>3</sub> , SiO <sub>4</sub> C <sub>graph</sub> (19%)	[50]
(17) Polytitanocarbosilance	h	75	SiC/TiC, C, O (SiC <sub>4-x</sub> O <sub>x</sub> )	[32,33]

<sup>a</sup>Pyrolytic conditions: a, >800 °C; b, 1,500 °C/Ar; c, 1,000 °C/Ar; d, 900 °C; e, 1,300 °C/Ar or vacuum; f, 1,350 °C/Ar; g, 1,350 °C/(Ar/NH<sub>3</sub>: 70/30); h, 840 °C.

<sup>b</sup>Yield in wt% of residue recovered at the pyrolysis condition.

<sup>c</sup>Precursors were heat-treated at the temperatures indicated before being pyrolyzed.

<sup>d</sup>Precursors were UV irradiated before being pyrolyzed.

<sup>e</sup>Precursors were treated with a catalyst at the indicated temperatures before being pyrolyzed.

<sup>f</sup>NI denotes “not indicated.”

<sup>g</sup>C<sub>graph</sub> denotes graphite.

(yield = 60%) [41]. A report by Sinclair [5] on polysilastyr-ene indicated a ceramic yield of 63% at 500 °C when UV cured. Copolymers and terpolymers reported by Carlesson and coworkers [39] are not included here because of space limitation. Unlike PDMS, which requires some sort of curing, conversion to an intermediate carbosilane polymer is unnecessary in the case of polysilastyr-ene [42] and vinylic silane,  $\text{Me}_3\text{Si}-(\text{MeSiH})_x-(\text{MeSiVi})-\text{SiMe}_3$  (Vi denotes vinyl), which gives mostly SiC in 72% yield (1,000 °C/inert gas) after cross-linking with 6% dicumyl peroxide at 250 °C [43]. Entries (7)–(17) are also based on PDMS. As the examples shown here indicate, PDMS is probably the most studied metalorganic precursor. Entries (7) and (8) are examples of use of catalysts for the conversion of PDMS to PCS without the use of autoclave [40,44]. Catalysts used other than  $\text{B}(\text{OR})_3$  and PBDPS (polyborodiphenylsiloxane [44,45]) are  $\text{MeBN}(\text{SiMe}_3)_2$  [40] and  $\text{B}(\text{NEt}_2)_3$  [40]. Entries (9)–(16) deal with fibers [45–50]. The difference between precursors (15) and (16) is the oxygen content [16% (mass) for NG100 and 11% for NG200 [50]]. The percentage composition of  $\text{SiC}_4(=\text{SiC})$ ,  $\text{Si}_2\text{O}_2$ ,  $\text{SiCO}_3$ ,  $\text{SiO}_4$ , and  $\text{C}_{\text{graph}}$  was 64/65, 9, 12, 15, and 35 for (15) and 78/81, 7, 7,

7, and 19 for (16), respectively, as determined by NMR studies [50].

Several other studies on Nicalon-based ceramic fibers have also been conducted in addition to the investigation of oxidation curing of PCS fibers and effect of oxygen in tensile strength of SiC fibers [51]. Similarly, studies dealing with the chemistry, characterization, modification, use, and applications of polysilanes and polycarbosilane are also available [52].

Data on various other polysilanes are presented in Table 58.2. The vinylic polysilane in entry (1) is that of Schilling's sodium-derived vinylic polysilane [54], the pyrolysis of which had been investigated by Schmidt and coworkers [53]. Fibers were prepared (and investigated [13]) from entries (2)–(4). In the case of entry (4), 1 wt% of PBDPS was added and the oxygen content in the residue was 1.4 wt%. The tensile strength and Young's moduli determination showed that when the oxygen content is > 1.4 or so, the heat resistance property was poor (at about 1,600 and 1,800 °C [13]). DMCS (dodecamethylcyclohexasilane) has also been investigated before for fiber production [58]. The system in entry (5) represents a family of polysilanes

**TABLE 58.2.** Pyrolysis data on polysilane precursors with various structures.

Precursors	Pyrolysis condition, yield, and composition			
	P <sup>a</sup>	Y	Residue and impurities	References
(1) Vinylic polysilane (Schilling's system)	a	57	SiC; C (17%) <sup>0</sup>	[53]
(2) HO-( $\text{Me}_2\text{Si}$ )-OH (AC, 470 °C) <sup>b</sup>	Fiber		SiC; O (0.35%); Si/C=1.35	[13]
(3) [ $\text{Me}_2\text{Si}$ ] <sub>6</sub> (DMCS) (AC, 480 °C) <sup>b</sup>	Fiber		SiC; O(0.2%); Si/C=1.41–1.35	[13]
(4) HO-( $\text{Me}_2\text{Si}$ )-OH+PBDPS (cat., 420 °C) <sup>c</sup>	Fiber		SiC; O (1.4%);	[13]
(5) {RR'Si[(CH <sub>2</sub> ) <sub>r</sub> ] <sub>s</sub> ] <sub>n</sub>	b	18–65	SiC;NDG	[54]
(6) H-(SiMeH)-H	a	77	SiC; O, H,=(Si <sub>1</sub> C <sub>0.9</sub> H<0.2O <sub>0.1</sub> )	[55]
(7) [(MeSiH) <sub>x</sub> (CH <sub>3</sub> Si) <sub>y</sub> ] <sub>n</sub>	c	12–27	SiC (77%); C (23%)	[56]
(8) [(MeSiH) <sub>x</sub> (CH <sub>3</sub> Si) <sub>y</sub> ] <sub>n</sub> (ca.) <sup>b</sup>		71–85	SiC (95%); Si(5%), ZrC/TC (<2%)	56
(9) [(MeSiH) <sub>x</sub> (CH <sub>3</sub> Si) <sub>y</sub> ] <sub>n</sub> (XL) <sup>d</sup>		60	SiC; Si (25.6%)	[56]
(10) Methylpolysilane	d	97 <sup>e</sup>	SiC;81%; SiO <sub>2</sub> : 12%; C: 7%; O: 2%	[57]
(11) Commercial Si-C-O fiber (Nicalon)	d	82	SiC; O (11%)	[57]
(12) -(Si(Me) <sub>2</sub> -C <sub>6</sub> H <sub>4</sub> ) <sub>n</sub> -, n=28		58	SiC; NDG	[59]
(13) Methylpolysilane (MeSi) <sub>x</sub> (RSi) <sub>y</sub> (R'Si) <sub>z</sub>	b	40–60	SiC; O impurity present	[60]
(14) (MeSiH) <sub>0.35</sub> (MeSiPh) <sub>0.4</sub> (MeSi) <sub>0.25</sub>		30 <sup>f</sup>	SiC; O impurity present	[61]
(15) (MeSiH) <sub>0.3</sub> (Me <sub>2</sub> Si) <sub>0.3</sub> (MeSi) <sub>0.4</sub>	f	20 <sup>g</sup>	SiC; O impurity present	[61]
(16)(MeSiH) <sub>0.3</sub> (MeSiPh) <sub>0.7</sub>	f	10 <sup>e</sup>	SiC; O impurity present	[61]
(17) Hydropolysilane	g	19–53	SiC; C (4–40%)	[62]
(18) [(MeSiH) <sub>30</sub> (PhSiMe) <sub>70</sub> ] <sub>n</sub> (I)	f	8.2–13.8	NDG	[63]
(19) [(MeSiH) <sub>25</sub> (PhSiMe) <sub>40</sub> (MeSi) <sub>35</sub> ] <sub>n</sub> (II)	f	8.2–13.8	NDG	[63]
(20) PPMCHS <sup>h</sup>		31	SiC; NDG	[64(a)]
(21) PPMCHS <sup>d</sup>		41	SiC; NDG	[64(a)]
(22) (MeSiH) <sub>x</sub> (CH <sub>2</sub> =CH-SiH) <sub>y</sub>	g		SiC	[64(b)]

<sup>a</sup>Pyrolytic conditions: a, 1,000 °C/N<sub>2</sub>; b, 1,200 °C; c, 950 °C/A; d, 540 °C/He; e, 600–900 °C/N<sub>2</sub>; f, 900 °C/N<sub>2</sub>; g, 1,400 °C/N<sub>2</sub>.

<sup>b</sup>Autoclave (AC) used at temperatures specified.

<sup>c</sup>Catalyst (group-IV metal complexes) used at temperatures specified.

<sup>d</sup>Cross-linked.

<sup>e</sup>Data are for fiber.

<sup>f</sup>When pyrolyzed in air at 900 °C, yield was 100%.

<sup>g</sup>When pyrolyzed in air at 900 °C, yield was 70%.

<sup>h</sup>PPMCHS= poly(permethylocyclohexasilane).

<sup>i</sup>When pyrolyzed in air at 900 °C, yield was 50%.

synthesized and investigated by Schilling [54]. Of the 15 polysilanes studied, the preferred R is Me or H while the preferred R' is vinyl. The polymers that gave the highest ceramic yields (64.5% and 56.6%) were prepared from a mixture of, respectively,  $\text{Me}_3\text{SiCl}/\text{MeSiHC1}_2/\text{CH}_2=\text{CHSiMeC1}_2$  and  $\text{Me}_2\text{SiC1}_2/\text{CH}_2=\text{CHSiMeC1}_2$  in 1.0/0.3/1.0 and 1/1 ratios, respectively [54]. The presence of microcrystalline  $\beta$ -SiC was confirmed by x-ray diffraction for the former system. The precursors can be directly converted to SiC, and impurities in the residue were not reported. The poly(methylsilane) (MPS) of entry (6) is reported [55] to produce near-stoichiometric (with minor H and O impurities), noncrystalline SiC at temperatures that are lower than some cases [55]. Polysilanes of entries (7)–(9) where  $(x + y = 1)$  gave a substantial amount of elemental Si when pyrolyzed. However, use of catalytic quantities of group-IV–metal–organometallic complexes or borate (such as  $\text{B}(\text{OSiMe}_3)_3$ ) resulted in cross-linking processes such that pyrolysis of these polysilanes gave close to stoichiometric SiC (>95 wt%) and only very little elemental Si. Fibers prepared from MPS [57] of entry (10) can be compared to that of entry (11) (with its higher oxygen content). The composition reported was determined using rule of mixtures calculation from elemental analysis data. Ceramic fibers with 2 wt% oxygen contain 80 wt% noncrystalline SiC having 2 nm crystallite size in a continuous glassy silicon oxycarbide phase. The excess carbon is thought to be in the form of microcrystalline, turbostratic pyrolytic carbon [57]. MPS fibers with low oxygen content (<1%) are expected to have more  $\beta$ -SiC polycrystallinity, improved thermal stability, and higher elastic modulus. The ceramic yields of entry (12) were 15% and 32% for  $n = 5$  and 13, respectively [59]. No additional compositional information was provided for these systems. The organic substituents of MPS entry (13) were methyl, phenyl, and *n*-octyl and various ratios (five different cases) of these were used.  $T_g$  values [by Dupont TMA (thermomechanical analyzer)] ranged from 53 to 155 °C while the oxygen content ranged from 0.42 to 2 wt%. The authors reported that modification of a branched polymethylsilane by substitution with higher alkyl or aryl groups allows control of preceramic polymer rheology and ceramic char composition (for melt spinning of fibers and production of stoichiometric SiC). The thermal sensitivity and degradation of linear and branched hydro-polysilane [61,62] and evaluation of cross-linking of hydro-polysilanes [63] have been investigated by Sawan and coworkers [61–63]. For entries (14)–(16), the ceramic yields were 100%, 70%, and 50% (at 900 °C) when pyrolyzed in air [61]. About 14 hydro-polysilanes [copolymers with methyl and phenyl substitutes in various combinations, entry (17)] were investigated by Shieh, Sawan, and Milstein [62]. The C/Si ratios ranged from 3.2 to 11.3 with one exception for which the ratio was 1.3. The residue of only four systems had free carbon greater than about 10% and the free carbon was indiscernible for several cases. The one with the highest yield [52.6%, prepared from a mixture

of  $\text{PhSiHC1}_2/(\text{CH}_3)_2\text{SiC1}_2/\text{CH}_3\text{SiC1}_3=50/25/15$ ] had a C/Si ratio of 5 and 5.7% free carbon. The work by Shieh and Sawan used different cross-linking agents [63]. The yields for I and II [entries (18) and (19)] were 8.2 and 38.6% before cross-linking. Using  $\text{C1CH}_2\text{C1}$ , tetravinylsilane, and trivinylmethylsilane as cross-linking agents, the yields were 9.2%, 21.6%, and 13.8% for I and 38.3%, 53.5%, and 47.5% for II, respectively.

#### Polycarbosilanes: Directly Synthesized Precursors

The synthesis of poly[(methylchlorosilylene)methylene] (PMCS-Cl) [65(a)] and poly(silapropylene) (PSP) [65(b)] have been reported by Bacque and coworkers [65,66]. Derivatives of PMCS-Cl where Cl has been replaced by H, D, -Si-, -NH-, -Si-, -NHMe-, -NMe<sub>2</sub>, etc. has been accomplished [67]. It was shown in further work by the same group [67] that derivatives prepared from PMCS-Cl by reacting the Si-Cl functionality with Na, K, Me<sub>2</sub>NH, MeNH<sub>2</sub>, NH<sub>3</sub>, and H<sub>2</sub>O and the Si-H functionality with 1,3-butadiene and divinylbenzene gave, upon pyrolysis (1,000 °C/Ar), relatively low ceramic yields which ranged from 11.4 to 77.6%. Of these the four highest yields were the Na, K, MeNH<sub>2</sub>, and H<sub>2</sub>O derivatives with yields, respectively, 77.6%, 59.3%, 53%, and 54.3%. The yields for the K, Na, MeNH<sub>2</sub> derivatives were for insoluble and unmeltable fractions of the product. All samples pyrolyzed at 1,200 °C were reported to contain O impurities (14–24 at.%) [67(b)]. Poly[(dimethylsilylene)methylene] [=poly(silabutylene)] has been converted to PSP [PSP-1, entry (1), Table 58.3]. The low ceramic yield for PSP-1 was attributed to the linearity of the polymers. PMCS-Cl and PSP were also synthesized by Wu and Interrante [68] by ring-opening polymerization of 1,3-dichloro-1,3-dimethyl-1,3-disilacyclobutane, which was in turn prepared from  $\text{C1}_2(\text{Me})\text{SiCH}_2\text{C1}$ . The PSP prepared this way is designed as PSP-2 in entry (2). The thermal properties of entries (1)–(6) should be evident from Table 58.3. Related work has dealt with the structural elucidation of a PCS [70] derived from  $\text{C1}_3\text{SiCH}_2\text{C1}$  and the ceramic evolution of PCS [71] prepared by the Yajima *et al.* process [48(d)]. The effect of thermal cross-linking is demonstrated by the data in entries (7) and (8). Interrante *et al.* [72] have also investigated Schilling's VPS [73,74] of entries (9) and (10). The approximate composition of the VPS was determined by NMR to be  $\{[\text{Si}(\text{Me})_3]_{0.32}[\text{Si}(\text{CH}=\text{CH}_2)\text{Me}]_{0.35}[\text{Si}(\text{H})\text{Me}]_{0.18}[\text{SiMe}_2]_{0.7}[\text{CH}_2\text{SiMe}]_{0.08}\}_n$ . The ceramic composition of entry (11) is close to  $\text{Si}_4\text{C}_5\text{O}_2$  and can be described as a continuum of  $\text{SiC}_4$  and/or  $\text{SiC}_{4-x}\text{O}_x$  tetrahedral species (and possibly contains free carbon) with homogeneity domain size less than 1 nm. Although details are not given here, SiC/AlN ceramics have been prepared by using polycarbosilane and appropriate polymers [77(a–c)]. Photoirradiation of poly[(methylsilylene)methylene] can rapidly lead to a crosslinked structure, which is then pyrolyzed at 1,200 °C to give a  $\beta$ -SiC ceramics (C:Si = 1.79:1) in 70% yield [77(d)].



**TABLE 58.3.** Pyrolysis data on poly(silapropylenes) (PSPs).

Precursors	Pyrolysis condition, yield, and composition			
	P <sup>a</sup>	Y	Residue and impurities	References
(1) $\text{-(Me}_2\text{Si-CH}_2\text{)-}$ $\rightarrow$ PSP-1(linear)	a	5	SiC; NDG	[65,66]
(2) $\text{Cl}_2\text{MeSi-CH}_2\text{Cl}$ $\rightarrow$ PSP-2	b	10	SiC; NDG	[68]
(3) PSP-2a $\text{-(CH}_3\text{SiH-CH}_2\text{)-}^b$	b	20	SiC; NDG	[68]
(4) PSP-2(TXL, 400 °C) <sup>c</sup>	c	66	$\beta$ -SiC (at 1,600 °C); NDG	[68]
(5) $\text{-(SiH}_2\text{-CH}_2\text{)-}$	b	80	SiC, NDG	[69]
(6) $\text{-(Me)}_2\text{Si-CH}_2\text{-}$	b	0		[69]
(7) $\text{-(SiH}_{2-x}\text{Et}_x\text{-CH}_2\text{)-}_{x=0.15}$	b	58–76	NDG	[72]
(8) $\text{-(SiH}_{2-x}\text{Et}_x\text{-CH}_2\text{)-}$ (TXL, 80–200 °C) <sup>c</sup>	b	80	$\beta$ -SiC <sup>d</sup> ; low C <sup>e</sup>	[72]
(9) VPS (Union Carbide Y-12044)	b	55	$\beta$ -SiC <sup>d</sup> ; C-rich	[72]
(10) VPS (Union Carbide Y-12044)	d	40	$\alpha$ -Si <sub>3</sub> N <sub>4</sub> ; C (1.8%)	[72,75]
(11) $\text{-(HSiCH}_3\text{-CH}_2\text{)-}$ (OX) <sup>f, g</sup>	e	85	SiC; SiC <sub>4-x</sub> O <sub>x</sub> ; C(?)	[76]

<sup>a</sup>Pyrolytic conditions: a, 1,000 °C/Ar; b, 1,000 °C/N<sub>2</sub>; c, 1,200 °C/N<sub>2</sub>; d, 1,000 °C/NH<sub>3</sub>; e, 1,200 °C inert gas.

<sup>b</sup>PSP-2a has a higher molecular weight than PSP-2 for entries 1 and 2, the yields are for PSP-1 and PSP-2.

<sup>c</sup>Thermal cross-linking at the temperatures indicated.

<sup>d</sup>Partially crystalline.

<sup>e</sup>Compare to VPS No. 9.

<sup>f</sup>Oxidative curing.

<sup>g</sup>Yajima *et al.* PCS.

Entries (1)–(4) in Table 58.4 are for polysilmethylene or polysilaethylene (PSM or PSE, respectively). PSM was synthesized by ring-opening polymerization of 1,3-disilacyclobutane [78] and the PSE's [entries (2)–(4)] from 1,1,3,3-tetrachloro-1,3-disilacyclobutane [79,80]. PSM is believed to be linear and can be used to make fibers or molded and shaped in various forms. The SiC obtained from PSM had amorphous and crystalline components at 900 °C [78]. The ceramic yield difference between PSE-I and PSE-II is attributed to a difference in molecular-weight distribution ( $M_n=10\,762$  and  $M_w=32\,823$  for PSE-I;  $M_n=7,480$  and  $M_w=25\,600$  for PSE-II [79]). NMR data on PSE ( $M_n=12\,300$  and  $M_w=33,000$ ) was consistent with the expected structure,  $(-\text{SiH}_2\text{-CH}_2\text{-})_n$ , and gave  $\alpha$ -SiC (at 1,000 °C/N<sub>2</sub>) with average crystallite size of 2.5 nm, indicating a high level of purity for the results that an initially cross-linked structure is by no means a requirement for high ceramic yields [80].

Entries (5)–(7) compare PCS (Dow Corning X9-6348,  $\{[-(\text{Me})_2\text{Si-CH}_2\text{-}]_{1.00}[-(\text{Me})_2\text{Si-CH}_2\text{-}]_{0.8}\}$ ) and poly(ethynyl)carbosilane prepared by chemical modification of PCS to provide a precursor with high solubility and latent reactivity [81]. The data in entry (5) are for the original PCS. Pyrolysis to 1,000 °C gave  $\beta$ -SiC with small crystal-lites [by x-ray diffraction (XRD)] [81]. In entries (8) and (9), data for poly(vinylsilane) (=polysilylethylene) and poly(dimethylsilylethylene) are provided [82,83]. The former was synthesized from  $\text{ViSiHC}_2$  and the latter from  $\text{ViSiHMe}_2$  (Vi=vinyl).

The data provided in entries (10)–(26) should be pretty self-explanatory. For entries (13)–(15), the structures given are only approximate (as are probably for many other cases, in general) and NMR results have shown (13)–(15) to be

composed of a mixture of PCS (74%) and polysilane (26%) [86]. The use of 10 mol% of the potential cross-linking agent 1,2-disilylethene ( $\text{H}_3\text{SiCH}_2\text{CH}_2\text{SiH}_3$ ) BSE during polymerization did not significantly increase the polymer molecular weight of the vinylsilane polymer in contrast to what was observed for methylsilane polymerization [86]. In the case of entry (21), when polysiltrimethylene was prepared from allyldiphenylsilane ( $\text{H}_2\text{C=CH-CH}_2\text{SiHPh}_2$ ) [88], the ceramic yield was 30%.

Overall the data presented here attempt to bring out the influence of  $\text{Si-CH=CH}_2$  and  $\text{Si-H}$  functional groups and the comparison of precursors with  $-\text{SiCH}_2-$ ,  $-\text{SiCH}_2\text{CH}_2-$ , and  $-\text{SiCH}_2\text{CH}_2\text{CH}_2-$  unit in the main chain. UV-irradiation of  $[-(\text{CH}_2\text{=CH})_2\text{SiCH}_2-]_n$  can lead to a crosslinked material, which then pyrolyzed at 1,000 °C to give SiC ceramics in 58% yield [80(c)].

Table 58.5 deals with several PCS precursors to SiC investigated by Schilling and coworkers. Those in entries (1)–(5) were based on K metal dechlorination of mixtures of vinylmethylchlorosilanes or methyltrichlorosilane [91]. This is a one-step preparation of branched PCS. For entries (3) and (5), the starting monomers are indicated since the structures of the PCS's were not provided. Those in entries (6)–(8) and (11) are K-derived while (9) and (10) were Na-derived [73,91(c)]. Precursor (6) was prepared from  $\text{Me}_3\text{Cl/MeSiCl}_2/\text{CH}_2\text{=CHSiMeCl}_2=0.85/0.3/1$ . When  $\text{Me}_2\text{SiCl}_2$  was changed to  $\text{MeSiHC}_2$ , the  $=\text{Si-H}$  modified PCS gave a "SiC" yield of 50% (1,200 °C). Precursor (7) was prepared by reaction of  $\text{H-C}\equiv\text{C-Na}$  with  $\{ -[\text{Si}(\text{Cl})\text{MeCH}_2]_x-[\text{SiMe}_2\text{CH}_2]_{1.0}-[\text{SiHMeCH}_2]_{0.8-x}-\}_n$ , while precursor (8) was obtained by self hydrosilylation of  $\text{CH}_2\text{=CH-SiHCl}_2$  followed by reduction with  $\text{LiAlH}_4$ . Precursor (9) was prepared using the same ratio as in (6)

**TABLE 58.4.** Pyrolysis data on various PCSs.

Precursors	Pyrolysis condition, yield, and composition			
	P <sup>a</sup>	Y	Residue and impurities	References
(1) Polysilmethylene (PSM)	a	85	SiC; NDG	[78]
(2) Polysilaethylene (PSE-I)	b	80	SiC; NDG	[79]
(3) Polysilaethylene (PSE-II)	b	60	SiC; NDG	[79]
(4) Polysilaethylene	c	87	β-SiC (at 1,000 °C); NDG	[80]
(5) PCS (Dow Corning X9-6348)	d	63 <sup>b</sup>	SiC; NDG	[82]
(6) Poly(ethynyl)carbosilane	d	74 <sup>b</sup>	SiC; NDG	[81]
(7) Poly(ethynyl)carbosilane (UV) <sup>c</sup>	d	85 <sup>b</sup>	SiC; no surface oxide contamination	[81]
(8) $\text{-(Si(H)}_2\text{-CH}_2\text{CH}_2\text{)-}$	b	30–40	SiC; slight excess C, H, O	[82,83]
(9) $\text{-(Si(Me)}_2\text{-CH}_2\text{CH}_2\text{)-}$	e	0	NDG	[84]
(10) PCS-I <sup>d</sup>	f	32	β-SiC; O (0.3–3%)	[84,85]
(11) PCS-II <sup>e</sup>	f	12	β-SiC; O (0.3–3%)	[84]
(12) PCS-III <sup>f</sup>	f	52	β-SiC; O (0.3–3%)	[84]
(13) $\text{ViSiH}_2\text{-SiViH-H}_2\text{SiVi}$	g	60	SiC; C-rich, 3% Ti (from catalyst)	[86]
(14) $\text{MeSiH}_2\text{-SiMeH-SiH}_2\text{Me}$	g	65	SiC; NDG	[86]
(15) Copolymer <sup>g</sup>	g	73	SiC (CSi = 1.3); NDG	[86]
(16) $\text{SiH}_3\text{-(C}_2\text{H}_4\text{SiH}_2\text{)}_n\text{-H(A)}$	g	12	NDG	[87]
(17) $\text{H}_3\text{Si-(C}_2\text{H}_4\text{SiH}_2\text{)}_n\text{-Vi}$	g	30	SiC; 0.19 C, 0.01 SiO <sub>2</sub>	[87]
(18) $\text{H}_2\text{ViSi-(C}_2\text{H}_4\text{SiH}_2\text{)}_n\text{-Vi}$	g	56	NDG	[87]
(19) $\text{-(SiViH-C}_2\text{H}_4\text{)-}_n\text{(B)}$	g	60	SiC; 2.21 C, 0.03 SiO <sub>2</sub>	[87]
(20) 2.5(A) + 1.0(B)	g	62	SiC; 1.41 C, 0.07 SiO <sub>2</sub>	[87]
(21) $\text{-(SiH}_2\text{-CH}_2\text{CH}_2\text{CH}_2\text{)-}_n$	h	45–50	SiC; NDG	[88]
(22) $\text{H-[SiH(C}_2\text{H}_4\text{SiH}_2\text{Me)]}_n\text{-H + Ti(cat.)}$	b	73	Si/C=1.01/1, -SiC (at 1,400 °C)	[89]
(23) $\text{-[SiH(C}_2\text{H}_4\text{SiHMe)]}_n\text{- + Ti(cat.)}$	b	73	Si/C=1.01/1, -SiC (at 1,400 °C)	[89]
(24) $\text{-[SiH(C}_2\text{H}_4\text{SiHMe)]}_n\text{- + no Ti}$	b	30	NDG	[89]
(25) $\text{[(Cl}_2\text{Si)}_{1.5}\text{SiCl(CH}_2\text{)}_3\text{]}_x$	b	22.6	NDG	[90]
(26) $\text{[(H}_2\text{Si)}_{1.5}\text{SiH(CH}_2\text{)}_3\text{]}_x$	b	30.9	NDG	[90]

<sup>a</sup>Pyrolytic conditions: a, 900 °C/Ar; b, 1,200 °C/(N<sub>2</sub>orAr); c, > 600 °C/N<sub>2</sub>; d, 950 °C/Ar; e, 550 °C/Ar; f, 1,000 °C; g, 1,400 °C/N<sub>2</sub>; h, 1,300 °C.

<sup>b</sup>Fibers.

<sup>c</sup>UV radiation.

<sup>d</sup>PCS-I= $\text{ViSiH}_2\text{-(C}_2\text{H}_4\text{-SiH}_2\text{)-[CH(Me)-SiH}_2\text{]-SiH}_3$ .

<sup>e</sup>PCS-II= $\text{H}_3\text{Si-[C}_2\text{H}_4\text{-SiH}_2\text{)-[CH(Me)-SiH}_2\text{]-SiMe}_3$ .

<sup>f</sup>PCS-III= $\text{ViSiH}_2\text{-(C}_2\text{H}_4\text{-SiH}_2\text{)-[CH(Me)-SiH}_2\text{]-SiH}_2\text{Vi}$ .

<sup>g</sup>30% vinylsilane/70% methylsilane.

**TABLE 58.5.** Pyrolysis data on PCSs prepared mostly by K and Na dechlorination of chlorisilanes.

Precursors	Pyrolysis condition, yield, and composition			
	P <sup>a</sup>	Y	Residue and impurities	References
(1) $\text{(Me}_3\text{Si)}_{0.5}\text{(CH}_2\text{-CH-SiMe)}_{1.0}\text{(SiMe}_2\text{)}_{1.0}$	a	18–43		[91]
(2) $\text{-(CH}_2\text{-SiMe}_2\text{)-}$	a	Nil		[91]
(3) $\text{ClCH}_2\text{SiMe}_2\text{Cl + MeSiCl}_3 \rightarrow \text{PCS}$	a	30.8		[91]
(4) $\text{-(CH}_2\text{CH(SiMe}_3\text{)-Si(Me)}_2\text{)-}_x$	a	Nil		[91]
(5) $\text{MeSiCl}_2 + \text{ViSiMe}_3 \rightarrow \text{PCS}$		40.9		[91]
(6) $\text{(Me}_3\text{-Si)}_{0.85}\text{(SiMe}_2\text{)}_{0.3}\text{(CH}_2\text{-CH-SiMe)}_{1.0}$	b	32		[74]
(7) $\text{-(Me-Si-CH}_2\text{-CH(Ph)-)}$	a	28		[74]
(8) $\text{-(Me-Si-CH}_2\text{-C(Me)=CHCH}_2\text{)-}$	a	25		[73,74]
(9) $\text{Me}_3\text{Si(SiMe}_2\text{)}_x\text{(SiViMe)}_y\text{SiMe}_3$	a	49.5	SiC; C and O	[74]
(10) $\text{Me}_3\text{Si(HSiMe)}_x\text{(SiViMe)}_y\text{SiMe}_3$	a	57.2	SiC; C and O	[74]
(11) $\text{Me}_3\text{SiCH}_2\text{CH(SiMe}_3\text{)}_y$		77.4	SiC; C and O	[74]
(12) BHMPCS <sup>b</sup>	a	11.1–53	SiC	[92,93]

<sup>a</sup>Pyrolytic conditions: a, 1,200 °C/Ar; b, 700 °C/N<sub>2</sub>.

<sup>b</sup>BHMPCS = branched hydrosilyl-modified polycarbosilanes.

but Na/solvent was used. Precursor (10) was a modification of (9) where MeSiHC1<sub>2</sub> was used instead of Me<sub>2</sub>SiC1<sub>2</sub>. Precursor (11) was prepared from Me<sub>3</sub>SiC1 and CH<sub>2</sub>=CHSiMe<sub>3</sub> using K/THE. When Na/solvent was used, there was no reaction. Entry (12) concerns hydrosilyl-modified polysilane precursors for SiC [92,93]. About ten different various cases were examined with ceramic yields in the range 11.1–53%.

Seyferth, Sobon, and Bonn have investigated photochemical and thermal reactions of small amounts (0.25–2 wt%) of polynuclear metal carbonyls for the purpose of cross-linking Si–H containing silicon polymers [95]. In entries (1)–(6) (Table 58.6), the effect on ceramic yield and composition are demonstrated, particularly in entry (6). Seyferth and Lang [96] have also demonstrated that *n*-BuLi/*t*-BuOK can be a most effective reagent for metallization of CH<sub>2</sub> groups in a SiCH<sub>2</sub>Si [e.g., in poly(dimethylsilylenemethylene), (Me<sub>2</sub>SiCH<sub>2</sub>)<sub>n</sub>] environment and some results are demonstrated in entries (7)–(10). Seyferth *et al.* [97] also investigated pyrolysis of hybrid polymers by reactions of precursors E and F [entries (11) and (12)] with various E/F ratios. An AIBN free radical initiator was used. The NMR-determined structure of PVSih<sub>3</sub> [(14)–(16)] was more complicated than the simplified representation as [CH<sub>2</sub>CH(SiH<sub>3</sub>)<sub>n</sub>]. The effect on the compositions can easily be discerned from the data in Table 58.6. Similar and related work by Seyferth and coworkers involving modifications and cross-linking of preformed precursors by using metal carbonyls, alkali-metal amide, and silylamides can be found in the literature [98,99]. Additionally, Seyferth and coworkers have demonstrated that multiple-phase ceramics can be prepared by pyrolysis of preceramic polymer/metal powder composites. The metal powders were oxides of Si and early transition metals [100]. This approach was particularly

useful to convert excess and/or unbound Si and C into metal silicides and carbides.

Work by several groups of investigators dealing with PCSs with regard to conversion and processing [101], NMR characterization [102], curing of PCS fibers [103], fabrication of C/SiC composites [104], mechanical properties [105], and other similar studies on PCS [106] are available but not reviewed here. Also not reviewed are publications on polysilanes [107] and polyhydrosilanes [108].

### Polysilylacetylenes

Table 58.7 lists some silicon–acetylene, silicon–olefin, silylene–diacetylene, and silylene–vinylene polymers. In the case of entry (6), R=Me, Et, *i*-Pr, *n*-Bu, *c*-Hx, *n*-Hx and Ph were investigated. Of these, the R=*c*-Hx and *n*-Hx cases gave higher ceramic yields of 76% and 72%, respectively [112]. In the case of entry (7), the three cases reported were with R=R'=Me, R=R'=Ph, and R=Ph and R'=Me with yields of 85%, 96%, and 95%, respectively [112].

### Polysiloxanes

Several polysiloxane systems that have been investigated as precursors to SiC are given in Table 58.8 and brief comments are made here only for a few cases. For entries (5) and (6), about 11 systems were investigated by Burns *et al.* [118]. They found formation of amorphous SiCO at 1,200 °C that continued to undergo Si–O to Si–C bond distribution as the temperature increased to 1,400 °C and a small amount of oxygen remained even at 1,800 °C. Trace amounts of β-SiC

**TABLE 58.6.** Pyrolysis data on various PCSs: Effect of modification and/or cross-linking of preformed precursors.

Precursors	Pyrolysis condition, yield, and composition			
	P <sup>a</sup>	Y	Residue and impurities	References
(1) Nicalon PCS (A)	a	55–60	SiC; C (15%)	[94,95]
(2) Nicalon PCS + metal carbonyls (cat., e.g., Ru)		83–88		[95]
(3) [(MeSiH) <sub>x</sub> (MeSi) <sub>y</sub> ] <sub>n</sub>	b	Low	1 SiC + 0.5Si	[95]
(4) [(MeSiH) <sub>0.65</sub> (MeSi) <sub>0.35</sub> ] <sub>n</sub> (B)		12		[95]
(5) (B) + 2%Ru <sub>3</sub> (CO) <sub>12</sub> (cat.)	b	55		[95]
(6) (A) + (B) + 2%Ru <sub>3</sub> (CO) <sub>12</sub> (cat.)	b	68	SiC (99%); C (1%)	[95]
(7) –(Me <sub>2</sub> SiCH <sub>2</sub> ) <sub>n</sub> –	c	0		[96]
(8) {[Me <sub>2</sub> SiCH <sub>2</sub> ] <sub>3</sub> [Me <sub>2</sub> SiCH(SiMe <sub>2</sub> Vi)]] <sub>n</sub> (C)	d	0–2		[96]
(9) [(MeSiH) <sub>0.8</sub> (MeSi) <sub>0.2</sub> ] <sub>n</sub> (D)	d	15–20	SiC (74%); Si (25%)	[96]
(10) 1(C) + 4(D) + AIBN(cat.)	d	68	SiC (91–94%); C (6–9%)	[96]
(11) [(MeSiH) <sub>0.4</sub> (MeSi) <sub>0.6</sub> ] <sub>n</sub> (E)	b	60	SiC (76%); C (24%)	[56,97,98]
(12) [MeViSi–C=C] <sub>n</sub> (F)	b	83	SiC (50%); C (50%)	[97]
(13) Various ratios of (E)/(F)=1.5–8	b	79–84	SiC (82–99%); C (1–18%)	[97]
(14) [CH <sub>2</sub> CH(SiH <sub>3</sub> ) <sub>n</sub> ] or PVSih <sub>3</sub>	e	39–47	NDG	[97]
(15) PVSih <sub>3</sub> + Zr-metallocene(cat.), UV		80	β-SiC (88.7%), C (0.7%), ZrC (0.6%)	[97]
(16) PVSih <sub>3</sub> (bulk pyrolysis)	f	39	β-SiC (94%), C (6%)	[97]

<sup>a</sup>Pyrolytic conditions: a, 1,200 °C/Ar; b, 1,000 °C/Ar; c, 600 °C/Ar; d, 900 °C/Ar; e, 960 °C/Ar; f, 1,500 °C.

**TABLE 58.7.** Pyrolysis data on polysilylacetylene and related precursors.

Precursors	Pyrolysis condition, yield, and composition			
	P <sup>a</sup>	Y	Residue and impurities	References
(1) $\text{-(Me}_2\text{Si-C}\equiv\text{C-SiMe}_2\text{-CH=CH-)}_n$	a	50,55	$\beta$ -SiC; excess C	[109]
(2) $\text{-(Si(Me)}_2\text{-C}\equiv\text{C-)}_n$	b	80	SiC (59.6%); C (40.4%)	[110]
(3) $\text{-(Si(Ph)}_2\text{-C}\equiv\text{C-)}_n$	b	81	SiC (29%); C (71%)	[110]
(4) $\text{-(PhSiMe-C}\equiv\text{C-)}_n$	b	77	SiC (35.5%); C (64.5%)	[110]
(5) $\text{-(Si(Me)}_2\text{-Si(Me)}_2\text{-C}\equiv\text{C-)}_n$	b	59	SiC (70.9%); C (29.1%)	[110, 111]
(6) $\text{-(R}_2\text{Si-C}\equiv\text{C-)}_n$	c	20–76	SiC; excess C	[112]
(7) $\text{-(RR' Si-C}\equiv\text{C-)}_n$	c	85–95	SiC; excess C	[112]
(8) $\text{-(Me(CH}_2\text{=CH)Si-C}\equiv\text{C-)}_n$	d	83	SiC (50%); C (50%)	[113]
(9) $\text{-(Me)}_2\text{Si-(Me)}_2\text{Si-C}\equiv\text{C-C}\equiv\text{C-}$	b	82	$\beta$ -SiC (59%); C (41%)	[114]
(10) $\text{-(Me}_2\text{Si-C}\equiv\text{C-C}\equiv\text{C-)}_n$	b	82	$\beta$ -SiC (40%); C (60%)	[114]
(11) $\text{-(Ph}_2\text{Si-C}\equiv\text{C-C}\equiv\text{C-)}_n$	b	80	$\beta$ -SiC (23.4%); C (76.6%)	[114]
(12) $\text{-(Ph(Me)Si-C}\equiv\text{C-C}\equiv\text{C-)}_n$	b	79	$\beta$ -Si (33.7%); C (66.3%)	[114]
(13) $\text{-(Me)}_2\text{Si-CH=CH-}$	b	27	SiC; NDG	[115]
(14) $\text{-(Et)}_2\text{Si-CH=CH-}$	b	16.7	SiC; NDG	[115]
(15) $\text{-[Ph(Me)Si-CH=CH-]}$	b	40	SiC; NDG	[115]

<sup>a</sup>Pyrolytic conditions: a, 1,200 °C/He; b, 1,000 °C/He; c, 1,100 °C/He; d, 1,000 °C/Ar.

**TABLE 58.8.** Pyrolysis data on polysiloxane SiC precursors.

Precursors	Pyrolysis condition, yield, and composition			
	P <sup>a</sup>	Y	Residue and impurity	References
(1) (DEDMS <sup>b</sup> + TEOS <sup>c</sup> )/H <sub>2</sub> O/EtOH	a	85	Si-C-O	[116]
(2) (DEDMS + TEOS)/H <sub>2</sub> O/EtOH	b	50	SiC <sup>d</sup> ; SiO <sub>2</sub> , C	[116]
(3) Polysiloxane <sup>e</sup>	c	76.9	Si <sub>1</sub> O <sub>1.36</sub> C <sub>2.7</sub> ( $\beta$ -SiC, trace)	[117]
(4) Polysiloxane	d	49.5	Si <sub>1</sub> O <sub>0.18</sub> C <sub>1.67</sub> ( $\beta$ -SiC, 90%)	[117]
(5) Polysiloxane	e	44.5	Si <sub>1</sub> O <sub>0.1</sub> C <sub>1.47</sub> ( $\beta$ -SiC, 97%)	[117]
(6) (PhSiO <sub>x</sub> ) <sub>r</sub> (MeSiO <sub>y</sub> ) <sub>s</sub> (Me <sub>2</sub> ViSi <sub>z</sub> ) <sub>t</sub>	f	67–77	Si-C-O with O (13.35–18.03 wt%)	[118]
(7) (PhSiO <sub>x</sub> ) <sub>r</sub> (MeSiO <sub>y</sub> ) <sub>s</sub> (Me <sub>2</sub> ViSi <sub>z</sub> ) <sub>t</sub>	e	35–49	SiC (68–100%), C <sup>f</sup> (0–31.6%)	[118]
(8) Polymethylsilsesquioxane (A)	c	77	Silicon oxycarbide and glassy C at 1,000 °C.	[119]
(9) Polyphenylsilsesquioxane (B)	c	63	Between 1,200 and 1,400 °C, amorphous silica, amorphous SiC, some crystalline	[119]
(10) 50(A)/50(B) copolymer	c	70	SiC, graphitic C found	[119]

<sup>a</sup>Pyrolytic conditions: a, 1,000 °C/Ar; b, firing at low temperature (e.g., 700 °C) and then at 1,550 °C; c, 1,400 °C/[Ar for entries (8)–(10)]; d, 1,600 °C; e, 1,800 °C/Ar; f, 1,100 °C/Ar.

<sup>b</sup>DEDMS = dimethyldiethoxysilane.

<sup>c</sup>TEOS = tetraethoxysilane.

<sup>d</sup>Partially amorphous, partially crystalline.

<sup>e</sup>Polysiloxane = (MeSiO<sub>1.5</sub>)<sub>0.75-x</sub>(PhSiO<sub>1.5</sub>)<sub>x</sub>(MeViSiO<sub>0.5</sub>)<sub>0.25</sub>.

<sup>f</sup>Turbostratic graphite.

were seen at 1,400 °C. By 1,600 °C, the carbothermic reduction was well underway and only a small percentage of oxygen remained in the material. At 1,800 °C, the pyrolysis is complete with the final product containing a substantial amount of  $\beta$ -SiC and excess C. The conversion process can be summarized as  $(\text{RSiO}_{1.5})_n \rightarrow \text{C}_x\text{Si}_y\text{O}_z \rightarrow y\text{SiC} + (x-y-z)\text{C} + z\text{CO}$ . If insufficient C is present, SiO is given off. As reported by Chen *et al.* [116(b)] the conversion can be envisioned to take place by polymer/copolymer  $\rightarrow \text{SiO}_2 + \text{C} \rightarrow \beta\text{-SiC}$  with the carbothermic reduction being represented by  $\text{SiO}_2 + 3\text{C} \rightarrow \text{SiC} + 2\text{CO}$ , which occurs at 1,550 °C. Overall, the conversion to SiC of the various systems investigated

are expected to have general commonality with the brief discussion above, and the original publications can be consulted for details. Other cases studied included redistribution reactions in polysiloxanes [120] and silsesquioxanes [121], arylsilsesquioxane gels, and related materials [122]. Additional examples can be found in a recent review [118(c)].

### Polydisilylazanes

Some representative polydisilylazanes [123–126] are presented in Table 58.9. The composition of a fiber of

**TABLE 58.9.** Pyrolysis data on polydisilylazane precursors.

Precursors	Pyrolytic condition, yield, and composition			References
	P <sup>a</sup>	Y	Residue and impurity	
(1) Methylpolydisilylazane		53	Si <sub>1</sub> C <sub>0.8</sub> N <sub>0.7</sub> O <sub>0.5</sub>	[123]
(2) [Me <sub>2.6</sub> (Si <sub>2</sub> ) <sub>1</sub> NH <sub>1.5</sub> ] <sub>11</sub> (A)	a	60	NDG	[124]
(3) (A) (1200) <sup>b</sup>	b	51	NDG	[124]
(4) (A) + additives <sup>c</sup>	a	51	Si <sub>1</sub> C <sub>0.8</sub> N <sub>0.2</sub> O <sub>0.03</sub>	[124]
(5) (A) (fiber)—aid cured	a		Si <sub>1</sub> C <sub>0.9</sub> N <sub>0.2</sub> O <sub>0.6</sub>	[124]
(6) (B) <sup>d</sup>	c	61	Si <sub>1</sub> C <sub>0.92</sub> N <sub>0.22</sub> O <sub>0.59</sub> (at 1,200 °C)	[125]
(7) PhVi-modified MPDZ resin (C)	a		SiC with residue containing O (11%), and N (13.3%)	[126]
(8) PhVi-modified MPDZ resin (C)	b	62	SiC <sup>e</sup> , O (0.4%), N (13.3%)	[126]
(9) (C)+boron (BBr <sub>3</sub> )	a		Residue contained B (1.2%), O (30.1%)	[126]
(10) (C)+ boron (BBr <sub>3</sub> )	d		Residue contained B (1.2%), O (0.13%).	[126]

<sup>a</sup>Pyrolytic conditions: a, 1,200 °C/Ar; b, 1,600 °C/Ar; c, 1,000 °C; d, 2,100 °C/Ar.

<sup>b</sup>Further pyrolysis of char from (A).

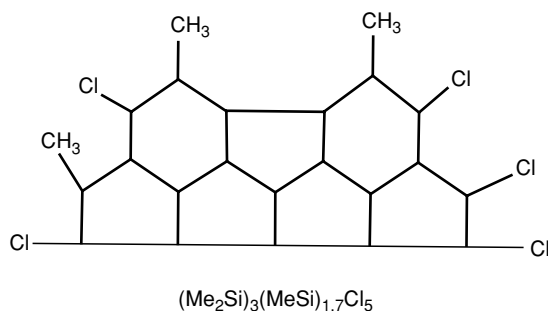
<sup>c</sup>When additives are used α-Si<sub>3</sub>N<sub>4</sub> and β-Si<sub>3</sub>N<sub>4</sub> were observed at temperatures as low as 1000 °C

<sup>d</sup>(B)=[(Me)<sub>2</sub>Si<sub>2</sub>]<sub>0.6</sub>[(Me)<sub>3</sub>Si<sub>2</sub>]<sub>0.4</sub>{(Me)<sub>4</sub>Si<sub>2</sub>]<sub>0.1</sub>[NHSi(Me)<sub>3</sub>]<sub>0.4</sub>}.  
<sup>e</sup>α-SiC (35%) and β-SiC (65%).

phenylvinyl-modified methylpolydisilylazane (MPDZ PhVi) [127] is also compared with other systems in Table 58.10 and in other related work [128].

### Methylchloropolysilanes

Baney and coworkers [125,130,131] have prepared a class of polyfunctional polysilanes from catalyzed Si–Si/Si–Cl bond redistribution of methylchlorodisilane, which gave polycyclic structures with approximately seven rings per molecule (for the reaction carried out at 250 °C). The proposed structure of this polymer designated as PCP-Cl-250 is shown below (Fig. 58.2). Pyrolysis of PCP-Cl-250 gave 80% yield (TGA, 1,200 °C) [125]. Using the Si–Cl reactive group, derivatives of PCP-Cl-250 have been made and references to the original works can be found in the reviews by Baney and Chandra [23(a)] and Laine and Babonneau [14]. The composition of the ceramics (at 1,200 °C) obtained for the oxygen (PCP-O-250) and methyl (PCP-M-250) derivatives are included in Fig. 58.2 [125]. The compositions of PCP-O-250 and PCP-Me-250 at 1,600 °C were reported to be SiC<sub>0.74</sub>O<sub>0.004</sub> and SiC<sub>0.63</sub>O<sub>0.02</sub>, respectively.



### 58.5.2 Si<sub>3</sub>N<sub>4</sub> Precursors

As opposed to the conventional methods of the preparation of Si<sub>3</sub>N<sub>4</sub>, which generally produced infusible and intractable products, the preparation of Si<sub>3</sub>N<sub>4</sub> from metalorganic precursors stemmed from the work of Verbeek and coworkers, who synthesized polysilazanes precursors for

**TABLE 58.10.** Composition calculated using the rule of mixture [127,129].

Fiber <sup>a</sup>	Composition (wt%)				
	SiO <sub>2</sub>	Si <sub>3</sub> N <sub>4</sub>	SiC	C	Si
MPDZ-PhVi	14.3	37.1	27.2	21.3	0
HPZ	5.8	71.3	18.5	4.4	0
SGN	26.8	0	61.6	11.6	0
CGN	19.1	0	90.9	10	0
MPS	1	0	94	0	4.3

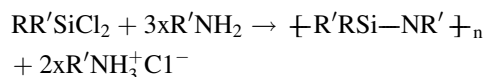
<sup>a</sup>Fibers were prepared from phenylvinyl-modified methylpolydisilylazane (MPDZ-PhVi), hydridopolysilazane (HPZ), Nicalon fiber with 15% oxygen (SGN), Nicalon fiber with 10% oxygen (CGN), and methylpolysilane (MPS).

Derivatives	Compositions
PCP-Cl-250	Si <sub>1</sub> C <sub>1</sub> O <sub>0.05</sub>
PCP-O-250	Si <sub>1</sub> C <sub>0.62</sub> O <sub>0.42</sub>
PCP-Me-250	Si <sub>1</sub> C <sub>0.53</sub> O <sub>0.15</sub>
Yajima's PCS	Si <sub>1</sub> C <sub>1.1</sub> O <sub>0.6</sub>

**FIGURE 58.2.** Proposed structure of PCP-Cl-250 and some related data.

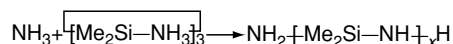
Si<sub>3</sub>N<sub>4</sub> [132]. There are several synthetic routes that are used nowadays for the preparation of Si<sub>3</sub>N<sub>4</sub> polymeric/ oligomeric precursors [22,133,134]. The reactions listed below and further manipulations of the same provide for the preparation of appropriate precursor [22,133]:

(i) Ammonolysis and aminolysis:

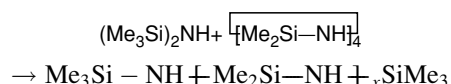


where R' and R are usually H and Me but can also be Et, Vi, Ph, etc.

(ii) Ring-opening polymerization:



or

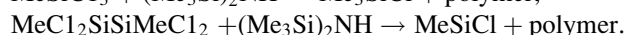
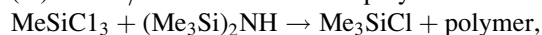


using transition metals such Ru<sub>3</sub>(CO)<sub>12</sub>/135 °C/1h/H<sub>2</sub> as catalyst for the latter.

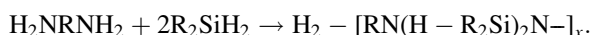
(iii) Deamination/condensation polymerization:



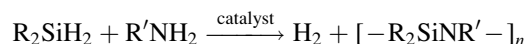
(iv) Si-Cl/Si-N redistribution polymerization:



(v) Catalytic dehydrocoupling-dehydrocyclization reactions:



(vi) Transition-metal catalyzed dehydrocoupling polymerization reactions:



An example of strong base is KH for reaction (v) and Ru<sub>3</sub>(CO)<sub>12</sub> is an example of a catalyst for (vi). If the substituents on the Si of the silane and amine monomers are different from H, SiC and C are usually obtained along with Si<sub>3</sub>N<sub>4</sub>. In a few cases Si can also be obtained. The SiC and the free and/or unbound C can be, in some cases, the major constituents. C-rich composites are particularly common where vinyl (Vi) and phenyl (Ph) groups are present and more C seems to be present with Ph than with Vi. It is, however, easy to reduce the C content to <1 wt% by carrying out the pyrolysis in NH<sub>3</sub> gas at temperatures >500 °C. Both the excess Si and C can also be converted to metal silicides and carbides if such multiphase composites are desired [100]. As the result of the lability of the Si-N bond due to the reaction ≡Si-N + H<sub>2</sub>O → ≡Si-OH + =N-H, oxygen can also be present in the form of SiO<sub>2</sub>, SiN<sub>2</sub>O<sub>2</sub>, etc. Although most organopolysilazanes give Si<sub>3</sub>N<sub>4</sub>, SiC,

and C, there are several cases in which >95% Si<sub>3</sub>N<sub>4</sub> has been obtained [135-138] with at least two cases with >99% Si<sub>3</sub>N<sub>4</sub> (with-out using NH<sub>3</sub> during the pyrolysis) [135,137].

### Pyrolysis of Si<sub>3</sub>N<sub>4</sub> Precursors

A variety of monomeric, oligomeric, and polymeric silazane systems including polydisilacyclobutasilazanes [139], cyclodisilazanes [140], and alkyl and arylsilsequiazanes [22,141] have been investigated as Si<sub>3</sub>N<sub>4</sub> precursors. In the tables that follow, some of these are examined in some details.

Results of pyrolysis of perhydropolysilazanes, polyorganosilazanes, and Si(NH<sub>2</sub>)<sub>4</sub> (after polymerization) are shown in Table 58.11. Seyferth and coworkers [138,142] has also investigated reactions of H<sub>2</sub>SiCl<sub>2</sub> and CH<sub>3</sub>SiHC<sub>12</sub> with CH<sub>3</sub>NH<sub>2</sub> and NH<sub>3</sub>, respectively, the products of which gave ceramic yields of 38% and 20%, respectively [142]. Other cases of reactions of RSiHC<sub>12</sub> and NH<sub>3</sub> with R=(CH<sub>3</sub>)<sub>2</sub>CH, (CH<sub>3</sub>)<sub>3</sub>C, Ph, and C<sub>6</sub>H<sub>5</sub>CH<sub>2</sub> have also been reported. Where a catalyst for ring-opening polymerization (ROP) was used, the ceramic yield for (CH<sub>3</sub>SiHNNH)<sub>x</sub> was 39%. Use of Ru<sub>3</sub>(CO)<sub>12</sub> and a mixture of [CH<sub>3</sub>SiHNNH]<sub>x</sub> and (Me<sub>3</sub>Si)<sub>2</sub>NH gave 74% ceramic yield. Work on the H<sub>2</sub>SiCl<sub>2</sub> + NH<sub>3</sub> system by Shimizu *et al.* [143] has demonstrated an increase of the molecular weight of the product from about 100 to about 100,000 by reacting the oligosilazane with various organic reagents, and the Si/N ratio changed from 1.01 to 1.0-1.03. Related work on the same system and treatment of the product with various amounts of pyridine in an autoclave at 120-150 °C increased the molecular weight, and the ceramic residue at 1,400 °C/N<sub>2</sub> (TGA) was 79.6% [144]. The residue contained Si (63.8%), N (28.7%), C (0.36%), O (2.7%), and H (0.11%). The OCMTS [entry (6)] was polymerized in the presence of KOMe. Similar work in which MeSiCl<sub>3</sub> was used for ROP of OCMTS and hexamethylcyclotrisilazane (HMCTS) and a mixture of OCMTS and HMCTS resulted in 70-80% ceramic yield (TGA 1,400 °C inert atmosphere), and the material contained Si, N, and C (no composition details were reported) [145].

Optimal candidate precursors for Si<sub>3</sub>N<sub>4</sub> can be -(H<sub>2</sub>Si-NH)-, -(H<sub>2</sub>Si-NHNH)-, -(MeSiH-NH)-, and -(SiH<sub>2</sub>-NMe)- because they can be converted to Si<sub>3</sub>N<sub>4</sub> upon pyrolysis by losing H<sub>2</sub> and/or CH<sub>4</sub> [153]. The precursors can be prepared from ammonolysis of H<sub>2</sub>SiCl<sub>2</sub> and MeHSiCl<sub>2</sub>, as an example:



But such systems are unstable and/or of low molecular weight to be directly useful. -(H<sub>2</sub>Si-NMe)<sub>n</sub>- is more stable in the absence of air and moisture but gives only 38-40% yield because of its low molecular weight [153]. Two approaches that have been undertaken to address such problems were developed by Laine and Blum [154] and Seyferth and coworkers [155]. Some results of work of

**TABLE 58.11.** Pyrolysis data on some silazane/polysilazane systems.

Precursors	Pyrolysis condition, yield, and composition			
	P <sup>a</sup>	Y	Residue and impurities	References
(1) Perhydropolysilazane $\text{-(H}_2\text{Si-NH)}_n\text{-}$ <sup>b</sup>	a	70	$\alpha\beta\text{-Si}_3\text{N}_4$ ; Si (trace)	[138,142]
(2) $(\text{SiH}_2\text{NH})_a(\text{SiH}_2\text{N})_b(\text{SiH}_3)_c$	b	80	$\alpha\text{-Si}_3\text{N}_4$ ; Si, O	[146]
(3) $(\text{H}_2\text{SiNH})_n$ <sup>c</sup>	c	82–93 <sup>c</sup>	$\text{Si}_3\text{N}_4$ ; Si	[147]
(4) $\text{Si}(\text{NH})_2/\text{NH}_4\text{Cl}$ (coprecipitate)	d	20	$\alpha\text{-Si}_3\text{N}_4$ (93%, 1,400 °C); Cl>1%	[137]
(5) $\text{-(Me)}_2\text{Si-NH-Si(Me)}_2\text{-}$ <sub>n</sub> OSZ1	e	57	$\text{Si}_3\text{N}_4$ ; SiC	[148]
(6) OCMTS + KOMe (cat.) <sup>d</sup>	e	76–79	SiCN; high C content	[149]
(7) OCMTS + KOMe (cat.)	f	69	$\alpha\text{-Si}_3\text{N}_4$ ; <0.2% C	[149(a)]
(8) PBSZ Fiber <sup>e</sup>	f	90	Amorphous Si–B–O–N fiber	[150]
(9) $\text{SiC}_{1.07}\text{N}_{1.17}\text{O}_{0.07}\text{H}_{3.63}$ (at 500 °C) <sup>f</sup>	g	83	$\text{Si}_3\text{N}_4$ ; SiC, Si (O)	[151]
(10) $\text{Si}(\text{NHEt})_4 \rightarrow$ precursor	c	55	$\text{Si}_3\text{N}_4$ ; C	[152]
(11) $\text{Si}(\text{NHEt})_4 \rightarrow$ precursor	h		$\alpha, \beta\text{-Si}_3\text{N}_4$ ; C <sub>graph.</sub>	[152]
(12) $\text{Si}(\text{NHEt})_4 \rightarrow$ precursor	i		$\alpha\text{-Si}_3\text{N}_4$ ; C <sub>graph.</sub>	[152]

<sup>a</sup>Pyrolytic conditions: a, 1,150 °C/N<sub>2</sub>; b, 1,100–1,300 °C/N<sub>2</sub>; c, 1,000 °C/N<sub>2</sub>; d, >400 °C/N<sub>2</sub>; e, 1,200 °C/N<sub>2</sub>; f, 1,200 °C/NH<sub>3</sub>; g, 1,600 °C/He; h, 1,500 °C/Ar; i, 1,600 °C/N<sub>2</sub>.

<sup>b</sup>n = 7–8.

<sup>c</sup>Depending on the preparation method.

<sup>d</sup>OCMTS=octamethylcyclotetrasilazane.

<sup>e</sup>Perhydropolysilazane + B(OMe)<sub>3</sub> → polyborosilazane(PBSZ).

<sup>f</sup>Composition is for polymer after being heated at 500 °C.

Laine and coworkers [136,156] are given in Table 58.12. Comparison of the data in entries (5), (8), and (9) can serve to illustrate the advantage gained by the use of transition-metal catalyst [the data in entry (5) were obtained by catalytic polymerization whereas that in (9) was not]. The effect of

increase in molecular weight, at least in these types of systems was illustrated by the pyrolysis studies on  $\text{MeNH-[H}_2\text{Si-NMe-}]_x\text{-H}$  oligomers and polymers [157]. By increasing the molecular weight from 600–700 to 2300, the ceramic yield increased from 40% to 60–65%,

**TABLE 58.12.** Pyrolysis and compositional data on some polysilazane systems.

Precursors	Yield <sup>a</sup>	Composition				
		Si <sub>3</sub> N <sub>4</sub>	SiC	C	N	O
(1) $(\text{MeHSi-NH})_x(\text{MeSiN})_y$ <sup>b</sup>	85	65	29	4		
(2) $[\text{H}_2\text{Si-NMe-}]_x[\text{H(NMe)Si-NMe}]_y$ <sup>b, c</sup>	63	75		18	6	
(3) $[\text{Me(H or NH)Si-NH}]^b$	57	64	25	10		
(4) $[\text{Ph(H)Si-NH-}]^b$	61	29	12	42		
(5) $[\text{H}_2\text{Si-NMe}]_x\text{-H}^d$	>80	97				
(6) $[\text{HSi(NH)}_{1.5}]_x[\text{SiNH(NHSiMe}_3)]_y^d$	50	96		2		2

Precursors	Yield <sup>a</sup>	Precursor <sup>e</sup>	Yield <sup>a</sup>
(7) $[\text{C}_6\text{H}_{13}(\text{H or NH)Si-NH}]^b$	35	(12) Poly(Si-phenylsilazane) <sup>f</sup>	75 <sup>g</sup>
(8) $-\text{[Me(H)SiNH-]}^b$	19–57	(13) Poly(Si-hexylsilazane) <sup>f</sup>	45 <sup>g</sup>
(9) $-\text{[H}_2\text{Si-NMe-]}^b$	40–63	(14) Poly(N-methylsilazane) <sup>f</sup>	61 <sup>g</sup> ; 49 <sup>h</sup>
(10) Poly(dimethylsilazane) <sup>f</sup>	Negligible	(15) Oligo(N-methylsilazane) <sup>f</sup>	48 <sup>g</sup> ; 41 <sup>h</sup>
(11) Oligo(Si-diethylsilazane) <sup>f</sup>	Negligible	(16) $(\text{SiViHNN})_x\text{-(SiMeH-NH)}_y$	71–84 <sup>i</sup>

<sup>a</sup>Residue wt% at 900 °C/N<sub>2</sub>.

<sup>b</sup>Reference [156(a)].

<sup>c</sup>Reference [153].

<sup>d</sup>Reference [136(a)].

<sup>e</sup>The composition of the residue from precursors (12)–(14) consisted of Si<sub>3</sub>N<sub>4</sub>, SiC, and C (impurity).

<sup>f</sup>Reference [156(b)].

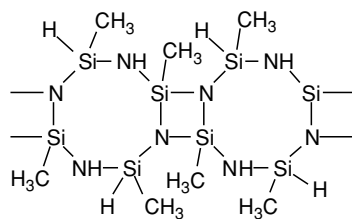
<sup>g</sup>To 800 °C.

<sup>h</sup>To 1,600 °C.

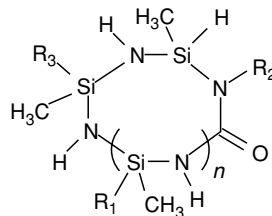
<sup>i</sup>Reference [220(h and i)].

while at the same time the viscosity increased from 1–3 to 100 P (the attainment of appropriate viscosity is also necessary for the purposes of preparing fibers and for use in coating [157]).

Methylhydridopolysilazane (MHPS) was prepared from  $\text{CH}_3\text{SiHCl}_2$  and  $\text{NH}_3$  [155], which gives  $[-\text{CH}_3\text{SiH}-\text{NH}-]_x$  (MHPS1), containing both cyclic and linear structures.



MHPS3


 Poly(ureasilazanes): PUSZ ( $R_1=R_2=R_3=H$ )

 PUMVS ( $R_1=H, CH=CH_2;$   
 $R_2=\text{alkyl}; R_3=\text{vinyl}$ )

**TABLE 58.13.** Pyrolysis data on some polysilazanes, polysilsesquiazanes, polyvinylsilazanes and polycarbosilazanes.

Polymers	Pyrolysis condition, yield, and composition				(A)	Pyrolysis condition, yield, and composition			
	P <sup>a</sup>	Y	Residue and impurity	References		Polymers	P <sup>a</sup>	Y	Residue and impurity
(1) ONMS <sup>b</sup>	a	48	$\alpha, \beta\text{-Si}_3\text{N}_4; \text{C}$	[161, 162(a)]	(12) PCSZ-I <sup>c</sup>	e	50	SiCN	[163]
(2) ONMS	b	40	$\text{Si}_3\text{N}_4; \text{C} (< 1\%)$	[161]	(13) PCSZ-II	e	70	SiCN	[163]
(3) PNMS <sup>d</sup>	c	63	$\alpha, \beta\text{-Si}_3\text{N}_4; \text{C}$	[153, 161]	(14) PCSZ-III	e	90	SiCN	[163]
(4) PNMS	b	65	$\alpha, \beta\text{-Si}_3\text{N}_4; \text{C}$	[153, 161]	(15) PCSZ(I-III)	f		$\beta\text{-SiC}; \text{C}$	[163, 164]
(5) APNMS <sup>e</sup>	c	80–85	$\alpha, \beta\text{-Si}_3\text{N}_4; \text{C}$	[162]	(16) TNMAPS <sup>f</sup>	g	Fiber <sup>g</sup>	SiC	[165]
(6) APNMS	b	72		[162]	(17) TNMAMS <sup>h</sup>	g	Fiber <sup>g</sup>	SiC	[165]
(7) CMS <sup>i</sup>		20		[162(b)]	(18) HSZ1 <sup>j, k</sup>	h	53	$\alpha\text{-Si}_3\text{N}_4; \text{Si} (62\%)$	[166]
(8) PCMS <sup>m</sup>	c	65–85	$\alpha, \beta\text{-Si}_3\text{N}_4;$ SiC, C	[162]	(19) HSZ2 <sup>n</sup>	h	48	$\alpha\text{-Si}_3\text{N}_4; \alpha\text{-SiC}, \text{Si} (62\%)$	[166]
(9) PCMS	d	80		[162]	(20) HSZ3 <sup>o</sup>	l	54	SiC, NDG	[167]
(10) APCMS <sup>p</sup>	e	95	$\alpha, \beta\text{-Si}_3\text{N}_4;$ SiC, C	[162]	(21) HSZ4 <sup>q</sup>	g	60	SiC, NDG	[168]
(11) APNES <sup>r</sup>	a	72–84	$\alpha, \beta\text{-Si}_3\text{N}_4$	[161, 162]	(22) HSZ5 <sup>c</sup>	g	74	SiNC, <sup>s</sup> C (< 3%), lowO	[136b, 169]

<sup>a</sup>Pyrolytic conditions: a, 800 °C/N<sub>2</sub>; b, 800 °C/NH<sub>3</sub>; c, 1200 °C/N<sub>2</sub>; d, 1200 °C/N<sub>2</sub>; e, 950 °C/Ar; f, 1600 °C/Ar; g, 1000 °C/N<sub>2</sub>; h, 1600 °C/He; l, 1000 °C/inert gas;

<sup>b</sup>ONMS = Oligo (N-methyl) silazane,  $\text{H}_2\text{N}-\text{SiH}_2-\text{NMe}-\text{H}$ .

<sup>c</sup>PCSZ-(I to III) = PSSZ heat-treated, respectively, at 335, 372, and 470 °C (in autoclave);

PSSZ =  $[\text{SiMe}_2][\text{Si}(\text{Me})_2-\text{NH}-\text{Si}(\text{Me})_2]_x$ .

<sup>d</sup>PNMS = poly(N-methyl) silazane,  $-\text{[SiH}_2-\text{NMe}]_x\text{[SiH}-(\text{NMe})_{1.5}]_y$ .

<sup>e</sup>APNMS = aminated PNMS.

<sup>f</sup>TNMAPS = tris (N-methylamino)phenylsilane.

<sup>g</sup>Weight loss insignificant up to 1000 °C.

<sup>h</sup>TNMAMS = tris (N-methylamino)methylsilane.

<sup>i</sup>CMS = cyclicmethylsilazane,  $(\text{MeSiH}-\text{NH})_n$ .

<sup>j</sup>HSZ1 and HSZ5 were both obtained from  $(\text{Me}_3\text{Si})_2\text{NH} + \text{HSiCl}_3$ .

<sup>k</sup>Related work to systems (18)–(22) can also be found in Refs. [170] and [171].

<sup>l</sup>No  $\beta\text{-SiC}$  detected.

<sup>m</sup>PCMS = polycyclicmethylsilazane obtained from CMS + KH.

<sup>n</sup>HSZ2 from  $(\text{Me}_2\text{SiH})_2\text{NH} + \text{HSiCl}_3$ .

<sup>o</sup>HSZ3 =  $[\text{Me}_{2.6}\text{Si}_2(\text{NH})_{1.5}(\text{NHSiMe}_3)_{0.4}\text{Cl}_{0.15}]_{13}$ .

<sup>p</sup>APCMS = aminated PCMS.

<sup>q</sup>HSZ4 =  $(\text{Me})_{2.6}(\text{Si})_1(\text{NH})_{1.5}(\text{NHSiMe}_3)_{0.4}$ .

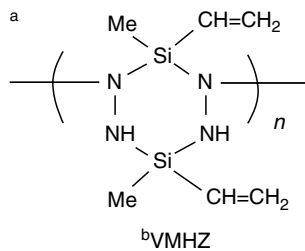
<sup>r</sup>APNES = aminated poly(N-ethyl)silazane,  $[\text{H}_2\text{Si}-\text{NEt}]_{nw}[\text{HSi}(\text{NH})_{0.5}-\text{NEt}]_x[\text{HSi}(\text{NH}_2)-\text{NEt}]_y[\text{HSi}(\text{NEtH})-\text{NH}]_z$ .

<sup>s</sup>Amorphous fiber.



TABLE 58.13. Continued.

Polymers	Pyrolysis condition, yield, and composition				(B)	Pyrolysis condition, yield, and composition			
	P <sup>a</sup>	Y	Residue and impurity	Refs.		Polymers	P <sup>a</sup>	Y	Residue and impurity
(1) VMHZ <sup>b</sup>	a	67	Si <sub>3</sub> N <sub>4</sub> , C, β-SiC (1,400 °C)	[172]	(12) VSA <sup>c</sup> (XL) <sup>d</sup>	f	83–85	Si <sub>3</sub> N <sub>4</sub> , SiC, C, Si	[177]
(2) VPS-I <sup>e</sup>	a	55	SiC	[173]	(13) VSA	f	59	Si <sub>3</sub> N <sub>4</sub> , SiC, C, Si	[177]
(3) VPS-I	b	47	amorph-Si <sub>3</sub> N <sub>4</sub> , < 2% C	[173]	(14) OVS <sup>f</sup>	f	83	SiCN, C	[178]
(4) VPS-II <sup>g</sup>	b		α-Si <sub>3</sub> N <sub>4</sub>	[174]	(15) OVNMS <sup>h</sup>	f	66	SiCN, C	[178,179]
(5) MPS-673 <sup>i</sup>	c	88	Si <sub>3</sub> N <sub>4</sub>	[175]	(16) OMS	f	46	SiCN, C	[178]
(6) HPZ-673 <sup>j</sup>	c	72	C: <0.4%	[175]	(17) VS/DMS <sup>k</sup>	f	63	SiCN, C	[178]
(7) PCS-823 <sup>l</sup>	c	81	O: 2.3–2.3%	[175]	(18) VS/MS <sup>m</sup>	f	77	SiCN, C	[178]
(8) MPS-673	d	52	SiC, Si-rich	[175]	(19) VS/MS <sup>n</sup>	g	72–87	Si <sub>3</sub> N <sub>4</sub> , SiC, C, SiO <sub>2</sub> (8.5%)	[179,180]
(9) HPZ-673	d	64	Si <sub>3</sub> N <sub>4</sub> , C	[175]	(20) PVSZ <sup>o</sup> (TXL) <sup>p</sup>	h	83	Si <sub>3</sub> N <sub>4</sub> , SiC, C, SiO <sub>2</sub>	[181]
(10) PCS-823	d	55	SiC, C rich	[175]	(21) PVSZ (UV) <sup>q</sup>	h	76	Si <sub>3</sub> N <sub>4</sub> , SiC, C, SiO <sub>2</sub>	[181]
(11) (A) <sup>r</sup>	e	40	Si <sub>3</sub> N <sub>4</sub>	[176]	(22) PMSZ <sup>s</sup>	h	81	Si <sub>3</sub> N <sub>4</sub> , SiC, C (7.5%), SiO <sub>2</sub>	[179]
					(23) PSSZ <sup>t</sup>	h	61	Si <sub>3</sub> N <sub>4</sub> , SiC, C, SiO <sub>2</sub> (8.4%)	[181]



<sup>b</sup>Pyrolytic conditions: a, 1,000 °C/N<sub>2</sub>; b, 1,000 °C/NH<sub>3</sub>; c, 1,500 °C/NH<sub>3</sub>; d, 1,200 °C/Ar; e, 1,400 °C/NH<sub>3</sub>; f, 1,000 °C/Ar, g, 1,400 °C/N<sub>2</sub>; h, 1,350 °C/Ar.

<sup>c</sup>VSA =  $\text{-(ViHSi-NH)-}_x$ .

<sup>d</sup>Cross-linked.

<sup>e</sup>VPS = vinyl polysilane; VPS-I =  $\{[(\text{SiMe}_3)_{0.32}][\text{SiViMe}]_{0.36}[\text{SiHMe}]_{0.18}[\text{SiMe}_2][\text{CH}_2\text{SiMe}_3]_{0.18}\}$

<sup>f</sup>OVS = oligovinylsilazane,  $\text{-(ViHSi-NH)-}_x$ .

<sup>g</sup>VPS-II =  $(\text{MeSi}_w(\text{ViSiMe})_x(\text{HSiMe})_y(\text{SiMe}_2)_z)_n$ .

<sup>h</sup>OVNMS = oligovinyl (N-methyl) silazane,  $\text{-(ViHSi-NMe)-}_x$ .

<sup>i</sup>MPS-673 = methylchloropolysilane heat-treated at 400 °C.

<sup>j</sup>HPZ-673 = hydridopolysilazane heat-treated at 400 °C.

<sup>k</sup>VS/DMS =  $\text{-(ViHSi-NH)-}_x(\text{Me}_2\text{Si-NH})_y$ .

<sup>l</sup>PCS-823 = polycarbosilane heat-treated at 550 °C.

<sup>m</sup>VS/MS =  $(\text{ViHSi-NH})_x(\text{MeHSi-NH})_y$ .

<sup>n</sup>Cross-linked and yield depended on heating rate (TGA).

<sup>o</sup>PVSZ =  $\text{-(ViHSi-NH)-}_x$ .

<sup>p</sup>Thermally cross-linked.

<sup>q</sup>UV radiation.

<sup>r</sup>(A) = Si<sub>1</sub>C<sub>1.93</sub>H<sub>4.7</sub>O<sub>0.01</sub>N<sub>0</sub>.

<sup>s</sup>PMSZ = poly(methylsilazane).

<sup>t</sup>PSSZ = phenylsilsequizane.

The cyclic product,  $[\text{CH}_3\text{SiH-NH}]_x$  can undergo ammonium-salt-induced polymerization to give a product (MHPS2). Dehydrocyclodimerization (DHCD) reaction of MHPS1 by using KH gives MHPS3 whose approximate structure can be expressed as  $(\text{CH}_3\text{SiH-NH})_{0.39}(\text{CH}_3\text{SiH-NCH}_3)_{0.04}(\text{CH}_3\text{SiN})_{0.57}$ . MHPS3 has been demonstrated to consist of the structure shown below. The ceramic

yields (TGA, 1,000 °C/N<sub>2</sub>) of MHPS1, MHPS2, and MHPS3 were found to be 20%, 36%, and 80–85%, respectively, thus illustrating the advantage gained by the DHCD reaction [the composition for MHPS3 consisted of Si<sub>3</sub>N<sub>4</sub>, SiC with some C and SiO<sub>2</sub>(?)]. Equally important other studies to increase molecular weight and/or yield by modifying preformed precursors have also been undertaken by

**TABLE 58.13.** *Continued.*

Precursors	(C)		Pyrolysis condition, yield, and composition	References
	P <sup>a</sup>	Y		
(1) $\text{-(SiViH-NH)-}$	a		Si <sub>3</sub> N <sub>4</sub> (30%); SiCN (26%), C (44%)	[182]
(2) $\text{-(SiViH-NMe)-}$	a		Si <sub>3</sub> N <sub>4</sub> ; SiC (9.7%), C, SiO <sub>2</sub> (5%)	[179]
(3) $\text{-(MeSiVi-NH)-}_x\text{-(XL)}^b$	b		$\alpha\beta\text{-Si}_3\text{N}_4$	[183]
(4) $\text{-(MeSiVi-NH)-}_x\text{-}$	c		$\alpha,\beta\text{-SiC}$	[183]
(5) $\text{-(MeSiVi-NH)-}_x$	d	64–67	NDG	[184]
(6) $\text{-(Me}_2\text{Si-NH)-}$	e	5–10	Si <sub>3</sub> N <sub>4</sub> (30–40%), NDG	[185]
(7) $\text{-(MeSiH-NMe)-}$	e	15–20	Si <sub>3</sub> N <sub>4</sub> (50–60%), NDG	[185]
(8) $\text{-(MeSiH-NMe)-}_{n/2}\text{-(MeSiH-NH)-}_{n/2}$	e	50–55	Si <sub>3</sub> N <sub>4</sub> (80–85%), NDG	[185]
(9) $[\text{MeSiH-NH}]_{0.8}[\text{MeSiVi-NH}]_{0.2}]_x$	f	54	NDG	[186] <sup>c</sup>
(10) $[\text{MeSiH-NH}]_{0.8}[\text{MeSiVi-NH}]_{0.2}]_x$ (CD) <sup>d</sup>	f	84	NDG	[186]
(11) $[\text{MeSiH-NH}]_{0.8}[\text{MeSiVi-NH}]_{0.2}]_x$	g		$\alpha,\beta\text{-Si}_3\text{N}_4$	[186]
(12) $[\text{MeSiH-NH}]_{0.8}[\text{MeSiVi-NH}]_{0.2}]_x$	h		$\beta\text{-SiC}$ ; Si (8%), N (1%)	[186]
(13) Polymethylsilazane	i	84	SiCN	[187]
(14) $[(\text{NH}_2)\text{SiH-N}(\text{CH}_3)]_x$	j		Si <sub>3</sub> N <sub>4</sub> (82%?)	[12b]
(15) $[(\text{CH}_3\text{NH})\text{SiH-N}(\text{CH}_3)]_x$	j		Si <sub>3</sub> N <sub>4</sub> (69%?); SiC <sup>d</sup>	[12b]
(16) $\text{-(NH}_2\text{)SiVi-NH-}_x$	j		Si <sub>3</sub> N <sub>4</sub> (74%?) + SiC + C <sup>e</sup>	[12b]
(17) $[(\text{NHCH}_3)\text{SiVi-N}(\text{CH}_3)]_x$	k		Si <sub>3</sub> N <sub>4</sub> (70%?) + SiC + C <sup>e</sup>	[12b]
(18) Me (Me) $\text{-(Si}_2\text{N}_2\text{Me}_2\text{-Vi(Me) + AIBN)}$	l	42	Si <sub>1</sub> N <sub>0.9</sub> C <sub>1.59</sub> O <sub>0.12</sub> H <sub>0.32</sub>	[140]

<sup>a</sup>Pyrolytic conditions: a, 1400 °C/Ar; b, 1500 °C; c, 1650 °C; d, 1000 °C/Ar; e, 800 °C/N<sub>2</sub>; f, 950 °C/N<sub>2</sub>; g, 1000 degC/NH<sub>3</sub> then 1600 °C/Ar; h, 1600 °C/Ar; i, 1300 °C/?; j, 1000 °C/N<sub>2</sub>; k, 1500 °C/N<sub>2</sub>; l, 1000 °C/He.

<sup>b</sup>Crosslinked.

<sup>c</sup>Related work can also be found in Ref. 188.

<sup>d</sup>Cured.

<sup>e</sup>Minor product.

several groups of scientists although these works are not discussed here in any detail [156–160].

In Table 58.13 [153,161–187] various polysilazanes, polysilsequizanes, polyvinylsilazanes, polycarbosilazanes, and some isocyanate modified systems [186,187] are presented. The data should be fairly self-explanatory and the original publications can be consulted for additional information.

The influence of pyrolysis atmospheres (inert versus oxidative and reactive), heating rates, duration of pyrolysis on ceramic yield, and composition can be gleaned from the various tables. There is, thus, a need to pay attention to the effects of pyrolysis conditions. As an example, work by Bahloul, Pereira, and Goursat [179,180] summarized in Table 58.14 can illustrate the point. While there was only very little change in the composition of VS/MS [entry (19), Table 58.13(b)] pyrolyzed at 1,200 and 1,400 °C in N<sub>2</sub> and Ar (for 1 h), the pyrolysis at 1,450 °C, 24 h in Ar, drastically changed the composition for VS/MS. For the purpose of comparison, compositional data are also included for VMSZ  $\text{-(ViSiH-NMe)-}$ . The theoretical formula for VMSZ is SiC<sub>3</sub>NH<sub>7</sub> and that for VS/MS SiC<sub>1.5</sub>NH<sub>5</sub>. The former precursor has a higher carbon content and led to about half as much SiC and about twice as much excess C although the compositions of Si<sub>3</sub>N<sub>4</sub> were comparable (at 1,400 °C).

Pyrolysis of poly(ureasilanes) (PUSZ) to 1,000 °C under an argon flow gives silicon carbonitride ceramics in 61–76% yield [189], which is significantly higher than that form the linear silazane oligomers  $\text{[-CH}_3\text{(H)Si-NH-]}_n$  of similar mass. The observed improvement may be a combined contribution from inclusion of urea bond linkage ( $\text{-NH-CO-NH-}$ ) and formation of a cyclic structure. Poly(ureamethylvinyl)silazane (PUMVS) can also be thermally converted to an infusible solid at  $T > 250$  °C. Subsequent pyrolysis of the cross-linked products at  $\sim 1,000$  °C yields amorphous silicon carbonitride (Si/C/N) ceramics

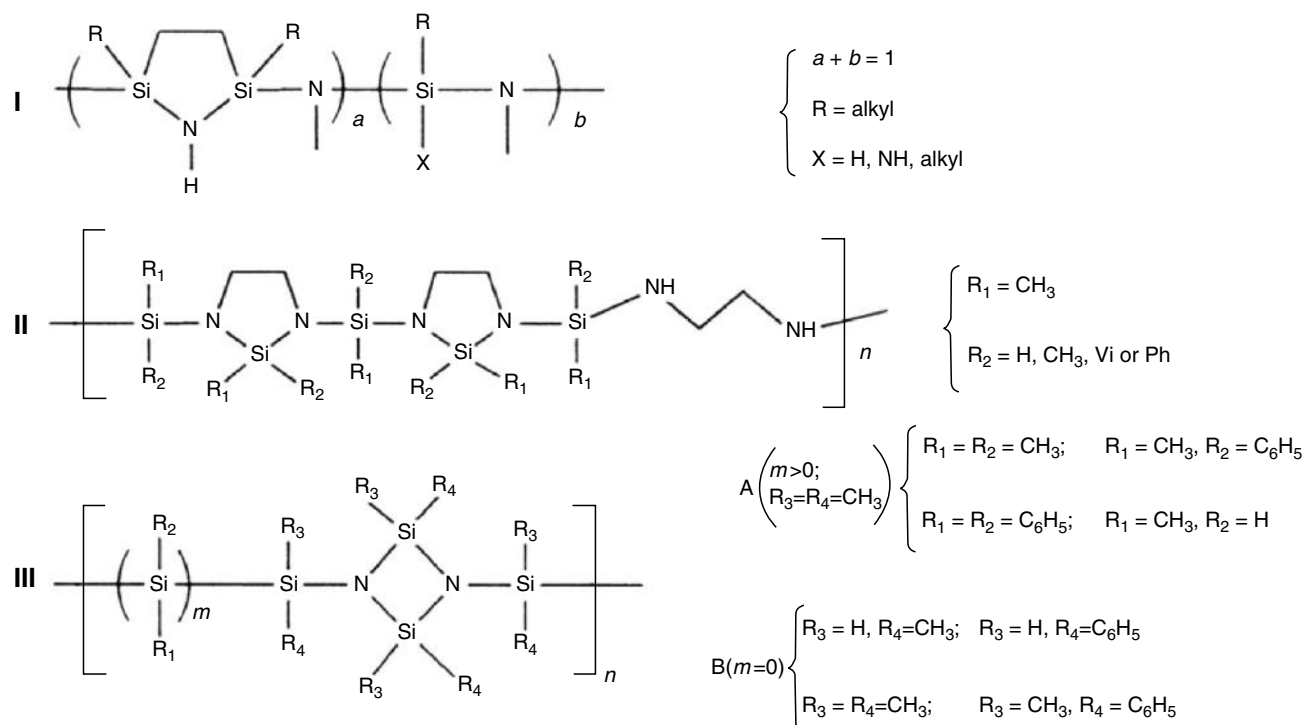
**TABLE 58.14.** *Composition of residue from VS/MS and VMSZ [179,180].*

Pyrolysis conditions	Composition (wt%)			
	Si <sub>3</sub> N <sub>4</sub>	SiC	SiO <sub>2</sub>	C
1,200 °C/Ar, 1 h	55.3	21.6	5.3	17.8
1,400 °C/Ar, 1 h	55.9	21.1	5.7	17.3
1,400 °C/N <sub>2</sub> , 1 h	54.3	20.2	8.5	17.0
1,400 °C/Ar, 1 h (VMSZ)	54.4	9.7	4.8	31.1
1,450 °C/Ar, 24 h	5.7	86.4	2.6	5.3

in ~70% yield with an empirical composition of  $\text{SiN}_{0.82}\text{C}_{0.86}$  [190].

### 58.5.3 Other Systems

There are at least three structurally related polysilazanes that contain cyclic disilazane structures in the main back-



(wt%) of the  $\text{Si}_3\text{N}_4$  residue was Si (57), N (37.9), C (0.3), H (0.2), and O (3.1), while that for the silicon carbonitride was Si (55.4), N (33.3), C (7.0), H (0.3), and O (1.0). System II with  $\text{R}_1 = \text{CH}_3$  and  $\text{R}_2$  being H,  $\text{CH}_3$ , Ph, and vinyl groups have been investigated [192–194]. As an example, the ceramic residue at 1,000 °C/ $\text{N}_2$  (TGA, 10 °C/min) for the  $\text{R}_1 = \text{CH}_3$  and  $\text{R}_2 = \text{vinyl}$  case was found to be 64% with an elemental composition of  $\text{Si}_1\text{N}_{1.07}\text{C}_{1.73}\text{O}_{0.13}$ . No pyrolysis data was reported for system IIIA [195,196]. Pyrolysis of IIIB (at 900 °C in  $\text{N}_2$ ) shows that the polymers with reactable Si–H group give higher ceramic yield (~69% when  $\text{R}_3 = \text{H}$  and  $\text{R}_4 = \text{CH}_3$ ) [197]. Upon heating to >1,500 °C, the pyrolyzed residues are crystallized to give  $\text{Si}_3\text{N}_4$  (~74 wt%) and SiC (~25%).

Furthermore, work by Baldus *et al.* [198] indicated that the novel compound  $\text{SiPN}_3$  has been prepared by reacting  $\text{Cl}_3\text{Si}-\text{N}=\text{PCl}_3$  with liquid ammonia, giving  $\text{SiPN}(\text{NH})(\text{NH}_2)_4$  (system IV) as a precursor. Pyrolysis of system IV is reported to proceed according to  $\text{IV} \rightarrow \text{SiPN}_3 + 3\text{NH}_3$  with a ceramic yield of 72% (900 °C/ $\text{NH}_3$ ). Crystalline  $\text{SiPN}_3$  is, in turn, reported

to decompose between 900 and 1,000 °C, giving  $\text{Si}_3\text{N}_4$  according to  $12\text{SiPN}_3 \rightarrow 4\text{Si}_3\text{N}_4$  (amorphous) +  $3\text{P}_4$  +  $10\text{N}_2$   $\xrightarrow{1,000^\circ\text{C}}$   $\alpha\text{-Si}_3\text{N}_4$  with a yield of 42.4%. The phosphorous and oxygen content was reported to be extremely low (200 and 200–400 ppm, respectively).

As seen in Table 58.12, pyrolysis of polysilazanes typically give silicon nitride/silicon carbide-based composites with chemical compositions at  $\text{Si}_x\text{C}_y\text{N}_z$  ( $z < 4/3x$ ). As a result of mismatched ratio among ceramic elements, the obtained ceramic residues often contain “free” carbon impurity, which may ultimately weaken the oxidativative stability at elevated temperature. Polysilazanes of formula  $[(\text{SiH}_2-\text{NH})_3(\text{MeSiH}-\text{NH})]_n$  and  $[(\text{SiH}_2-\text{NH})_3(\text{SiH}_2-\text{NMe})]_n$  [199], which are designed specifically to release  $\text{Si}_3\text{N}_4/\text{SiC}$  composites, are shown to be pyrolyzed into ceramics in 77 and 83% yields, respectively. Cross-linking of the polymer samples significantly improves their ceramic yield to ~94%. Neutron wide angle scattering proved the absence of “free” carbon phase in the  $\text{Si}_3\text{N}_4/\text{SiC}$  composites. Additional examples of polysilazanes can be found in reviews [200,201].

### 58.6 PYROLYSIS ON SOME BORON-CONTAINING PRECURSORS

Recent studies have shown that incorporation of boron element into silicon-based ceramics increases their thermal stability and retard crystallization [202–204]. For example, the materials of the binary system Si—N start to crystallize at  $T=1,000\text{ }^{\circ}\text{C}$  forming  $\alpha\text{-Si}_3\text{N}_4$ , while metastable solid solutions of the ternary and quaternary systems Si—C—N and Si—B—C—N withstand crystallization up to 1,450 and 1,700  $^{\circ}\text{C}$ , respectively [205]. In order to form an amorphous uniform phase in the final multinary ceramics, the ceramic elements are preferably distributed homogeneously in the preceramic polymers. The general consensus in the ceramics community is that the quaternary system Si—B—C—N as well as the ternary systems Si—B—N and Si—B—C would be particularly suitable for producing amorphous ceramics that resist the microstructural changes even at top loads.

Some representative examples are listed in Table 58.15. Thermal condensation of borazine ( $\text{B}_3\text{N}_3\text{H}_6$ ) with silazanes

produces copolymers with highly branched structures (entry 1 and 2). Pyrolysis of the borazine-containing polymer in the entry 1 yields B/N/Si ceramics with trace carbon contamination, while that in the entry 2 gives B/N/Si/C ceramics. Both ceramic products are amorphous up to 1,400  $^{\circ}\text{C}$  [206]. Hydroboration of 2,4,6-trimethyl-2,4,6-trivinylcyclotrisilazane (TMTVS) with borazine affords the polymer in the entry 4, which leads to B/N/Si/C ceramics upon pyrolysis at 1,000  $^{\circ}\text{C}$  [208]. In comparison with the borazine-containing polymers in the entry 1 and 2, the polymer in the entry 4 gives a higher ceramic yield, as hydroboration in the latter maintains the structural integrity of cyclotrisilazane ring. In the entry 5, hydroboration of TMTVS with borane in dry toluene gives polymers **A** (a colorless liquid), **B** (a hard glassy solid), and **C** (a white powder) [209]. Polymers **B** and **C** can not be redissolved once the solvent is removed, indicating a relatively high degree of branching or cross-linking and a higher content of boron (than polymer **A**). The relative contents of boron element in the ceramic products are in the same order found in the polymer precursors:  $\text{A} < \text{B} < \text{C}$  (the empirical formula for precursors **A**,

**TABLE 58.15.** Pyrolysis data on boron-containing precursors with various structures.

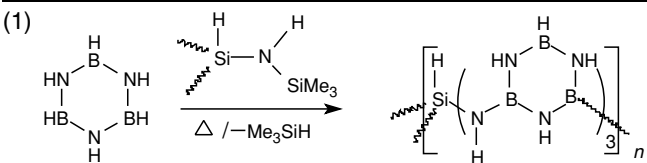
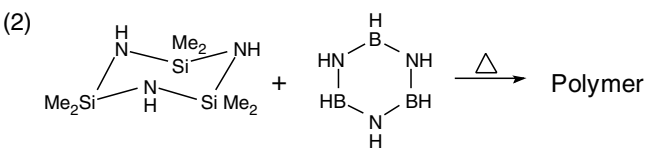
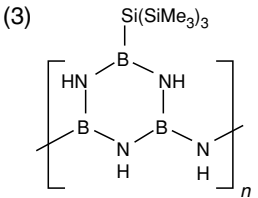
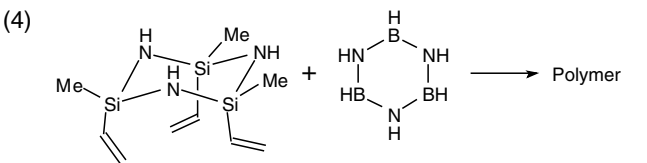
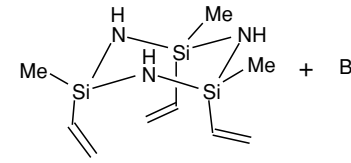
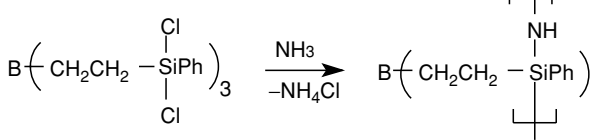
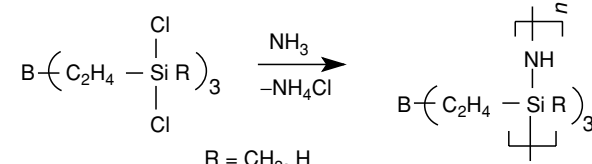
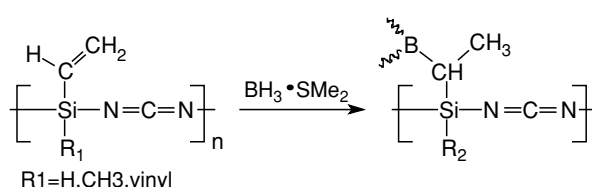
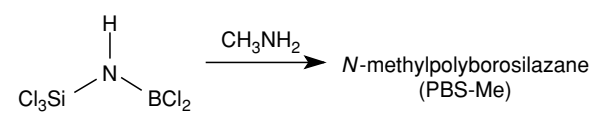
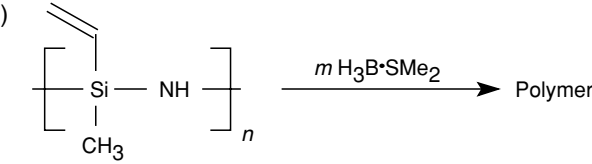
Polymer precursors	Pyrolysis condition, yield, and composition				
	Pyrolytic condition	Yield (%)	System	Composition	References
(1) 	1,400 $^{\circ}\text{C}$ (Ar)	38–42	B/N/Si	From $\text{B}_{1.00}\text{N}_{1.05}\text{Si}_{0.17}\text{C}_{0.01}$ to $\text{B}_{1.00}\text{N}_{1.17}\text{Si}_{0.19}\text{C}_{0.05}$	[206]
(2) 	1,400 $^{\circ}\text{C}$ (Ar)	43–58	B/N/Si/C	From $\text{B}_{1.00}\text{N}_{1.40}\text{Si}_{0.35}\text{C}_{0.21}$ to $\text{B}_{1.00}\text{N}_{1.48}\text{Si}_{0.37}\text{C}_{0.23}$	[206]
(3) 	1,400 $^{\circ}\text{C}$ (N <sub>2</sub> )	47%	B/N/Si/C	$\text{B}_{1.00}\text{N}_{1.28}\text{Si}_{0.29}\text{C}_{0.10}$	[207]
(4) 	1,000 $^{\circ}\text{C}$ (Ar)	73–77	B/N/Si/C	—	[208]

TABLE 58.15. Continued.

Polymer precursors	Pyrolysis condition, yield, and composition				
	Pyrolytic condition	Yield (%)	System	Composition	References
(5) 	1,000 °C (N <sub>2</sub> )	40–55	B/N/Si/C	B <sub>0.29</sub> N <sub>2.13</sub> Si <sub>3.0</sub> C <sub>4.18</sub> B <sub>0.82</sub> N <sub>2.58</sub> Si <sub>3.0</sub> C <sub>5.03</sub> B <sub>1.93</sub> N <sub>2.40</sub> Si <sub>3.0</sub> C <sub>5.83</sub>	[209]
(6) 	1,050 °C (Ar)	75	B/N/Si/C	From B <sub>1.0</sub> N <sub>2.8</sub> Si <sub>2.9</sub> C <sub>4.5</sub> to B <sub>1.0</sub> N <sub>2.8</sub> Si <sub>3.0</sub> C <sub>4.4</sub>	[210]
(7) 	1,000 °C (Ar)	83 (R=H) 52–55 (R=CH <sub>3</sub> )	B/N/Si/C	—	[211– 212]
(8) 	1,100 °C (Ar)	53 (R <sub>1</sub> =H) 63 (R <sub>1</sub> =CH <sub>3</sub> ) 70–75 <sup>a</sup>	B/N/Si/C	—	[211, 215, 216]
(9) 	1,200 °C (N <sub>2</sub> )		B/N/Si or B/N/Si/C	B <sub>1.0</sub> N <sub>2.3</sub> Si <sub>1.0</sub> C <sub>0.8</sub>	[216, 217]
(10) 	1,400 °C (Ar)		<i>m/n</i> = 0	<b>D:</b> SiC <sub>1.6</sub> N <sub>1.0</sub> <b>E:</b> SiC <sub>1.5</sub> N <sub>1.0</sub> B <sub>0.15</sub> <b>F:</b> SiC <sub>1.6</sub> N <sub>1.0</sub> B <sub>0.22</sub> <b>G:</b> SiC <sub>1.7</sub> N <sub>1.0</sub> B <sub>0.28</sub> <b>H:</b> SiC <sub>1.7</sub> N <sub>1.0</sub> B <sub>0.37</sub>	[218]

molar ratio (*m:n*) = 0, 1:8, 1:5, 1:4, and 1:3.

<sup>a</sup>R<sub>1</sub>=vinyl, R<sub>2</sub>=-C<sub>2</sub>H<sub>4</sub>B=.

**B**, and **C** are Si<sub>3.0</sub>N<sub>3.0</sub>B<sub>0.33</sub>C<sub>9.0</sub>H<sub>22.0</sub>, Si<sub>3.0</sub>N<sub>3.0</sub>B<sub>1.0</sub>C<sub>9.0</sub>H<sub>24.0</sub>, Si<sub>3.0</sub>N<sub>3.0</sub>B<sub>3.0</sub>C<sub>9.0</sub>H<sub>30.0</sub>, respectively).

Pyrolysis of poly(organoborosilazane) (entry 6) under argon at 1,050 °C gives an amorphous ceramics, which resist crystallization up to 1,700 °C and thermally degradation up to 2,200 °C [210]. It should be noticed that the ratio of ceramic elements (B:Si:N) in the ceramic chars is about the same as that in the polymer precursors, illustrating the importance to control the ratio of ceramic elements in the preceramic polymers. Ceramic fibers can be obtained from this type of polymer for high temperature application

[212]. Boron-containing polysilylcarbodi-imides (entry 8) also give amorphous ceramics upon pyrolysis to 1,100–1,400 °C, whose compositions as thermolyzed ceramics are located in or close to the phase fields BN + Si<sub>3</sub>N<sub>4</sub> + C, BN + Si<sub>3</sub>N<sub>4</sub> + SiC + C, BN + SiC + C, or BN + B<sub>4+δ</sub>C + SiC + C. Comparison of ceramics from five different samples at 1,600–2,000 °C shows that the SiC-poor (Si<sub>3</sub>N<sub>4</sub>-rich) materials are not high-temperature stable, whereas SiC-rich (Si<sub>3</sub>N<sub>4</sub>-poor) materials are mass stable up to 2,000 °C [215(b)]. Pyrolysis of N-methylpolyborosilazane (entry 9) produces amorphous SiBN<sub>3</sub>C ceram-

ics, which is stable up to 1,800 °C with respect to weight loss and microstructure changes [217]. The polymer precursor can be processed to a green fiber by melt-spinning, which then undergoes an intermediate curing step and successive pyrolysis into ceramic fiber.

Controlled hydroboration of  $[-\text{MeSi}(\text{Vi})-\text{NH}-]_n$  with  $\text{BH}_3$  leads to precursors with different content of boron (entry 10), which are then converted to ceramics at 1,400 °C [218]. The thermal stability of the obtained amorphous ceramics is strongly dependent on the boron content. The boron-free ceramics (sample **D**), which is obtained from the pyrolysis of the parent polymer  $[-\text{MeSi}(\text{Vi})-\text{NH}-]_n$ , decomposes at about 1,500 °C. The decomposition temperatures of the boron-modified ceramics **E** and **F** are raised to 1,650 °C and 1,900 °C, respectively, showing that boron not only retards the crystallization of SiC and  $\text{Si}_3\text{N}_4$  but also protects the thermodynamically not stable  $\text{Si}_3\text{N}_4$  against decomposition at elevated temperature.

### 58.7 CONVERSION STUDIES, USES, AND APPLICATIONS

Conversion of a precursor to its respective ceramics involves numerous reactions. During the pyrolysis process, volatile organic species are generated and eliminated, which may drastically lower the ceramic yield. Cross-linking of the preceramic polymers before pyrolysis is often necessary to help retention of the ceramic elements in the solid states, thereby improving the desirable ceramic yields. As an additional example, pyrolysis of linear poly(vinylsilane),  $[-\text{CH}_2-\text{CH}(\text{SiH}_3)-]_n$ , in argon to 1,500 °C gives only about 40% ceramic yield. The crosslinked (but still soluble) poly(vinylsilane), however, substantially improves the ceramic yield to 70–80% [219].

In order to control the chemical composition and microstructure of the final ceramic produce, it is of great value to understand the nature, rates, and mechanisms of the gaseous product evolution at various stages of the thermal conversion process. Mass spectrometry (MS) in conjunction with TGA provides useful suggestions about the reaction mechanisms responsible for the mass loss. XRD and solid state NMR ( $^{11}\text{B}$ ,  $^{13}\text{C}$ ,  $^{15}\text{N}$ , and  $^{29}\text{Si}$ ) becomes a powerful tool to reveal chemical environmental changes in the ceramic residues during the pyrolysis conversion. There are several cases of studies dealing with conversions processes as studied by NMR [220] other than those already cited and with uses and/or applications as fibers, films, coatings, binders, etc. For example, the pyrolytic conversion of polysilazane precursors  $[(\text{ViSiH}-\text{NH})_{0.5}-(\text{MeSiH}-\text{NH})_{0.5}]$  to ceramics is studied by means of TGA, MS, solid-state NMR, and X-ray diffraction [220(f,g)]. Mass losses of ~3% and ~11% were observed at 200–400 °C (releasing ammonia) and 400–800 °C (releasing methane, hydrogen, and to a lesser extent, ethene and propene), respectively, producing a ceramic char

in about 80% yield. Although the major chemical composition change of the ceramics occurs within the temperature range of 400–800 °C, the amorphous silicon carbonitride was formed in 800–1,400 °C (by  $^{29}\text{Si}$  and  $^{13}\text{C}$  NMR data), and crystallization in the ceramics can only be observed after heating the ceramics to above 1,450 °C.

Currently, preceramic polymers are successfully used to produce ceramic fibers, coatings, joints, porous materials, nanotubes, and ceramic composites. For further appraisal of the efforts in uses and/or applications of SiC and  $\text{Si}_3\text{N}_4$  precursors, the references in the Ref. [1,7,14] and other reviews [221–227], as well as in some of the recent work [228] pertaining to fiber processing and property thereof, uses and/or applications can be consulted. Thermal stability of the ceramic composite products has been constantly improved for high-temperature engine applications [229,228(1)], which will enable high-efficiency use of energy resources and reduce burden on the environment. Precursor-derived sintered SiC fibers are stable at 2,200 °C [230]. Smooth continuous SiC films have been recently demonstrated through pyrolysis of polymethylsilyne  $[\text{SiMe}]_n$  [231]. Porous ceramic foams with variable cell sizes (100–600  $\mu\text{m}$ ) [232–240] and ceramic microtubes [241–243] can be obtained via pyrolysis of a preceramic polymer. Blend of different preceramic polymers can lead to a phase-separated mixture in nanosized domain. Direct pyrolytic conversion of such phase-separated mixture to ceramics [244] could retain the microstructure developed in the polymer blend, thereby offering an attractive route to nano ceramic composites. The composition of the SiC– $\text{Si}_3\text{N}_4$  composites can be controlled by adjusting the ratio of polymer precursors (e.g., polysilanes and polycyclodisilazanes) in the blends [245].

### 58.8 SUMMARY

Preceramic polymers offer an exciting alternative route to fabricate ceramics. In principle, these polymers can be fabricated into any desirable shapes, and then converted through pyrolysis to ceramics. Over the past two and half decades, research activities in this field have led to the development of many useful materials, which include commercial transformation of polycarbosilane into silicon carbide fiber (NICALON). Pyrolytic conversion of a preceramic polymer to its ceramics products typically accompanies a high level of volume shrinkage, which remains to be a barrier for the full development of preceramic polymer technology. The volume shrinkage can be minimized by choosing the polymer of high ceramic yields and using a controllable pyrolytic degradation condition, which allows cross-linking prior to the ceramic conversion. Conversion of molecular precursors into hybrid materials with desirable nanostructures remains to be a challenge [246,247].

This review has attempted to focus on ceramic yields and compositions of residues obtained from a host of SiC and

Si<sub>3</sub>N<sub>4</sub>/SiC precursors, and the presence of deleterious impurity elements is very apparent in most cases. The impurities in the form of SiO<sub>2</sub>, excess Si and C, etc. can lead to decomposition reactions as well as affect crystallization, thermodynamic, and kinetic reactions, particularly at high temperatures. Combined interests in energy conservation and nano science will continue to foster activities in the multicomponent ceramic products of suitable microstructures, which exhibit superior thermal stability for the fuel-efficient high-temperature engine and other applications. Protective defect-free ceramic coatings, which are covalently bond to carbon fibers or light metal surfaces to extend their service life, will enable advanced technology in various industries such as automobile [248], if cost effective ceramic composites is realized.

## ACKNOWLEDGMENTS

Support from NASA through Center for High Performance Polymers and Composites is acknowledged.

## REFERENCES

- (a) K. J. Wynne and R. W. Rice, *Annu. Rev. Mater. Sci.* **14**, 297 (1984); (b) M. Birot, J.-P. Pillot, and J. Dunogues, *Chem. Rev.* **95**, 1443 (1995); (c) A. R. Bunsell and M.-H. Berger, *J. Eur. Ceram. Soc.* **20**, 2249 (2000).
- (a) D. L. Segal, *Br. Ceram. Trans. J.* **85**, 184 (1986); (b) K. Komeya, *Am. Ceram. Soc. Bull.* **63**, 1158 (1984); (c) N. N. Ault and S. D. Hartline, *Am. Ceram. Soc. Bull.* **5**, 773 (1987); (d) S. B. Hanna, N. A. L. Mansour, A. S. Tails, and H. M. A. Abd-allah, *Br. Ceram. Trans. J.* **84**, 18 (1985).
- S. Yajima, K. Okamura, J. Hayashi, and M. Omori, *J. Am. Ceram. Soc.* **59**, 324 (1976).
- J. P. Riggs, *Encycl. Polym. Sci. Eng.* **2**, 640 (1988);
- R. A. Sinclair, in *Ultrastructure Processing of Ceramics, Glasses and Composites*, edited by L. L. Hench and D. R. Ulrich (Wiley-Interscience, New York, 1984), p. 256.
- (a) R. W. Rice, *Am. Ceram. Soc. Bull.* **62**, 889 (1983); (b) B. E. Walker, Jr., R. W. Rice, P.F. Becker, B. A. Bender, and W. S. Coblenz, *Am. Ceram. Soc. Bull.* **62**, 619 (1983); (c) R. Baney and G. Chandra, in *Concise Encyclopedia of Polymer Science and Engineering*, edited by J. I. Kroschwitz and P. M. Siegel (Wiley-Interscience, New York, 1990), p. 899; (c) D. Segal, *Chemical Synthesis of Advanced Ceramic Materials* (Cambridge University Press, New York, 1989).
- For an overview see: (a) D. Seyferth, *Adv. Chem. Ser.* **245**, 131 (1995); (b) R. M. Laine and A. Sellinger, Si-containing ceramic precursors. In *The Chemistry of Organic Silicon Compounds*, vol. 2, chapter 39, edited by Z. Rappoport and Y. Apeloig (John Wiley & Sons Ltd., 1996), pp. 2245–2315; (c) J. Livage, C. Sanchez and F. Babonneau, Molecular precursor routes to inorganic solid. In *Chemistry of Advanced Materials: An Overview*, chapter 9, edited by L. V. Interrante and M. J. Hampden-Smith (Wiley-VCH, 1998), pp. 389–448; (d) R. Richter, G. Roewer, U. Böhme, K. Busch, F. Babonneau, H. P. Martin, and E. Müller, *Appl. Organomet. Chem.* **11**, 71 (1997).
- G. Pouskouleli, *Ceram. Int.* **15**, 213 (1989).
- G. D. Soraru, F. Babonneau, and J. D. Mackenzie, *J. Non-Cryst. Solids* **106**, 256 (1988).
- (a) C. H. Anderson and R. Warren, *Composites* **15**, 16 (1984); (b) C. H. Anderson and R. Warren, *Composites*. **15**, 101 (1984).
- (a) A. Zangvil, Y.-W. Chang, N. Finnegan, and J. Lipowitz, *Ceram. Int.* **18**, 271 (1992); (b) A. Kato, H. Mizumoto, and Y. Fukushige, *Ceram. Int.* **10**, 37 (1984).
- (a) O. Devverdier, M. Monthieux, D. Mocaer, and R. Pallier, *J. Eur. Ceram. Soc.* **12**, 27 (1993); (b) B. Kanner and R. E. King III, in *Silicon-Based Polymer Science: A Comprehensive Resource*, edited by J. M. Zeigler and F. W. G. Fearon (American Chemical Society, Washington, D.C. 1990), p. 607; (c) G. S. Bibbo, P. M. Benson, and C. G. Pantano, *J. Mater. Sci.* **26**, 5075 (1991).
- K. Okamura, H. Ichikawa, M. Takeda, T. Sefachi, N. Kaoai, and M. Nishii, U.S. Patent No. 5,283,044 (February 1, 1994).
- R. M. Laine and F. Babonneau, *Chem. Mater.* **5**, 260 (1993).
- D. Seyferth, C. Strohmann, H. J. Tracy, and J. L. Robinson, *Mater. Res. Soc. Symp. Proc.* **249**, 3 (1992).
- R. M. Laine, Y. D. Blum, R. D. Hamlin, and A. Chow, National Technology Information Service Technical Report No. 5, Order No. AD-A178136, 1987.
- M. C. Parche, in *Kirk-Othmer Encyclopedia of Chemical Technology*, vol. 4, edited by H. F. Mark, J. J. Meketta, Jr., and D. F. Othmer, 2nd edition (Interscience, John Wiley, New York, 1964), pp. 114–132.
- (a) A.R. Verma and P. Krishna, in *Polymorphism and Polytypism in Crystals* (Wiley, New York, 1966); (b) *Gmelin Handbook of Inorganic Chemistry*, 8th ed., edited by J. Schlichting, G. Czack, E. Koch-Bienemann, P. Kuhn, and F. Schroder (Springer, New York, 1984), Suppl. vol. B2, Si-Silicon; (c) P. T. B. Shaffer, *Acta Crystallogr.* **B 25**, 477 (1969).
- (a) R. Marchand, Y. Laurent, and J. Lang, *Acta Crystallogr.* **B 25**, 2157 (1969); (b) K. Kato, Z. Inoue, K. Kijima, and J. Kawada, *J. Am. Ceram. Soc.* **58**, 90 (1975); (c) R. Gran, *Acta Crystallogr.* **B 35**, 800 (1979).
- (a) *Silicon Carbide-1973*, edited by R. C. Marshall, J. W. Faust, Jr., and C. E. Ryan (University of South Carolina Press, Columbia, 1974); (b) *Silicon Carbide Ceramics*, edited by S. Somiya and Y. Inomata (Elsevier Applied Science, London, 1991).
- (a) G. R. Terwillinger, *J. Am. Chem. Soc.* **57**, 48 (1974); (b) T. Ekstrom, *Mater. Forum* **17**(1), 62 (1993); (c) R. N. Katz, *Ind. Ceram.* **17**(3), 158 (1997).
- R. West, *J. Organomet. Chem.* **300**, 327 (1986).
- (a) R. Baney and G. Chandra, in *Encyclopedia of Polymer Science and Engineering*, edited by H. F. Mark, N. M. Bikales, C. G. Overberger, G. Menges, and J. I. Kroschwitz (Wiley-Interscience, New York, 1988), Vol. 13, p. 312, and references therein; (b) P. Trefonas, in *Encyclopedia of Polymer Science and Engineering*, edited by H. F. Mark, N. M. Bikales, C. G. Overberger, G. Menges, and J. I. Kroschwitz (Wiley-Interscience, New York, 1988), vol. 13, p. 162.
- R. R. Wills, R. A. Markle, and S. P. Mukherjee, *Am. Ceram. Soc. Bull.* **62**, 904 (1983).
- R. D. Miller and J. Michl, *Chem. Rev.* **89**, 1359 (1989).
- Z. F. Zhang, Y. Mu, F. Babonneau, R. M. Laine, J. E. Harrod, and J. A. Rahn, in *Inorganic and Organometallic Oligomers and Polymers*, edited by J. F. Harrod and R. M. Laine (Kluwer Academic, Boston, 1991), p. 127.
- H. R. Allcock, in *Chemical Processing of Advanced Materials*, edited by L. L. Hench and J. K. West (Wiley, New York, 1992), p. 699.
- G. Soula, in *Inorganic and Organometallic Polymers with Special Properties*, edited by R. M. Laine (Kluwer Academic, Boston, 1992), p. 31.
- R. West, in *Inorganic Polymers*, edited by J. E. Mark, H. R. Allcock, and R. West (Prentice Hall, Englewood Cliffs, NJ, 1992), p. 186.
- R. Richter, G. Roewer, K. Leo, and B. Thomas, *Friberg. Forschungsh. A* **832**, 99 (1993).
- (a) *Silicon-Based Polymer Science: A Comprehensive Resource*, edited by J. M. Zeigler and F. W. G. Fearon (American Chemical Society, Washington, D.C., 1990), Chaps. 31–34; (b) P. Kochs In *Silicon in Polymer Synthesis*, edited by H. R. Kricheldorf (Springer, Berlin 1996), pp.223–287.
- T. Yamamura, *Polym. Prepr. (Am. Chem. Soc. Div. Polym. Chem.)* **25**, 8 (1984).
- F. Babonneau, J. Livage, G. D. Soraru, G. Carturan, and J. D. Mackenzie, *New J. Chem.* **14**, 539 (1990).
- S. Yajima, J. Hayashi, M. Omori, and K. Okamura, *Nature* **261**, 683 (1976).
- R. West, L. Nozue, X.-H. Zhang, and P. Trefonas, *Polym. Prepr. (Am. Chem. Soc. Div. Polym. Chem.)* **25**, 4 (1984).
- R. West, L. D. David, P. I. Djurovich, H. Yu, and R. Sinclair, *Am. Ceram. Soc. Bull.* **62**, 899 (1983).

37. R. West, L. D. David, P. L. Djurovich, K. L. Stearley, K. S. V. Srinivasan, and H. Yu, *J. Am. Chem. Soc.* **103**, 7352 (1981).
38. R. Riedel, K. Strecker, and G. Petzow, *J. Am. Chem. Soc.* **72**, 2071 (1989).
39. D. J. Carlsson, J. D. Cooney, S. Gauthier, and D. J. Worsfold, *J. Am. Ceram. Soc.* **73**, 237 (1990).
40. F. Duboudin, M. Birot, O. Babot, J. Dunogues, and R. Galas, *J. Organomet. Chem.* **341**, 125 (1988).
41. M. A. Abu-eid, R. B. King, and A. M. Kotliar, *Eur. Polym. J.* **28**, 315 (1992).
42. B. I. Lee and L. L. Hench, in *Science of Ceramic Chemical Processing*, edited by L. L. Hench and D. R. Ulrich (Wiley, New York, 1986), p. 345.
43. B. L. Lee and L. L. Hench, *Mater. Res. Soc. Symp. Proc.* **73**, 815 (1986).
44. T. Ishikawa, M. Shibuya, and T. Yamamura, *J. Mater. Sci.* **25**, 2809 (1990).
45. (a) S. Yajima, Y. Hasegawa, K. Okamura, and T. Matsuzawa, *Nature*, **273**, 525 (1978); (b) S. Yajima, *Philos. Trans. R. Soc. London Ser. A*, **294**, 419 (1980).
46. W. Toreki, C. D. Batich, M. D. Sacks, M. Salaam, and G. J. Choi, *Mater. Res. Soc. Symp. Proc.* **271**, 761 (1992).
47. S. Yajima, K. Okamura, J. Hayashi, and M. Omori, *J. Am. Ceram. Soc.* **59**, 324 (1976).
48. (a) Y. Hasegawa, M. Iimura, and S. Yajima, *J. Mater. Sci.* **15**, 720 (1980); (b) S. Yajima, Y. Hasegawa, J. Hayashi, and M. Kimura, *J. Mater. Sci.* **13**, 2569 (1978); (c) Y. Hasegawa and K. Okamura, *J. Mater. Sci.* **21**, 321 (1986); (d) H. Ichikawa, F. Machino, S. Mitsuno, T. Ishikawa, K. Okamura, and Y. Hasegawa, *J. Mater. Sci.* **21**, 4352 (1986); (e) Y. Hasegawa, *J. Mater. Sci.* **24**, 1177 (1989).
49. R. J. P. Corriu, D. Leclercq, P. H. Mutin, and A. Vioux, *Chem. Mater.* **4**, 711 (1992).
50. (a) P. H. Hommel, J. L. Miquel, and A. P. Legrand, *Industrie Ceramique* **849**, 344 (1990); (b) M. Takeda, J.-I. Sakamoto, Y. Imai, and H. Ichikawa, *Compos. Sci. Technol.* **59**, 813 (1999).
51. (a) R. A. Petrisko and G. L. Stark, 33rd International SAMPE (The Society for the Advancement of Materials Process Engineering) Symposium, edited by G. Carrillo, E. D. Newell, W. D. Brown, and P. Phelan, Anaheim, CA, March 7-10, 1988; (b) K. Okamura, M. Sato, T. Matsuzawa, and Y. Hasegawa, *Polym. Prepr. (Am. Chem. Soc. Div. Polym. Chem.)* **25**, 6 (1984); (c) T. Taki, S. Maeda, K. Okamura, M. Sato, and T. Matsuzawa, *J. Mater. Sci. Lett.* **6**, 826 (1987); (d) T. Mah, N. L. Hecht, D. E. McCullum, J. R. Hoenigman, H. M. Kim, A. P. Katz, and H. A. Lipsitt, *J. Mater. Sci.* **19**, 1191 (1984); (e) C. Laffon *et al.*, *J. Mater. Sci.* **24**, 1503 (1989).
52. (a) R. H. Baney and J. H. Gaul, Jr., U.S. Patent No. 4,310,651 (January 12, 1982); (b) D. Reyx, J. M. N. Martins, and I. Campistrone, *Makromol. Chem.* **194**, 87 (1993); (c) R. D. Miller, *Polym. News* **12**, 326 (1987); (d) R. West, in *Ultrastructure Processing of Ceramics, Glasses and Composites*, edited by L. L. Hench and D. R. Ulrich (Wiley-Interscience, New York, 1984), p. 235; (e) F. Yenca, Y. L. Chen, and K. Matyjaszewski, *Polym. Prepr. (Am. Chem. Soc. Div. Polym. Chem.)* **28**, 222 (1987); (f) S. M. Bushnell-Watson and J. H. Sharp, *J. Therm. Anal.* **40**, 189 (1993).
53. W. R. Schmidt, L. V. Interrante, R. H. Doremus, T. K. Trout, P. S. Marchetti, and G. E. Maciel, *Chem. Mater.* **3**, 257 (1991).
54. C. L. Schilling, Jr., U.S. Patent No. 4,783,516 (November 8, 1988).
55. (a) Z. F. Zhang, F. Babonneau, R. M. Laine, Y. Mu, J. P. Harrod, and J. A. Rahn, *J. Am. Ceram. Soc.* **74**, 670 (1991); (b) M. F. Gozzi, M. D. C. Goncalves, and I. V. P. Yoshida, *J. Mater. Sci.* **34**, 155 (1999); (c) B. Boury, N. Bryson and G. Soula, *Appl. Organomet. Chem.* **13**, 419 (1999).
56. (a) D. Seyferth, T. G. Wood, H. J. Tracy, and J. L. Robison, *J. Am. Ceram. Soc.* **75**, 1300 (1992); (b) M. F. Gozzi and I. V. P. Yoshida, *Macromolecules* **28**, 7235 (1995); (c) B. Boury, N. Bryson, and G. Soula, *Chem. Mater.* **10**, 297 (1998).
57. J. Lipowitz, G. E. LeGrow, T. F. Lim, and N. Langley, *Ceram. Eng. Sci. Proc.* **9**, 931 (1988).
58. (a) S. Yajima, J. Hayashi, and M. Omori, *Chem. Lett.* September (9), 931 (1975); (b) S. Yajima, K. Okamura, and J. Hayashi, *Chem. December (12)*, 1209 (1975); (c) S. Yajima, M. Mori, J. Hayashi and K. Okamura, *Lett.* June (6), 551 (1976).
59. J. G. Noltes, in *Transformation of Organometallics into Common and Exotic Materials: Design and Activation*, edited by R. M. Laine, (Martinus Nijhoff, Amsterdam, 1988), p. 97.
60. D. R. Bujalski, G. E. LeGrow, and T. F. Lim, *Polym. Prepr. (Am. Chem. Soc. Div. Polym. Chem.)* **28**, 396 (1987).
61. T. M. Hsu and S. P. Sawan, *Polym. Prepr. (Am. Chem. Soc. Div. Polym. Chem.)* **33**, 1034 (1992).
62. (a) Y. T. Shieh, S. P. Sawan, and J. B. Milstein, *Polym. Prepr. (Am. Chem. Soc. Div. Polym. Chem.)* **33**, 1044 (1992); (b) Y. T. Shieh and S. P. Sawan, *J. Polym. Res.* **1**(4), 367 (1994); (c) Y. T. Shieh and S. P. Sawan, *J. Appl. Polym. Sci.* **58**, 2013 (1995).
63. Y. T. Shieh and S. P. Sawan, *Polym. Prepr. (Am. Chem. Soc. Div. Polym. Chem.)* **31**, 1042 (1992).
64. (a) K. Kumar, *J. Polym. Sci. C* **26**, 25 (1988); (b) F. I. Hurwitz, T. A. Kacik, X.-Y. Bu, J. Masnovi, P. J. Heimann, and K. Beyene, *J. Mater. Sci.* **30**, 3130 (1995).
65. (a) E. Bacque, J. P. Pillot, M. Birot, and J. Dunogues, *Macromolecules* **21**, 30 (1988); (b) **21**, 34 (1988).
66. E. Bacque, J. P. Pillot, M. Birot, and J. Dunogues, in *Transformation of Organometallics into Common and Exotic Materials: Design and Activation*, edited by R. M. Laine, (Martinus Nijhoff, Amsterdam, 1988), p. 116.
67. (a) E. Bacque, J. P. Pillot, M. Birot, J. Dunogues, P. Lapouyade, E. Bouillon, and R. Pailler, *Chem. Mater.* **3**, 348 (1991); (b) E. Bouillon, R. Pailler, R. Naslain, E. Bacques, J. P. Pillot, M. Birrot, I. Dunogues, and P. V. Huong, *Chem. Mater.* **3**, 356 (1991).
68. H. J. Wu and L. V. Interrante, *Chem. Mater.* **1**, 564 (1989).
69. (a) H. J. Wu and L. V. Interrante, *Polym. Prepr. (Am. Chem. Soc. Div. Polym. Chem.)* **33**, 210 (1992); (b) L. V. Interrante, C. W. Whitmarsh, W. Sherwood, H.-J. Wu, R. Lewis, and G. Maciel, NATO ASI Ser., Ser. E: Appl. Sci. **297** (Appl. Organomet. Chem. Prepar. Process. Adv. Mater.), 173 (1995); (c) Q. Liu, H.-J. Wu, R. Lewis, G. E. Maciel, and L. V. Interrante, *Chem. Mater.* **11**, 2038 (1999).
70. C. K. Whitmarsh and L. V. Interrante, *Organometallics* **10**, 1336 (1991).
71. C. Laffon, A. M. Flank, P. Lagarde, and E. Bouillon, *Physica B* **158**, 229 (1989).
72. L. V. Interrante, C. K. Whitmarsh, T. K. Trout, and W. R. Schmidt, in *Inorganic and Organometallic Polymers with Special Properties*, edited by R. M. Laine (Kluwer Academic, Netherlands, 1992), p. 243.
73. C. L. Schilling, Jr. and T. C. Williams, *Polym. Prepr. (Am. Chem. Soc. Div. Polym. Chem.)* **25**, 1 (1984).
74. C. L. Schilling, Jr., *Brit. Polym. J.* **18**, 355 (1986).
75. W. R. Schmidt, V. Sukumar, W. J. Hurley, R. Garcia, L. V. Interrante, R. H. Doremus, and G. M. Renlund, *J. Am. Ceram. Soc.* **73**, 2412 (1990).
76. E. Bouillon, D. Mocaer, J. F. Villeneuve, R. Pailler, R. Naslain, M. Monthieux, A. Oberlin, C. Guimon, and G. Pfister, *J. Mater. Sci.* **26**, 1517 (1991).
77. (a) C. L. Czekaj, M. L. J. Hackney, W. J. Hurley Jr., L. V. Interrante, G. A. Sigel, P. J. Schields, and G. A. Slack, *J. Am. Ceram. Soc.* **73**, 352 (1990); (b) L. V. Interrante, W. R. Schmidt, S. N. Shaikh, R. Garcia, P. S. Marchetti, and G. E. Maciel, in *Chemical Processing of Advanced Materials*, L. L. Hench and J. R. West, eds. (Wiley, New York, 1992), p. 777; (c) J. A. Jensen, U.S. Patent No. 5,229,468 (July 20, 1993); (d) B. E. Fry, A. Guo, and D. C. Neckers, *J. Organomet. Chem.* **538**, 151 (1997).
78. (a) T. L. Smith, Jr., U.S. Patent No. 4,631,179 (December 23, 1986); (b) Q. Liu, H.-J. Wu, R. Lewis, G. E. Maciel, and L. V. Interrante, *Chem. Mater.* **11**, 2038 (1999).
79. H.-J. Wu and L. V. Interrante, *Polym. Prepr. (Am. Chem. Soc. Div. Polym. Chem.)* **32**, 588 (1991).
80. (a) H.-J. Wu and L. V. Interrante, *Macromolecules* **25**, 1840 (1992); (b) L. V. Interrante, Q. Liu, I. Rushkin, and Q. Shen, *J. Organomet. Chem.* **521**, 1 (1996); (c) W. Habel, A. Oelschläger, and P. Sartori, *J. Organomet. Chem.* **486**, 267 (1995).
81. K. J. Thorne, S. E. Johnson, H. Zheng, J. D. Mackenzie, and M. F. Hawthorne, *Chem. Mater.* **6**, 110 (1994).
82. B. Boury, R. J. P. Corriu, D. Leclercq, P. H. Mutin, J. M. Planeix, and A. Moux, *Organometallics* **10**, 1457 (1991).
83. R. J. P. Corriu, D. Leclercq, P. H. Mutin, J. M. Planeix, and A. Vioux, *Organometallics* **12**, 454 (1993).
84. B. Boury, R. J. P. Corriu, D. Leclercq, H. Mutin, J. M. Planeix, and A. Vioux, in *Inorganic and Organometallic Polymers with Special*



- Properties*, edited by R. M. Laine (Kluwer Academic, Netherlands, 1992), p. 255.
85. V. B. Boury, L. Carpenter, and R. J. P. Corriu, *Angew. Chem. Int. Ed. Engl.* **29**, 785 (1990).
  86. (a) J. Masnovi, X. Y. Bu, K. Beyene, P. Heimann, T. Kacilc, A. H. Andrist, and F. I. Hurwitz, *Mater. Res. Soc. Symp. Proc.* **271**, 771 (1992); (b) J. Masnovi, X. Y. Bu, P. Conroy, A. H. Andrist, F. I. Hurwitz and D. Miller, *Mater. Res. Soc. Symp. Proc.* **180**, 779 (1988).
  87. B. Boury, R. J. P. Corriu, and W. E. Douglas, *Chem. Mater.* **3**, 487 (1991).
  88. B. Boury, L. Carpenter, R. Corriu, and H. Mutin, *New J. Chem.* **14**, 535 (1990).
  89. R. J. P. Corriu, M. Enders, S. Huille, and J. E. Moreau, *Chem. Mater.* **6**, 15 (1994).
  90. (a) W. Habel, B. Hamack, C. Hover, and P. Sartori, *J. Organomet. Chem.* **467**, 13 (1994); (b) P. Sartori, W. Habel, B. V. Aefferden, and L. Mayer, *Chem. Ind.* **12**, 54 (1990).
  91. (a) C. L. Schilling, Jr., J. P. Wesson, and T. C. Williams, *J. Polym. Sci. Polym. Symp.* **70**, 121 (1983); (b) C. L. Schilling, Jr., J. P. Wesson, and T. C. Williams, *Am. Ceram. Soc. Bull.* **62**, 912 (1983); (c) C. L. Schilling, Jr. NTIS Technical Report 83-3, Order No. AD-A141649, 1983; (d) C. L. Schilling, Jr. and T. C. Williams, NTIS Technical Report 83-2, Order No. AD-A141558, 1983.
  92. C. L. Schilling, Jr., U.S. Patent No. 4,472,591 (September 18, 1984).
  93. C. L. Schilling, Jr., NTIS Technical Report 83-1 Order No. AD-A141546, 1983.
  94. S. Yajima, *Am. Ceram. Soc. Bull.* **62**, 893 (1983).
  95. (a) D. Seyferth, C. A. Sobon, and J. Boren, *New J. Chem.* **14**, 545 (1990); (b) D. Seyferth, T. G. Wood, H. J. Tracy, and J. L. Robison, *J. Am. Ceram. Soc.* **75**, 1300 (1992).
  96. (a) D. Seyferth and H. Lang, *Organometallics* **10**, 551 (1991); (b) D. Seyferth and H. Lang, in *Ultrastructure Processing of Advanced Materials*, edited by D. R. Uhlmann and D. R. Ulrich (Wiley, New York, 1992), p. 667.
  97. D. Seyferth, G. E. Koppetsch, T. G. Woods, H. J. Tracy, J. L. Robinson, P. Czubarow, M. Tasi, and H. G. Woo, *Polym. Prepr. (Am. Chem. Soc. Div. Polym. Chem.)* **34**, 223 (1993).
  98. T. G. Wood, Ph.D. Thesis, Massachusetts Institute of Technology, Cambridge, MA., 1984.
  99. D. Seyferth, N. Bryson, D. P. Workman, and C. A. Sobon, *J. Am. Ceram. Soc.* **74**, 2687 (1991).
  100. D. Seyferth, H. Lang, C. A. Sobon, J. Borm, H. J. Tracy, and N. Bryson, *J. Inorg. Organomet. Polym.* **2**, 59 (1992).
  101. (a) E. Bouillon *et al.*, *J. Mater. Sci.* **26**, 1331 (1991); (b) D. M. Kalyon and S. Kovenklioglu, *Adv. Polym. Tech.* **7**, 191 (1987).
  102. (a) C. Gerardin, F. Taulelle, J. Livage, M. Birot, and J. Dunogues, *Bull. Magn. Reson.* **12**, 84 (1988); (b) T. Taki, *J. Inorg. Organomet. Polym.* **2**, 269 (1992).
  103. (a) K. Okamura, T. Matsuzawa, and Y. Hasegawa, *J. Mater. Sci. Lett.* **4**, 55 (1985); (b) K. Okamura, M. Sato, and Y. Hasegawa, *J. Mater. Sci.* **2**, 769 (1983); (c) K. Okamura and T. Seguchi, *J. Inorg. Organomet. Polym.* **2**, 171 (1992); (d) D. W. Matson, R. C. Petersen, and R. D. Smith, *Mater. Lett.* **4**, 429 (1986); (e) M. Takeda, Y. Imai, H. Ickikawa, T. Ishikawa, and K. Okamura, *Ceram. Eng. Sci. Proc.* **13**, 209 (1992); (f) Y. Hasegawa, *J. Inorg. Organomet. Polym.* **2**, 161 (1992).
  104. X. J. Wang, F. R. Liu, and C. R. Zhang, in *Material Research Society International Symposium Proceedings*, edited by Y. Han (North-Holland, Amsterdam, 1991), vol. 2, p. 93.
  105. K. Okamura, T. Mutsuzawa, M. Sato, Y. Higashiguchi, S. Morozumi, and A. Kohyama, *J. Nucl. Mater.* **141-143**, 102 (1986).
  106. (a) J. J. Poupeau, D. Abbe, and J. Jamet, *Mater. Res. Soc. Symp. Proc.* **17**, 287 (1984); (b) M. J. Morris, V. E. McGrath, S. Norris, W. G. Stibbs, R. J. P. Emsley, and J. H. Sharp, *Proc. Eur. Conf. Adv. Mater. Process.* 2nd. vol. 3, 259 (1991); (c) W. P. Weber and S. Q. Zhou, U.S. Patent No. 5,171,810 (December 15, 1992); (d) M. J. Michalczyk, U.S. Patent No. 5,270,429 (December 14, 1993); (e) C. K. Whitmarsh and L. V. Inerrante, U.S. Patent No. 5,153,295 (October 6, 1992); Whitmarsh and L. V. Inerrante; (f) M. Yazdi, D. Dollimore, and D. Agar, *Thermochim. Acta* **144**, 159 (1989); (g) T. Seguchi and K. Okamura, *Keobunshi Kakeo* **42**, 163 (1993).
  107. (a) D. Seyferth and Y.-F. Yu, U.S. Patent No. 4,639,501 (January 27, 1987); (b) R. A. Sinclair and R. West, *Meet Res. Soc. Symp. Proc.* **32**, 387 (1984); (c) K. Koga, S. Nagano, S. Mizuta, and M. Nakayama, U.S. Patent No. 4,374,793 (February 22, 1983); (d) T. D. Tilley, U.S. Patent No. 5,229,481 (July 20, 1993); (e) H.-G. Woo and T. D. Tilley, in *Ultrastructure Processing of Advanced Materials*, edited by D. R. Uhlmann and D. R. Ulrich (Wiley, New York, 1992), p. 651; (f) R. C. West and L. D. David, U.S. Patent No. 4,324,901 (April 13, 1982) (g) R. C. West, U.S. Patent No. 4,260,780 (April 7, 1981).
  108. K. A. Brown-Wensley and R. A. Sinclair, U.S. Patent No. 4,537,942 (August 27, 1985)
  109. (a) T. J. Barton, S. Ijadi-Maghsoodi, and Y. Pang, U.S. Patent No. 5,241,029 (August 31, 1993); (b) N. I. Baklanova, V. N. Kulyukin, N. Z. Lyakhov, G. Y. Turkina, O. G. Yarosh and M. G. Voronkov, *J. Mater. Synth. Proc.* **5**, 443 (1997).
  110. S. Ijada-Maghsoodi, Y. Pang, and T. J. Barton, *J. Polym. Sci.* **28**, 955 (1990).
  111. M. Ishikawa, Y. Hasegawa, T. Hatano, and A. Kunai, *Organometallics* **8**, 2741 (1989).
  112. S. Ijadi-Maghsoodi, X. P. Zhang, Y. Pang, M. Meyer, M. Akinc, and T. J. Barton, *Polym. Prepr. (Am. Chem. Soc. Div. Polym. Chem.)* **32**, 577 (1991).
  113. (a) D. Seyferth, Y.-F. Yu, and G. H. Wiseman, U.S. Patent No. 4,719,273 (January 12, 1988); (b) D. Seyferth, G. H. Wiseman, Y.-F. Yu, T. S. Targos, C. A. Sobon, T. G. Wood, and G. E. Koppetsch, in *Silicon Chemistry*, edited by J. Y. Corey, E. R. Corey, and P. P. Gaspar (Ellis Harwood, Chichester, UK, 1988), p. 415.
  114. (a) S. Ijadi-Maghsoodi and T. J. Barton, *Macromolecules* **23**, 4485 (1990); (b) R. J. P. Corriu, P. Gerbier, C. Guérin, and B. Henner, *J. Mater. Chem.* **10**, 2173 (2000).
  115. Y. Pang, S. Ijadi-Maghsoodi, and T. J. Barton, *Macromolecules* **26**, 5671 (1993).
  116. (a) F. Babonneau, K. Thorne, and J. D. Mackenzie, *Chem. Mater.* **1**, 554 (1989); (b) K. C. Chen, K. J. Thorne, A. Chemseddine, F. Babonneau, and J. D. Mackenzie, *Mater. Res. Soc. Symp. Proc.* **121**, 571 (1988).
  117. R. B. Taylor and G. A. Zank, *Polym. Prepr. (Am. Chem. Soc. Div. Polym. Chem.)* **32**, 586 (1991).
  118. (a) G. T. Burns, R. B. Taylor, Y. Xu, A. Zangvil, and G. A. Zank, *Chem. Mater.* **4**, 1313 (1992); (b) D. R. Bujalski, S. Grigoras, W.-L. Lee, G. M. Wieber, and G. A. Zank, *J. Mater. Chem.* **8**, 1427 (1998); (c) G. A. Zank, in *Silicon-Containing Polymers*, edited by R. G. Jones, W. Ando, and J. Chrojnowski (Kluwer Academic Publishers, Dordrecht, 2000), pp. 697-726.
  119. F. I. Hurwitz, P. Heimann, S. C. Farmer, and D. M. Hembree, Jr., *J. Mater. Sci.* **28**, 6622 (1993).
  120. (a) V. Belot, R. J. P. Corriu, D. Leclercq, P. H. Mutin, and A. Vioux, *J. Polym. Sci. A Polym. Chem.* **30**, 613 (1992); (b) J. R. Fox, D. A. White, S. M. Oleff, R. D. Boyer, and P. A. Budinger, *Mater. Res. Soc. Symp. Proc.* **73**, 395 (1986); (c) P. H. Mutin, *J. Am. Ceram. Soc.* **85**, 1185 (2002).
  121. V. Belot, R. J. P. Corriu, D. Leclercq, P. H. Mutin, and A. Vioux, *J. Mater. Sci. Lett.* **9**, 1052 (1990).
  122. K. J. Shea, D. A. Loy, and O. Webster, *J. Am. Chem. Soc.* **114**, 6700 (1992).
  123. R. H. Baney, G. T. Burns, J. P. Cannady, and T. K. Hilty, in *Organosilicon and Bio-organosilicon Chemistry*, edited by H. Sakurai (Ellis Harwood, Chichester, 1985), p. 269.
  124. R. H. Baney, in *Ultrastructure Processing of Ceramics, Glasses and Composites*, edited by L. L. Hench and D. R. Ulrich (Wiley-Interscience, New York, 1984), p. 245.
  125. R. H. Baney, J. H. Gaul, Jr., and T. K. Hilty, *Mater. Res. Soc. Symp. Proc.* **17**, 253 (1984).
  126. D. C. Deleuw, J. Lipowitz, and J. A. Rabe, U.S. Patent No. 5,268,336 (December 7, 1993).
  127. J. Lipowitz and G. L. Turner, *Polym. Prepr. (Am. Chem. Soc. Div. Polym. Chem.)* **29**, 74 (1988).
  128. (a) J. Lipowitz, H. A. Freeman, R. T. Chen, and E. R. Prack, *Adv. Ceram. Mater.* **2**, 121 (1987); (b) R. M. Salinger, T. D. Barnard, C. T. Li, and L. G. Mahone, *Soc. Adv. Mater. Process Eng. Q.* **19**, 27 (1988).
  129. D. R. Stull and H. Prophet, *JANAF Thermochemical Tables*, 2nd ed., NSRDS-NBS Publication No. 37 (National Bureau of Standards, Washington, D.C., 1971).
  130. R. H. Baney, J. H. Gaul, Jr., and T. K. Hilty, *Organometallics* **2**, 859 (1983).
  131. R. H. Baney, *Chemtech* **18** (12), 738 (1988).

132. (a) G. Winter, W. Verbeek, and M. Mansmann, U.S. Patent No. 3,892,583 (July 1, 1975); (b) W. Verbeek, U.S. Patent No. 3,853,567 (December 10, 1974).
133. R. M. Laine, Y. D. Blum, D. Tse, and R. Glaser, in *Inorganic and Organometallic Polymers*, ACS Syrup. Series No. 360, edited by M. Zeldin, K. J. Wynne, and H. R. Allcock (American Chemistry Society, Washington, D.C., 1988), p. 124, and references therein.
134. Y. Nakaido, Research Institute for Special Inorganic Materials Report No. 9 (1991), p. 139.
135. D. L. Delaet, Patent Cooperation Treaty International Publication No. WO 91/19688 (December 26, 1991).
136. (a) R. M. Laine, Y. D. Blum, A. Chow, R. Hamlin, K. B. Schwartz, and D. J. Rowcliffe, *Polym. Prepr. (Am. Chem. Soc. Div. Polym. Chem.)* **28**, 393 (1987); (b) G. E. Legrow, T. F. Lim, J. Lipowitz, and R. S. Reaach, *Am. Ceram. Soc. Bull.* **66**, 363 (1987).
137. (a) S. Ampuero, P. Bowen, and T. A. Ring, *Mater. Res. Soc. Symp. Proc.* **287**, 227 (1993); (b) T. Yamada, T. Kawahito, and T. Iwai, *J. Mater. Sci. Lett.* **2**, 275 (1983); (c) K. S. Mazdiyasn and C. M. Cooke, *J. Am. Ceram. Soc.* **56**, 628 (1973).
138. D. Seyferth, C. C. Prud'Homme, and G. H. Wiseman, U.S. Patent No. 4,397,828 (August 9, 1983).
139. (a) G. T. Burns, C. K. Saha, G. A. Zank, and H. A. Freeman, *J. Mater. Sci.* **27**, 2131 (1992); (b) C. K. Saha and H. A. Freeman, *J. Mater. Sci.* **27**, 4651 (1992); (c) G. T. Burns, European Patent Application No. EP 295062 A2 (June 8, 1988); (d) G. T. Burns, U.S. Patent No. 4,774,312 (September 27, 1988).
140. E. Duguet and M. Schappacher, *Pct. Int. Application No. WO 92/17527* (October 15, 1992).
141. (a) G. T. Burns and G. A. Zank, *Polym. Prepr. (Am. Chem. Soc. Div. Polym. Chem.)* **34**, 343 (1993); (b) G. T. Burns, T. P. Angellotti, L. F. Hanneman, G. Chandra, and J. A. Moore, *J. Mater. Sci.* **22**, 2609 (1987).
142. (a) D. Seyferth and G. H. Wiseman, *Polym. Prepr. (Am. Chem. Soc. Div. Polym. Chem.)* **25**, 10 (1984); (b) D. Seyferth, G. H. Wiseman, and C. Prud'Homme, *J. Am. Ceram. Soc.* **66** (1) C-13 (1983) (c) D. Seyferth, G. H. Wiseman, and C. Prud'Homme, *Mater. Res. Soc. Symp. Proc.* **17**, 263 (1984).
143. Y. Shimizu, Y. Tashiro, H. Aoki, M. Ichiyama, H. Nishii, T. Kishi, K. Okuda, and T. Isoda, European Patent Application No. EP 544959A1 (December 30, 1991).
144. O. Funayama, M. Aral, and T. Isoda, European Patent Application No. EP 303498A1 (August 12, 1988).
145. (a) Y. Nakaido and N. Kozakai, *Nippon Kagaku Kaishi* **7**, 1080 (1989); (b) Y. Nakaido, T. Matsuura, D. Yamashita, M. Okabe, and S. Ishikita, *Nippon Kagaku Kaishi* **5**, 487 (1990).
146. M. Arai, S. Sakurada, T. Isoda, and T. Tomizawa, *Polym. Prepr. (Am. Chem. Soc. Div. Polym. Chem.)* **28**, 407 (1987).
147. O. Funayama, T. Isoda, H. Kaya, T. Suzuki, and Y. Tashiro, *Polym. Prepr. (Am. Chem. Soc. Div. Polym. Chem.)* **32**, 542 (1991).
148. A. A. Gallo, U.S. Patent No. 4,778,907 (October 18, 1988).
149. (a) D. Bahloul, M. Pereira, and P. Goursat, *Ceram. Int.* **18**, 1 (1992); (b) F. Sirieix, P. Goursat, A. Lecomte, and A. Dauger, *Compos. Sci. Technol.* **37**, 7 (1990).
150. O. Funayama, H. Nakahara, A. Tezuka, T. Ishii, and T. Isoda, *J. Mater. Sci.* **29**, 2238 (1994).
151. M. G. Salvetti, M. Pijolat, M. Soustelle, and E. Chassigneux, *Solid State Ionics* **63-65**, 332 (1993).
152. D. M. Narsavage, L. V. Interrante, P. S. Marchetti, and G. E. Maciel, *Chem. Mater.* **3**, 721 (1991).
153. R. M. Laine, *Platinum Met. Rev.* **32**, 64 (1988).
154. (a) Y. Blum and R. M. Laine, *Organometallics* **5**, 2081 (1986); (b) R. M. Laine and Y. Blum, U.S. Patent No. 4,612,383 (September 16, 1986).
155. (a) D. Seyferth and G. H. Wiseman, *J. Am. Ceram. Soc.* **C-132** (1984); (b) D. Seyferth, G. H. Wiseman, J. M. Schwark, Y.-F. Yu, and C. A. Poutasse, in *Inorganic and Organometallic Polymers* (ACS Symp. Proc. No. 360), edited by M. Zeldin, K. J. Wynne, and H. R. Allcock (American Chemistry Society, Washington, D.C., 1988), p. 144; (c) D. Seyferth and G. H. Wiseman, in *Science of Ceramic Chemical Processing*, edited by L. L. Hench and D. R. Ulrich (Wiley, New York, 1986), p. 354; (d) D. Seyferth and G. H. Wiseman, U.S. Patent No. 4,482,669 (November 13, 1984); (e) D. Seyferth, in *Transformation of Organometallics into Common and Exotic Materials: Design and Activation*, edited by R. M. Laine (Nijhoff, Dordrecht, 1988), p. 133; (f) R. M. Stewart, N. K. Dando, D. Seyferth, and A. J. Perrotta, *Polym. Prepr. (Am. Chem. Soc. Div. Polym. Chem.)* **32**, 569 (1991); (g) H. N. Han, D. A. Lindquist, J. S. Haggerty, and D. Seyferth, *Chem. Mater.* **4**, 705 (1992); (h) N. R. Dando and A. J. Perrotta, *Chem. Mater.* **5**, 1624 (1993); (i) D. Seyferth and R. M. Stewart, *Appl. Organomet. Chem.* **11**, 813 (1997).
156. (a) K. A. Youngdahl, R. M. Laine, R. A. Kennish, T. R. Cronin, and G. G. A. Balavoine, *Mater. Res. Soc. Symp. Proc.* **121**, 489 (1988); (b) Y. D. Blum, K. B. Schwartz, and R. M. Laine, *J. Mater. Sci.* **24**(5), 1707 (1989).
157. R. M. Laine, Y. D. Blum, R. D. Hamlin, and A. Chow, in *Ultrastructure Processing of Advanced Ceramics*, edited by J. D. Mackenzie and D. R. Ulrich (Wiley, New York, 1988), p. 761.
158. (a) J. D. Bolt and F. N. Tebbe, U.S. Patent No. 4,730,026 (March 8, 1988); (b) J. J. Lebrun and H. Porte, U.S. Patent No. 4,689,832 (August 25, 1987); (c) J. M. Schwark, *Polym. Prepr. (Am. Chem. Soc. Div. Polym. Chem.)* **34**, 294 (1993).
159. (a) M. Matsumoto, K. Niwada, and S. Tanaka, *Jpn. Kokai Tokkyo Koho JP 61072607 A2* (April 14, 1986); (b) M. Balasubramanian and P. Choudhury, U.S. Patent No. 5,010,157 (December 9, 1988) (c) Y. Takeda, M. Takamizawa, T. Takeno and A. Hayashida, European Patent Application EP 323062 (December 9, 1988).
160. (a) D. Seyferth, H. Lang, H. J. Tracy, C. Sobon, and J. Borm, *Polym. Prepr. (Am. Chem. Soc. Div. Polym. Chem.)* **32**, 581 (1991); (b) D. Seyferth, J. M. Schwark, and Y. F. Yu, U.S. Patent No. 4,767,876 (August 30, 1988); (c) D. Serferth, Y. F. Yu, and T. S. Targos, U.S. Patent No. 4,705,837 (November 10, 1987); (d) D. Seyferth and Y. F. Yu, U.S. Patent No. 4,650,837 (March 17, 1987); (e) D. Seyferth, T. G. Wood, and Y. F. Yu, U.S. Patent No. 4,645,807 (February 24, 1987) (f) D. Seyferth and J. M. Schwark, U.S. Patent No. 4,720,532 (January 19, 1988).
161. Y. D. Blum, K. B. Schwartz, E. J. Crawford, and R. M. Laine, *Mater. Res. Soc. Symp. Proc.* **121**, 565 (1988).
162. (a) Y. D. Blum, G. A. McDermott, and A. S. Hirschon, in *Inorganic and Organometallic Oligomers and Polymers*, edited by J. F. Harrod and R. M. Laine (Kluwer Academic, Netherlands, 1991), p. 161; (b) Y. D. Blum, G. A. McDermott, R. B. Wilson, and A. S. Hirschon, *Polym. Prepr. (Am. Chem. Soc. Div. Polym. Chem.)* **32**, 548 (1991).
163. D. Mocaer, R. Pailler, R. Naslaih, C. Richard, J. P. Pillot, J. Dunogues, C. Gerardin, and F. Taulelle, *J. Mater. Sci.* **28**, 2615 (1993).
164. (a) D. Mocaer, R. Pailler, R. Naslain, C. Richard, J. P. Pillot, and I. Dunogues, *J. Mater. Sci.* **28**, 2632 (1993); (b) D. Mocaer, R. Pallier, R. Naslain, C. Richard, J. P. Pillot, J. Dunogues, O. Delverdier, and M. Monthieux, *J. Mater. Sci.* **28**, 2639 (1993); (c) D. Mocaer, R. Pailler, R. Naslain, C. Richard, J. P. Pillot, J. Dunogues, C. Darnez, M. Chambon, and M. Lahaye, *J. Mater. Sci.* **28**, 3049 (1993); (d) D. Mocaer, G. Chollon, R. Pailler, L. Filipuzzi, and R. Naslain, *J. Mater. Sci.* **28**, 3059 (1993).
165. B. G. Penn, J. G. Daniels, F. E. Ledbetter III, and J. M. Clemons, *Polym. Eng. Sci.* **26**, 1191 (1986).
166. (a) J. P. Cannady, U.S. Patent No. 4,543,344 (September 24, 1985); (b) J. P. Cannady, U.S. Patent No. 4,540,803 (September 10, 1985).
167. (a) J. Lipowitz, J. A. Rabe, and T. M. Carr, *Polym. Prepr. (Am. Chem. Soc. Div. Polym. Chem.)* **28**, 411 (1987); (b) J. Lipowitz, J. A. Rabe, and T. M. Carr, in *Inorganic and Organometallic Polymers* (ACS Symposium Series 360), edited by M. Zeldin, K. J. Wynne, and H. R. Allcock (American Chemical Society, Washington, D.C., 1988), p. 156; (c) J. H. Gaul, Jr., U.S. Patent No. 4,340,619 (July 20, 1982).
168. R. H. Baney, *Polym. Prepr. (Am. Chem. Soc. Div. Polym. Chem.)* **25**, 2 (1984).
169. G. E. Legrow, T. F. Lim, J. Lipowitz, and R. S. Reaach, *Mater. Res. Soc. Symp. Proc.* **73**, 553 (1986).
170. J. H. Gaul, Jr., U.S. Patent No. 4,312,470 (January 26, 1982).
171. J. P. Cannady, U.S. Patent No. 4,535,007 (August 13, 1985).
172. N. Brodie, J. P. Majoral, and J.-P. Disson, *Inorg. Chem.* **32**, 4646 (1993).
173. W. R. Schmidt, P. S. Marchetti, L. V. Interrante, W. J. Hurley, Jr., R. H. Lewis, R. H. Doremus, and G. E. Maciel, *Chem. Mater.* **4**, 937 (1992).
174. W. R. Schmidt: V. Sukumar, W. J. Hurley, Jr., R. Garcia, R. H. Doremus, L. V. Interrante, and G. M. Renlund, *J. Am. Ceram. Soc.* **73**, 2412 (1990).
175. G. T. Burns and G. Chandra, *J. Am. Ceram. Soc.* **72**, 333 (1989).
176. K. Okamura, M. Sato, and Y. Hasegawa, *Ceram. Int.* **13**, 55 (1987).

177. N. S. C. K. Yive, R. Corriu, D. Leclercq, P. H. Mutin, and A. Vioux, *New J. Chem.* **15**, 85 (1991).
178. N. S. C. K. Yive, R. J. P. Corriu, D. Leclercq, P. H. Mutin, and A. Vioux, *Chem. Mater.* **4**, 141 (1992).
179. D. Bahloul, M. Pereira, and P. Goursat, *J. Am. Ceram. Soc.* **76**, 1163 (1993).
180. D. Bahloul, M. Pereira, and P. Goursat, *J. Am. Ceram. Soc.* **76**, 1156 (1993).
181. (a) N. S. C. K. Yive, R. J. P. Corriu, D. Leclercq, P. H. Mutin, and A. Vioux, *Chem. Mater.* **4**, 1263 (1992); (b) J. Bill, J. Seita, G. Thurn, J. Dürr, J. Canel, B. Z. Janos, A. Jalowiecki, D. Sauter, S. Schempp, H. P. Lamparter, J. Mayer, and F. Aldinger, *Phys. Status Solidi A* **166**, 269 (1998).
182. (a) C. M. Gerardin, F. Taulelle, and J. Livage, *Mater. Res. Soc. Symp. Proc.* **287**, 233 (1993); (b) C. Gerardin, F. Taulelle, and J. Livage, *J. Chim. Phys.* **89**, 461 (1992); (c) D. Bahloul, P. Goursat, and A. Lavedrine, *J. Eur. Ceram. Soc.* **11**, 63 (1993).
183. (a) W. Toreki, C. D. Batich, M. D. Sacks, and A. A. Morrone, *Ceram. Eng. Sci. Proc.* **11**, 1371 (1990); (b) W. Toreki, N. A. Creed, and C. D. Batich, *Polym. Prepr. (Am. Chem. Soc. Div. Polym. Chem.)* **31**, 611 (1990); (c) A. A. Morrone, W. Toreki, and C. D. Batich, *Mater. Lett.* **11**, 19 (1991).
184. (a) A. Lavedrine, D. Bahloul, P. Goursat, N. C. K. The, R. Corriu, D. Leclercq, H. Mutin, and A. Viola, *J. Eur. Ceram. Soc.* **8**, 221 (1991); (b) J. Lücke, J. Hacker, D. Suttor and G. Ziegler, *Appl. Organomet. Chem.* **11**, 181 (1997).
185. B. Arkles, *J. Electrochem. Soc.* **133** (1), 233 (1986).
186. (a) J. M. Schwark, U.S. Patent No. 4,929,704 (May 29, 1990); (b) J. M. Schwark and M. J. Sullivan, *Mater. Res. Soc. Symp. Proc.* **271**, 807 (1992); (c) J. M. Schwark, *Polym. Prepr. (Am. Chem. Soc. Div. Polym. Chem.)* **32**, 567 (1991); (d) A. Kojima, S. Hoshii, and T. Muto, *J. Mater. Sci. Lett.* **21**, 757 (2002).
187. Y. Abe, T. Ozai, Y. Kuno, Y. Nagao, and T. Misono, *J. Inorg. Organomet. Polym.* **2**, 143 (1992).
188. (a) J. M. Schwark, U.S. Patent No. 5,155,181 (October 13, 1992); (b) J. M. Schwark, U.S. Patent No. 5,021,533 (June 4, 1991); (c) J. M. Schwark, U.S. Patent No. 5,032,649 (July 16, 1991); (d) U.S. Pat. 5,001,090 (Mar. 19, 1991), J. M. Schwark, U.S. Patent No. 5,001,090 (March 19, 1991).
189. D. Seyferth, C. Strohmann, N. D. Dando, and A. J. Perrotta, *Chem Mater.* **7**, 2058 (1995).
190. Y. L. Li, E. Kroke, R. Riedel, C. Fasel, C. Gervais, and F. Babonneau, *Appl. Organomet. Chem.* **15**, 820 (2001).
191. T. Vaahs, M. Bruck, and W. D. G. Boker, *Adv. Mater.* **4**, 224 (1992).
192. K. Feng, A. Rodriguez, and Y. H. Mariam, *Polym. Mater. Sci. Eng. (ACS)* **69**, 337 (1993).
193. K. Feng and Y. H. Mariam, *Appl. Organomet. Chem.* **7**, 253 (1993).
194. (a) K. Feng and Y. H. Mariam, *Macromolecules* **24**, 4729 (1991); (b) K. Feng and Y. H. Mariam (Figure 47.1 are unpublished results).
195. Z. Du, J. Chen, and T. Han, *Chin. J. Polym. Sci.* **7**, 31 (1989).
196. H. Qiu, S. Yu, H. Ren, and Z. Du, *Polym. Bull.* **27**, 607 (1992).
197. X. Bao and M. J. Edirisinghe, *J. Mater. Chem.* **10**, 395 (2000).
198. H.-P. Baldus, W. Schnick, J. Lucke, U. Wannagat, and G. Bogedain, *Chem. Mater.* **5**, 845 (1993).
199. M. Hörz, A. Zern, F. Berger, J. Haug, K. Müller, F. Aldinger, and M. Weinmann, *J. Eur. Ceram. Soc.* **25**, 99 (2005).
200. A. Soum In *Silicon-Containing Polymers*, edited by R. G. Jones, W. Ando, and J. Chojnowski (Kluwer Academic Publishers, Dordrecht, 2000), pp. 323–349.
201. E. Kroke, Y. L. Li, C. Konetschny, E. Lecomte, C. Fasel, and R. Riedel, *Mater. Sci. Eng.* **R 26**, 97 (2000).
202. R. Riedel, A. Kienzle, W. Dressler, L. Ruwisch, J. Bill, and F. Aldinger, *Nature* **382**, 796 (1996).
203. B. Jaschke, U. Klingebiel, R. Riedel, N. Doslik, and D. Gadow, *Appl. Organomet. Chem.* **14**, 671 (2000).
204. H.-P. Baldus and M. Jansen, *Angew. Chem. Int. Ed. Engl.* **36**, 328 (1997).
205. R. Riedel and W. Dressler, *Ceram. Int.* **22**, 233 (1996).
206. T. Wideman, K. Su, E. E. Remsen, G. A. Zank, and L. G. Sneddon, *Chem. Mater.* **7**, 2203 (1995).
207. D. Srivastava, E. N. Duesler, and R. T. Paine, *Eur. J. Inorg. Chem.* 855 (1998).
208. Q. D. Nghiem, J.-K. Jeon, L.-Y. Hong, and D.-P. Kim, *J. Organomet. Chem.* **688**, 27 (2003).
209. W. R. Schmidt, D. M. Narsavage-Heald, D. M. Jones, P. S. Marchetti, D. Raker, and G. E. Maciel, *Chem. Mater.* **11**, 1455 (1999).
210. (a) Z.-C. Wang, F. Aldinger, and R. Riedel, *J. Am. Ceram. Soc.* **84**, 2179 (2001); (b) J. Bill, T. W. Kamphowe, A. Müller, T. Wichmann, A. Zern, A. Jalowiecki, J. Mayer, M. Weinmann, J. Schuhmacher, K. Müller, J. Peng, H. J. Seifert, and F. Aldinger, *Appl. Organomet. Chem.* **15**, 777 (2001).
211. F. Aldinger, M. Weinmann, and J. Bill, *Pure Appl. Chem.* **70**, 439 (1998).
212. R. Riedel, J. Bill, and A. Kienzle, *Appl. Organomet. Chem.* **10**, 241 (1996).
213. S. Bernard, M. Weinmann, D. Cornu, P. Miele, and F. Aldinger, *J. Eur. Ceram. Soc.* **25**, 251 (2005).
214. M. Weinmann, R. Haug, J. Bill, F. Aldinger, J. Schuhmacher, and K. Müller, *J. Organomet. Chem.* **541**, 345 (1997).
215. (a) A. Müller, P. Gerstel, M. Weinmann, J. Bill, and F. Aldinger, *Chem. Mater.* **14**, 3398 (2002); (b) A. Müller, J. Peng, H. J. Seifert, J. Bill, and F. Aldinger, *Chem. Mater.* **14**, 3406 (2002).
216. H. P. Baldus, O. Wagner, and M. Jansen, *Key Eng. Mater.* **89**, 75 (1994).
217. P. Baldus, M. Jansen, and D. Sporn, *Science* **285**, 699 (1999).
218. A. Müller, P. Gerstel, M. Weinmann, J. Bill, and F. Aldinger, *J. Eur. Ceram. Soc.* **20**, 2655 (2000).
219. D. Seyferth, M. Tasi, and H. G. Woo, *Chem. Mater.* **7**, 236 (1995).
220. S. J. Ting, C. J. Chu, and J. D. Mackenzie, *J. Mater. Res.* **7**, 164 (1992); (b) G. D. Soraru, F. Babonneau, and J. D. Mackenzie, *J. Mater. Sci.* **25**, 3886 (1990); (c) G. R. Hatfield and K. R. Carduner, *J. Mater. Sci.* **24**, 4209 (1989); (d) F. Babonneau, J. Livage, and R. M. Laine, *Polym. Prepr. (Am. Chem. Soc. Div. Polym. Chem.)* **32**, 579 (1991); (e) J. Lipowitz, J. A. Rabe, and T. M. Carr, *Spectrosc. Lett.* **20**, 53 (1987); (f) D. Bahloul, M. Pereira and C. Gerardin, *J. Mater. Chem.* **7**, 109 (1997); (g) D. Bahloul, M. Pereira and C. Gerardin, *J. Mater. Chem.* **7**, 117 (1997); (h) H. Q. Ly, R. Taylor, R. J. Day, and F. M. Heatley, *J. Mater. Sci.* **36**, 4037 (2001); (i) C. Gervais, F. Babonneau, L. Ruwisch, R. Hauser, and R. Riedel, *Can. J. Chem.* **81**, 1359 (2003).
221. T. F. Cooke, *J. Am. Ceram. Soc.* **74**, 2959 (1991).
222. K. Okamura, *Composites* **18**, 107 (1987).
223. J. Lipowitz, *Am. Ceram. Soc. Bull.* **70**, 1888 (1991).
224. W. Wade Adams and S. Kumar, in *Ultrastructure Processing of Advanced Materials*, edited by D. R. Uhlmann and D. R. Ulrich (Wiley, New York, 1992), p. 343.
225. N. R. Langley, G. E. LeGrow, and J. Lipowitz, in *Reinforced Ceramic Composites*, edited by K. S. Mazdiyasi (Noyes, Park Ridge, NJ, 1989), p. 63.
226. W. H. Atwell, P. Foley, W. E. Hauth, R. E. Jones, N. R. Langley, and R. M. Salinger, Final Report No. AFWAL-TR-86-4146 (1989).
227. (a) D. J. Pysker, K. C. Goretta, R. S. Hodder, Jr., and R. E. Tressler, *J. Am. Ceram. Soc.* **72**, 284 (1988); (b) B. Jaschke, U. Klingebiel, R. Riedel, N. Doslik, and D. Gadow, *Appl. Organomet. Chem.* **14**, 671 (2000).
228. (a) T. Shimoo, H. Chen, and K. Okamura, *J. Mater. Sci.* **29**, 456 (1994); (b) W. Habel, B. Hamack, C. Nover, and P. Sartori, *J. Organomet. Chem.* **467**, 13 (1994); (c) D. R. Bujalski, G. A. Zank, and T. D. Barnard, U.S. Patent No. 5,262,553 (November 16, 1993) (d) Y. Yokoyama, T. Nanba, I. Yasui, H. Kays, T. Maeshima, and T. Isoda, *J. Am. Ceram. Soc.* **74**, 654 (1991); (e) T. Ishikawa, T. Yamamura, and K. Okamura, *J. Mater. Sci.* **27**, 6627 (1992); (f) K. E. Gonsalves, T. D. Xiao, and P. R. Strutt, *Ind. J. Technol.* **31**, 436 (1993); (g) S. T. Schwab *et al.*, *Polym. Prepr. (Am. Chem. Soc. Div. Polym. Chem.)* **34**, 296 (1993); (h) G. Passing, H. Schonfelder, R. Riedel, and R. J. Brook, *Br. Ceram. Trans.* **92**, 21 (1993); (i) W. Toreki, G. J. Choi, C. D. Batich, M. D. Sacks, and M. Saleem, *Ceram. Eng. Sci. Proc.* **13**, 198 (1992); (j) A. Herzog and U. Vogt, *Adv. Eng. Mater.* **4**, 877 (2002); (k) F. Cao, X.-D. Li, J.-H. Ryu, and D.-P. Kim, *J. Mater. Chem.* **13**, 1914 (2003); (l) L. Macdonald, *Ceramic Transactions*, 144 (*Advanced SiC/SiC Ceramic Composites: Developments and Applications in Energy Systems*), 87–95 (2002); (m) A. Herzog and U. Vogt, *Adv. Eng. Mater.* **4**, 877 (2002); (n) A. Herzog and U. Vogt, *Ceram. Eng. Sci. Proc.* **23**, 19 (2002); (o) J. Clade, E. Seider, and D. Sporn, *J. Eur. Ceram. Soc.* **25**, 123 (2005).
229. P. Baldus, M. Jansen, and D. Sporn, *Science* **285**, 699 (1999).
230. T. Ishikawa, Y. Kohtoku, K. Kumagawa, T. Yamamura, and T. Nagasawa, *Nature (London)* **391**, 773 (1998).

231. M. W. Pitcher, S. J. Joray, and P. A. Bianconi, *Adv. Mater.* **16**, 706 (2004).
232. P. Colombo and M. Modesti, *J. Am. Ceram. Soc.* **82**, 573 (1999).
233. P. Colombo and M. Modesti, *J. Sol-Gel Sci. Technol.* **14**, 103 (1999).
234. P. Colombo and J. R. Hellmann, *Mat. Res. Innovat.* **6**, 260 (2002).
235. I.-K. Sung, S.-B. Yoon, J.-S. Yu, and D. P. Kim, *Chem. Commun.* 1480 (2002).
236. M. R. Nangrejo and M. J. Edirisinghe, *J. Porous Mater.* **8**, 131 (2002).
237. P. Colombo, J. R. Hellmann, and D. L. Shellman, *J. Am. Ceram. Soc.* **85**, 2306 (2002).
238. P. Colombo and E. Bernardo, *Compos. Sci. Technol.* **63**, 2353 (2003).
239. T. Takahashi and P. Colombo, *J. Porous Mater.* **10**, 113 (2003).
240. Y. W. Kim, S. H. Kim, H. D. Kim, and C. B. Park, *J. Mater. Sci.* **39**, 5647 (2004).
241. R. Melcher, P. Cromme, M. Scheffler, and P. Greil, *J. Am. Ceram. Soc.* **86**, 1211 (2003).
242. P. Colombo, K. Perini, G. Bernardo, T. Capelletti, and G. Maccagnan, *J. Am. Ceram. Soc.* **86**, 1025 (2003).
243. Q.-M. Cheng, L. V. Interrante, M. Lienhard, Q. Shen, and Z. Wu, *J. Eur. Ceram. Soc.* **25**, 233 (2005).
244. (a) L. V. Interrante, K. Moraes, Q. Liu, A. Puerta, and L. G. Sneddon, *Pure Appl. Chem.* **74**, 2111 (2002); (b) K. Moraes, J. Vosburg, D. Wark, L. V. Interrante, A. R. Puerta, L. G. Sneddon, and M. Narisawa, *Chem. Mater.* **16**, 125 (2004).
245. X. Bao and M. J. Edirisinghe, *Mater. Technol. (Poulton-le-Fylde, United Kingdom)* **15**(2), 137 (2000).
246. M. Sternitzke, *J. Eur. Ceram. Soc.* **17**, 1061 (1997).
247. R. J. P. Curriu, *Angew. Chem. Int. Ed.* **39**, 1376 (2000).
248. (a) C. K. Narula, A. Varshney, M. P. Everson, P. Schmitz, L. F. Allard, A. Gandopadhyay, T. S. Lewkbandara, C. H. Winter, P. Czubarow, and D. Seyferth, *Mater. Res. Soc. Symp. Proc.* **495**, 287 (1998); (b) M. Buchmann, R. Gadow, E. Scherer, and M. Speicher, *Ceram. Trans.* **139**, 3 (2002).